PALEOGEOGRAPHY, SEDIMENTOLOGY AND BASIN DEVELOPMENT OF THE EOCENE RAPAHOE GROUP IN THE PUNAKAIKI-WESTPORT AREA.

A thesis

submitted in partial fulfilment

of the requirements for the Degree

of

Master of Science in Geology

in the University of Canterbury

by

Helen Lever

University of Canterbury

1999

Frontispiece: the Inland Pack Track crosses the Pororari River on a beautiful Wets Coast day. Typical outcrop can be seen to the lower right, in this case the Blue Bottom Group.

Abstract

The Rapahoe Group as presently defined consists of marine and marginal marine sediments deposited during a regional transgressive cycle, which occur between Brunner Coal Measures and Nile Group Limestones. It is proposed that the Rapahoe Group be expanded to include all transgressive deposits that underlie the Nile Group Limestones, including the Brunner Coal Measures. The limestone in and around the quarry at Cape Foulwind should also be included as the Cape Foulwind limestone rather than part of the Oligocene Waitakere Limestone, as it is formed during a fluctuating transgression in the Eocene rather than high-stand conditions in the Oligocene, even though the two are similar in composition.

The basin between Punakaiki and Westport is a narrow N to NE trending basin controlled on the west by the Cape Foulwind Fault and on the east by the complex Paparoa Tectonic Zone. Maximum subsidence occurred on the SE margin of the basin, but due to post-Oligocene uplift and erosion most of the evidence for the nature of this margin has been removed. The Cape Foulwind Fault is an enigmatic structure, its orientation, exact location and history is unknown. Slide deposits and the occurrences of Miocene Welsh Formation limestone onlapping basement on the eastern side of the basin suggest a land mass to the east, that was not transgressed until the Miocene. A similar land mass to the southeast was probably transgressed in the latest Eocene, however, all direct evidence of landmasses to the east of the basin has been removed by erosion caused by post-Oligocene uplift.

The Little Totara Sand can be subdivided at most outcrops and was deposited in a number of different shoreline environments, including beach, dune and tidal bar and channels. At Gibsons Beach and the Cape Foulwind Quarry it is underlain by a laminated silt and clay sequence up to 50 cm thick, that contains lenses of coarser sand and is very carbon rich. This is inferred to be

a lagoon deposit. The Little Totara Sand is time transgressive as it occurs both over and underlying the limestone at the Cape Foulwind Quarry.

A basin wide transgression-regression-transgression sequence has been recognised in all closely examined sections, the regression culminating in the Lower Whaingaroan with a surface of erosion or sub-aerial exposure recognised in most sections. This unconformity is correlated with an unconformity in the Inangahua and Buller Gorge regions, and possibly with breccia deposits around the mouths of the Little Wanganui and Mokihinui Rivers, but similar unconformities are not recorded for Greymouth, Buller Coalfields or Murchison areas. The regression and unconformity are therefore thought to be due to local tectonic events, rather than regional or global changes in sea-level.

Table of Contents:

List of Figures:

List of Tables

Chapter 1

Introduction

Aim of Thesis

The aim of this thesis is to interpret the paleogeography and Eocene development of the basin during the deposition of the Rapahoe Group, which consists of near-shore marine sediments that range in age from Kaiatan to Lower Whaingaroan. The interpretation of paleogeography is largely reliant on the inference of environment of deposition from analysis of structure, texture, composition, and fossil content of the five formations in the Rapahoe Group.

Location of study area

The area studied includes the limited inland exposure in the upper reaches of the Punakaiki and Pororari Rivers, and the coastal cliffs and river and road cuttings to the exposures of Rapahoe Group around the Cape Foulwind area (fig. 1.1). From the coastal exposures around Punakaiki to the Four Mile River the study area falls into the Paparoa National Park, and much of this area is covered in thick native bush or in regenerating scrubland.

Previous Work

The area under study forms part of two geological maps, the Westport and Charleston map by Nathan (1975b), and the Punakaiki map by Laird (1988). Both of these are at 1:63,360

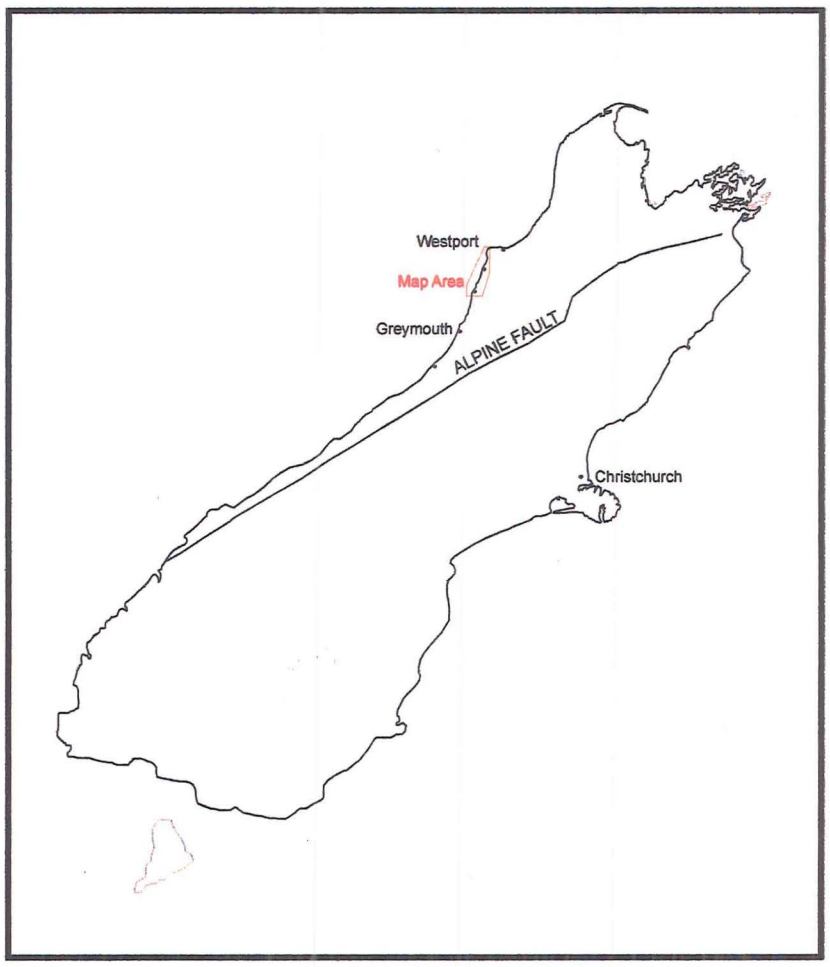

Figure 1.1: Location of the field area for this thesis. See the map in the back pocket for details of outcrop locations. The red line encloses the Paparoa National Park.

scale, but the map in the back of this thesis is presented at 1:50,000 scale in line with current practices. The Rapahoe Group is particularly extensive around the Greymouth region where it was first described (Gage 1952) and a brief history of the grouping and naming of the sediments now included in the Rapahoe Group is presented in Chapter 3. Several general overviews of sedimentation on the West Coast through the Tertiary are published (Laird and Lewis 1976, Nathan *et al.* 1986). Both the underlying Brunner Coal Measures and the overlying Nile Group Limestones have been studied: many different aspects of the Brunner Coal Measures have been studied especially around Charleston where the formation is particularly thick (Soong and Blattner 1986, Newman 1985, Sykes and Lindqvist 1993 etc.). The limestones in the Punakaiki-Westport area were studied as part of an M.Sc. thesis (Anderson 1984), and also Smale (1990) investigated the sources for various suites of heavy minerals in Cretaceous and Cenozoic sediments. Some studies have also been carried out on the fossils of the Rapahoe Group. Henderson (1975) examined the collection of spatangoids held by the New Zealand Geological Survey, which contained many samples collected by H.G. Wellman during his mapping of the West Coast region; and a more recent paper by Feldmann and Maxwell (1990) details an unusual decapod crustacean fauna found near Punakaiki.

Geological History

Until the Cretaceous, New Zealand was a small part of a convergent margin of the Gondwana continent. Around 105 Ma, subduction in most of the New Zealand region stopped. The cessation of subduction was inferred to be caused by the collision of the southward stepping spreading ridge between the Phoenix and Pacific Plates with the subduction zone east of New Zealand, causing the subduction zone to become blocked from north to south as each segment of the ridge arrived (Bradshaw 1989). This led to extension occurring across the New Zealand continental

crust, as the subduction zone became locked up, and the Pacific plate continued to move slowly away from Gondwana. After a period of extension across the whole of New Zealand north of the collision zone, a spreading ridge in what is now the Tasman Sea developed. The first ocean crust in the Tasman Sea is dated at around 82 Ma. The extension across the New Zealand crust from 105-100 Ma resulted in an overall thinning of the crust and the formation of numerous WNW-ESE trending basins, in Westland, Fiordland, and Canterbury, NE trending in the Campbell Plateau and parts of Otago. The later basins forming around 70 Ma on the West Coast tend to trend NNE-SSW (Laird 1994). The early basins in the Buller and Westland regions contain coarse breccias and local basal tuffs (the Pororari Group), dated in the Buller Gorge at 101±5 Ma (Bradshaw 1997). Associated intrusions along extensional faults have ages that range from 105 Ma (Baker and Seward 1996) to 78 Ma (Adams and Nathan 1978, and Muir *et al.* 1994).

During the mid Cretaceous, rapid uplift and continental extension led to the development and unroofing of a metamorphic core complex (the Paparoa Metamorphic Core Complex; Lewthwaite 1995), where mid crustal rocks have been exposed to weathering and erosion. The Charleston Metamorphic Group also includes some undeformed granites that vary in age between 105 (±5) to 92 Ma (S.D. Weaver pers. comm. 1999, Graham and White 1990). The ending of ductile deformation of the Charleston Metamorphic Group was estimated to be between 110 and 90 Ma (Kimbrough and Tulloch 1989), more recent studies place it around 105 ±5 Ma (S.D. Weaver pers. comm. 1999). Foliations in the Charleston Metamorphic Group typically strike north to northeast (White 1994, Lewthwaite 1995). When the sea floor spreading in the Tasman began in about 82 Ma WNW-ESE fractures were reactivated. NNE orientated rifting began ca. 70 Ma (Laird 1994) along the West Coast and the South Taranaki Basin. The development and occurrence of these rifts was probably controlled by reactivation of mid Cretaceous transfer faults developed between the opening New Caledonia Basin and the Tasman Sea spreading.

The Tasman Sea stopped spreading around 53 Ma. The cessation of spreading has been linked with a shift in relative plate motion (Australia began moving northward faster) meaning that the Tasman rift was no longer the optimum orientation for spreading. Sea floor formation began to occur in the southeast Tasman Sea, beginning about 47 Ma (Lamarche *et al.* 1997). The spreading system propagated northwards, breaking off part of the Campbell Plateau (Wood *et al.* 1996) and causing extension throughout south Westland. Extension continued to occur across the New Zealand Continent throughout the Eocene, although the early Eocene was a period of 'tectonic quiescence' (Nathan *et al.* 1986), resulting in a widespread unconformity over much of Westland. This unconfomity may be related to the adjustment period between spreading in the Tasman Sea and spreading in the southeast Tasman. The Rapahoe Group is deposited in a series of north to northeast trending fault controlled basins (fig. 1.2), that were actively extending through the mid Eocene to Oligocene. The greatest thickness of Rapahoe Group Sediment occurs in the Paparoa Trough to the east of Greymouth. This trough is controlled by the movement along the Paparoa Teconic Zone, several related faults that apparently had a scissor movement in the Eocene (Laird 1968, fig. 1.3). In the south around Greyounth, the western side of the zone is down faulted, and up to 2000 m of sediment was deposited during the Eocene (Nathan *et al.* 1986) including conglomerate beds (the Omotumoto Formation,Nathan 1974). Around Westport the eastern side of the tectonic zone is down faulted, again with conglomerate beds adjacent to the fault (Laird 1968).

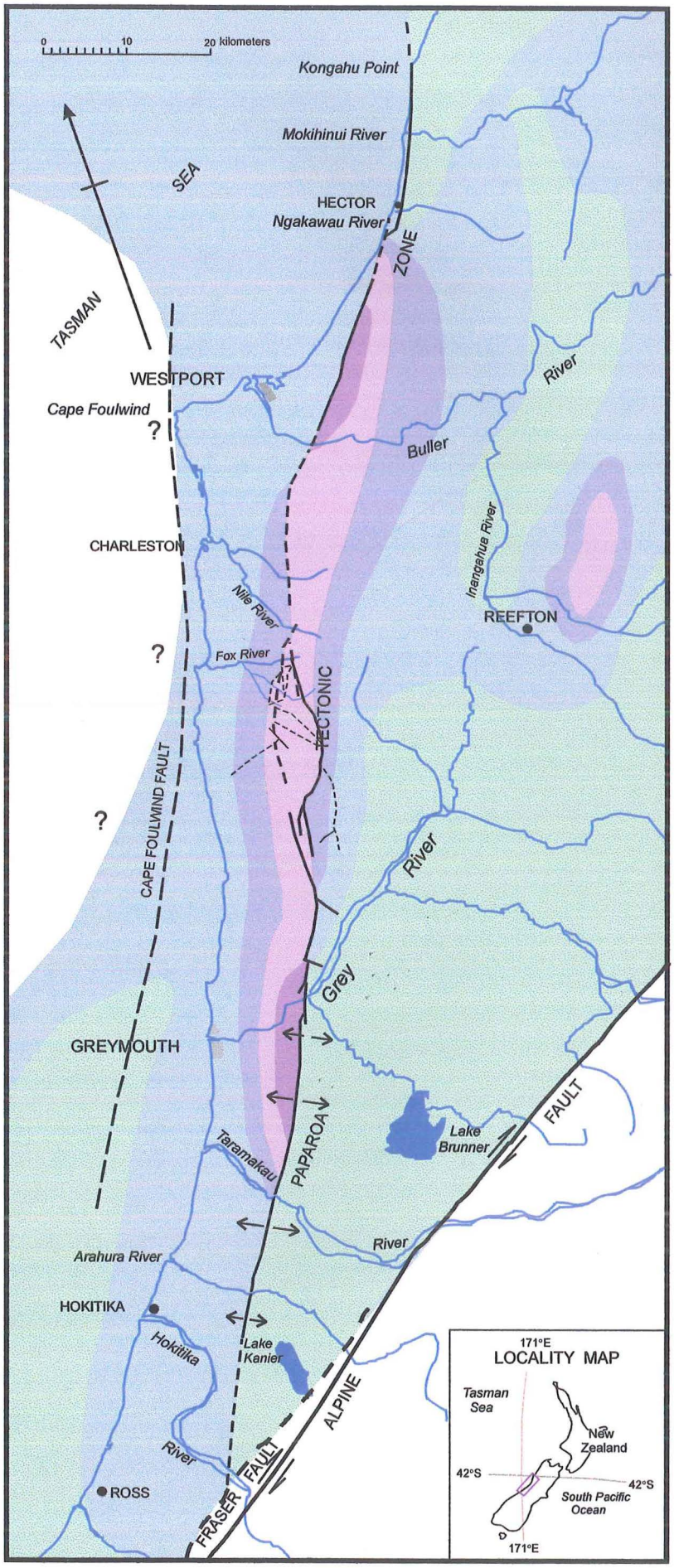

Figure 1.2: Map of North Westland showing approximate location of major faults and fault zones, with the thickness of Eocene sediments overlain. Modified from Laird (1968) and Nathan *et al.* (1986).

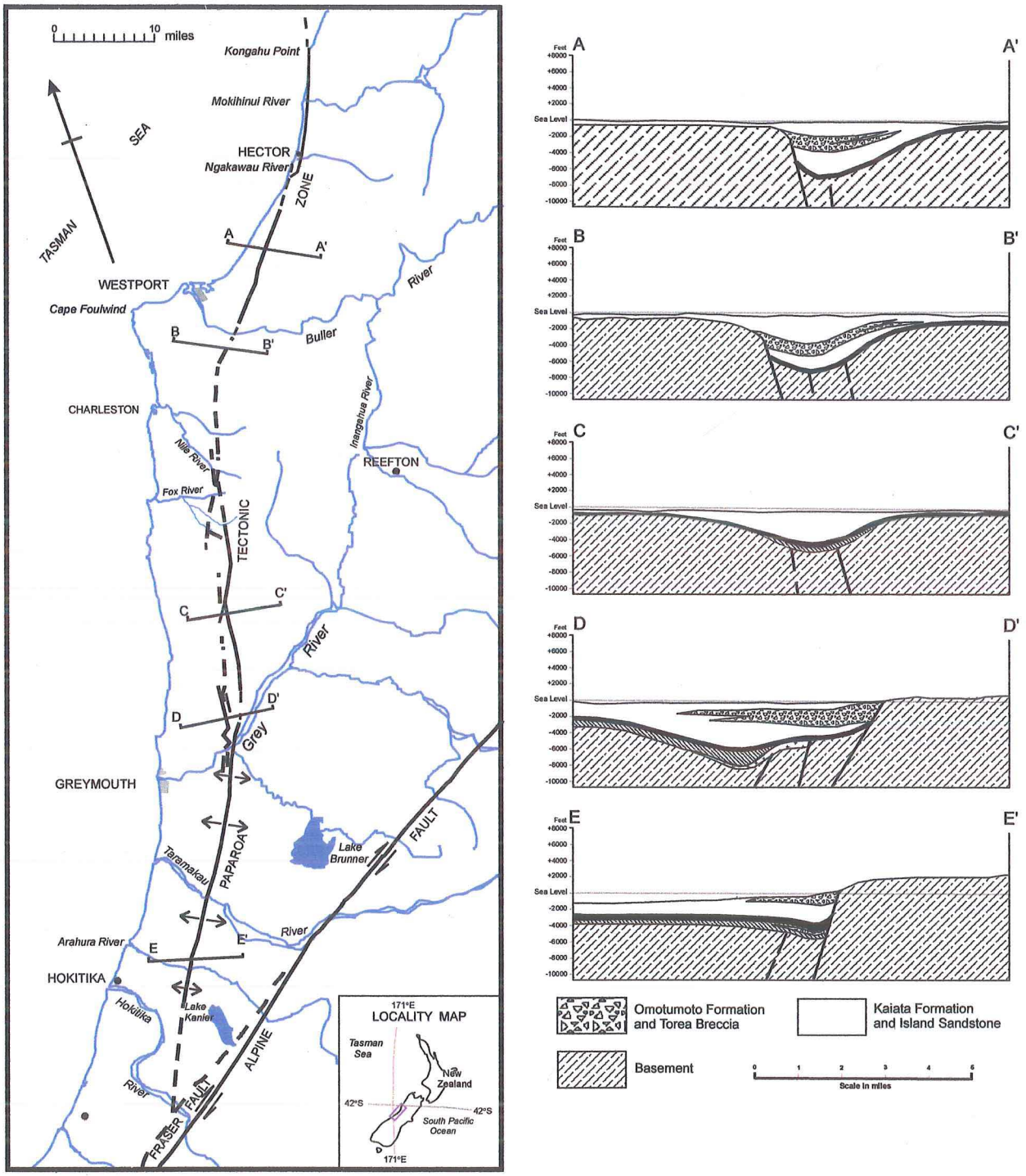

Figure 1.3: The location of some of the structural elements of the Paparoa Tectonic Zone, and cross sections across the zone during the Eocene, the section locations are shown on the map. The reconstructions are based largely on coal rank from the Brunner Coal Measures. From Laird (1968).

However, around the Punakaiki-Charleston area the simple scissor movement hypothesis breaks down. The fault here is supposed to be down faulting on the east, but conglomerates and local basement occurrences on the western side suggest that the eastern side was uplifted during the Eocene (M.G. Laird pers. comm. 1999). Unfortunatly, post-Oligocene uplift of the eastern side and subsequent erosion have removed any Eocene sediments that may have been deposited, so no direct evidence for the relative positions of the two sides of the fault zone during the Eocene has been removed. The Paparoa Tectonic Zone controls the subsidence along the eastern side of the Punakaiki-Charleston basin, as the Cape Foulwind Fault controls the subsidence along the western margin. Most of the subsidence occurred in the east: unfortunately this area has little useful exposure of the Rapahoe Group due to post-Oligocene uplift.

The whole of New Zealand was subsiding from the mid Eocene due to the lower thermal buoyancy the further away from the spreading ridges the thinned continent drifted, and this resulted in a regional transgression. The effects of the extension during the Eocene are printed over this transgression, and are seen predominantly in differences in the thickness of sediments across and between basins. Active faulting can be inferred to occur in the Punakaiki-Westport Basin from the occurrences of Eocene sediment gravity flows on the eastern side of the basin, and from changes in the thickness of Eocene units across the basin (Laird 1988).

Over time the orientation of spreading shifted, and the southeast Tasman spreading ridge transforms carried increasing oblique movement. The northward propagation of the ridge and the rate of spreading slowed and stopped in the Late Oligocene to Miocene as New Zealand became involved in the convergent margin developing between the Pacific and Australian plates. The convergent regime eventually resulted in the reactivation in the reverse sense of the same Cretaceous faults that frequently form the boundaries of Paleocene basins in, so the basins became inverted. The inversion and subsequent erosion of these basins resulted in much of the

information about the Eocene and Oligocene sedimentation and tectonic activity being lost. The uplift of the eastern side of the Paparoa Tectonic Zone since the Miocene has eroded all Tertiary cover down to the Charleston Metamorphic Group, and so it is unknown what sediments were deposited over this area during the Eocene.

Chapter 2:

Methods

Field Work

The West Coast has a well deserved reputation for being very wet. This is not to say that the sun does not shine, for Westport has one of the highest average hours of sunshine in the South Island, but rather that if there are clouds in the sky then it is either about to rain, it is raining or it has just finished raining. The climate however tends to be warmer than the East Coast, and this warmth, combined with abundant rain and high sunshine hours leads to lush, rapid growth, both of native rainforest, and of exotic flora such as gorse, blackberry, lupins, assorted grasses and *Cannabis sativa* all of which is calculated to make field work on the Coast a little tricky.

Much of the field area is in the recently established Paparoa National Park (see fig. 1.1). The rest of the area is either owned by D.O.C. and being encouraged to revert to native bush, or overgrown due to somewhat indifferent farming. The presence of the National Park discouraged any attempt to clean up or create outcrop on a large scale. The high rainfall does aid in forming large and extensive river systems, but the exposures in these tend still to be covered by bush, or the wet slopes slip frequently enough to cover outcrops. The forest ranges from rainforest, to regenerating broadleaf and gorse, to stumpy beach and broom in the higher areas. None of the vegetation types are easy to move about in, and all are excellent at concealing outcrops. The rate of erosion, whether by direct weathering, slips or plant root

action, is such that outcrops are created and disappear in a short time.

The land rises precipitously from the ocean (fig. 2.1), most beaches are backed by cliffs that beautifully expose the Rapahoe Group and overlying Limestones, but which make access difficult. These coastal cliffs are where much of the information for this thesis has come, as investigations in the many rivers and gullies showed that they seldom contained any exposure of the Rapahoe Group, and where they did, it was very limited. The large volumes of gravel in the river beds frequently obscured any outcrop and the river tends to erode the softer Rapahoe Group causing overlying limestone to collapse. The limestone overlies the Rapahoe Group, and forms steep sided gorges in the rivers and their tributaries. The end of the Rapahoe Group and the start of limestone outcrops are marked across the field area by cliffs of limestone, few of which show the contact with the underlying sandstones and mudstones.

The other places where useful outcrops of the Rapahoe Group are found are in road cuttings and old and current mines. The road cuttings are kept clear by regular trimming, but still often need vigorous cleaning and clearing of plants to see any useful exposures. However, these have proved most useful in unravelling the history of the Little Totara Sand. Unfortunately, many of the old mine sites have become overgrown, and a lot of collapse, slips and weathering has obscured much of the marvellous outcrop exposed by the miners. The Brighton mine in particular no more than 20 years ago still had well exposed Little Totara Sand, which could be seen in contact with Brunner Coal Measures below and Island Sandstone above, and the drives into the Brunner Seam were still open. Now the valley is completely filled with regenerating broadleaf and supple-jack forest, over a mixture of gorse and blackberry. The road and railway are almost overcome, and the buildings are collapsing. The exposure of the Island - Little Totara contact is gone, and the Brunner - Little Totara can

Perpendicular Point, looking south, as seen from the beach. The point is composed of rhythmically layered Island Sandstone, on which birds nest (hence the white markings). The lowest part of the cliff (obscured) is well laminated with scours and hummocky cross-stratification. F14P14.

Brighton Coal Mine, looking west. The access to this part of the mine is through the gut in the middle background (broadleaf, gorse and ferns) or scrambling up Limestone Creek, which runs from the lowest right corner behind the spur. This outcrop, which is reached after a scramble up a slope in excess of 70° on Brunner Coal Measures. The Little Totara Sand outcrop is an almost vertical cliff (extreme left of photo). F4P9.

Figure 2.1: Sea cliffs and steep hills in the field area.

only be seen in the stream and a single steep outcrop, currently in the process of slipping off the hillside (fig. 2.1). Other mines are similarly overgrown, and several no longer have visible access tracks leading into them (Waitakere Opencast). Those exposures that do exist show only the Brunner - Little Totara Sand contact, and the Little Totara - Kaiata contact is lost in lowland between these outcrops and the cliffs that mark the beginning of limestone exposure.

Fortunately the coastal cliffs provide good sections through the succession, numerous points marking the hardest or most calcareously cemented parts, which frequently include the contacts between the Rapahoe Group and the overlying limestone. During several months of fieldwork I examined the sedimentary structures, textures and relationships of the various formations, and satisfied myself that I had found all the available outcrops to study.

During fieldwork I took many photographs of the outcrops, sedimentary structures, trace fossils and scenic photos. These are listed, with location and description in Appendix VI. Many have been used in the text to illustrate the appearance of the various formations and their structures and other features.

Samples

Samples were taken for analysis from all localities visited. Appendix II contains a complete list of samples, locations, fieldbook references and analyses performed. The samples are referred to throughout this thesis using the field numbering system, HLS numbers. This numbering system is correlated with University of Canterbury rock collection numbers for future reference in Appendix II.

Laboratory Work

Samples from the various units were analysed in several ways. Six Little Totara Sand samples, six Island Sandstone samples and eight Kaiata Mudstone samples were disaggregated, sieved and pipetted to study the grain size distribution, the results of which are presented in Appendix V (see also Chapter 4). Indurated samples of Kaiata Mudstone and Island Sandstone were thin sectioned, and point counted for composition (Appendix IV). Samples from the Kaiata Mudstone and Island Sandstone were also disaggregated and sieved to extract microfossils, which were collected and identified (Appendix III). The Little Totara Sand was examined for texture and composition, but no micro- or macrofossils were found.

All Little Totara Sand samples disaggregate readily, and often do not need the addition of a dispersant when washed before size analysis. Island Sandstone and Kaiata Mudstone samples, on the other hand, tend to be slightly cemented, and cling together, and samples from the cemented bands were impossible to disaggregate without mechanical pounding, which would result in broken fossils and an altered grain size distribution. Thus only those samples that could be easily disaggregated were sieved for size analysis, however Laird (pers. comm. 1999, see Chapter 4) showed that the cemented and uncemented bands in the Island Sandstone had the same grain size distribution.

A part of each sample was taken for microfossil extraction, these were heated with detergent or Calgon in water, until the sediment was completely broken down, or further treatment produced no changes. Then the sediment was wet sieved through a 2.25ϕ and 4.00ϕ sieve and both the sand and mud fractions were kept and dried. The dry sediment was examined, and the amount of sand and mud estimated. The microfossils were extracted and identified.

For size analysis of Island and Kaiata samples, about 20 grams of sample was heated with distilled water and Calgon, until disaggregated or further heating resulted in no change. Then

samples that were not fully disaggregated were mechanically ground in water with a pestle in a mortar. The samples were then wet sieved through a 4.00ϕ sieve, and sand and mud fractions were dried in an oven. The sand fraction was dry sieved and weighed, and the mud fraction was weighed, and placed in a settling column for pipette analysis. The calculated cumulative percentage (calculated in an Excel program) from these analyses were put into SigmaPlot, from Jandel Scientific Software, which produced the graphs in Chapter 4.

XRD analysis was performed on two samples of clay from the Kaiata Mudstone, extracted during pipette analysis, and the results from the two samples came out very similar, the more concentrated sample being represented by the graph in fig. 4.11.

Chapter 3:

Stratigraphy of the Rapahoe Group

Introduction

The purpose of this chapter is to introduce the formations and lithologies that are included in the Rapahoe Group. The formation names have a long and complicated history, mainly because the grouping and description of the various formations and members used has always depended on which part of the West Coast the work was done on. Nathan (1974, 1975a, 1975b, Nathan *et al.* 1986) was the first to propose a classification that could be used in all parts of the West Coast.

The formations that make up the Rapahoe Group are described here in this chapter, with their distribution and stratigraphic relationships. The descriptions here are compilations of previous work and data collected during field work for this thesis. Chapter 4 contains more detail about each unit, including composition, texture, structure and facies variation.

The name Rapahoe Group was first proposed by Nathan (1974), following his field-work for the Buller, North Westland and Greymouth geological maps. Most of Nathan's proposed groups and formations have since been accepted into common usage. Nathan (1974) rejected the common practice of defining a group as a set of sediments that are deposited in the same cycle of sedimentation, so that a group may contain diverse lithologies. He set out to group the West Coast sediments by similar lithologies. However, the stratigraphy of the West Coast is such that the groups he defined are usually cycles of sedimentation anyway. The Rapahoe Group as he defined it also contains some rather diverse lithologies, as the Little Totara Sand and other sand bodies Nathan (1974) included are very different in appearance, composition, diagenetic

alterations and depositional environment to the other units. The Rapahoe Group as defined by Nathan (1974) is almost a cycle of sedimentation, being those marine and marginal marine sediments deposited during overall transgression from fluvial deposits to limestones, although this definition should also include the Brunner Coal Measures, as they are the first sediments deposited in the transgression.

The only group that Nathan (1974) proposed that was not generally accepted into use is the Mawheranui Group, which brought together the fluvial Paparoa Coal Measures and the fluvial/estuarine Brunner Coal Measures. The two coal measure units are difficult to differentiate in the Greymouth area, but are separated by a major unconformity elsewhere. The complete difference in paleoenvironment, tectonic context, coal composition and sedimentation style means that lumping the two can be very misleading, and does not give a true picture of the development of the region (see also Gage 1975, Lewis 1975 and Laird 1988). The type section of the Brunner Coal Measures occurs in the Greymouth Coal Field, where the two coal units are difficult to differentiate. The Brunner is also unusual in this area in that it contains Paleocene strata; elsewhere the Brunner is entirely Eocene. The status of the Brunner Coal Measures and the Paparoa Coal Measures is undecided at this time. Bishop (1991) included the Paparoa Coal Measures in the Pakawau Group and the Brunner Coal Measures in the Rapahoe Group, however Ward (1997) rejects both reassignments based on inconsistencies in lithology and distribution. Nunweek (in prep. 1999) proposes the formation of the Brunner Formation (in the Rapahoe Group), that would contain as members Coal Measures and Transitional conglomerate units, as well as differentiating Eocene and Paleocene coal seams. Brunner Coal Measures have also been included in the Maruia Formation (in the Murchison Basin) by Suggate (1984) and Roder and Suggate (1990).

The name Mawheranui was originally used by Morgan (1911), when he introduced the term Mawheranui Series to describe the coal measures of the Greymouth area (fig. 3.1).

The series then contained the Paparoa and Brunner Coal Measures, the Island Sandstone and the Kaiata Mudstone (thought to contain a coal seam). Gage (1952) grouped the Island sandstone, Kaiata Mudstone, Omotumotu Beds and Port Elizabeth Beds in an informal Lower Tertiary Formation. Nathan (1974) proposed that the Omotumotu and Port Elizabeth Beds be grouped with the Kaiata Mudstone into the Kaiata Formation, and that all three have member status. The Omotumotu Member does not occur in the study area. The "Port Elizabeth Member" is basically Kaiata Mudstone with rhythmic cementation, and it tends to be slightly coarser than Kaiata Mudstone. The difference between the two members is slight, gradational and ambiguous, and I have chosen not to use the Port Elizabeth Member in my field area, so that the Kaiata Formation consists entirely of Kaiata Mudstone. Nathan (1975b) however, recognised Port Elizabeth beds at Cape Foulwind (Gibsons Beach), and the top part of the Kaiata Mudstone at Woodpecker Bay could be assigned to Port Elizabeth beds, but was not distinguished as such by Laird (1988), and was mapped within his Kaiata Formation.

Nathan (1974) included several sand bodies in his Rapahoe Group, the Little Totara Sand, the Lyell Sand and the Te Wharau Sand. Only the Little Totara Sand occurs in this study area. Since the definition of the Rapahoe Group by Nathan (1974) as containing the Kaiata Formation, the Island Sandstone and the various sand bodies, the group has had added to it the Fossil Creek Formation (Laird 1988), who grouped this formation into the Rapahoe Group on the basis of its age and *probable* depositional relationship to the rest of the Rapahoe Group. The Fossil Creek Formation has no sedimentological contacts with the rest of the group and its relationship to the rest of the Rapahoe group is therefore uncertain.

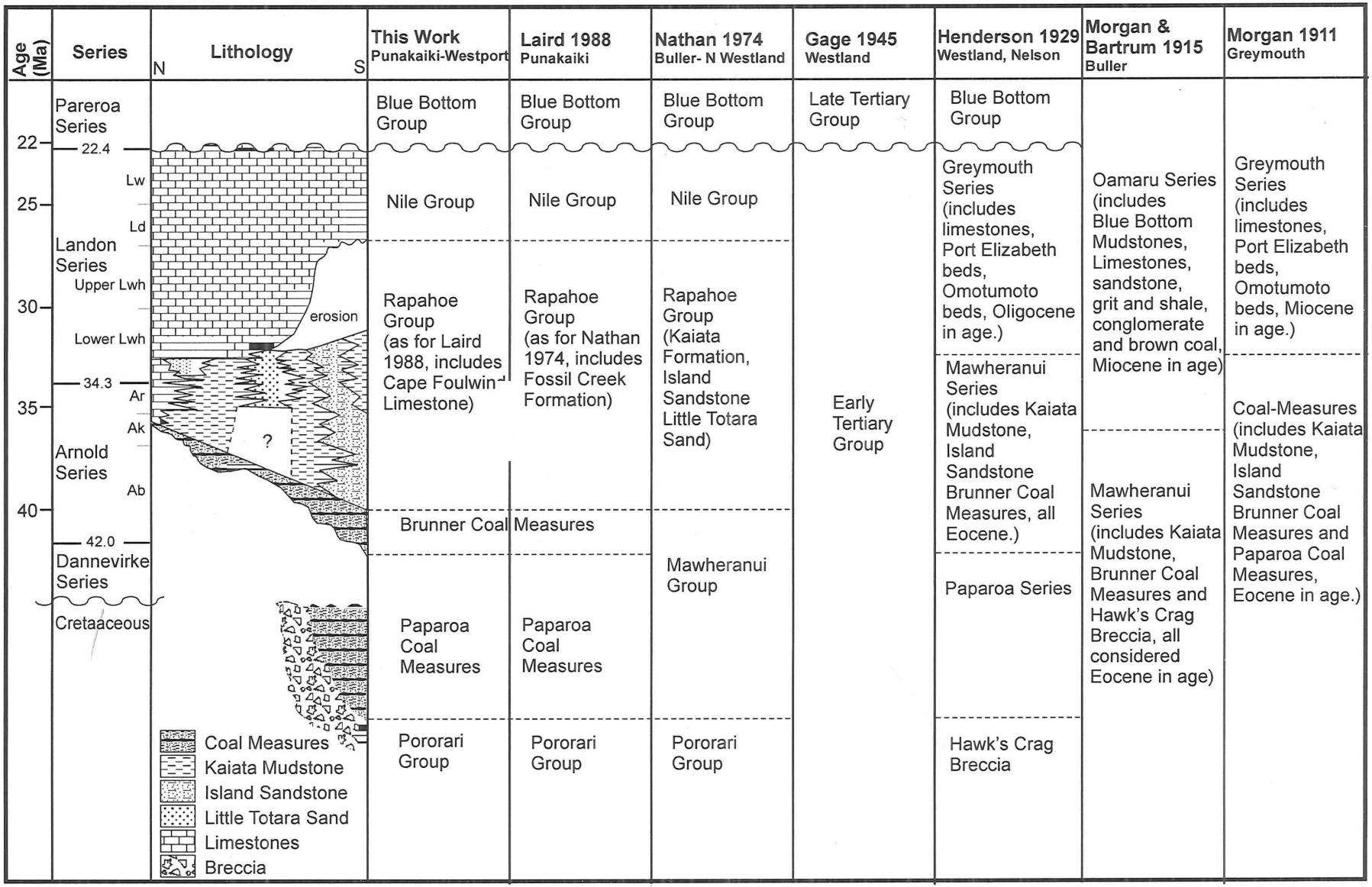

Figure 3.1: The changes in stratigraphic nomenclature and grouping over time. In the earliest papers, the practice of using microfossils and other methods to date sections was not widely in use, and all dates are reckoned relative to other beds.

If the Rapahoe Group is defined as all those marine and marginal marine sediments associated with the regional marine transgression, then it should logically include all the sediments deposited between the basement or *fluvial* coal measures, and the first occurrence of widespread limestones representing the maximum transgression. This would include the Brunner Coal measures, as they represent fluvial/esturine peat swamps (Newmann 1985), and therefore they are the first deposit of the transgression. Including the Brunner Coal Measures in the Rapahoe Group would mean the group would represent one cycle of sedimentation. The limestones are the result of a different set of conditions, and so belong to a different group. The Cape Foulwind Limestone, however, is formed during the transgression and is clearly interbedded with the Kaiata Mudstone. It is an integral part of the Rapahoe Group, and including it in the Waitakere Limestone is very misleading as it is not related to the widespread shallow conditions under which the Waitakere Limestone was deposited. The widespread and thin Waitakere deposits cannot be convincingly demonstrated to be continuous with the Cape Foulwind Limestone which is much more limited in extent.

Although the Brunner Coal Measures should be included as a formation in the Rapahoe Group, they are not included here because of space and time restraints. In this thesis, the Rapahoe Group is defined as those marine and marginal marine sediments that occur between the Coal Measures or equivalent sands, and the first *widespread* Oligocene Limestones. By this definition the limestone quarried at Cape Foulwind for cement is also a part of the Rapahoe Group and is described as such below. The limestone is described as a separate formation, rather than a member within the Kaiata Formation. The Rapahoe Group ranges in age from Kaiatan (Eocene) to Lower Whaingaroan (Oligocene).

Formations in the Rapahoe Group

Little Totara Sand: rl (Nathan 1974)

DISTRIBUTION: The Little Totara Sand outcrops in cliffs from Meybille Bay to Limestone Creek; further south it is overstepped by Island Sandstone. The formation is 30 m thick at Brighton Coal Mine, but thins rapidly to the south, and is cut off abruptly to the north by the Limestone Creek Fault, suggesting activity on the fault in the Eocene. North of the fault, between Kaipakati Point and the Redjacket Mine, it occurs as 1-2 m thick layers, intermittently inter-fingering with basal Kaiata Mudstone resting on Brunner Coal Measures. North of Redjacket Mine the formation becomes thicker, and it reaches its greatest thickness of 210 m near the Little Totara River. In the Okari and Cape Foulwind areas the formation overlies the Kaiata Mudstone: in the Okari Lagoon area it interfingers with algal limestone and muddy sandstone, and reaches a thickness approaching 200 m according to Nathan (1975b).

DESCRIPTION: The Little Totara Sand consists mainly of coarse to fine, well-sorted to poorly-sorted, white mica-feldspar-quartz sand, with indistinct bedding, and very common large and small scale cross bedding, scour surfaces including granule concentrations, grading and thin conglomerate layers. The Little Totara Sand's most distinctive feature is bimodal roundness in the quartz grains. Most outcrops show that the formation consists of several sections, each consisting of different degrees and types of cross stratification, and different grain size distributions, often with distinct current direction distributions, separated by planar erosion surfaces. The sections also differ in the amount of organic carbon, and iron oxide cementation present, as laminae or blobs. Few recognizable plant root structures remain, due to diagenetic alteration and remobilisation.

STRATIGRAPHIC RELATIONS: The formation rests on Brunner Coal Measures from Meybille Bay to Limestone Creek, locally directly on the coal seam, but usually separated by up to 1 m of finely laminated fine sandstone, and at Brighton Coal Mine separated by a quartz gravel lag deposit. It is overlain with a 1-2 m gradation by Island Sandstone. It occurs sporadically and thinly north of Kaipakati Point, where it interfingers with basal Kaiata Formation. From the Redjacket Mine northwards to the Little Totara River, Little Totara Sand rests on Brunner Coal Measures, usually several meters above the coal seam. Often there is evidence for reworking of Brunner Sands (fluvial) by Little Totara Sand processes (marginal marine), so a gradational contact over several meters can be recognized in some places, Little Totara Sand being distinguished by bimodal roundness. In the North, at Okari Lagoon and Cape Foulwind, the Little Totara Sand rests on Kaiata Mudstone: the contact is a disconformity, with considerable erosion and the deposition of a carbon-rich lagoonal silt inbetween, although the contact appears conformable (fig. 3.2). The Little Totara Sand is also reported to underlie the Cape Foulwind Limestone in parts of the quarry (Lewis pers. comm. 1999), here occurring at both the top and bottom of the sequence.

AGE: Kaiatan to Lower Whaingaroan on microfossil evidence: the base of Little Totara Sand becomes younger towards the North.

DEPOSITIONAL ENVIRONMENT: The Little Totara Sand was deposited in a variety of shoreline environments: different outcrops show internal differences in environment, and environment also changes vertically within an outcrop. These environments include dunes, beaches and tidal sandbars.

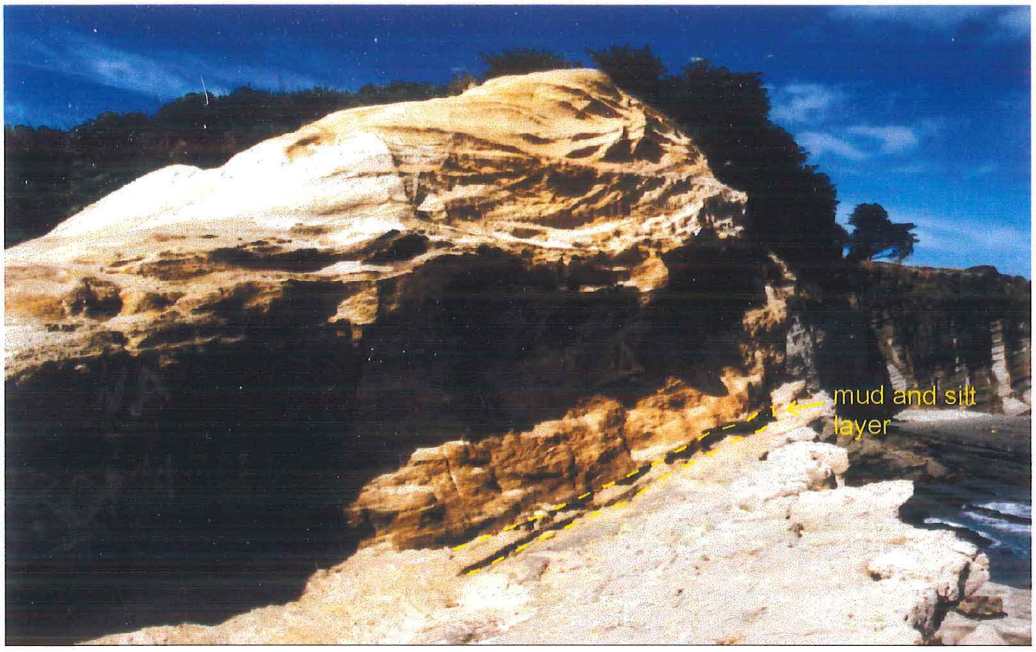

a: mud and silt layer between top surface of the Kaiata Mudstone and the Little Totara Sand at Gibsons Beach. The layer here is of variable thickness, no more than 15 cm. F4P37

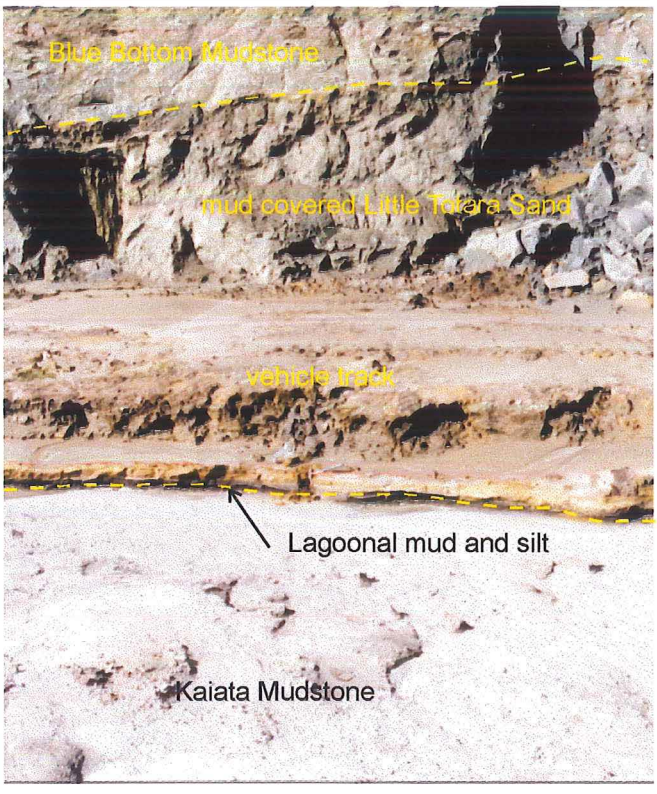

b: Contact between the Kaiata Mudstone and the Little Totara Sand at the Cape Foulwind Quarry. The mud and silts between the two formations is much thicker here than at Gibsons Beach, up to 40 cm. The silt contains sand lenses, representing washover events from the nearby beach and dune environments. The trace fossils in the top surface of the Kaiata Mudstone don't contain such coarse fills here, possibly indicating deeper erosion. F11P4.

Figure 3.2: The boundary between the Kaiata Mudstone and the Little Totara Sand in the Cape Foulwind area. The boundary has been considered to be conformable, but there is evidence for considerable erosion and the deposition of a lagoonal silt between the two formations.

Kaiata Formation: rk (Gage 1952 after Morgan 1911)

DISTRIBUTION: The Kaiata formation crops out on the eastern limb of the Barrytown Syncline between the Punakaiki and Pororari rivers. Small erosional remnants also occur in the east of the Pike River Coalfield (Laird 1988), and in the offshore Haku-1 drillhole. The formation also occurs in Woodpecker Bay, where it interfingers to the south with Island Sandstone and at the base with Little Totara Sand and rests on Brunner Coal Measures. To the north the formation thins and eventually pinches out north of Four Mile Road. The thickness is highly variable, up to 900 m thick in the Pororari River, but thinning rapidly to the southwest, being only 70 m thick at the Punakaiki River and pinching out to the south. In Woodpecker Bay it averages 200 m in thickness. The thickness in the Charleston area, where it overlies Brunner Coal Measures and underlies Little Totara Sand is uncertain, but the formation thickens to the north, reaching 130 m thick at Gibsons Beach, where it pinches out locally around a basement high.

DESCRIPTION: The Kaiata Formation in this area consists of moderately well to poorly sorted, micaceous and glauconitic, dark brown or grey, calcareous sandy mudstone. At Kaipakati Point where it interfingers with the Island Sandstone, the two formations are distinguished by sand content and colour. The Kaiata formation is strongly burrowed and generally shows no internal lamination. It is rhythmically layered, the layer frequency variable and generally increasing towards the top of the formation, although in some areas (Charleston) the layers are not visible. The cemented layers reach up to 40% $CaCO_3$ and intervening layers vary between 5% and 15% $CaCO_3$ (Laird 1988).

STRATIGRAPHIC RELATIONS: On the eastern limb of the Barrytown Syncline and in the Pike River Coalfield, the Kaiata Formation rests conformably on, but apparently with relatively rapid transition into, the Island Sandstone (Laird 1988). In Woodpecker Bay it interfingers with and grades into Island Sandstone southwards, and rests conformably, but with rapid transition

over 1 to 2 m, on Brunner Coal Measures. It overlies the Little Totara Sand north of the Redjacket mine, until north of Four Mile Road it grades into the Little Totara Sand. Around the Charleston region it underlies the Little Totara Sand, and at Cape Foulwind it rests conformably on Brunner Coal Measures, and is overlain after an erosional break by Little Totara Sand.

AGE: Kaiatan to basal Whangaroan in the southern part, basal Runangan to lower Whaingaroan around Cape Foulwind on microfossil evidence.

DEPOSITIONAL ENVIRONMENT: Shallow marine offshore, probably with restricted circulation and low oxygen conditions, a gulf or embayment.

Island Sandstone: ri (Hector 1877)

DISTRIBUTION: The Island Sandstone crops out extensively in the upper reaches of the Pororari and Punakaiki rivers, and in the Pike River Coalfield (Laird 1988). It also occurs extensively from Punakaiki to Kaipakati Point, where it interfingers with and grades into Kaiata formation. It overlies Brunner Coal measures in the Pororari River, reaching a maximum thickness of 850 m, but it thins rapidly to the south, being 420 m thick in the Punakaiki River and 180-200 m in the Pike River Coalfield (Laird 1988). At Perpendicular point it is 270 m thick, but thins to the north and at Pahautane Point it is 200 m thick, at Seal Island it is only 20 m thick, as it is interfingering with and grading into Kaiata Formation.

DESCRIPTION: The formation consists of moderately well to poorly sorted, brown-grey, fine to very fine muddy calcareous sandstone. Although locally parallel lamination, cross-bedding, scouring and hummocky cross-stratification is visible, burrowing is intense and lamination is commonly destroyed. Outcrops show rhythmic layering developed by alternating cemented and less well cemented horizons (see Chapter 7). The more resistant well cemented layers average 36% $CaCO_3$ cement, with total $CaCO_3$ including detrital shells rising over 50%. The cement has

generally replaced a matrix, inferred to be muddy and calcite rich. At Perpendicular Point, above a section with well developed convoluted parallel laminations, about 30 cm of the sandstone is cemented with quartz (chalcedony), filling voids left by dissolution of original calcite cement. The percentage of quartz reaches 23% in concretions within one narrow (10 cm) layer. North of Perpendicular Point, there are prominent scours and channels in the basal meters of the formation, and well developed hummocky cross-stratification,with bioturbatedhorizons between packages of laminated sands.

STRATIGRAPHICRELATIONS:Except in the northwest,Island Sandstone rests conformably on Brunner Coal Measures. Between Limestone Creek and Meybille Bay it rests on Little Totara Sand with a gradation of 1 to 2 m, and south of Meybille Bay it rests directly on Meybille Granite. Around Kaipakati Point it grades laterally into and interfingers with Kaiata Formation. At Pahautane and Kaipakati the glauconite content and calcium carbonate content increases towards the top of the formation, the actual contact with the overlying limestones marked by an uncemented sand horizon at Pahautane and a highly cemented Rhodolith band at Kaipakati Point and Seal Island (see Chapter 5). In the upper Pororari and Punakaiki rivers the Island Sandstone is overlain conformably if abruptly by the Kaiata Formation.

AGE: Kaiatan to basal Whaingaroan on microfossil evidence.

DEPOSITIONALENVIRONMENT:Shallowmarine offshore, inner shelf, at least partly above storm wave base.

Cape Foulwind Limestone: rc (new formation)

DISTRIBUTION: The Cape Foulwind Limestone is limited to a granitic basement high at Cape Foulwind, where it is quarried. Resedimented algal limestone material occurs in the basal (Runangan) part of the Kaiata formation at Gibsons Beach, and also just below the Little Totara Sand contact (Lower Whaingaroan). Algal debris from the Limestone also occurs in the Okari Lagoon area, where it inter-fingers with sandy Kaiata Mudstone (upper part) and Little Totara Sand. The limestone reaches a maximum of 60 m thickness in the Quarry.

DESCRIPTION: White to blue-grey muddy to sandy algal biosparite, to pink-cream algal biosparite, scattered mud and sand laminae and lenses. Algal material consists of broken material and rare in-situ colonies. It also occurs as thin bands of cemented muddy algal biosparite inter-bedded with bands of Kaiata Mudstone containing scattered algal material. Glauconitic in places, especially in muddy and sandy parts, the glauconite usually occurs as glauconitized fossils and algae in the limestones, although granular glauconite becomes common in some mud layers.

STRATIGRAPHIC RELATIONS: The formation rests unconformably on weathered Cape Foulwind "Granite", sands correlated with Brunner Coal Measures, or on Brunner Coal Measures. It inter-fingers laterally with Kaiata Mudstone and Little Totara Sand. In the Quarry, the limestone either grades up through glauconitic, muddy algal sands into Kaiata Mudstone, or is overlain abruptly by another algal limestone, white to yellow-grey in colour, probably the Waitakere Limestone. Karst features in the top of this limestone reach down into parts of the Cape Foulwind Limestone.

AGE: Lower Runangan to Whaingaroan on microfossil evidence.

DEPOSITIONAL ENVIRONMENT: Shallow marine, with clear water conditions, a basement high probably relatively close to a shoreline, well within the photic zone, 0-15 m water depth.

Fossil Creek Formation: rf (Laird 1988)

DISTRIBUTION: The formation occurs as a narrow fault-bounded strip between the headwaters of Fossil and Dilemma creeks, and in a similar structural situation in Henniker Creek.

DESCRIPTION: The lower half of the formation in the type section consists dominantly of pebbly mudstone, with clasts up to 5 cm. Thinner interbedded units include coarse sandstone and fine conglomerate with clasts up to 60 cm, thin beds of parallel laminated sandstone, and slump horizons. The upper half consists of well bedded, fine to medium, dm-bedded sandstone showing parallel lamination and frequent grading. In Henniker Creek the formation consists mainly of massive pebbly sandstone, or mudstone and breccia containing clasts up to 50 cm in diameter. A thickness of 140 m occurs in the type section; in Henniker Creek approximately 40 m is preserved.

STRATIGRAPHIC RELATIONS: The formation is everywhere in fault contact with other units.

AGE: Runangan to basal Whaingaroan on microfossil evidence.

DEPOSITIONAL ENVIRONMENT: The common presence of graded beds, pebbly mudstones, and slump horizons suggests deposition by sediment gravity flows in a subsiding basin.

Chapter 4:

Sedimentology

Introduction

This chapter details the sedimentary characteristics of the various formations within the Rapahoe Group. Composition, textures, structures and trace fossil assemblages are described and discussed for the Little Totara Sand, the Kaiata Mudstone and the Island Sandstone. Details of the evidence for the paleoenvironmental interpretations in Chapter 8 are included in these descriptions. Grid references for locations mentioned in the text are for the NZMS series 260 1:50,000 maps, or for the geological map in the map pocket at the back of this thesis. Textural information is presented in Appendix V, (see Chapter 2 for methods); compositional information was gained from point counting and visual estimation of thin sections (Cape Foulwind Limestone, Kaiata Mudstone and Island Sandstone) and grain counts of loose sand samples from the Little Totara Sand. Information on the structure, texture and extent of the Cape Foulwind formation is difficult to aquire; an attempt was made to access quarry records, but the information did not arrive in time to be included here. OSH regulations restrict movement within the quarry itself.

Cape Foulwind Formation

Field Relationships:

The Cape Foulwind Limestone has previously been included in the Waitakere Limestone, based on the similar lithology. The limestone differs from the Waitakere in its relationship to surrounding lithologies, limited extent, and age, although it contains a similar assemblage of algal and other fossil material. The thickest and purest limestone in the Cape Foulwind Quarry is approximately lower Runangan in age, and occurs about 30 m below the contact with the overlying Little Totara Sand which is Lower Whaingaroan in age (based on microfossil dating). The limestone is limited to the area on and around a basement high, consisting of Cape Foulwind "Granite", weathered granite and associated sands (see map, in pocket). The shallow water around this high proved ideal for the growth of coralline algae. The debris from broken algal growths accumulated and a complex relationship developed between the massive limestone accumulating on the basement high and the surrounding debris fields, mud and sand deposits. The size and thickest part of the algal deposits varied over time, resulting in the complex interbedding of Kaiata Mudstone, various sands and algal limestone seen in the Cape Foulwind Quarry.

At the time of the deposition of overlying Little Totara Sand, the deposition of algal limestone had reduced to an area perhaps 200 meters across in the far north side of the present quarry, where algal limestone interbedded with Kaiata Mudstone is overlain abruptly by a yellowish algal limestone, probably the Waitakere Limestone (fig. 4.1).

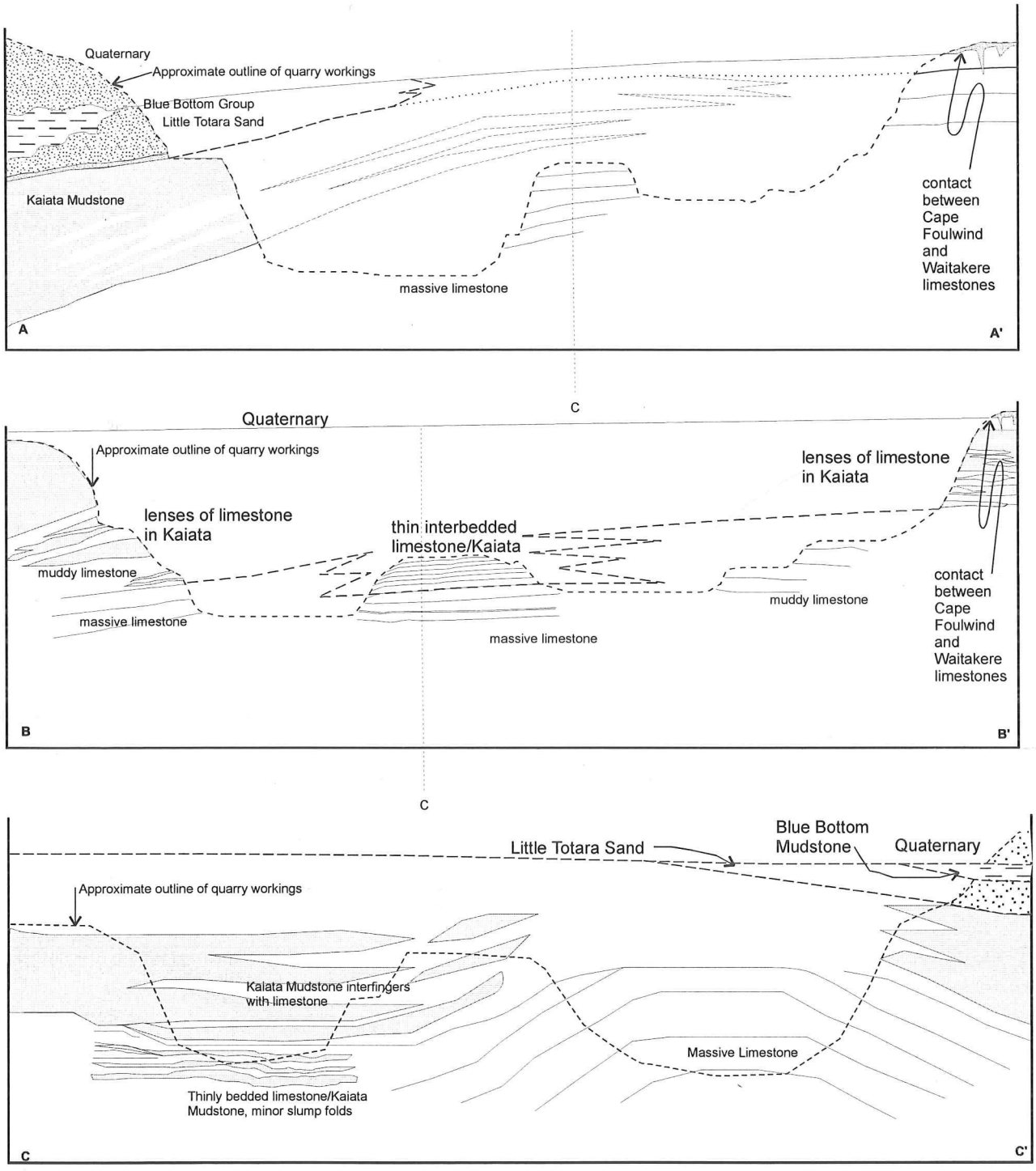

Figure 4.1: Diagrammatic representation of the probable facies relationships at the Cape Foulwind Quarry. Not to scale.

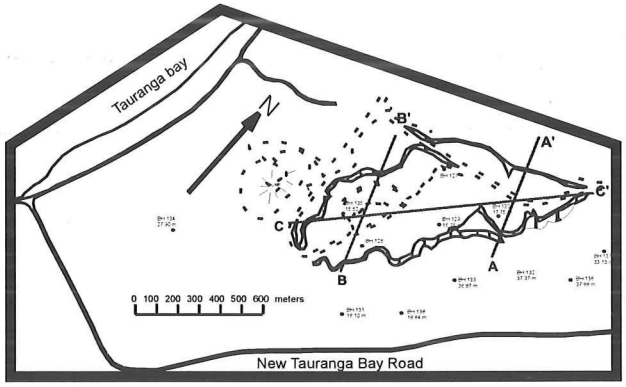

Both Anderson (1984) and MacGregor (1983) considered the Eocene "Waitakere Limestone" at the Cape Foulwind Quarry as part of the Waitakere, and MacGregor acknowledged that the limestone may not have been deposited continuously through to the Oligocene (MacGregor 1983, p. 387). While I cannot solve this question completely, the following observations were made at the quarry:

1. A quarried face shows layers and lenses of limestone interbedded with Kaiata Mudstone, with the amount of mudstone increasing upwards (fig. 4.2a). A sharp upper boundary to this sequence is overlain by a yellowish, massive algal limestone, maximum 6 meters thick here, topped by modern soils.
2. The yellow, massive algal limestone in another face showed karst (or paleokarst) formation that penetrated into the underlying muddy Limestone sequence (the sink holes are filled with orange-black sands, presumably Quaternary in age).
3. Cape Foulwind Limestone on the SE side of the quarry grades up into and interfingers with Kaiata Mudstone dated as Runangan-Whaingaroan. The mudstone is unconformably overlain by Little Totara Sand of Lower Whaingaroan age (Srinicasan and Vella, 1974).
4. Broken, rounded fragments of algae are present in the coarse burrow fills below the Kaiata/Little Totara Sand disconformity at Gibsons Beach (fig. 4.2b).

The yellow massive limestone is inferred to be the Waitakere Limestone, equivalent to the outcrop that occurs at Gibsons Beach, based on its appearance, thickness and the presence of karst features. Limestone lenses in the Kaiata Mudstone, decrease in frequency and thickness up to the massive yellow limestone, probably result from algal debris being washed off the paleohigh. Even where there is Cape Foulwind Limestone directly below the massive, yellowish limestone inferred to be Waitakere Limestone, a sharp boundary occurs between the two units.

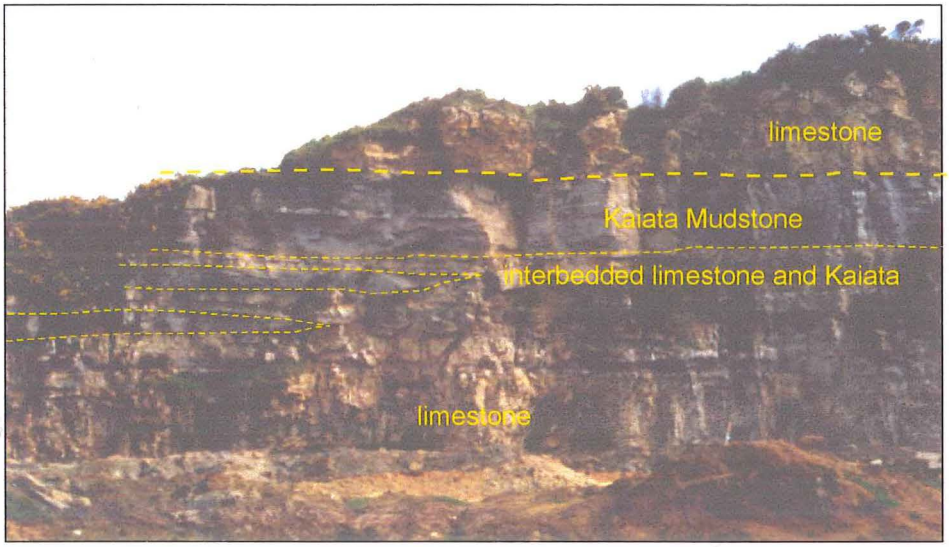

a: Photograph of a quarried face, Milburn Cement Quarry. The face illustrates the relationship between massive limestone, Kaiata Mudstone and the overlying yellowish limestone, above the dotted line, in the northern part of the Quarry. The limestone layers are lensoid in shape, the limestone lenses pinch out to the left implying transport from right to left in this face.

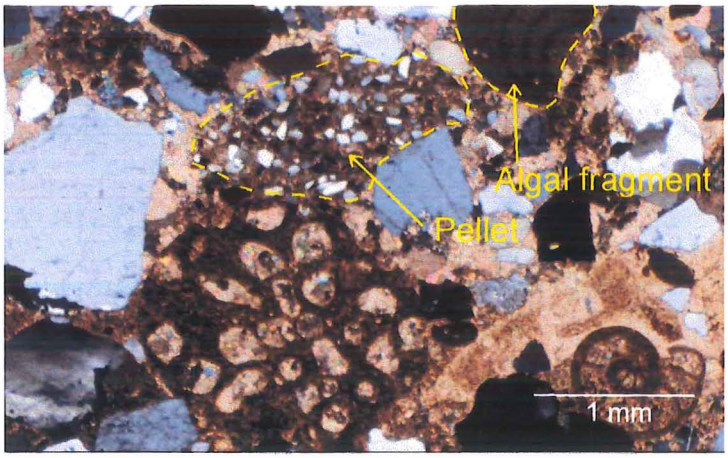

b: Coarse sand and granule fill from a burrow in the top surface of the Kaiata Mudstone, Gibsons Beach. Fill contains abundant coarse detritals, as well as foraminifera, bryozoa, pellets and algal fragments, and is extensively calcite cemented.

Figure 4.2: Cape Foulwind Limestone interbedded with Kaiata Mudstone, and algal debris in coarse sandy burrow fill.

The presence of algal material in the coarse sand-filled burrows beneath the Kaiata/Little Totara Sand disconformity (fig. 4.2b) implies that the algal limestone was either being eroded or there was still some algal growth occurring at this time. The fragments have been transported at least 1 km from the quarry and are all broken and rounded. On the SE side of the quarry, where the algal limestone grades up into glauconitic Kaiata Mudstone, the algal limestone had ceased to be deposited by late Runangan-basal Whaingaroan times (based on dating of the Kaiata Mudstone using Foraminifera).

The Waitakere Limestone is absent from the southern sides of the quarry, probably due to erosion in the Miocene before the deposition of Blue Bottom mudstones. This erosion is responsible for the paleokarst in the top of the Waitakere Limestone at Gibsons Beach, and may also be the cause of the paleokarsting in the limestone at the quarry, but the sinkholes are now filled with Quaternary black sands.

Texture and Composition:

The Cape Foulwind Limestone varies from 98.75% $CaCO_3$ (MacGregor 1983), to very sandy, muddy or glauconitic especially where it grades into overlying and underlying mud and sandstones. MacGregor (1983) studied the Cape Foulwind Limestone as part of his description of the Waitakere Limestone. He represented the variation in the entire Waitakere Limestone as a series of eight facies, two of which occurred only in the quarry at Cape Foulwind. From my own investigations, the Cape Foulwind Limestone can be divided into the following four lithofacies:

1. Massive, poorly sorted, sand to gravel rudstone, coralline algal biosparite. Contains rhodoliths, broken branch fragments, foraminifera, echinoid plates, crinoid stems, bryozoan fragments (frequently attached to coralline algae), and small quantities of brachiopod and mollusc fragments (fig. 4.3d). Quartz/feldspar quantities are negligible. This is the most common facies, representing the majority of the massive limestone. It is

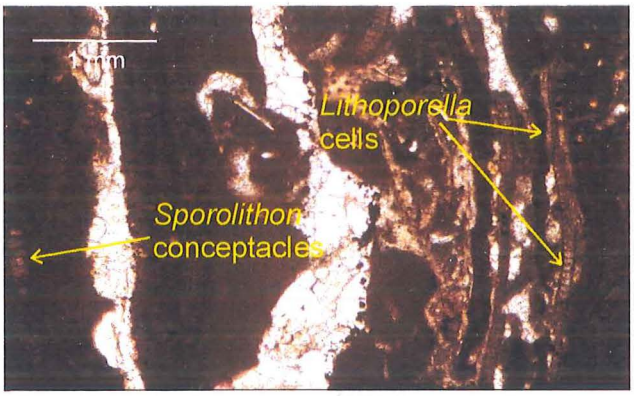

a: HLS 92. Cape Foulwind Limestone: layers within a rhodolith from facies 2, displaying *Lithoporella* layers and *Sporolithon* conceptacles. The bright bands are calcite veins. ppl.

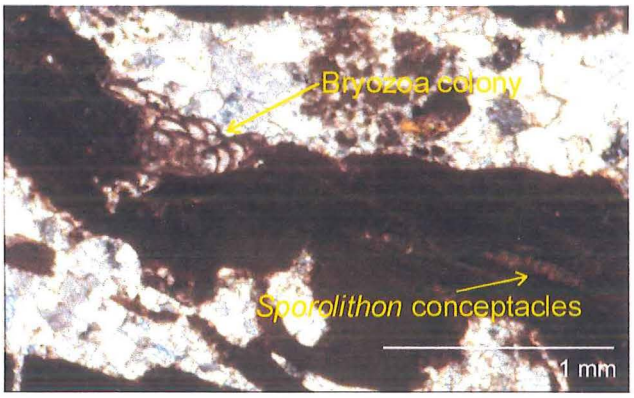

b: HLS 92. Cape Foulwind Limestone: a layer within a rhodolith from facies 2. *Sporolithon* conceptacles and a bryozoa colony in the rhodolith surface. cpl.

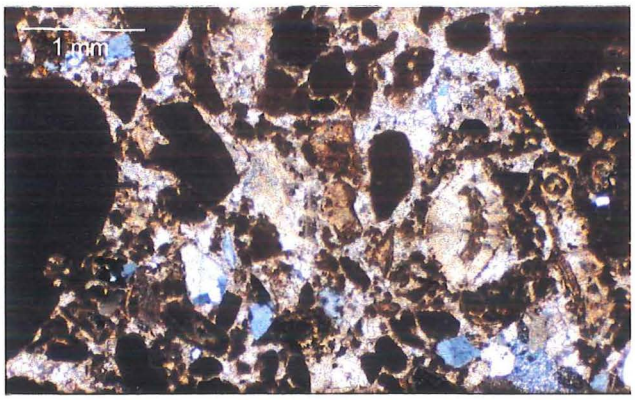

c: HLS 92. Cape Foulwind Limestone, facies 2. Matrix containing small to medium fragments of corralline algae, foraminifera, echinoderm fragments, other fossils, detrital quartz, feldspar, micas and rock fragments and mud (now calcite cement). Larger algal fragments are seen to left and right. cpl.

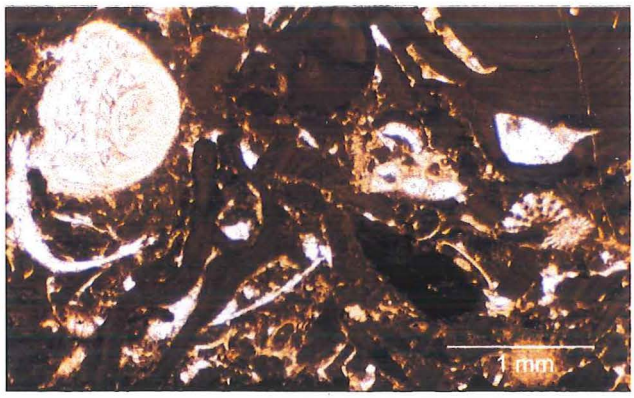

d: HLS 91. Cape Foulwind Limestone, facies 1. Matrix of limestone consisting of small to medium fragments of corralline algae, foraminifera, crinoid stems and other fossil fragments. No detritals and little mud in the matrix. ppl.

Figure 4.3: Photomicrographs of Cape Foulwind Limestone samples.

sometimes interbedded with thin beds of muddy or sandy limestone, but occurs frequently as massive, 25-30 cm beds. $CaCO_3$ content reaches 98% (MacGregor 1983). HLS 91 which is representative of this lithofacies contains 96.5% $CaCO_3$ (see Appendix IV), the remainder being authigenic opaque minerals, mainly oxidised iron. Pressure solution between algal grains is common in some parts, although much of the limestone has no grain solution present. MacGregor (1983) suggested bioturbation as a possible reason why parts of the limestones have lots of stylolites other parts do not. The amount of cement in this lithofacies varies from 13-33% (MacGregor 1983). This facies takes in MacGregor's Type 1 to Type 4 limestones, which are distinguished mainly by variations in the percentage of rhodoliths, algae, and other allochems. They are also distinguished by whether they are interbedded with sand layers, mud layers or impure limestones, and also the presence of burrows.

2. Very poorly sorted, sandy and silty, medium to very coarse floatstone coralline algal biosparite. Incomplete recrystallization of the matrix has left areas that show pelloidal micritic texture. The facies is dominated by algal fragments (50-60% including rhodoliths) up to 6 mm long, and also contains bryozoa, brachiopod, mollusc and echinoderm fragments (fig. 4.3c). Contains approximately 6% detrital grains, mainly rockfragments, that range in size from granule to silt. The limestone has 85-90% $CaCO_3$, detrital material and glauconite (filling voids in fossils and grains) make up remainder of rock. Rhodoliths up to 3 cm long are common; where they can be observed, nuclei consist mainly of fragments of algae. *Lithoporella* and *Sporolithon* have both been positively identified from this facies (figure 4.3a&b). The percentage of cement is 23.5% in HLS 92, mainly because of the replacement of matrix by spar. This facies marks the beginning of the transition into Kaiata Mudstone in the southern section of the quarry.

3. Poorly sorted, silty to coarse sandy floatstone, muddy coralline algal biomicrite to biosparite. Contains assorted foraminifera and other fossils, algal fragments are varied in size, some very large, all separated by a micaceous muddy, sometimes blue/grey matrix. The largest algal fragments are assumed to be in situ. The muddy matrix may be recrystallized to spar. This facies is probably equivalent to Macgregor's Type 6 limestones.
4. Poorly sorted, fine to medium sand packstone, sandy algal biosparite. Contains foraminifera, echinoderm fragments, bivalve shells and bryozoa. Weakly cemented, with a high percentage of detrital sand. This facies is transitional to underlying Little Totara Sands and calcareous sands correlated with the Brunner Coal Measures (containing no coal material at the quarry). This lithofacies also occurs as thin beds within the massive limestones. It is equivalent to MacGregor's Type 8 limestones.

Facies 1 only rarely contains glauconite. Facies 2 and facies 3 commonly contain glauconite. Facies 4 only contains glauconite were the facies interfingers with glauconitic algal limestone. Generally glauconite occurs as glauconitized fossils (usually foraminifera) or algal fragments. Glauconite tends to be associated more with the inter-bedded calcareous silts (Kaiata Mudstone) than with the purer algal sands. Facies 1 tends to occur as massive beds up to 30 cm thick, divided by layers of mud, silt and sand often no more than a few centimeters in thickness. In some places the deposition of limestone is interrupted for several meters (fig 4.4), where sandy or muddy limestone or sand and mud layers are deposited.

The occurrences of algal debris in the Kaiata Mudstone at Gibsons Beach and also at the Okari Lagoon area are inferred to be deposited by storm induced debris flows, where the higher energy of storm waves has destabilized the accumulated debris on the paleohigh, and also created more debris by breaking delicate branched algal growths. The bands of algal limestone at Gibsons

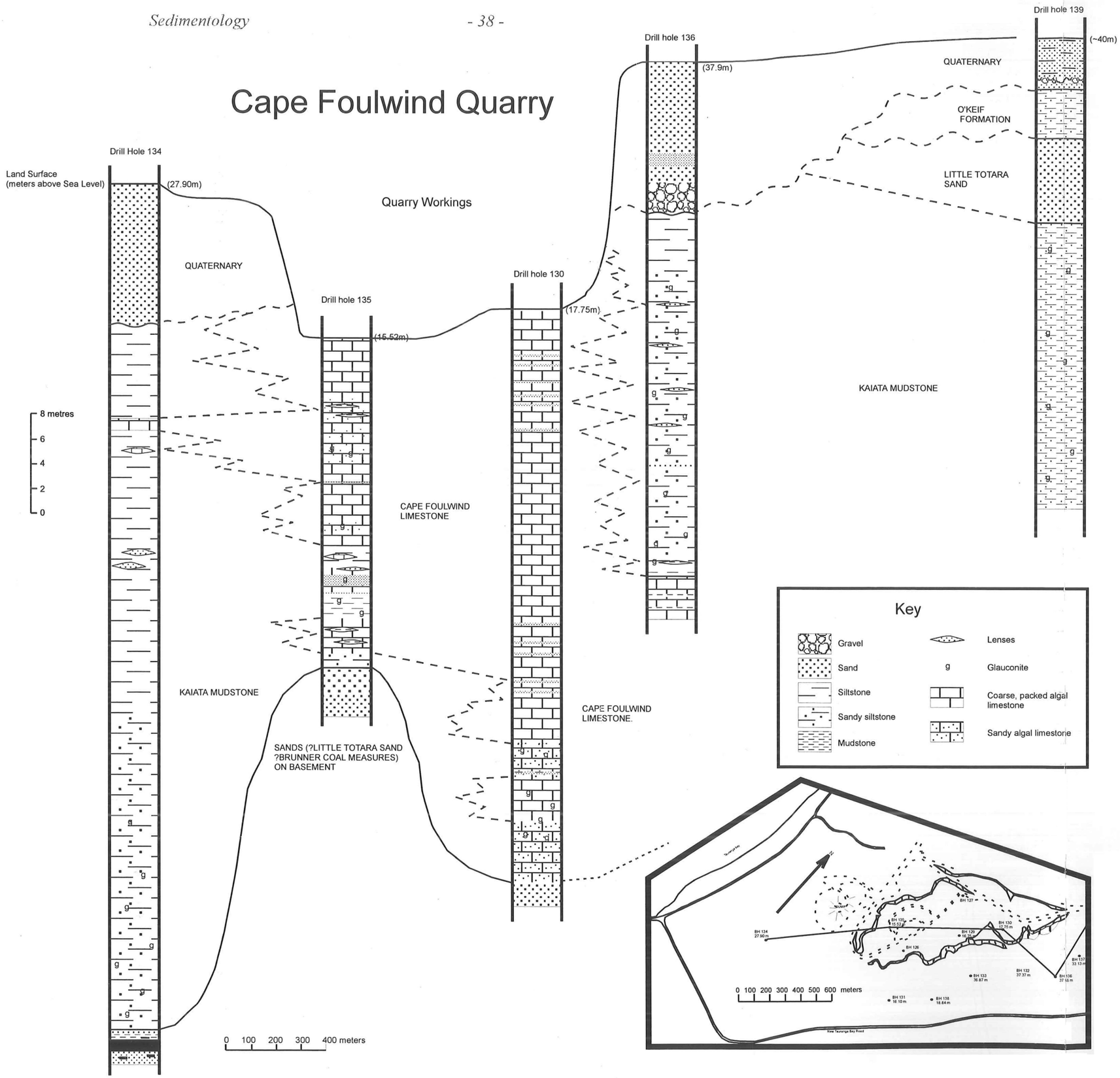

Figure4.4: Correlation of facies of limestone and mudstone from borehole data. The variation within the limestone is considerable, and the extent of the limestone is limited.

Beach have scoured bases, and often display graded bedding, with rhodoliths concentrated at the base (see MacGregor 1983). The algal debris at Okari Lagoon also have scoured channels, cross bedding (in some sand layers) and gravel associated with them. They occur some distance from the quarry, and probably represent a channel carrying algal material down from the basement high where the quarry now exists.

Island Sandstone

Composition:

Most Island Sandstone samples are subfeldsarenites (see fig. 4.5). The exceptions to this grouping are coarser, not bioturbated and contain an unusual chalcedony cement, which made distinguishing lithic grains and grains replaced by microcrystalline quartz difficult. Table 4.1 shows the composition of samples from cemented bands (cement ranges from 23.5% to 53.25%).

The rock fragments observed in the coarser grain fraction are mainly granitic fragments, and very few sedimentary fragments are observed in samples from the western side of the basin where total rock fragments average 3.2%. The major reason for the small amount of rock fragments is the fine grain size of the sand- and mudstones, which mean that the granitic fragments would be broken into individual crystals before being deposited. The largest number of rock fragments in a singel sample occurs in HLS 61, which is a coarse burrow fill in the upper most Kaiata Mudstone, containing 10.5% rock fragments. The large percentage of rock fragments is entirely due to the large grain size (maximum granule sized) of the sediment that allows the coarse grained granitic and metamorphic rock fragments to survive.

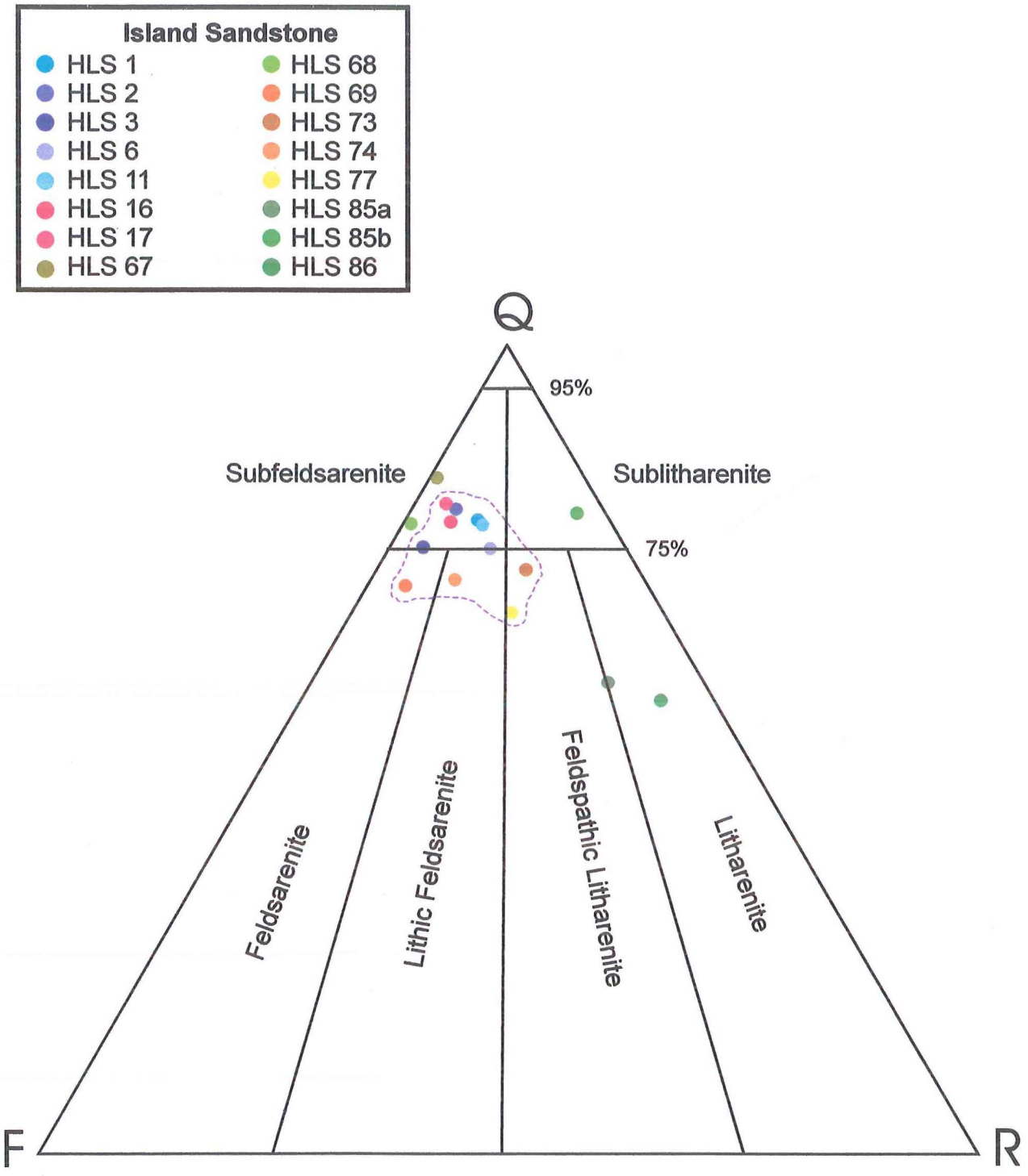

Figure 4.5: QRF Diagram for the Island Sandstone. Smithy's Beach samples are blue, samples from near the chlacedony cemented layer are green and the two samples from near the contact with the limestone in Woodpecker Bay are in red. All other samples from Punakaiki, Limestone Creek and Bullock Creek are in orange colours. Purple dashed line encloses majority of "normal" Island Sandstone.

Table 4.1: Composition of the Island Sandstone from point counting thin sections from cemented bands. Data is presented as percentages which are calculated by averaging point counting results (see Appendix IV).

HLS #	Quartz	Feld-spars	Mica	Rock frags	Detrital Opaque	Other Detrital	Matrix	Calcite Cement	Fe oxid Cement	Quartz Cement	Algal grains	Shells Fossils	Glauc onite
1	18.25	3.25	2.50	1.75	2.00	0.00	0.00	25.50	20.75	0.00	0.00	16.00	8.75
2	22.75	4.50	1.50	1.25	3.50	0.00	0.00	32.75	0.00	0.00	5.50	15.75	13.00
3	10.75	3.00	0.50	0.50	3.50	0.00	6.00	25.75	5.50	0.00	0.00	36.25	8.25
6	24.25	4.75	8.00	3.25	2.25	5.00	5.25	42.00	3.50	0.00	0.00	1.00	0.75
11	33.75	6.00	4.50	4.00	1.75	4.00	2.50	37.75	2.00	0.00	0.00	3.25	0.50
16	29.50	6.50	3.00	1.75	3.25	1.00	0.00	39.75	0.00	0.00	0.00	7.00	7.25
17	25.50	5.25	2.25	1.00	3.50	0.00	0.00	41.00	0.00	0.00	0.00	14.25	7.25
67	20.75	3.75	3.25	0.00	2.00	0.00	0.00	33.00	2.00	19.25	0.00	13.25	0.00
68	20.50	5.75	2.75	0.00	2.25	0.00	0.00	45.00	0.00	2.00	0.00	18.25	0.00
69	11.00	4.00	2.75	0.50	2.00	0.50	0.00	53.25	6.00	0.00	0.00	20.50	0.75
73	31.75	5.25	3.75	6.75	8.75	1.50	1.00	30.50	2.75	0.00	0.00	8.00	0.00
74	16.25	4.50	2.25	2.00	2.50	0.00	0.00	23.50	12.00	0.00	0.00	26.75	10.25
77	35.75	8.25	2.50	9.50	3.75	7.25	0.00	0.00	33.00	0.00	0.00	0.00	0.00
85a	15.25	2.50	2.50	8.00	0.50	2.25	0.00	41.00	0.75	0.00	6.25	21.00	0.00
85b	17.50	0.75	3.25	3.75	3.00	1.00	0.00	26.00	5.50	22.25	0.00	16.75	1.25
86	19.25	1.75	2.25	13.00	1.00	0.50	0.00	28.50	3.75	6.00	0.00	19.50	4.50
Avg:	22.05	4.36	2.97	3.56	2.84	1.44	0.92	32.83	6.09	3.09	0.73	14.84	3.91

On the eastern side of the basin, where the greatest thickness of Rapahoe Group was deposited (in the headwaters of the Punakaiki and Pororari rivers), sedimentary rock fragments and chert fragments are more common and total rock fragments represent 9.5% of the Island Sandstone sample from Punakaiki Gorge (HLS 77, Table 4.1). However, the opaque cement, high alteration, and occurrence of sericitised feldspar obscure grains sufficiently to make identification difficult. Rock fragments include chert, mudstone and siltstone. The contrast of unaltered grains with highly altered grains of feldspar may suggest that some recycling has occurred. The Fossil Creek Formation is a series of sediment gravity flows from a nearby continental margin (Laird 1988). Although the unit is completely fault bounded, it is likely that its present location on the far eastern margin of the Punaiki-Charleston Basin is not far from where it was deposited. The pebbles in the formation consist predominantly of quartz, but also include hornfels, gneiss, granite and limestone (Laird pers. comm. 1999). The quartz, hornfels and gneiss is derived from the Charleston Metamorphic Group, which forms the basement to the east of the Paparaoa Tectonic Zone in this area; the granite is likely to have come from one of the many isolated intrusions that occur throughout the metamorphic complex and the Greenland Group. The limestone presence is difficult to explain, because no limestones of this age were thought to exist in this area. However, it is unknown what sedimentary rocks existed on the basement east of the Paparoa Tectonic zone, it is entirely possible that some Paleocene or Eocene sediments and limestones were deposited in a small fault-bounded basin that were later reworked into the Rapahoe Group, or they represent basin margin deposits, formed in shallow embayments on a coastline, that are equivalent with the Rapahoe Group (see Chapter 8).

On the western side of the basin, the highest concentration of rock fragments occurs in coarse sand and granule-filled burrows in the uppermost part of the Kaiata Mudstone, directly underlying the black to orange carbonaceous and iron rich muddy very fine sands (probably deposited in a

lagoonal environment) which occur under the Little Totara Sand at Gibsons Beach (K29 834387) and the Cape Foulwind Quarry (K29 828365). Here the rock fragments reach up to 11% (see Appendix IV), and many of these are granite fragments. The sandstone also contains epidote, muscovite, minor biotite, strained quartz, serrated polycrystalline quartz, 2:25% microcline as well as other K-feldspar and minor plagioclase, fossils (including algal fragments) and rounded grains containing silt-sized particles, mud and fossils that are interpreted as fecal pellets. The presence of strained and polycrystalline quartz implies a metamorphic source, probably the Cape Foulwind gneissic granite (D. Shelley pers. comm. 1999). The unstrained quartz grains must have come from an un-metamorphosed granitic source, possibly some local deposits of undeformed granites, an as yet unknown granite west of the Cape Foulwind Fault, or a granite in the Paparoa Range.

The low proportion of rock fragments (in the same sand size as they occur on the eastern side) on the western side of the basin implies a difference in source between the two sides of the basin, which supports the inference that sediment was being supplied from both sides, and therefore that areas were being actively eroded on both the east and west sides of the basin as late as the Lower Whaingaroan (the age of the burrow fills at Gibsons Beach and beginning of Nile Group deposition inland). The basement on either side of the basin differed in composition, the eastern side having more sediments being eroded, as well as the granite and gneisses supplying the fresh feldspars and quartz to the basin. The western side of the basin may have all been like the metamorphosed granitic rocks exposed at Cape Foulwind, which are thought to be part of the ridge that marks the location of the Cape Foulwind Fault (Davey 1977). The dominance of opaque cement (iron oxides, probably haematite, see Chapter 7) in the eastern Island Sandstone may reflect a greater abundance of mafic minerals.

Textures:

The cemented layers in the Island Sandstone differ from the surrounding uncemented sediment only in the amount of calcite cement that they contain (fig. 4.6, Laird 1999 pers. comm.). The grain size analyses of Island Sandstone in Fig. 4.6 come from cemented and uncemented layers in a single outcrop. The curves are similar except at the finest end, where the curves for cemented samples have a lower angle. The difference implies that the cemented layers seem to contain a greater proportion of clay sized material, which is not the expected result.

The Island Sandstone is in general a poorly sorted, very fine skewed, leptokurtic silty sandstone (see Appendix V). The distribution of grain sizes tends to be bi or tri-modal (fig. 4.7), however the sand fraction is well sorted with a coarse tail. The poor sorting of the overall sample is due to the large proportion of 'matrix' present in the sandstone. The sandstone is still mainly grain supported, however a large amount of matrix can be inferred to have been present due to the occurrence of unsupported detrital grains in cement. The matrix has been mostly converted to calcite cement in the cemented bands. Bioturbation in most of the Island Sandstone has throughly mixed any segragation of grain sizes in bedding that may have existed.

The laminations in Island Sandstone sample HLS86a are distinguished in thin section by a difference in the proportion of calcite cement, which is partially replacing a matrix. The difference in cement content probably accounts for the grooved weathering pattern characteristic of laminated outcrops.

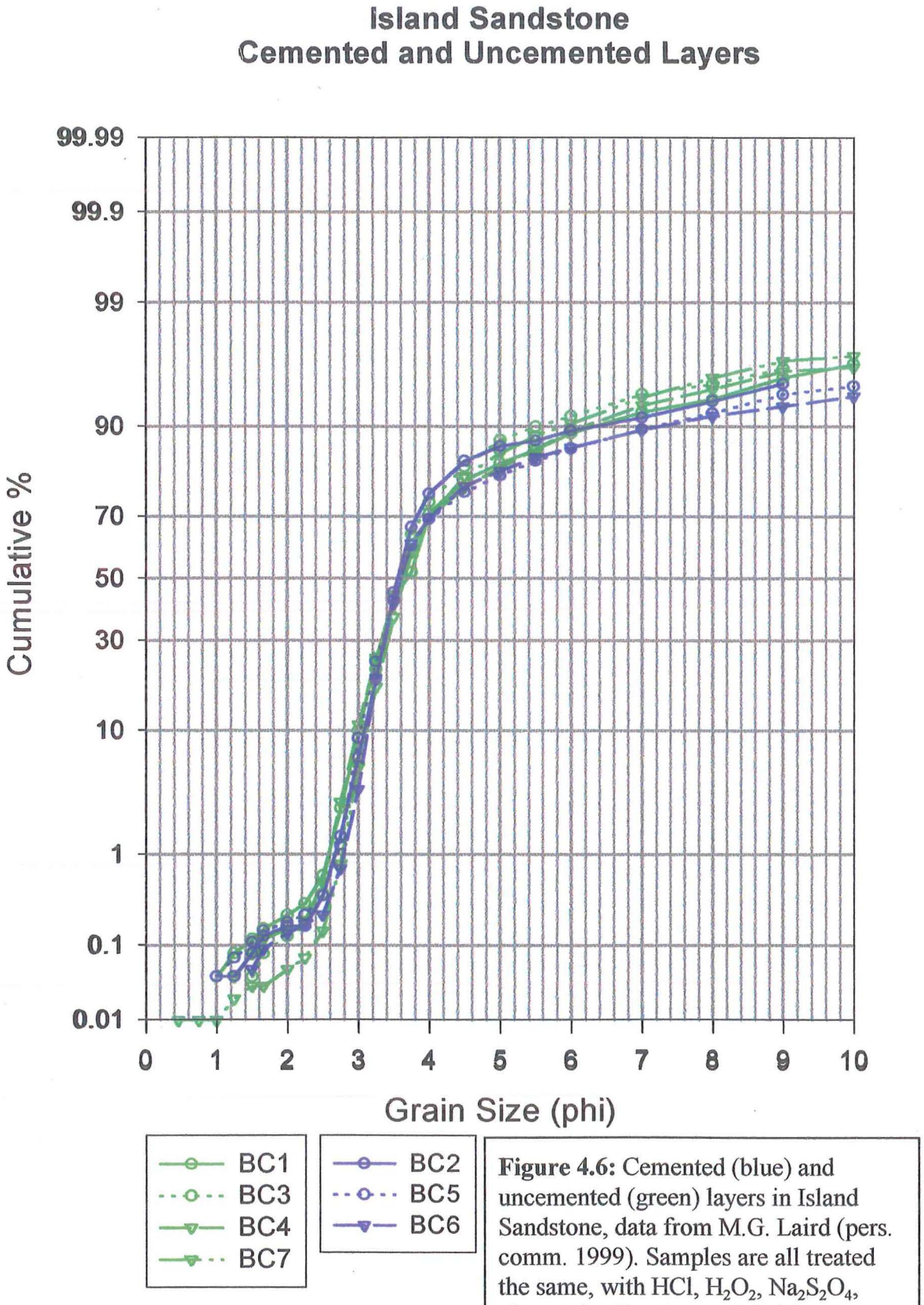

Figure 4.6: Cemented (blue) and uncemented (green) layers in Island Sandstone, data from M.G. Laird (pers. comm. 1999). Samples are all treated the same, with HCl, H_2O_2, $Na_2S_2O_4$, ultrasonic vibrating and shaking.

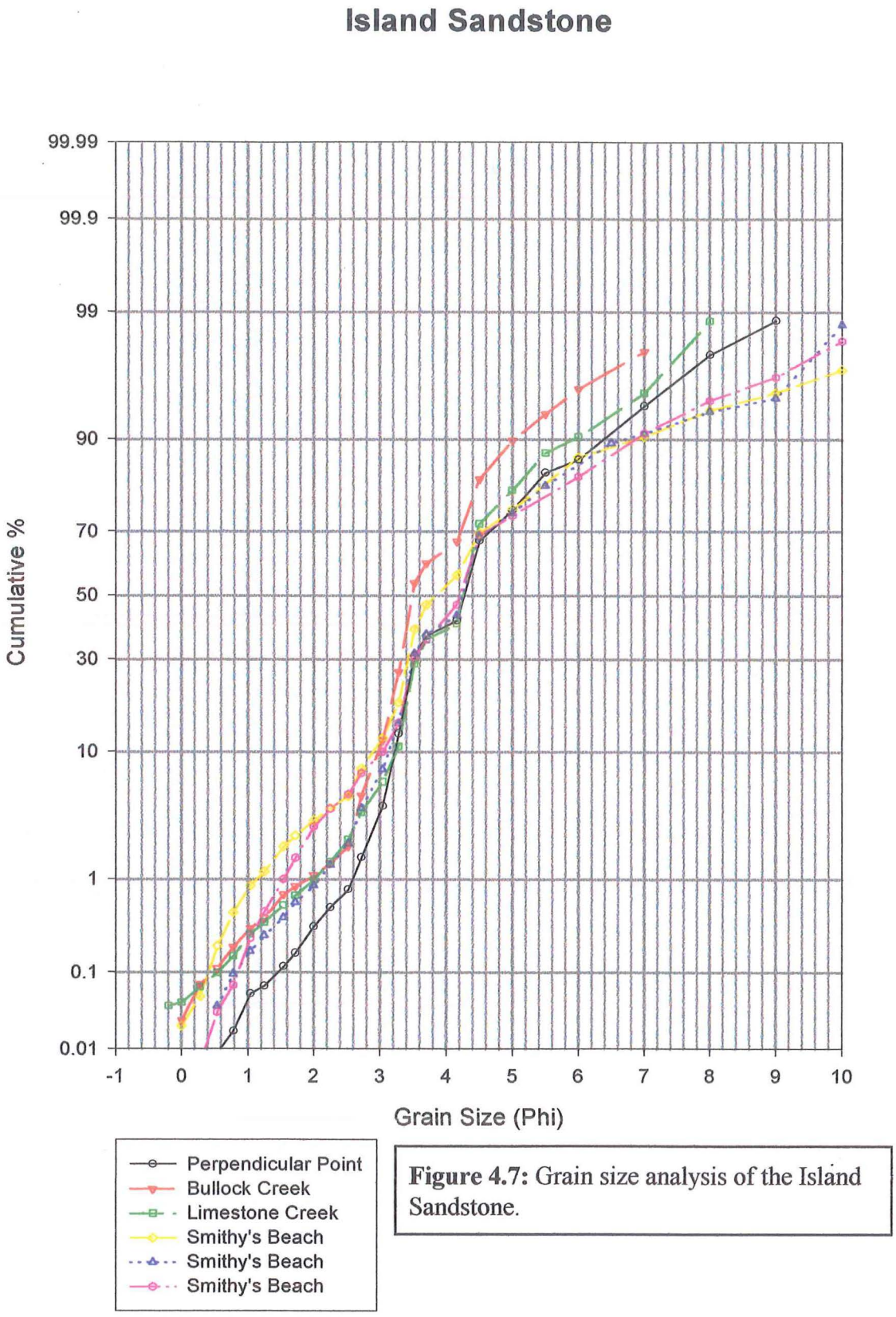

Figure 4.7: Grain size analysis of the Island Sandstone.

Structures:

The Island Sandstone is normally bioturbated. However, in several locations around Perpendicular Point, a section of the Island sandstone that is well laminated is exposed.

On the north side of Perpendicular Point, the base of the sandstone is not exposed, and it is unknown whether the large fallen blocks that occur between the area of the contact and the first cliffs of sandstone are in situ or not. These blocks are of bioturbated sandstone with rhythmic cemented bands, as are the cliffs above the beach. The sandstone in wave-washed cliffs closer to the Point is laminated, and contains scours, hummocky cross-stratification (fig. 4.8c), graded bedding, and cross-bedding. Some bioturbated horizons exist, where traces extend down into laminated sands, and the bioturbated section is truncated by the base of the next packet of laminated sands (fig. 4.8a&b). There are also crenulated laminations, probably caused by slumping shortly after deposition as the deformation is entirely plastic with no fractures or microfaults.

To the south of Perpendicular Point, laminated Island Sandstone also occurs in a small bay. Here the laminated section is thinner, and apparently (the contact does not outcrop) overlies bioturbated, rhythmically cemented sandstone. There is also a section of convoluted bedding in the laminated section; the convolutions are more extreme with tight isoclinal folds and weird shapes (fig. 4.8d). The laminations are caused by differences in the grain size, and especially the amount of cement present (probably caused by different amounts of matrix or carbonate material). The difference in cementation makes the laminations stand out in weathered outcrops. The top of the laminated section grades into bioturbated sandstone, with the laminations gradually becoming more and more disrupted. Above this gradation, a horizon occurs which contains pink irregular concretions. The whole layer and about 10 cm either side of it is cemented with chalcedony and quartz (see Chapter 7), which is infilling pores dissolved into an original calcite

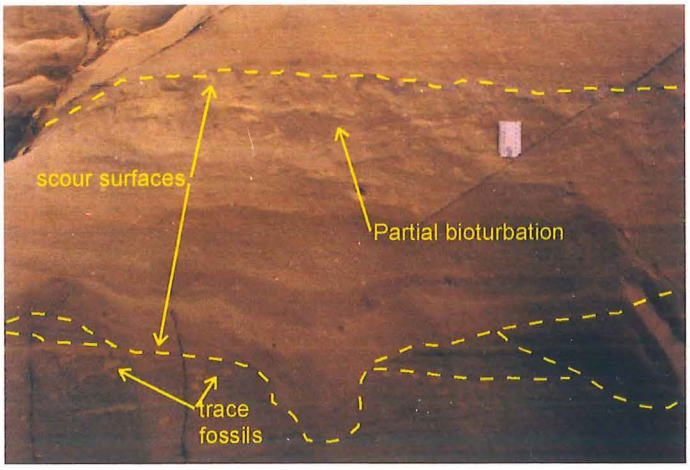

a: Laminated sandstone with two bioturbated layers cut off by more laminations, note the uneven bottom surface of the middle set of laminations and curved shape of laminations. Ruler is 10 cm long. F14P7

b: detail of partially bioturbated layer truncated by laminated sandstone. This is the upper erosion surface from (a). Ruler is 10 cm long. F14P8

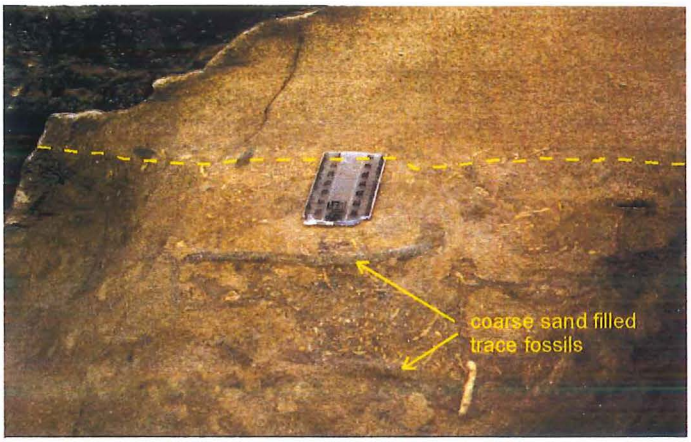

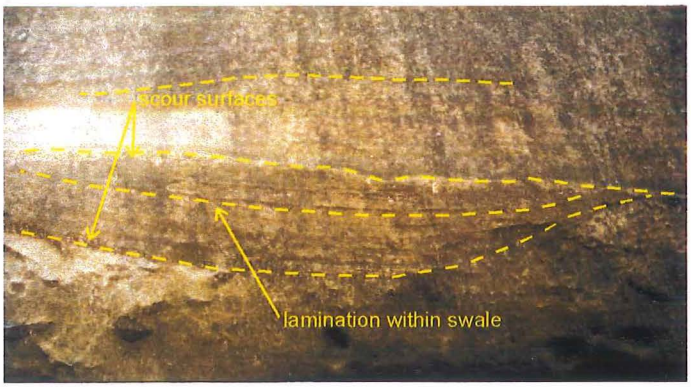

c: a swale in finely laminated sandstone, cut by an uneven erosion surface. F14P9

d: Convoluted bedding in a layer of Island Sandstone about 50 cm thick. F10P23

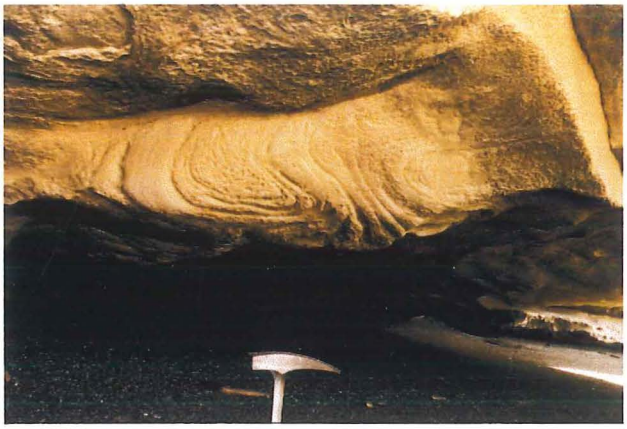

Figure 4.8: Photographs of laminated to bioturbated sandstone, in the basal part of the Island Sandstone on the north side of Perpendicular Point.

cement. The sandstone above this is bioturbated and rhythmically cemented.

Around Perpendicular Point, there are a number of occurrences of large oyster shells (up to 25 cm long). They occur on cemented bands that show a high number of network burrows, and also in sand that shows no obvious surface for them to colonise. Sometimes the clusters are obviously transported (they are no longer in growth position) but other occurrences of oyster clusters are so large that any transportation could only be a very short distance. Their presence and habit implies breaks in sedimentation long enough for the shells to reach their large size.

In the laminated section north of Perpendicular Point, especially where there are alternating laminated and bioturbated sections, but also where channels cross-cut each other, it is obvious that the sedimentation was episodic. The time between episodes of sedimentation varied, sometimes allowing significant thickness of bioturbated sediment to build up, but at other times either the interval was not long enough or the next event was of sufficient magnitude to wipe out all evidence of bio-activity.

Hummocky cross-stratification has long been associated with deposition by storm waves (e.g. Harms et al. 1975), and its presence in the laminated sands of the Island Sandstone supports deposition by episodic storm events. The preservation of the laminated sediments implies that the successive storm events were of sufficient magnitude to rework the sediment to a depth below the level to which the bioturbation extended. The change from laminated sediments to bioturbated sediments may suggest a decrease in the sedimentation rate, allowing trace makers to bioturbate the entire thickness of a storm deposit before the next occurs. The decrease in sedimentation could be caused by deepening or by a decrease in sediment supply, perhaps by tectonic influences or by the gradual submergence of local sources of sediment (Meybille Bay Granite). The change may also be the result of decreasing depth of penetration of storm events, either by climatic change or by deepening of depositional environment. The increasing mud content of the overlying sediment

suggests that a deepening occurred, which would both decrease sediment supply and reduce the effectiveness of the storm waves to rework the sediment. The change is gradational, but this is a gradual increase in the completeness of bioturbation, and may not represent a gradual change in conditions, the change in paleodepth may have been abrupt. As in the Smithy's Beach section, the rhythmically cemented, bioturbated part of this sequence displays flucuating mud content, which shows up as differences in colour, weathering style, and cementation. Unfortunately, the outcrop around Perpendicular Point is inaccessible for study, as it consists of a vertical cliff.

On the north side of Kaipakati Point (K30 746061), cemented bands change orientation part-way up the cliff, and merge up dip (fig. 4.9). As the cemented bands are *assumed* to be parallel to bedding (bioturbation obscures the real relationship) this feature may represent an unconformity of some kind. Similar angular relationships between cemented bands are not observed anywhere else, in the immediate vicinity or at the same point in the succession further along Smithy's Beach. The change may represent onlap of sediment onto a surface scoured by a slip, although the surface of the cemented band underneath the change shows no scour features. The foraminiferal assemblages on either side of the change are very similar, and neither can be dated accurately (HLS 82&83, see Appendix III).

Trace Fossils:

The Island Sandstone contains abundant trace fossils. The sandstone is in general well bioturbated, with few original structures preserved. Against this fabric of bioturbation several different types of trace can be seen. The Island Sandstone shows the *Cruziana* Ichnofacies. This ichnofacies contains the greatest diversity of traces, and indicates sublittoral-open shelf environments with moderate energy (Lewis and McConchie 1994, Chapter 8). In the uncemented layers of Island Sandstone, most traces are horizontal to inclined, however vertical, frequently nodular *Ophiomorpha* traces are common (fig. 4.10e).

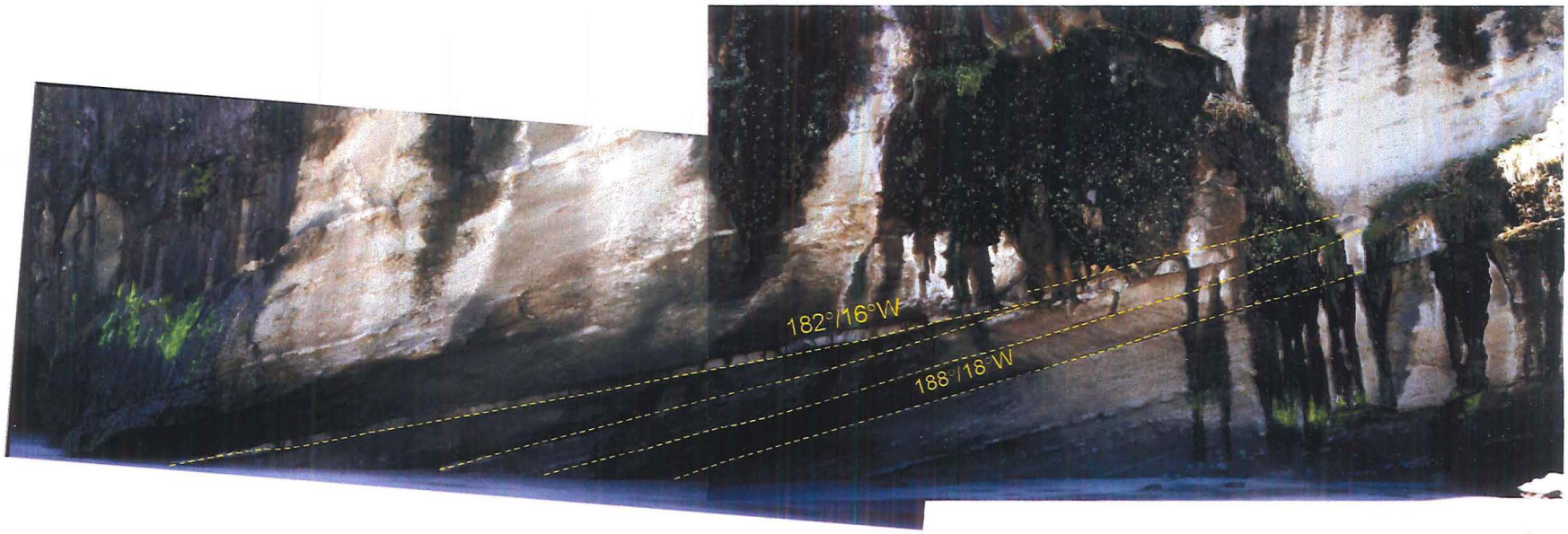

Figure 4.9: merging relationship of cemented layers at the north end of Smithy's Beach.

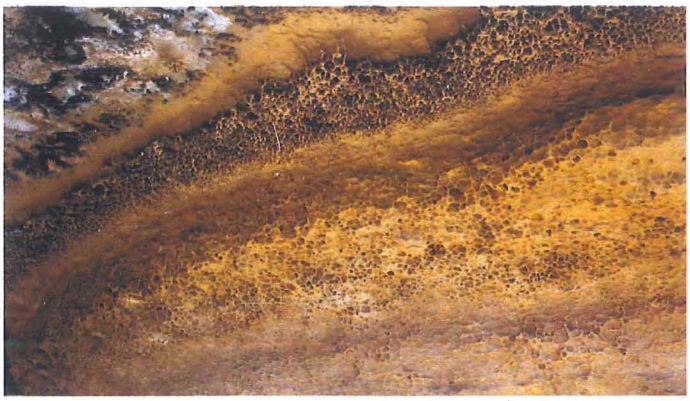

a: network traces weathering out on the underside of cemented bands. F3P30

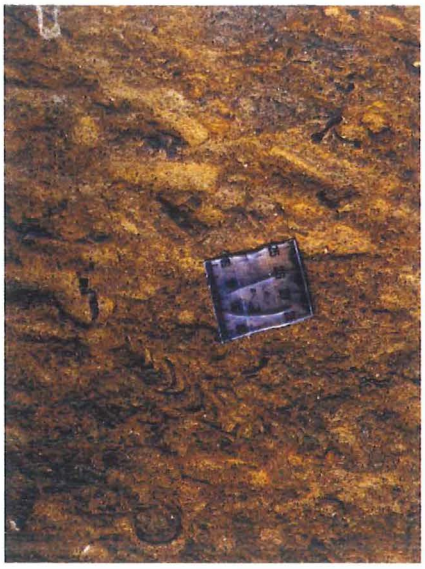

d: Bioturbated sandy Island Sandstone. F2P15

b: Bioturbated muddy Island Sandstone, around concretion layer (concretion to left of photograph). F3P10

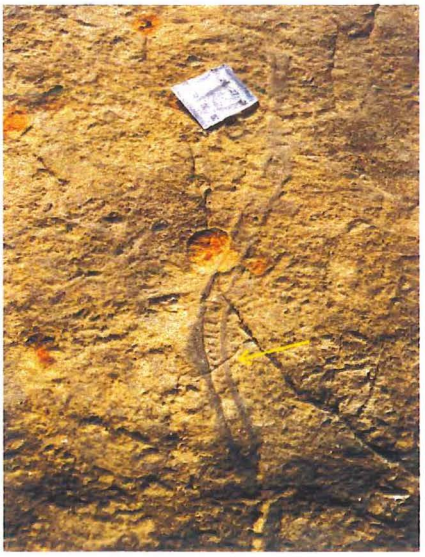

e: *Ophiomorpha* in sandy Island Sandstone, ruler is 4 cm long. F2P17

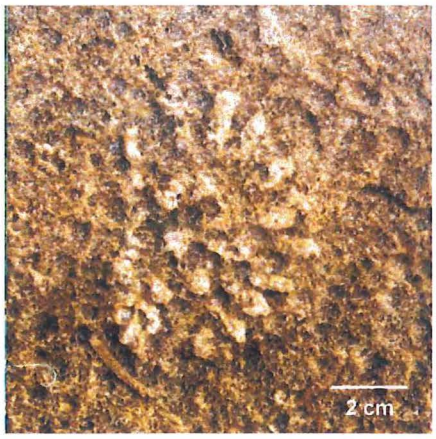

c: *Dactyloidites* on underside of cemented layer. F7P9

Figure 10: Trace fossils in the Island Sandstone

The horizontal and inclined traces include what may be rare *Zoophycus* (Lewis pers. comm. 1999), numerous narrow mud-rich traces, and *Scolicia* (echinoid burrowing traces) (fig 4.10b&d). The fossil spatangoids responsible for *Scolicia* are common, crushed but whole in the outcrops, although extracting them is very difficult. Y-branching *Thallassinoides* burrows are often present on the surfaces of cemented bands, and other network burrows are exposed in cemented bands because the preferentially cemented burrows are more resistant to weathering (fig. 4.10a). In one location the feeding trace *Dactyloidites* is exposed on the underside of a resistant quartz and calcite cemented unit along with cross-cutting, back-filled traces (fig 4.10c). *Dactyloidites otttoi* (Genitz 1849), which the traces closely resemble, is associated with moderate to high energy environments and warm water conditions (De Gilbert *et al.* 1995).

Traces that closely resemble crosscutting channels and trough cross bedding are present in the lower part of the Island Sandstone at Smithy's Beach (K30 746057). These traces can occur isolated within completely bioturbated sandstone, and are cut themselves by smaller, deeper tier traces. They most closely resemble the trace fossil *Teichichnus* (Lewis pers.comm. 1999), however the traces reach up to approximately 1 m in width, and have other characteristics that have not been previously described for *Teichichnus*. The traces are defined by lighter and darker laminations, possibly concentrated organic matter (fig. 4.11).

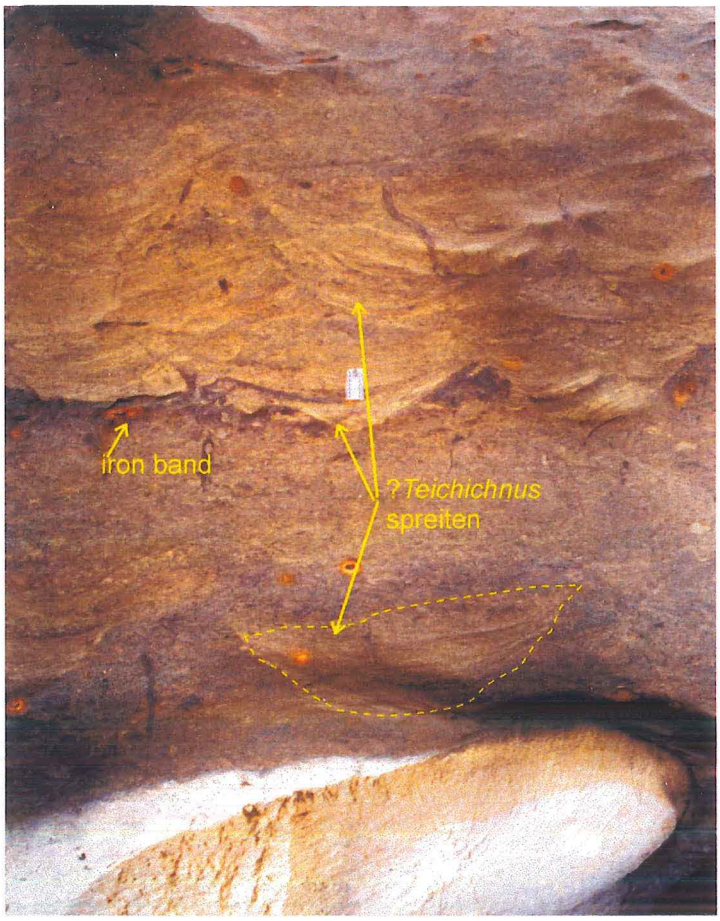

a: ?*Teichichnus* spreiten in bioturbated muddy sandstone, Smithy's Beach, ruler is 10 cm long. F15P11.

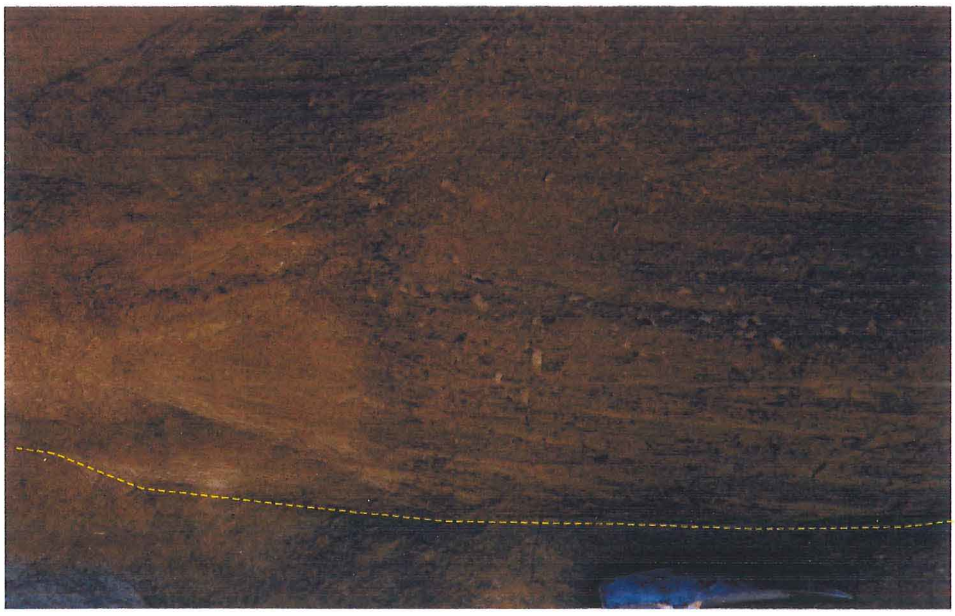

b: Cross cutting ?*Teichichnus* spreiten in bioturbated muddy Island Sandstone, Smithy's Beach. F2P20.

Figure 4.11: Photographs of ?*Teichichnus* ichnogenus in Island Sandstone at Smithy's Beach. The traces are unusually large for this genus.

Kaiata Mudstone

The Kaiata Mudstone has for a long time been used by workers on the West Coast as a name for all brownish to grey muddy sediments of Eocene age. The Kaiata Mudstone does not consist of a single body of sediment, but rather is divided into several bodies in several basins with different depocenters. The deposition of Kaiata Mudstone type sediment is related to the supply of sediment, the sediment type and environment of deposition. The Kaiata Mudstone occurs both in the Greymouth area, and around Westport, but is not thought to be connected between these locations (Nathan *et al.* 1986, Nathan 1975b).

Composition:

Analysis of clay (extracted during pipetted analysis) from two Kaiata Mudstone outcrops (HLS78 Punakaiki River Gorge and HLS34 Four Mile River) showed a mixture of kaolinite, illite and vermiculite (fig. 4.12). Vermiculite can be a swelling clay, and may account for many of the slimy characteristics of Kaiata Mudstone outcrops. The assemblage may be diagenetic in origin, as kaolinite and illite are formed in different chemical conditions. Marine pore water chemistry tends to produce illite/smectite mixed-layer clays and pyrite, whereas acid leaching (possibly derived form coal measures) produces kaolinite (e.g. Burley and MacQuaker 1992). Vermiculite is commonly produced by alteration of biotite (Chamley 1989), smectite is commonly altered by deeper diagenesis to illite and chlorite, and chlorite can be altered by weathering to vermiculite (Burley and MacQuaker 1992). Chamley (1989) noted occurrences of kaolinite forming at the same time as the illite-smectite transition, which also tends to produce chlorite. The vermiculite found in the samples may be the result of modern temperate weathering of the Kaiata Mudstone.

The blue-grey colour of the Kaiata Mudstones is probably caused by organic substances (Pantin 1969). Nathan and Smale (1983) found the organic carbon content of the Kaiata Mudstone

Geochemistry Laboratory, Department of Geological Sciences, University of Canterbury, New Zealand

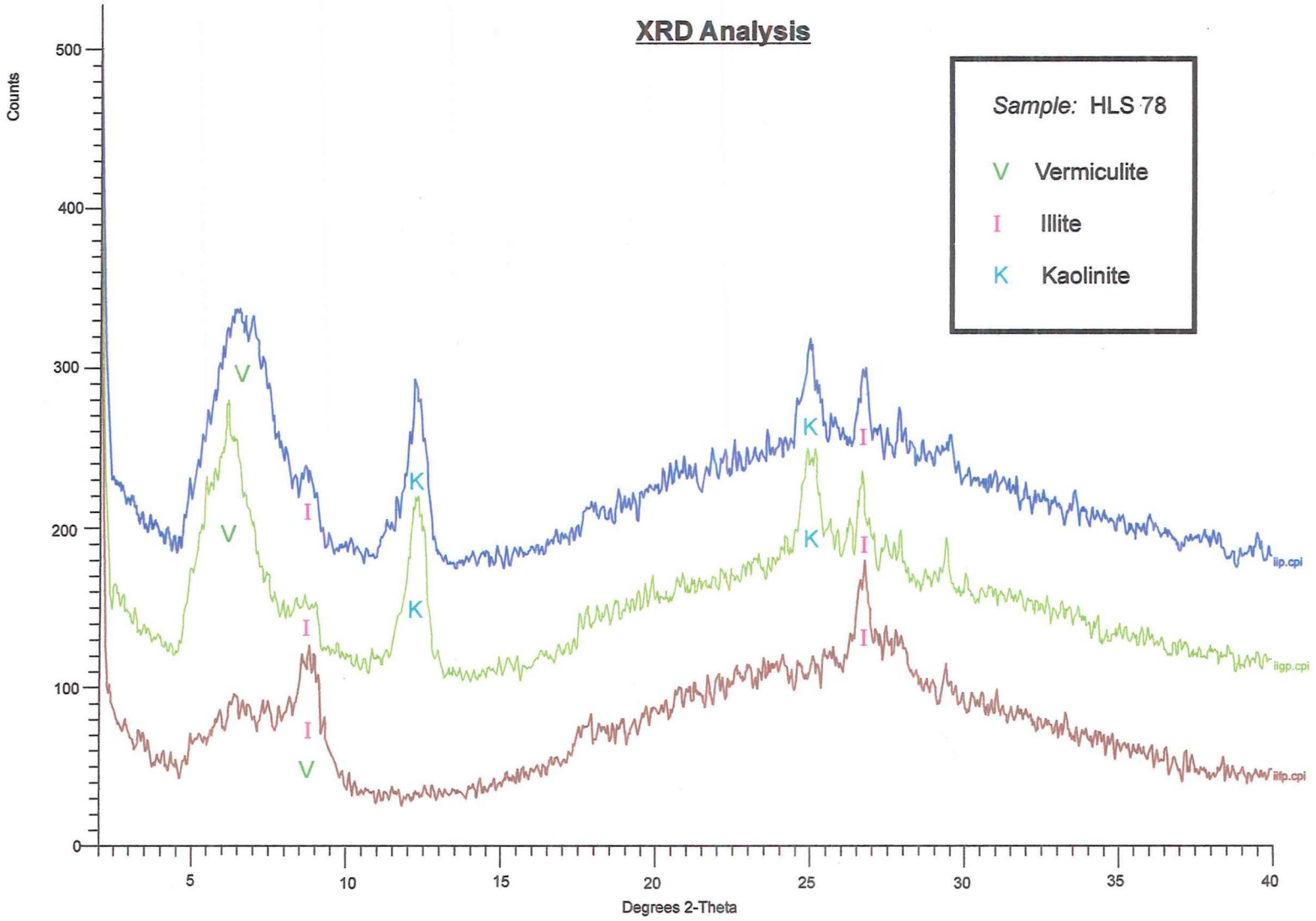

Figure 4.12: XRD analysis of Kaiata Mudstone sample HLS 78 from the Punakaiki River Gorge. Another sample, HLS 34 ur Mile River, gave the same results at a lesser concentration.

averages about 1%. Iron compounds may be inferred to be present based on the growth of pryrite and the iron staining observed in thin section. The pyrite occurs as cubic and anhedral grains in the sediment, microfossil replacement and concretion of burrow fills.

The detrital composition of the Kaiata Mudstone varies from place to place, mainly in the amount and types of micas that occur in the silt fraction. Many of the mica flakes appear to be brown to black when observed in reflected light, although micas seen in thin section rarely display pleochroism. These grains may be biotite (or muscovite) flakes that have been altered after deposition.

The Kaiata Mudstone has a similar detrital composition to the Island Sandstone. The major difference is the lack of significant rock fragments, which is caused by the fine grain size of the siltstones (fig. 4.13).

Texture:

The Kaiata Mudstone is in general a poorly sorted, fine skewed, leptokurtic sandy muddy siltstone. The amount of sand and clay depends on both the area and the position of the sample within the stratigraphic sequence. The sand content of the Kaiata Mudstone generally increases towards the top and bottom of the sequence. The sand content of samples collected ranges from about 8% near the middle of the sequence, to 58% near the top of the sequence. The clay content varies from 2.46% to 34.23%, while the silt content does not vary as much and averages 60.13%. The distribution of grain sizes tends to be bi-modal, with a mode (sometimes two) in the sand fraction and a mode in the coarse silt fraction (fig 4.14). The Kaiata Mudstone grain size analyses have a similar shape to the Island Sandstone curves, and overlap with sandstone curves (fig. 4.15).

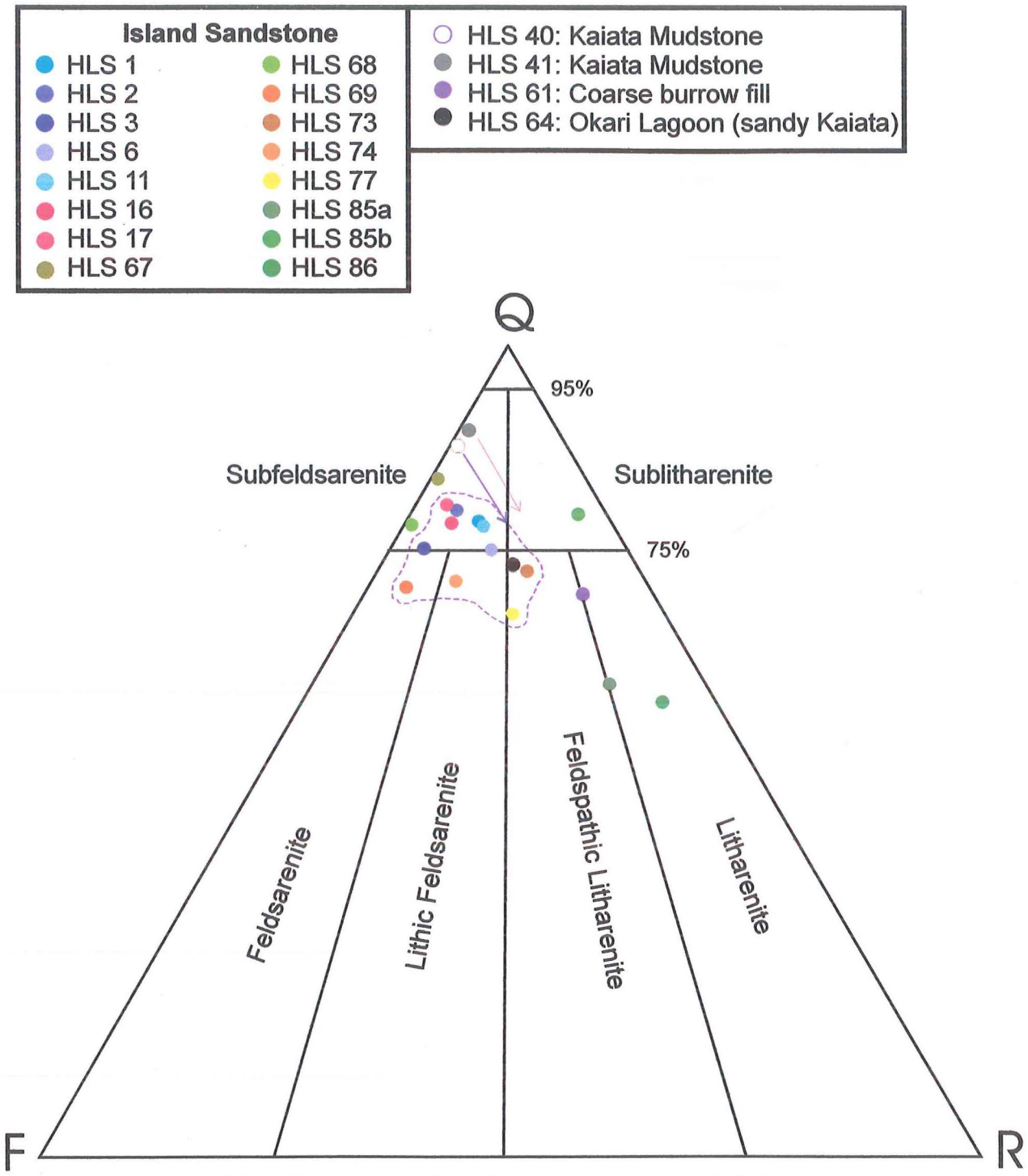

Figure 4.13: QRF Diagram for the Island Sandstone and Kaiata Mudstone. Smithy's Beach samples are blue, samples from near the chlacedony cemented layer are green and the two samples from near the contact with the limestone in Woodpecker Bay are in red. All other samples from Punakaiki, Limestone Creek and Bullock Creek are in orange colours. Dashed line encloses majority of "normal" Island Sandstone. The sandy Kaiata sample form Okari Lagoon plots within normal Island Sandstone composition. HLS 61 plots as a Litharenite due to its coarse grain size and therefore abundant rock fragments. The two Kaiata Mudstone samples from Gibsons Beach plot to the extreme left because of their small grain size and therefore fewer rock fragments. Adding rockfragments in the same proportions as occur in the Island Sandstone makes the composition shift down the arrows.

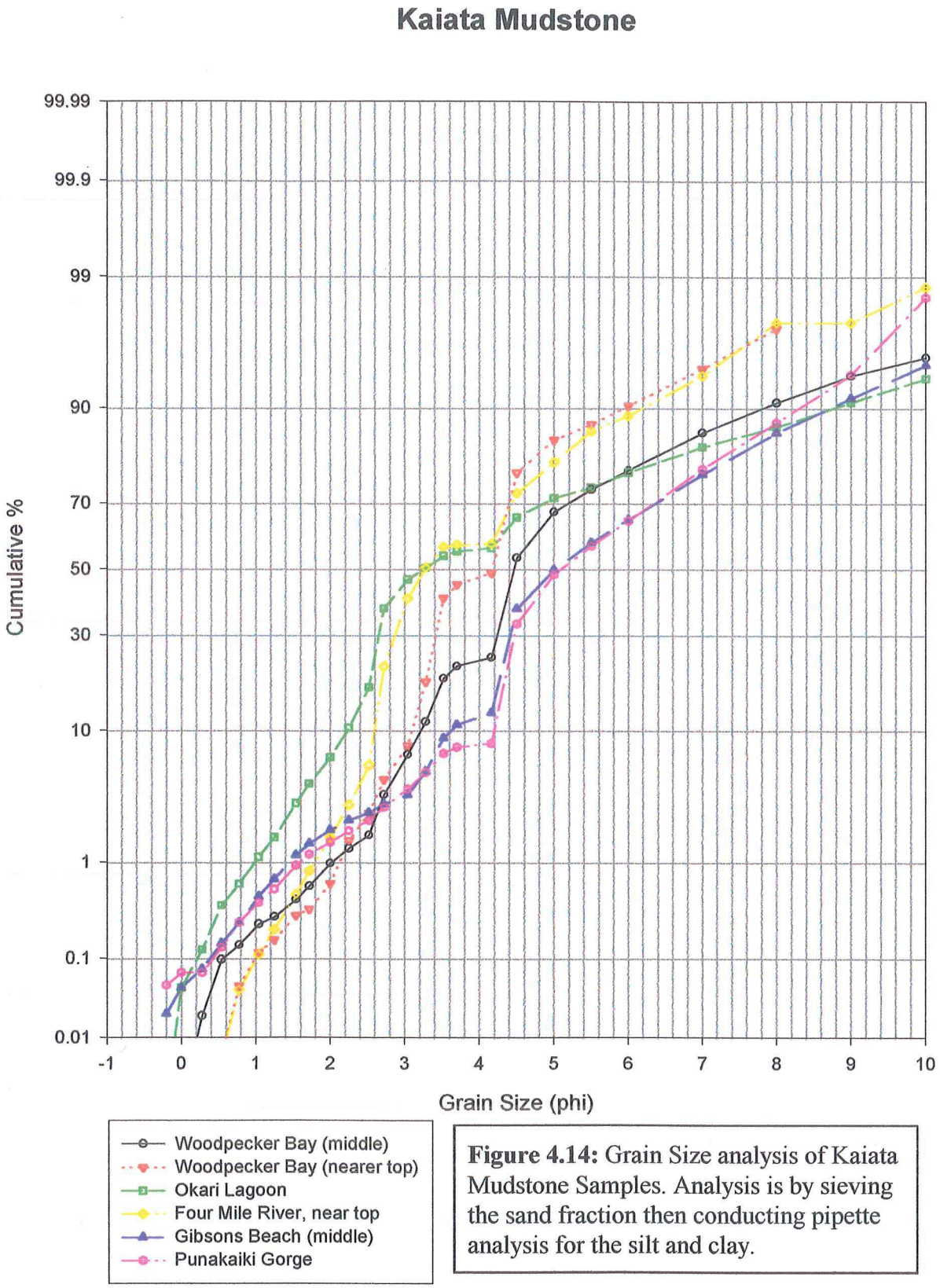

Figure 4.14: Grain Size analysis of Kaiata Mudstone Samples. Analysis is by sieving the sand fraction then conducting pipette analysis for the silt and clay.

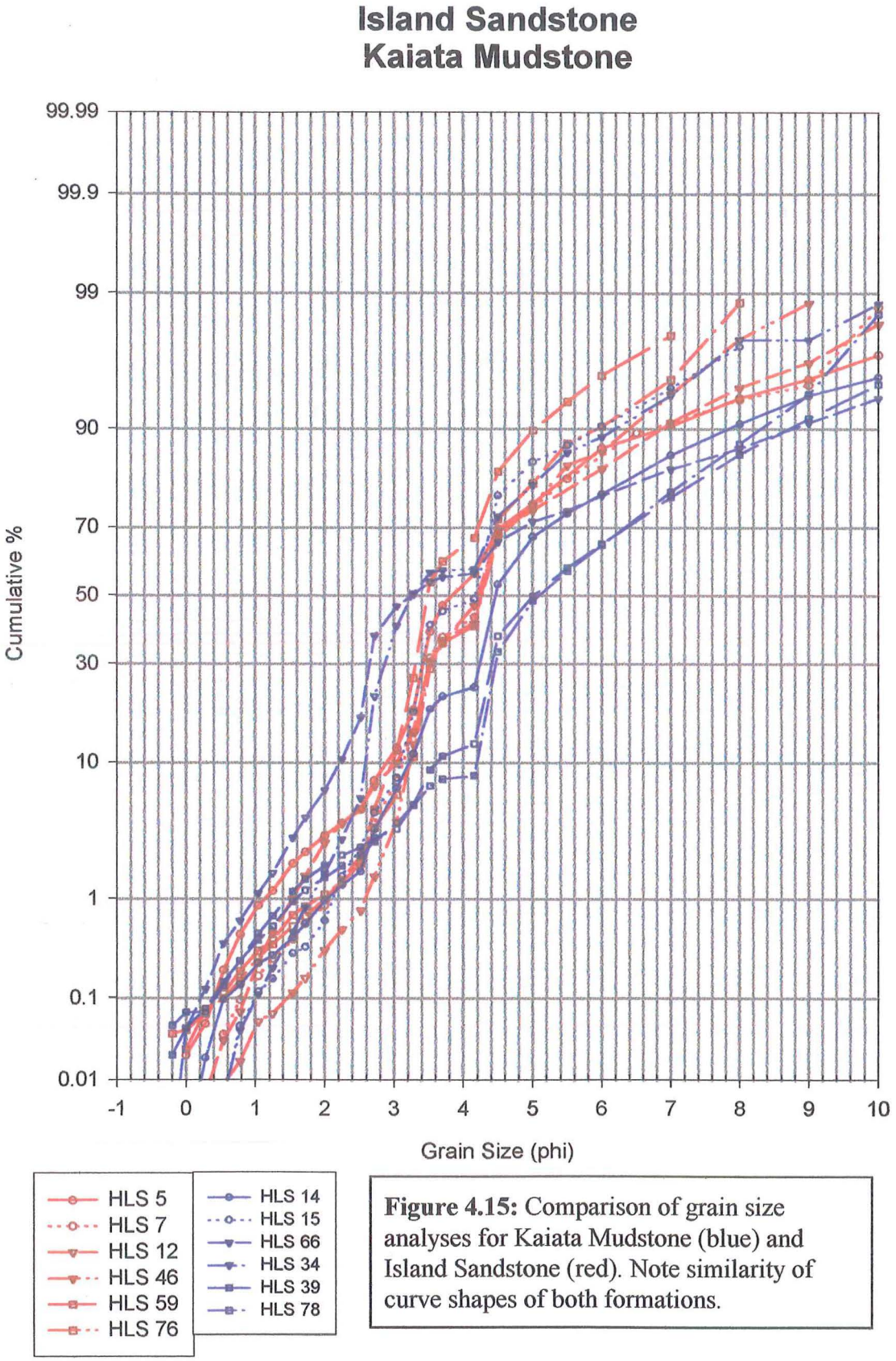

Figure 4.15: Comparison of grain size analyses for Kaiata Mudstone (blue) and Island Sandstone (red). Note similarity of curve shapes of both formations.

When Kaiata samples were disaggregated (using Calgon) and sieved for size analysis, it was found that the mudstone contained a large percentage of pellets, that were resistant to disaggregation. The proportion of pellets reached up to 25% of the total sample. Pellets are not included in the size analyses, as the weight of the sample was corrected after their presence was detected.

The cemented layers that occur in the top part of the Kaiata Mudstone are no different from the surrounding less-cemented mudstone in grain size, sorting or fossils content, just as in the Island Sandstone. Trace fossils can be observed to pass through the boundary between cemented layer and mudstone with no discontinuity, hence the cementation must have occurred after traces were created. In some places the cemented layers have gradational lower and upper contacts, that is the percentage of calcite cement decreases gradually, rather than being concentrated in a layer of set width. The layers also vary in width along strike, and frequently become strings of concretions rather than a continuous layer. The variation supports the theory that some of the rhythmic layering is caused by lateral merging of concretions. There is no observed difference between the concreted layers and the sediment between them in terms of fossils content, to give a reason why cementation is restricted. The rhythmic nature of the layering may be caused by initiation of cementation below the sea-floor (see Chapter 7).

Structures:

No bedding structures are preserved in the Kaiata Mudstone, with the exception of three claystone layers in the mudstone at Gibsons Beach. Everywhere else the Kaiata Mudstone is bioturbated.

The three claystone layers mentioned previously occur in the middle of the section, in the part with the finest overall grainsize (fig. 4.16). The mudstone here is massive and weathers in a flaking pattern, with no cemented bands. Two claystone layers occur close together (75 cm apart),

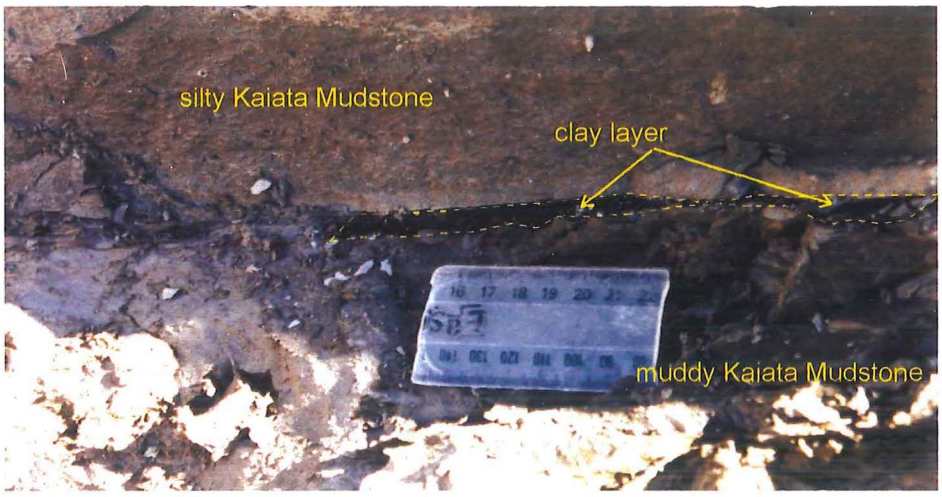

a: Thin clay layer (dark colour on excavated surface) in Kaiata Mudstone at Gibsons Beach. The muddy Kaiata under the clay layer is very rich in microfossils. F11P10.

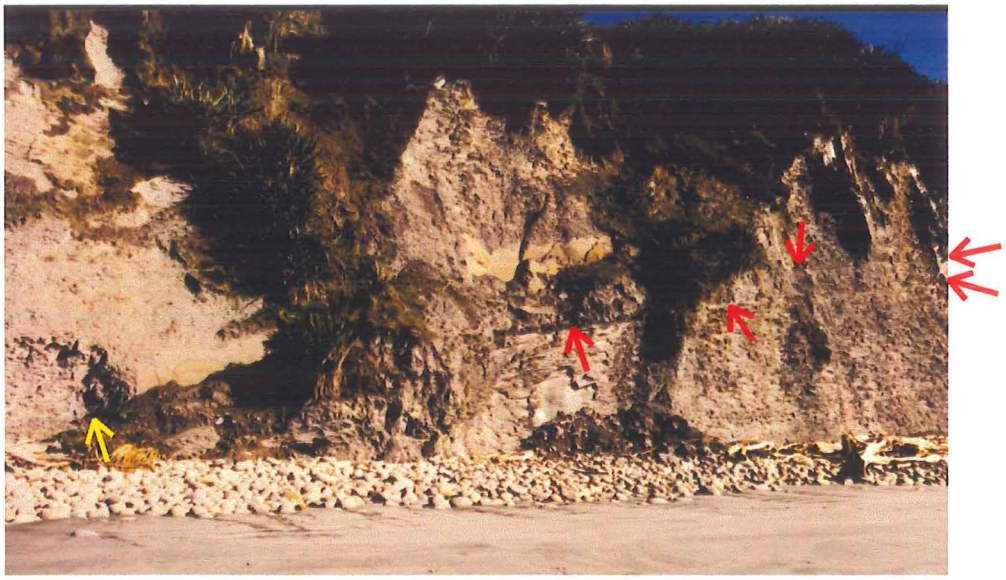

b: Two clay layers (red arrows) in Kaiata Mudstone at Gibsons Beach. The location of **a** is marked by a yellow arrow on the left side, it corresponds to the upper of the two that can be seen on the right. F11P13.

Figure 4.16: Clay layers in the Kaiata Mudstone at Gibsons Beach.

and the other occurs above, close to the lowest cemented band. The claystone layers consist of bands approximately 5 mm thick of almost pure clay. There is a change in grain size over the middle claystone layer, which also has mudstone containing almost 45% mostly benthic foraminifera (HLS88u see Appendix III), which probably represents a condensed section. The overlying sediment is 74% silt and 22% clay, the mudstone under the claystone layer is 65% silt and 34% clay. The claystone layer itself is flat and even and no scoured surfaces either below or above the layers are seen. These layers are inferred to represent periods of almost no detrital deposition, the middle one at least preceded by slowing of deposition. Gomez and Fernandez (1994) described three different types of condensed section:

1. Stratigraphic, caused by decreasing sediment supply. This may be caused by climatic changes, reducing erosion and transport (e.g. the changes in appearence and preservation of sequences observed by Ruffell and Rawson 1994), or by slowing uplift of the eroding source areas. A eustatic or tectonic driven sea-level rise can also decrease sediment supply, by effectively creating greater accommodation space closer to shore, and pushing the shoreline further inland so that sediment does not reach the more basinward locations. The maximum of a transgression often produces condensed sections in the rock record (e.g. Winn et al. 1998).
2. Sedimentary, caused by a decrease in the accumulation rate. The decrease in accumulation can be related to decreasing subsidence or accommodation space, or increasing depth.
3. Taphonomic, caused by the mixing of fossil assemblages by recycling of fossils from underlying beds.

The claystone layers are inferred to be a case of stratigraphic condensation, where the sedimentation rate has decreased. The lack of bioturbation of the claystone layers is unusual, surface and infaunal trace makers should have mixed the clay as it was being deposited, yet there

is no evidence for any biogenic activity in the claystone layer. This may imply some change in conditions that temporarily removed trace makers from this environment, allowing the clay to be buried relatively undisturbed. The lack of bioturbation supports the inference of an event origin for the claystone layers. Stratigraphic condensed sections are fundamentally controlled by sediment supply. The sediment supply to a basin can also be controlled by climate (Ruffell and Rawson 1994), the position and strength of currents entering the basin, as well as changes in relative sea-level. Stratigraphic and sedimentary condensations are not diagnostic of deep ocean conditions. The grain size is smallest around these claystone layers, and increases towards the top (sand and granule filled burrows) and bottom (to sandy siltstone, HLS39 see Appendix V) of the succession. The gradual decrease in grain size towards the middle of the succession implies a gradual process of decreasing sediment supply, and decreasing energy, rather that decreasing accommodation space which would probably lead to coarsening towards the claystone layers.

The fining of sediment towards the middle of the succesStion could be caused by a decreasing sediment supply due to lessening erosion, but there is no evidence for tectonic activity around and after the clay layers (debris flows from the quarry, or in the quarry) to account for the increase of sediment supply needed to cause the regression towards the top of the section. The most likely explanation for the sequence is a rise in relative sea-level to a maximum at the first clay layer. After the first clay layer a condensed section is topped by another clay layer. After this sedimentation is more rapid, until the third clay layer, which represents another transgressive maximum. Then the sediment gradually becomes more silty, eventually becoming sandy in the part now eroded between the Kaiata Mudstone and the Little Totara Sand. The sands that underlie the Kaiata Mudstone are non-marine to marginal marine. The section at Gibsons Beach is inferred to represents a transgressive sequence of fining upwards and deepening siltstones to mudstones, with a fluctuating maximum transgression represented by the three claystone layers, followed by

a regressive sequence of coarsening upward silts to shoreline sands.

At Woodpecker Bay, the Kaiata Mudstone grades upwards and laterally into the Island Sandstone. The two units are very similar in composition, and are distinguished primarily on the basis of sand content (see section on Island Sandstone). They also tend to have different colours in weathered outcrops, the Island Sandstone appearing orange-brown, wheras the muddier Kaiata appears blue-grey. The Island Sandstone has a significant amount of ferric oxide or hydroxide as cement (3-30%) which may be caused by oxygen rich depositional conditions or by later oxdation, while the Kaiata Mudstone tends to contain pyrite crystals, probably representing anoxic conditions just below the sediment-water interface.

In the lower part of the Kaiata Mudstone there are several well cemented horizons, with uneven surfaces, that have blocks or groups of large *Ostrea* shells deposited around them. The *Ostrea* fossils occur sparsley not in life position, and also occasionally in clusters approximately in life position: the size of the clusters means that the oysters were probably not transported far from their growth positions.

The oysters, probably *Crassostrea* sp., usually prefer rocky substrates (Beu *et al.* 1990), but in the Island Sandstone and Kaiata Mudstone they occur in several locations on apparently sandy or muddy substrates, and are generally longer than 15 cm, the reach up to 25 cm long. Their large size and thickness of their shells may be a response to surviving on a shifting substrate of sand and mud. Trace fossils are extremely numerous and diverse in the layers, and include abundant networks beneath the layer surface which are weathering out and exposed due to a difference in cementation. The traces are seen more in these layers due to the differences in cementation, but similar network burrows are not generally associated with other cemented layers, indicating these layers may represent firmgrounds. The burrows tend to be larger than the thin, purple traces seen elsewhere in the section and often have oxidised rims. These horizons are sandier and more

cemented than those that occur towards the middle of the sequence. Little Totara Sand also infingers with the lower part of the Kaiata Mudstone in the area (Laird 1999 pers. comm.).

In the middle of the sequence at Woodpecker Bay, the Kaiata is muddier, has less distinct cemented layers, and the trace fossils tend to be smaller. The possible fimgrounds, abundant cemented network traces and large oyster clusters that occur lower in the section are not apparent in the central part of the section. The upper part of the section gets progressively sandier eventually grading into the Island Sandstone approximately 15 m below the rhodolith layers. The Woodpecker Bay sequence is also inferred to be a transgression-regression sequence. The rhodolith layer at the top of the sequence also displays shallowing textures and a eroded upper surface (see Chapter 5).

Trace Fossils:

The Kaiata Mudstone is bioturbated, and individual trace fossils are rarely observed, especially in the muddier sections. The trace fossils that are preserved in the mudstone vary from very thin (5 mm wide) sinuous burrows that are orientated both horizontally and vertically, to large (up to 3 cm wide) burrows that frequently have pale oxidised rims (fig. 4.17). Echinoid plates and occasional spatangoid echinoid fossils in the mudstone suggest spatangoids are the cause ofsome of the bioturbation. The abundant infaunal biota implies that the oxygen content of the sea-water was relatively high, but the oxidation in burrows beneath the surface implies that the sediment was probably anoxic not far below the sediment-water interface.

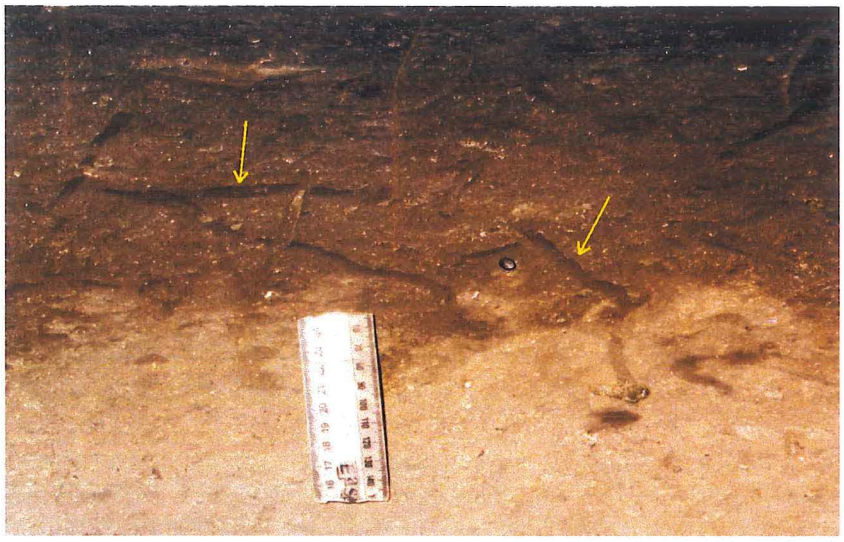

a: Thin mud filled burrows in the Kaiata Mudstone, Gibsons Beach. F5P11.

b: Larger traces with pale oxidised rims, Kaiata Mudstone, Gibsons Beach. F5P3.

c: *Thallassinoides* type burrows filled with very coarse sand, top surface of the Kaiata Mudstone, Gibsons Beach. F4P35.

Figure 4.17: Trace fossils in the Kaiata Mudstone. The types of traces found depends on the type of sediment present. The smaller, purple traces in **a** are found in the muddier parts of the Kaiata Mudstone in all areas, while the larger traces in **b** and **c** are found in the siltier and sandier parts.

Little Totara Sand

Composition:

The Little Totara Sand consists mainly of quartz grains, with less common feldspar and muscovite. Rock fragments are infrequent, except in the granule to gravel grain sizes, where they tend to be polycrystalline quartz grains and granitic rock fragments. The heavy minerals present include beryl, ilmenite, monazite, rutile, spessartine, topaz, tourmaline, zircon and zoisite (Yetton 1975). The composition indicates derivation of the Little Totara Sand from a quartz rich granite. Yetton (1975) suggested that the abundant tourmaline could be derived from a gneissic source to the west, although it could also be derived from the pegmatites in the local granites. Some feldspars have been altered to white powdery and soft clay, probably illite. This alteration is probably responsible for the small quantities of clay that are present in the Little Totara Sand, and may also account for the relatively small number of feldspars identified.

Texture:

The Little Totara Sand's most distinctive feature is bi-modal roundness. The rounder grains tend to be in the medium to coarse sand sizes, and the bimodality decreases towards the coarser and finer sizes. The coarser grains, granules and gravels are all superficially rounded, and the finer grain sizes are angular. Most Little Totara Sand samples contain 10-30% rounded grains. Little Totara Sand samples that are not bimodally rounded occur where the Little Totara Sand is interbedded with the Waitakere Limestone, and in isolated unusual beds.

The Little Totara Sand tends to be poorly sorted, although the grains are frequently sorted into laminations that are well sorted within themselves (fig. 4.18). Most of the silt and clay fractions may be caused by the breakdown of feldspar minerals.

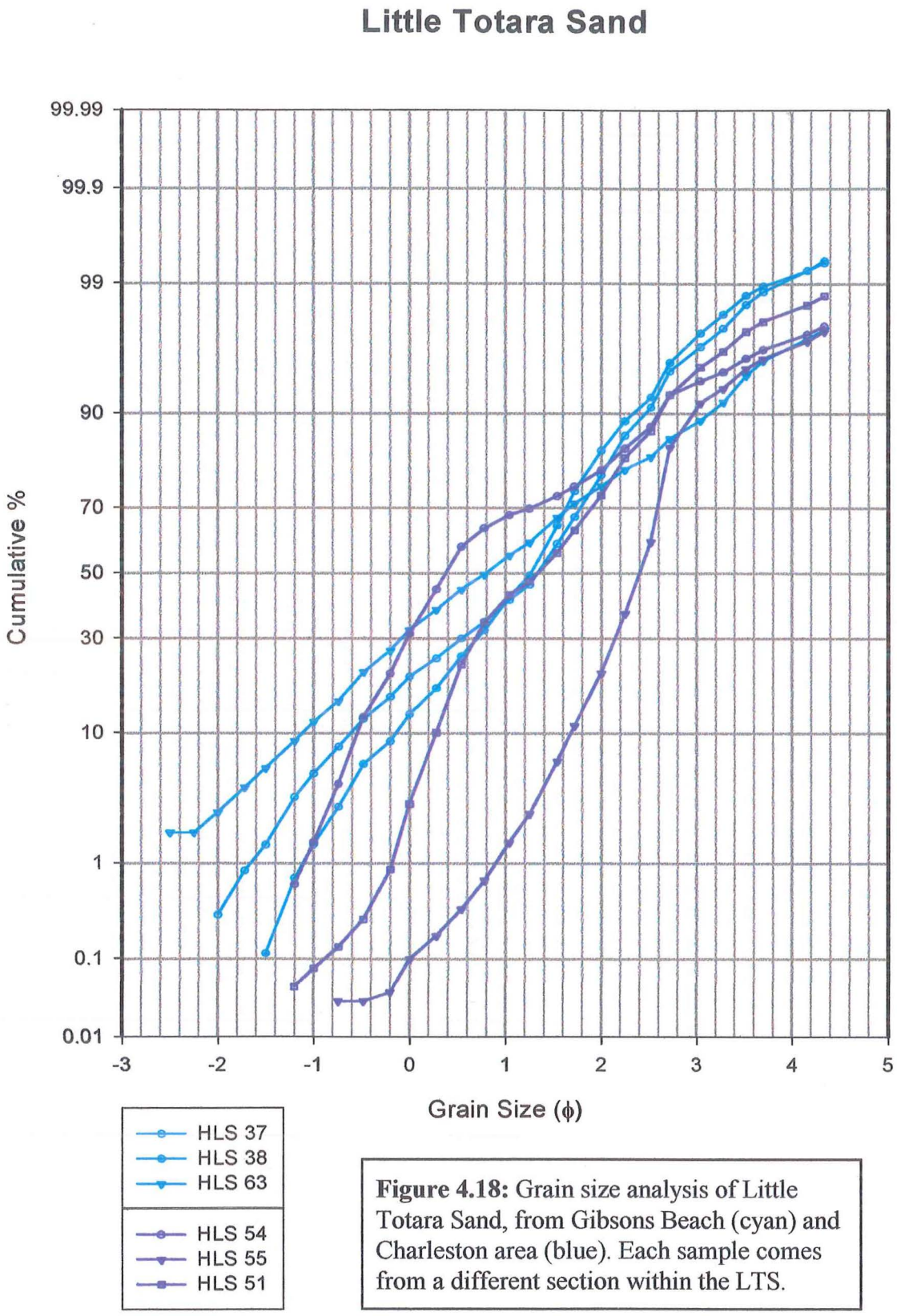

Figure 4.18: Grain size analysis of Little Totara Sand, from Gibsons Beach (cyan) and Charleston area (blue). Each sample comes from a different section within the LTS.

The single leptokurtic sample (HLS55, see Appendix V)was also unusual in that it did not display a high degree of bi-modal roundness, containing less than 3% rounded grains. The sample comes from a single cross bedded channel fill in a section of Little Totara Sand that displays mica drapes and at least two directional cross-bedding, interpreted as a tidal channel to beach complex. The analysed samples all come from different sections of the Little Totara Sand, but several have very similar grain size distributions (fig. 4.17: HLS37&38), implying that section breaks do not necessarily represent shifts in environments, but can also represent erosion events.

The bi-modal roundness suggests that rounded quartz grains had a longer history of erosion before being deposited. These grains could have been trapped an environment for a long period of time, or the grains could be recycled from another sediment, so subjecting the grains to two episodes of transport and erosion. The whole length of Little Totara Sand deposition is probably not enough to achieve the roundness of any of the quartz grains, so it is more likely that the rounded grains are recycled from a previous sediment. This inference is supported by the concentration of rounded grains into particular size ranges (which size ranges varies with location), which implies that these grains are derived from a local sand deposit. The most likely source of these recycled grains is the Brunner Coal Measures, which are reworked by Little Totara Sand processes in several locations (K30 803142 to 802152), resulting in a gradual increase of the proportion of rounded grains. Yetton (1975) suggests that the heavy mineral suites of the Brunner Coal Measures and the Little Totara Sand are related in that the Little Totara Sand suite is a more abraded and weathered version of the suite found in the Brunner Coal Measures. A great quantity of Brunner Coal Measures must have been completely eroded to provide the rounded grains for the Little Totara Sand. However Brunner Coal Measures are found underlying the Rapahoe Group everywhere in the field area (except around basement highs at Cape Foulwind and Charleston), so the sand may have been derived from an area either west of the Cape Foulwind

Fault, or east of the Paparoa Tectonic Zone. Other possible sources include sands from the Pororari Group and possibly (but unlikely due to probably being buried) the Paparoa Coal Measures.

Structures:

The Little Totara Sand contains abundant sedimentary structures that have not been obscured by trace fossils as have the structures of the other formations. The few traces observed consist mostly of simple vertical burrows that do not stand out from the surrounding sands, which tends to indicate high energy conditions (Bronley 1996). Little Totara Sand outcrops are commonly dividable into sections based on grain size and types and sizes of sedimentary structures. The Little Totara Sand contains trough cross bedding, planar cross bedding, dune cross bedding, scours, herringbone cross bedding, lag deposits, coarse debris flows, mud drapes, flaser bedding, massive sections and clay layers. It also has abundant blobs of dark brown to black or orange iron oxide coatings and cementation, which are probably the result of diagenetic modification of the opaque minerals in the sand.

In the Little Totara Sand outcrops between K30 796135 to K30 802152, around an uneven basement with a least one area that was exposed during Little Totara Sand deposition (road cutting at K30 797136), the structures include herringbone cross bedding, trough cross-bedding, flaser bedding and mica drapes (fig. 4.19). There are also lenses of coarser grained sediments: gravel and rip-up-clasts, probably deposited by storms. The local occurrences of herringbone cross-bedding implies that the Little Totara Sand in this area was deposited in a tidal environment, although the prevalance of one direction of cross-bedding in most sections implies that one tide was recorded dominantly, probably the ebb tide (Heward 1981). Although cross bedding in several directions can also occur on offshore bars, it is unlikely that energy conditions would allow the settling of

a: herringbone cross-bedding. Small scale sets of trough cross-beds overlain by a thicker set of straight foresets. Road cutting. F15P12.

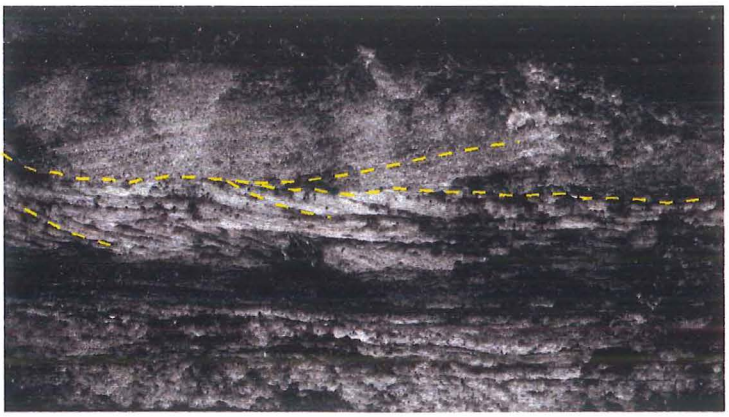

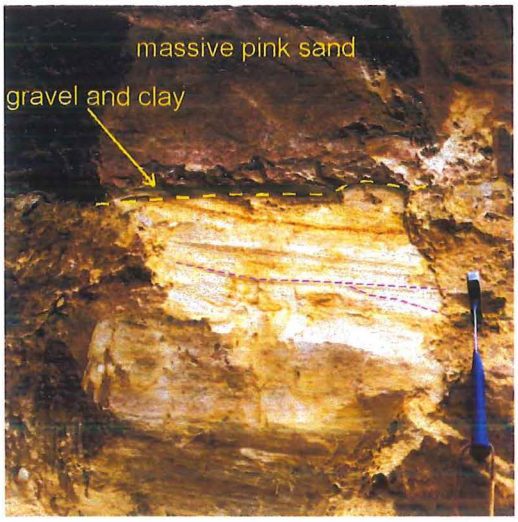

b: massive, coarse pink sand bed overlying cross-bedded medium to fine sand. Road cutting. F6P13.

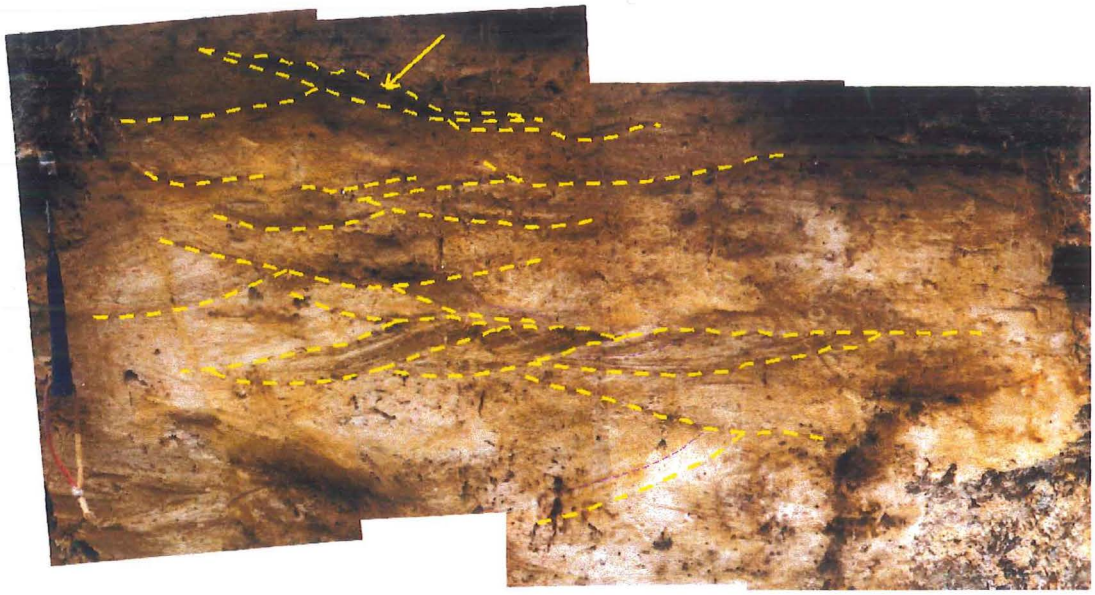

C: F6P7-F6P10, trough cross bedding, mica drapes (arrow), and two directions of cross-bedding.

Figure 4.19: Sedimentary Structures in the Little Totara San...

mica rich mud layers on a tidal bar. The outcrop with the greatest lateral and vertical extent in this area at K30 803144-803142 displays the abrupt contact with the underlying Brunner Coal Measures, here represented by carbonaceous sediments and sandstone. The outcrop can be subdivided into at least three different sections, characterised by

1. coarse sand lenses, layers of coarse and fine sands (lowest).
2. trough cross bedding in at least two directions, with mica drapes on some surfaces.
3. massive, coarse pink-coloured sand, separated from section two by a clay layer on an erosive surface (top section) (4.19b).

Section 3 (HLS54) has no discernable sedimentary structures, is pink-coloured (presumably from iron oxides), and is coarser than underlying Little Totara Sand. Unfortunately the outcrop does not show the top of this section. The massive bed was likely deposited rapidly, probably as the result of a storm event. The section with two directional cross-bedding is inferred to represent a very shallow to inter-tidal environment. The trough cross bedding, scours and coarse grain size suggest that the section was formed in a tidal channel, where the mica drapes were deposited at the turning of the tide. The section with coarse sand lenses was probably deposited in a beach environment (berm to backshore), where the original laminae have been disturbed by trace fossil activity and erosion, to form lenses. The coarser sand laminations and lenses represent storm deposition, while the finer represent wind and fine weather transport (Heward 1981).

Herringbone cross-bedding occurs at K30 797136, where the Little Totara Sand pinches out against a basement high and where two faults cut across the basement and overlying sands. Further north, in a pit on a forestry access road at K30 804177, large scale cross-bedding can be seen. The sand is iron stained and poorly sorted. Reay (1975) found this exposure to contain a very thick bed of curved cross-bedding, which is now not exposed in the pit. The size of the bedding, poor sorting and carbonaceous material suggested subaerial dunes as the environment of

deposition (Reay 1975). The current directions here are consistently to the SW (fig. 4.20), almost parallel to the axis of the basin. At K30 804182, flaser bedding is formed by segregation of quartz-feldspar sands and mica rich sands, possibly indicating a tidal environment.

In McLaughlins Pit, near Charleston, the Little Totara Sand can be divided into two sections. The lower section is characterised by wavy and indistinct cross-bedding, disseminated patches of iron oxides and carbon, relatively smooth erosion surfaces and irregular patches of iron staining (fig. 4.21). Above a major erosional surface, the cross-bedding becomes more distinct, larger scale and distinctly multi-directional. Here the rare iron minerals and staining are concentrated in foreset beds, and along erosional surfaces. The larger cross beds tend to be concave up (fig. 4.21). The wavy bedding and lack of distinct cross-bedding in the lower section implies oscillating or low energy flows. This section is inferred to have been deposited in a beach backshore environment, where strong water flows do not last long enough to produce high angle cross-bedding, and wind deposited sands cause most of the distinct cross-bedding. The dominant flow direction in this area is to the S or SW, possibly representing ebb-tide flow (fig. 4.20). The larger cross-bedding and sorting of sand grains in the upper section implies higher energy deposition, possibly aeolian dunes. Above this section, the Little Totara Sand grades into and interfingers with the Watakere Limestone, which is thought to have been deposited between low tide and 20 m depth (MacGregor 1983). The Little Totara Sand that interfingers with this limestone is noticeably finer (and more angular) than the Little Totara Sand lower in the section. Young (1964) noted cross-bedding in running sands overlying the coal seam (Little Totara Sand) at McLaughlins Quarry, and commented that it gave the impression of being deposited at least partially by wind, rather than water currents.

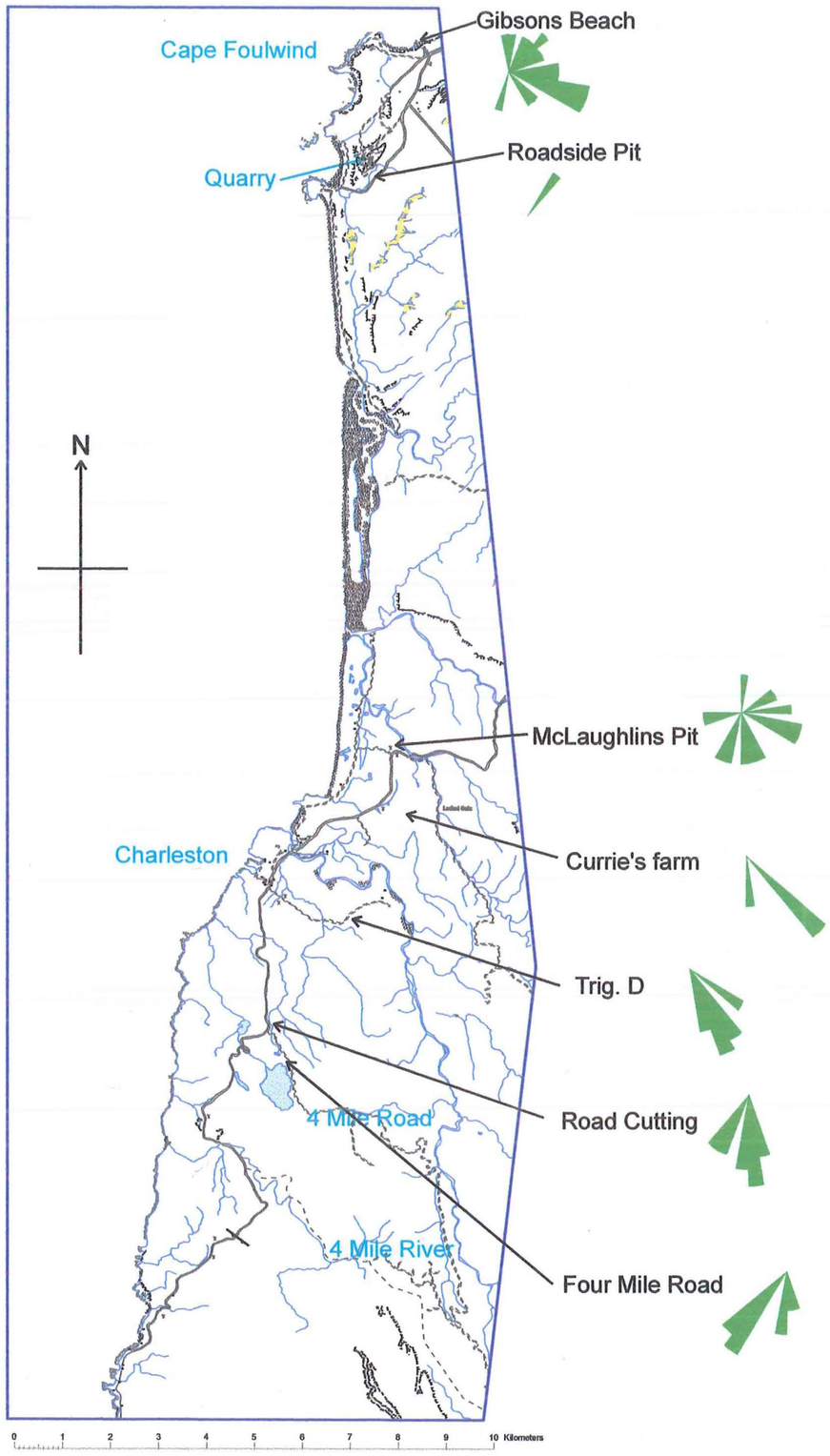

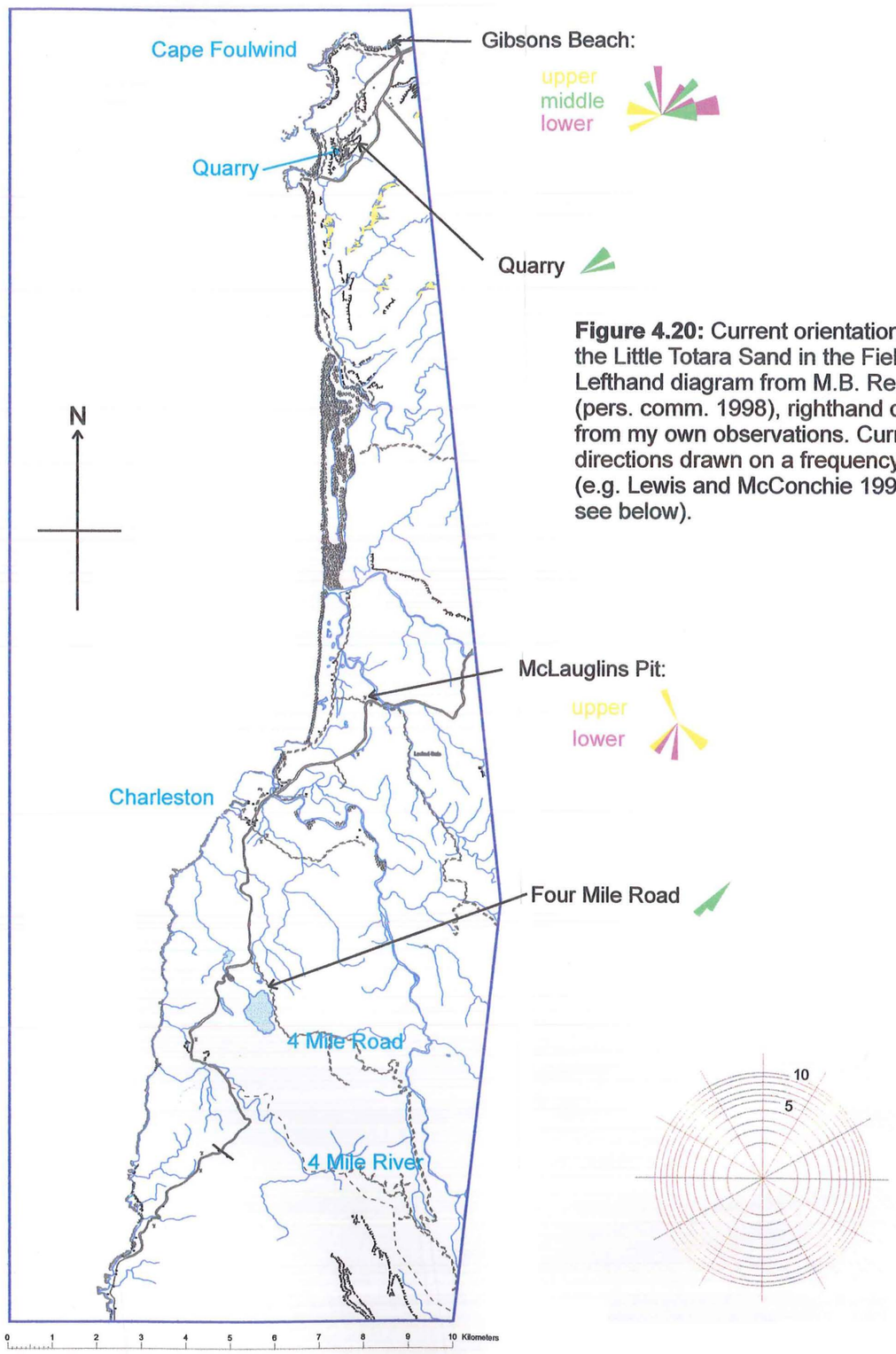

Figure 4.20: Current orientations for the Little Totara Sand in the Field area. Lefthand diagram from M.B. Reay (pers. comm. 1998), righthand diagram from my own observations. Current directions drawn on a frequency net (e.g. Lewis and McConchie 1994, see below).

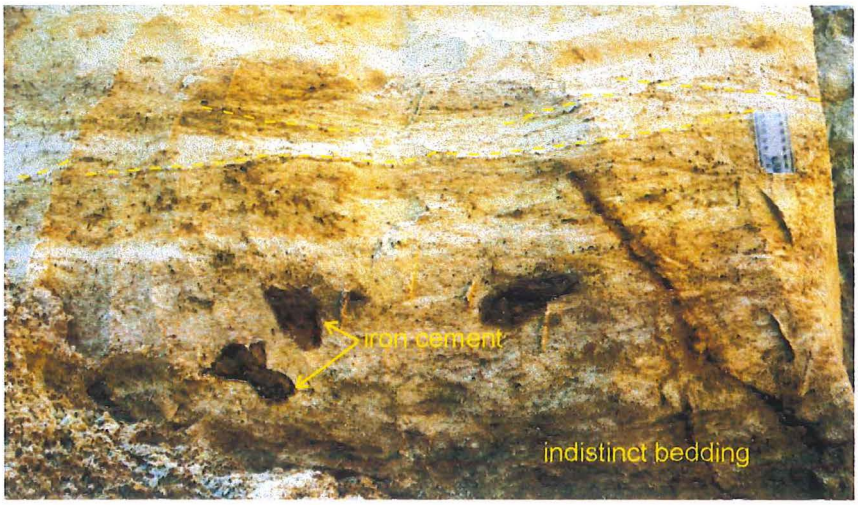

a: Iron cement blobs, indistinct and wavy bedding and cross bedding in McLaughlins Quarry. F12P4.

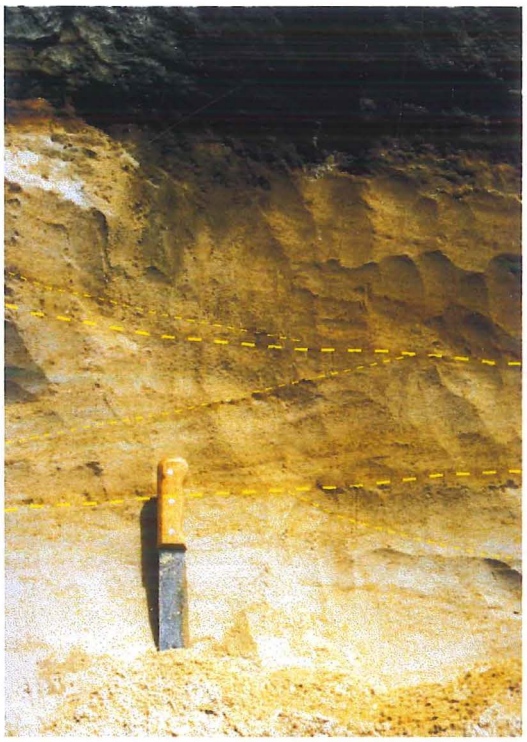

b: Two directions of cross bedding in a road side cutting above McLaughlins Quarry. Heavier dashed lines indicate erosion surfaces. F12P6.

Figure 4.21: Photographs of Little Totara Sand sedimentary structures.

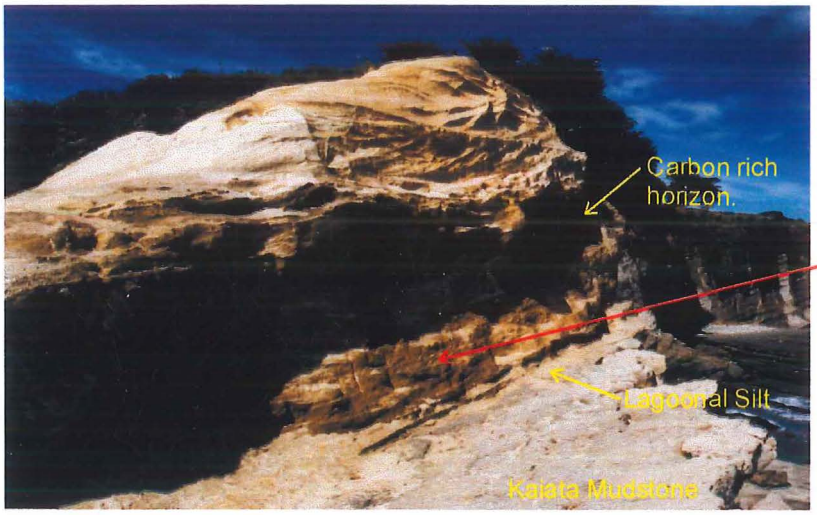

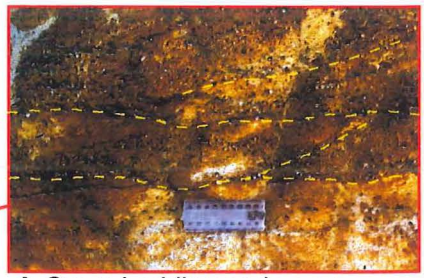

d: Cross bedding and scour surfaces with granule concentrations (dotted yellow lines). F5P1.

c: The first two sections of the Little Totara Sand at Gibsons Beach, separated by a layer of carbonaceous silts and mud. The upper section in this photograph has large scale, concave dune cross-bedding, the lower section has much smaller scale cross bedding. F4P37.

At Gibsons Beach, the Little Totara Sand can be divided into at least three sections. Directly underneath the clean, white-yellow Little Totara Sands, there is a 10 cm thick bed consisting of laminated very fine sands, silts and muds. The laminations vary in colour (black, brown, orange or grey) and grain size (silt, muddy silt, sandy silt, mud). Lenses and broken layers are common, possibly indicating bio-activity. There are erosion surfaces that cut laminations within the silts. Coarse sand grains and sand lenses can be found within the bed. The black colour is caused by the presence of carbon in the sediment. These sediments are inferred to be lagoonal deposits, that include lenses of sand from the laterally adjacent dune environment. The Little Totara Sand directly overlying the lagoonal silts is characterised by straight, small-scale cross-bedding (10 to 20 cm sets), with granules concentrated on the lee faces and on the erosional surfaces between sets. The top of this section also shows scours, channels and tabular cross-bed fills. Overlying the lowest section is a layer of variable thickness (up to 50 cm) of brown-black indurated sandstone. The next two sections contains much larger scale low to high angle cross bedding, with iron oxide staining and granules concentrated on the lee faces (fig. 4.21). These sections are separated by an erosional surface with quartz gravel and clay concentrated along it. The current directions for all three sections are scattered but tend to be most common in the N to E directions (fig. 4.20). The large size fractions are concentrated in foreset laminae and in the erosion surface below cross-bedded sets, otherwise the size and sorting of the sands the first layer suggests deposition predominantly in an aeolian dune system.

Trace Fossils:

There are very few trace fossils in the Little Totara Sand, mostly consisting of simple vertical burrows, ranging in size from 5 mm disturbances in laminae to 10 mm burrows. In many exposures carbonaceous material occurs, and what may be rootlets are also seen. This implies at

least some degree of subaerial exposure in some parts of the Little Totara Sand. Carbonaceous horizons and rootlets are especially common in area around K30 803144, especially the forestry road section.

Chapter 5:

Rhodoliths

Introduction

Rhodoliths (literally red-stones) are "...nodules and detached branch growths with a nodular form composed principally of coralline algae..." (Bosellini and Ginsburg 1971). The successive algal layers have white, pink or red colours and are formed by deposition of lime in the cell walls of the algae. The skeleton produced distinguishes rhodoliths from oncoliths and other algal deposits that bind sediment to produce structures. Rhodoliths have also been called rhodolites (Bosellini and Ginsburg 1971), and rhodoids (Peryt 1983).

The presence of rhodoliths, their size, morphology, growth pattern, species composition and arrangement within the sediment, all have the potential to provide much information about the environment of deposition. Many papers have been published on how and where rhodoliths grow, in modern seas and in ancient environments from interpretations of fossil occurrences (e.g. Bosence 1976, Bosence 1983b, Manker and Carter 1987 and Martin *et al.* 1993).

Rhodoliths require certain light and nutrients to grow. To attain a sub-spherical shape, they also need frequent overturning. The different genera of algae have different tolerances to light, temperature and surface conditions. Changes in genera of algae within rhodoliths can indicate changes in conditions, depth, temperature and energy of the environment (Bosence 1983a). Branched or columnar forms also occur, and the morphology of rhodoliths is considered to be related to the energy of their formative environment (Bosence 1983a). The delicate branched forms occur only in low energy environments, because high energy waves and currents easily

break the branches off. The encrusting forms occur in high energy environments where they are frequently turned to expose new surfaces for colonisation.

Bosellini and Ginsburg (1971) thought that rhodoliths occur only in "relatively shallow water", where wave or tidal currents turn them frequently. Living rhodoliths have since been reported in clear water at depths of 150m (Tsuji 1993). When rhodoliths are found too far down for sufficient light to reach them (about 150 m), they are considered relict. Most rhodoliths form between 0 and 50 m water depth (Bosence 1983b).

A little previous work has been done on the occurrence and environmental significance of rhodoliths in the New Zealand region. The presence of rhodoliths in Cenozoic carbonates is mentioned briefly in Nelson (1978). A paper published on New Zealand rhodoliths by Burgess and Anderson (1983), briefly describes locations and structures of "rhodolite" occurrences, and their brief environmental interpretation generalises for all the rhodolith occurrences they studied. They conclude that most deposits occurred as algal shoals, that they formed in shallow marine conditions of less than 50 m water depth, on upfaulted blocks "forming submarine topographic highs" (Burgess and Anderson 1983, p. 253) and that the most likely mechanism for turning was storm activity due to the wide range of shapes in any deposit of rhodoliths.

A study of the Waitakere Limestone overlying the Little Totara Sand near Charleston (MacGregor 1983) describes eight facies ranging from rhodoliths through algal debris to almost pure micrite. Macgregor (1983) interprets this limestone as a shallow-water temperate algal carbonate that ranges in age from upper Eocene (Runangan) to lower Oligocene (Whaingaroan). In the Charleston region, the limestone is interbedded and gradational with the Little Totara Sand for several meters, becoming progressively less sandy upwards. It is composed of calcareous algae (rhodoliths and broken branches), bryozoa fragments, echinoderm plates, foraminifera, minor quartz sand and calcite cement at Charleston. MacGregor reached the conclusion that the

Waitakere Limestone was deposited in clear-water, *c.* 20°C, 0-12 m depth, near shore conditions. MacGregor infers sea-grass banks from the presence of certain foraminifera, which implies quiet conditions for some of the facies, while others are associated with near-shore active environments.

A recent paper by Lee *et al.* (1997) describes coralline algae found encrusting basaltic pebbles-cobbles in association with bryozoa, serpulids, bivalves, foraminifera and brachiopods near Oamaru. The authors interpreted the fauna as Runangan, from shallow (25-50m) water depths and subtropical temperatures. Whaingaroan rhodoliths also occur on the flanks of volcanoes in the Oamaru area.

Rhodoliths are found in several places within the present study: within the algal limestone at Cape Foulwind, in the Waitakere Limestone and at Kaipakati Point. The occurrence of calcareous algae at Cape Foulwind is dealt with in Chapter 3, and the rhodoliths from Kaipakati Point are detailed here. The rhodoliths are concentrated into layers on Seal Island and Kaipakati Point, and found individually as far south as Pahautane Point. They are stratigraphically confined at the contact of the Rapahoe Group with overlying sandy, glauconitic limestone (Tiropahi Limestone) at Woodpecker Bay. At Punakaiki, the overlying limestone is the Potikohua Limestone, a polyzoan biosparite (Laird 1988). The contact with the Island Sandstone here varies from gradational to an erosional unconformity exposed particularly well in Bullock Creek where there are no rhodoliths associated with either sandstone or limestone.

The Rhodolith layers

The internal morphology of the rhodolith zone changes across Kaipakati Point and Seal Island (fig. 5.1). Near the limestone contact at Pahautane Point, isolated rhodoliths are commonly associated with bivalve shells and worm tubing.

Along the southern side of Kaipakati Point, sparse rhodoliths form two layers separated by about 10cm, a thick upper layer (15-20 cm) and thin (5-10 cm) lower layer of scattered rhodoliths. Isolated rhodoliths occur above and below these layers.

On the north side of Kaipakati point, the rhodoliths form a concentrated layer, with glauconite content and calcite cementation in the underlying sediment increasing upwards towards it. The rhodolith layer here contains much sediment and *Pectin, Ostrea* and other mollusc shells, echinoid shells, bryozoa fragments and serpulid worm tubes, and the sediment above the band also contains many shells and scattered rhodoliths. The band varies laterally from sparse rhodoliths in a sandy matrix, to mass rhodoliths in a single layer with a lessening concentration upward, to two concentrated layers separated by about 10cm of sparse rhodoliths, and with a decreasing rhodolith concentration above the layers. The thickness of the band from first rhodolith appearance to last is about 150 cm.

On Seal Island, there are several distinct bands of rhodoliths. On the south side of the island, there are two distinct, narrow, cemented bands dipping south: the lower layer is thin (maximum 7 cm) and changes in thickness laterally, eventually grading into less cemented lenses northwards. On the eastern face a thick west dipping cemented layer weathers out and can be traced from the upper layer on the south side of the island. Several lenses of rhodoliths occur in the sediment below, the equivalent of the lower band. To the north the layers are again separate cemented narrow bands and appear to be dipping northwards. The outcrop patterns suggest that the greatest concentration of rhodoliths has probably been eroded: it may have occurred close to the current

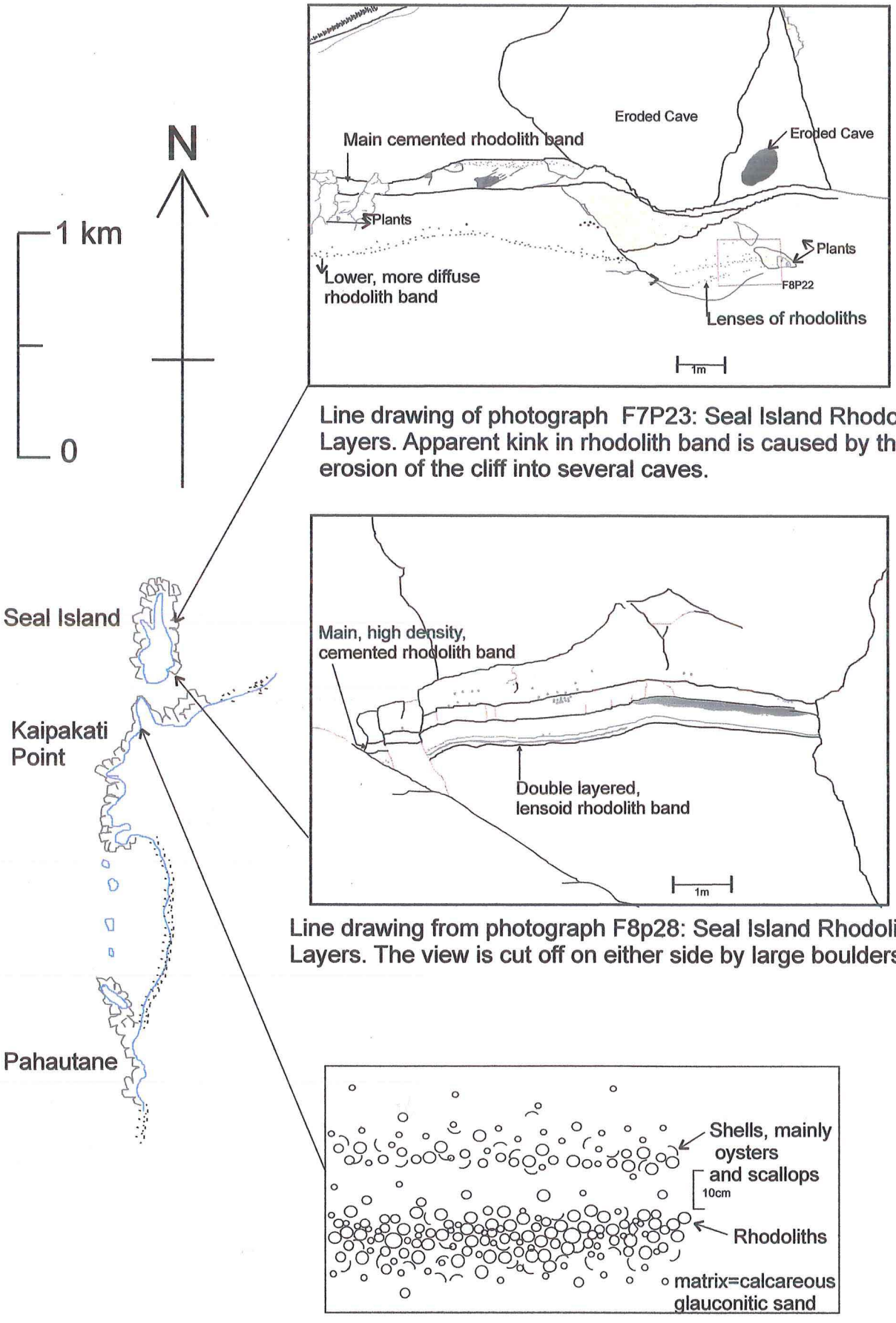

Figure 5.1: Rhodolith band morphology on Kaipakati Point and Seal Island.

edge of the island, where a strip of sand connects Seal Island to the main beach at low tide. During deposition and rhodolith growth I infer that the rhodolith layers formed part of a bar of rhodoliths, raised and thick at the centre but thinning and sloping down to the seafloor. Calcite cementation of the thicker parts of the bar probably occurred on the seafloor as it does in modern algal reefs (Jindrich 1983), adding to the long term stability of the rhodolith mound.

Where the rhodolith zone on Seal Island is largely composed of one thick layer, the composition of that layer changes both vertically and laterally. In some parts the layer is composed entirely of rhodoliths with a matrix of broken branches. In some places, however, there exists a gradation from bottom to top, from algal sand and granules, composed entirely of broken algal branches, through a transition zone of around 20 cm thickness, into rhodoliths in algal sand matrix. The outcrop shows a rapid lateral transition into the rhodolith facies to the south, this probably represents a channel, an erosion of the bar as it was originally and redeposition of the coarser algal sediment. The change from fine to coarse algal sediment deposited implies an increase in energy, probably caused by a drop in relative sea-level, bringing the bar well into the reach of normal waves and tidal currents. The band where this transition is observed is about 1.4 m thick (Fig 5.2b).

Stratigraphic Location:

The rhodolith band marks the boundary between the Island Sandstone and the Tiropahi Limestone. Below the rhodolith band the Island sandstone becomes progressively more calcite rich, also containing more shell fragments and glauconite. Above the rhodoliths the sediment still contains a lot of detrital sands and silt, and the glauconite content decreases upwards (Table 5.1, fig. 5.2a).

Rhodolith Layer at Seal Island. Layer is approximately 1.4 m thick: lower 40 cm consists of fine algal debris, the top 80 cm contains rhodoliths up to 5 cm in length, the middle is transitional. To the right, the coarse rhodolith infills a channel, the finer material is eroded (arrowed). F11P22.

Island sandstone (bottom of picture) separated from Tiropahi Limestone by thin, poorly sorted detrital sandstone layer. Pahautane Point. F2P5.

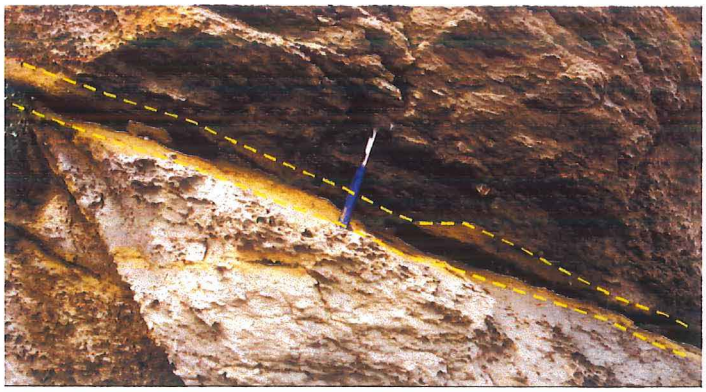

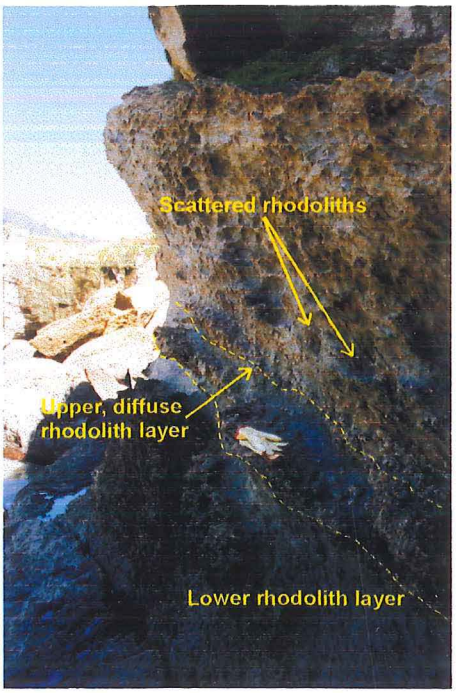

Rhodolith layers at Kaipakati Point. Two layers separated by about 10cm of sediment. Note the scattered rhodoliths above the layers. F3P29.

Figure 5.2b: Rhodolith layers as the boundary between Island Sandstone and Limestones, compared with the boundary at nearby Pahautane Point.

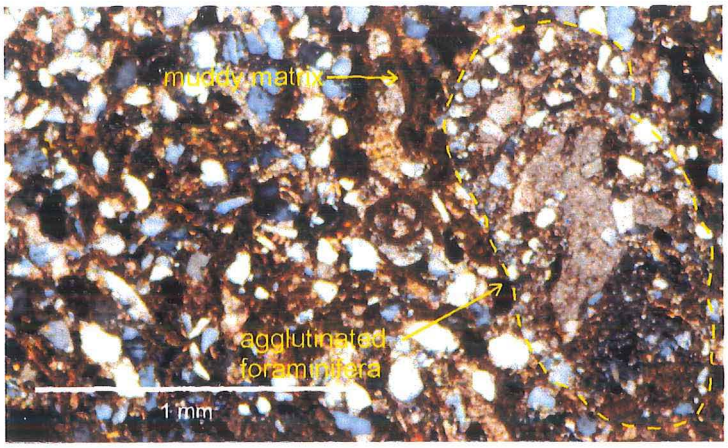

a: HLS 16. Island Sandstone 3.5 m below the rhodolith layers. cpl.

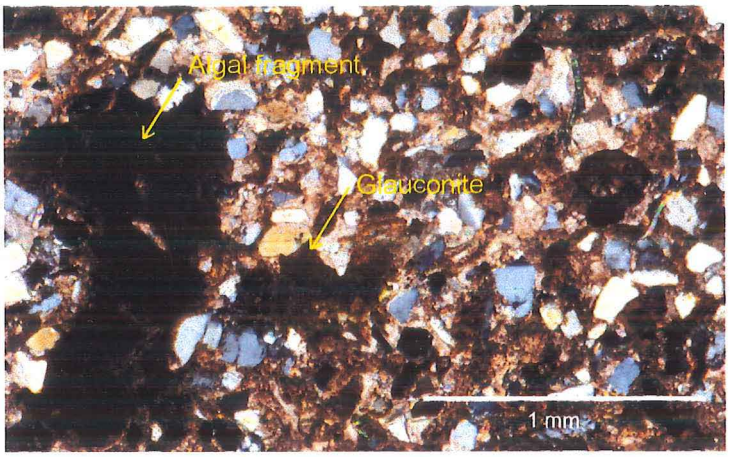

b: HLS 17. Island Sandstone 1 m below the rhodolith layers. cpl.

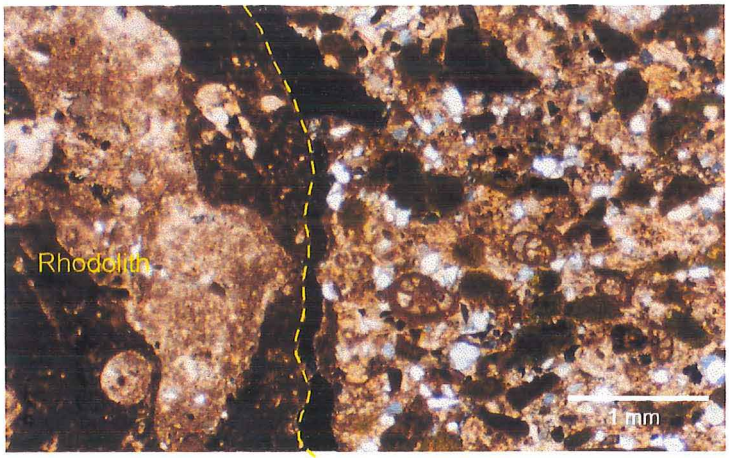

c: HLS 80. Rhodolith in sandy glauconitic limestone, 1 m above rhodolith layer: cpl.

Figure 5.2a: Succession of lithologies up to Rhodolith layers.

Table 5.1: Selected composition data related to distance from rhodolith layers.

Distance from rhodolith layers	Detrital grains	Calcite cement (=matrix)	Glauconite	Shells, algal material.
3.5 m below (HLS 16)	45.0%	39.75%	7.25%	8.0%
1.0 m below (HLS 17)	35.25%	41%	7.25%	14.25%
1.0 m above (HLS 80)	16.25%	34.0%	15.0%	32.25%

At the Pahautane section, where only scattered rhodoliths occur, there is evidence for an erosion event between the two units. Bryozoan-rich sandstone is overlain abruptly by a thin (5 cm) band of poorly-cemented orange sandstone, inferred to be deposited rapidly by currents, which is overlain by highly bryozoan-rich limestone (fig. 5.2b). All rhodoliths occur below this horizon. There is also evidence in the limestone here for cessation of sedimentation and erosion events (shell accumulations and abrupt changes in glauconite concentrations associated with intense burrowing) close to the contact with the Island Sandstone. At Kaipakati Point, there is little evidence for erosion in the limestones, except the inference that the deposition of the rhodoliths in this area is from currents downslope from the maximum concentration near Seal Island. On Seal Island itself, the rhodolith layer shows evidence of irregular smooth holes dissolved into both matrix and rhodoliths that are filled with glauconitic sand. These holes appear to have been created after initial cementation of the rhodolith band and infilled with the next episode of sedimentation. The lateral and vertical extent of solution is difficult to determine given the inaccessibility of the outcrop.

Rhodoliths

Bosence (1983) suggests a descriptive classification of rhodoliths, based on the number of species identified in a nodule, the shape of the nodule, and the growth or branching pattern of the algae (Table 5.2).

Table 5.2: Classification of rhodoliths by Bosence (1983)

Monospecific (mono)	Spheroidal (S)	Laminar (L): concentric (con) or boxwork (box)
Multispecific (multi)	Ellipsoidal (E)	Branching (B): classes 1, 2, 3, 4
	Discoidal (D)	Columnar (C)

e.g. Multispecific, discoidal, laminar concentric (or Multi. D. L. con) rhodolith

All rhodoliths in the Kaipakati Point area are multispecific (see below), laminar concentric with uneven surface, showing creases or crenulations and bulbous projections. The rhodoliths range in size from tiny fragments of branches, to large uneven balls 12 cm in diameter. The coralline algae have encrusted shell material including bryozoan colonies, small blobs or patches of sediment and frequently broken fragments of other rhodoliths. Broken branches of algal growths are frequently found in the matrix and as the nucleus of encrusting rhodoliths. Bryozoa have often colonised the surface of a rhodolith, before being overgrown by the next phase of algal growth (fig. 5.3).

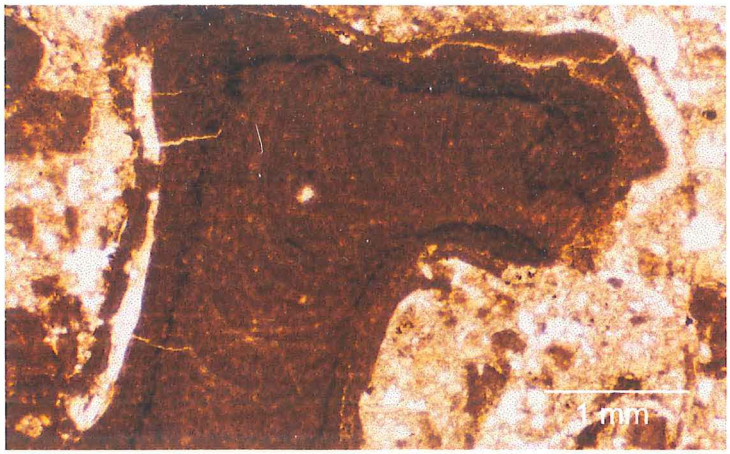

a: HLS 81a. Bent rhodolith branch covered by a layer of encrusting algae. ppl.

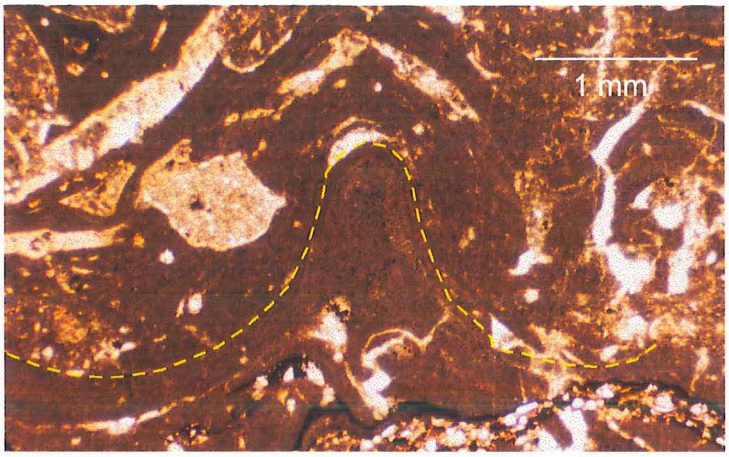

b: HLS 81a. Crenulated layers within a rhodolith. ppl

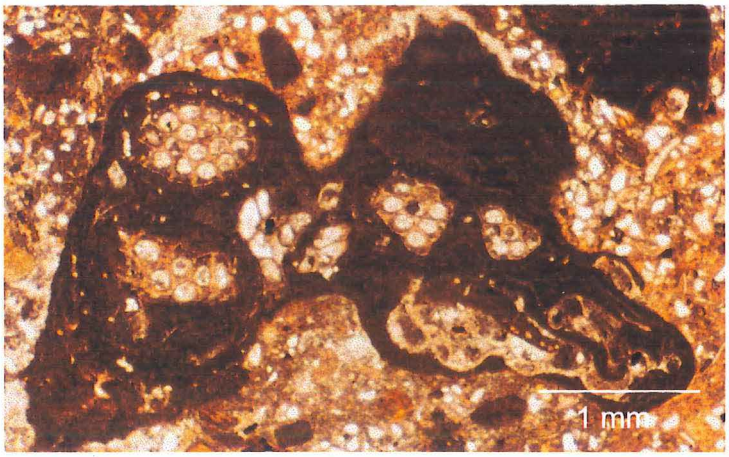

c: HLS 79. Algal encrustation of a bryozoan colony. ppl

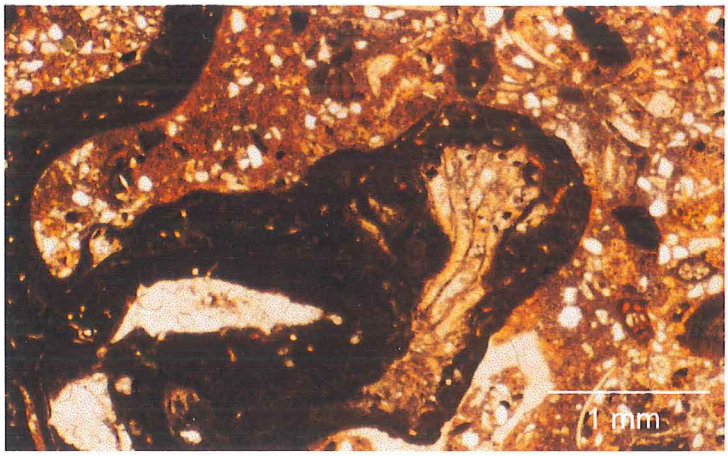

d: HLS 79. Bryozoa on the surface of a rhodolith is encrusted by algae. ppl

Figure 5.3: Branch forms, encrusting habits, uneven surfaces and inter-relationship with bryozoa.

Algal Genera:

Determining which genera of algae are responsible for the formation of these rhodoliths is difficult. The identification of algae relies upon the arrangement of the cell structure and the arrangement, location, number and morphology of 'conceptacles'- reproductive cavities within algal layers (Wray 1977). Hence any recrystallization, alteration or cementation can distort, dissolve or obscure these important features and make identification impossible. Despite the widespread cementation and solution present in the rhodolith band, enough features remain to positively identify some genera of algae (conceptacles and cell structure). The fabric of cells is clearly visible in most cases, and the presence of conceptacles is the main criteria used here for positive identification of genera. However, many layers of algae have none of the diagnostic features, or these have been removed or obscured by diagensis, and the listing of identified genera will surely represent only some of the algae responsible for rhodolith formation.

Adding to the confusion of identifying the genera of algae is the ongoing taxonomic debate over the naming and taxonomic position of many genera of coralline algae. The generic names used here are hopefully up to date at the time of publication.

Descriptions of the genera identified here come are found in Johnson (1961), Adey and MacIntyre (1973), Wray (1977), Anderson (1984), Bosence (1991) (for some taxonomic debate), Minnery (1990) and Ghosh and Maithy (1996). The only algal genus positively identified from the rhodoliths is *Sporolithon* (formerly *Archaeolithothamnium*, see Ghosh and Maithy 1996), which appears to be the major culprit in the formation of the Rhodoliths. Probably identifications include *Lithothamnion* (formerly *Lithothamnium*) and *Mesophyllum*, which are relatively common and *Lithoporella* which has a distinctive cell structure, but is very rare and possibly *Lithophyllum* (fig. 5.4).

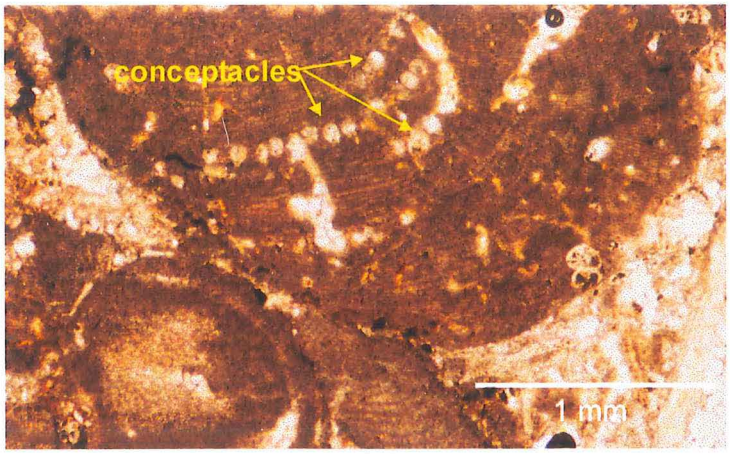

a: HLS 81a. Sporolithon. ppl

b: HLS 18. Lithoporella? ppl

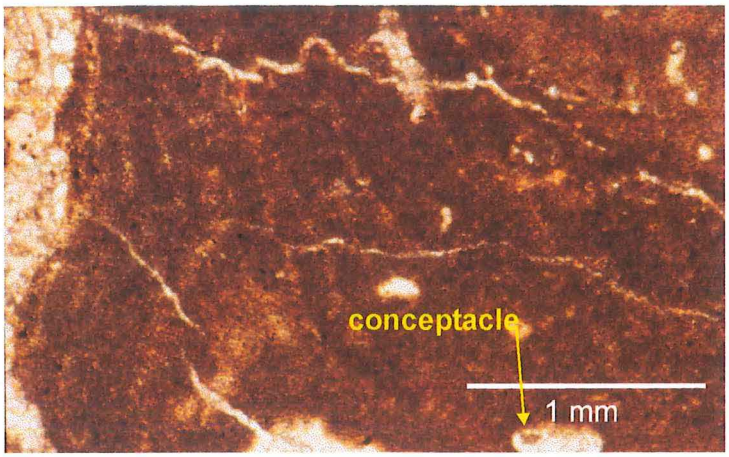

c: HLS 89. Lithothamnion? ppl

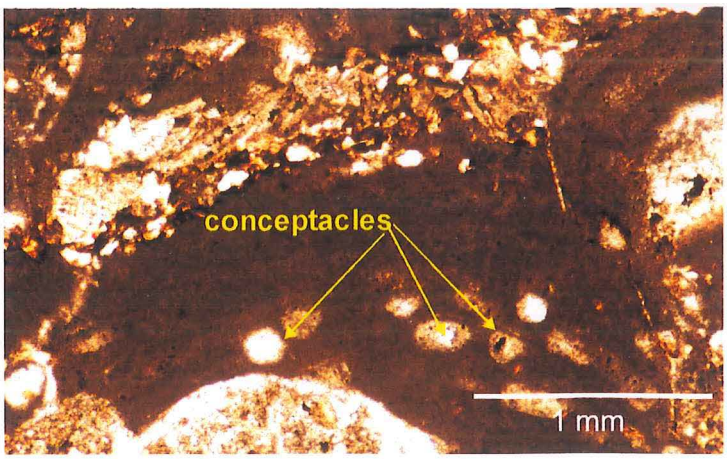

d: HLS 81a. Mesophyllum? ppl

Figure 5.4: Various genera of algae, showing distinctive features.

MacGregor (1983) identified *Archaeolithothamnium*, *Lithothamnium*, *Lithophyllum*, *Lithoporella*, and other melobesiids in the Waitakere Limestone. Anderson (1984) found *Lithothamnium*, *Lithophyllum*, *Melobesia*, and *Mesophyllum* in the Nile Group Oligocene Limestones, although his definition of *Lithothamnium* is the same as MacGregor (1983), Wray (1977) and others use for *Archaeolithothamnium*.

Anderson (1984) illustrated some of the controversy surrounding the interpretation of the paleoenvironmental ranges of calcareous algae genera: different authors have quoted many different ranges for each genera. In the literature *Archaeolithothamnium*, *Mesophyllum* and *Lithoporella* are generally considered to be tropical to subtropical forms, while *Lithothamnium* is considered primarily a cold water form, although thin crusts have been reported from tropical algal reefs (Johnson 1961, Adey and MacIntyre 1973). Identification of species allows more precise temperature and estimates of paleobathymetry, but in this study specific identification is impossible with the state of preservation of the rhodoliths. *Lithophyllum* is considered to occur in tropical to temperate waters, in strong light conditions (shallow depth or clear water) (Wray 1977). It lives at shallower depths in cooler water than it can in the tropics, where it is found up to 100 m water depth. Both *Archaeolithothamnium* and *Lithothamnium* are found from shallow to deep water, but not in intertidal zones. Banner and Simmons (1994) found fossil *Archaeolithothamnium* in depth controlled facies correlated with depths of 15-60 m. They infer these depth ranges using comparisons with modern calcareous algae occurrences, where the depth of algal growth is limited by light penetration. Bosence (1991) provides a general paleobathymetry depth/abundance chart for the Neogene occurrences of calcareous algae:

Intertidal-20 m: *Neogoniolithon*, *Porolithon*, *Lithphyllum* and *Hydrolithon*.

20-40 m: *Neogoniolithon*, *Lithphyllum*, *Hydrolithon*, *Titanoderma* and *Mesophyllum*.

40-60 m: *Mesophyllum* dominant with *Archaeolithothamnium*, *Lithothamnium* and *Lithophyllum.*

60-100 m: *Mesophyllum* and *Lithothamnium* with *Archaeolithothamnium* and *Lithophyllum* (Bosence 1991

However, this chart has not been tested for Paleogene coralline algae occurrences, so it should not be used without caution for Eocene – Oligocene rhodoliths.

Solution Cavities:

On Seal Island the sediment that is frequently included within algal layers and between rhodoliths is considerably finer and less glauconite rich than the sediment that occurs in cavities in the top part of the cemented rhodolith band (fig 5.5). The cavities can be up to 7cm across, but tend to be no larger than 2 cm in diameter, and are often sub-spherical in cross-section. These cavities, containing different sediment (Table 5.3) and often eroded into large rhodoliths and areas of cemented algal fragments, are evidence for an episode of solution in the rhodolith band, after pore-filling cementation had occurred, but before stylolites, calcite veins and the replacement of matrix by calcite cement occurred. The sediment infilling the cavities frequently contains broken fragments of algal branches and debris, some of which show evidence of solution.

Table 5.3: Comparison between cavities and algal sediment in two samples

	Detrital (Qtz, feldspar, etc	Calcite cement	Algal material	Fossils	Glauconite
HLS 89: Algal part	8 %	29.75%	49%	10%	0%
HLS 89: Cavity	16.5%	39.5%	20.5%	6.75%	15%
HLS 81b: Algal part	3.25%	22.5%	63.5%	8%	0.25%
HLS 81b: Cavity	10.25%	43.75%	16.75%	12.5%	9.75%

The occurrence of burrows filled with finer, algal and less glauconitic sediment in the lower part of the layers suggests that many of the cavities may be have been burrows, whose outlines have been altered completely by subsequent solution.

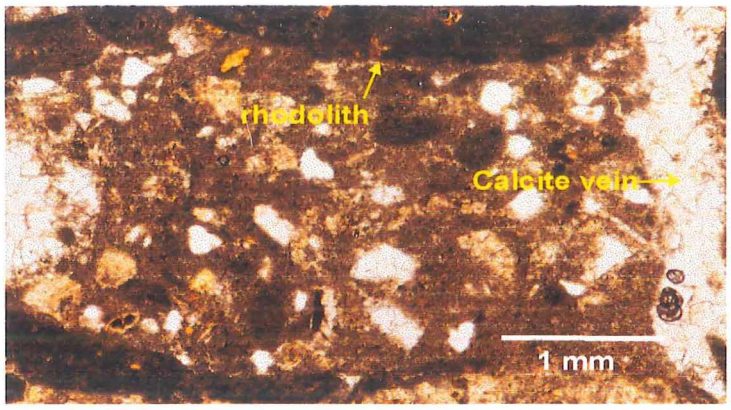

a: HLS 81b. Sediment within rhodolith band. ppl

b: HLS 81b. Sediment outside rhodoliths. ppl

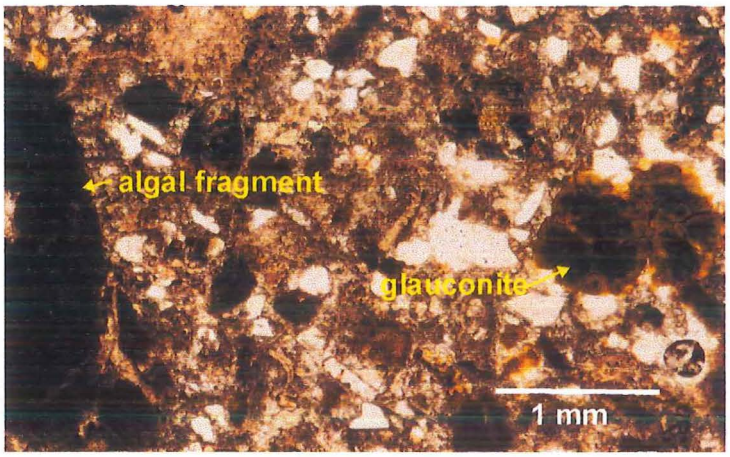

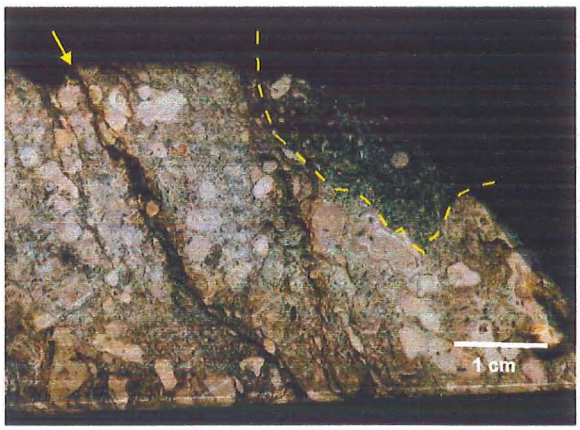

c: Scanned image of a block from the rhodolith band on Seal Island. Dotted line encloses a sediment filled cavity, arrow indicates stylolite.

f: Scanned image of a cavity in cemented rhodolith mass (arrowed).

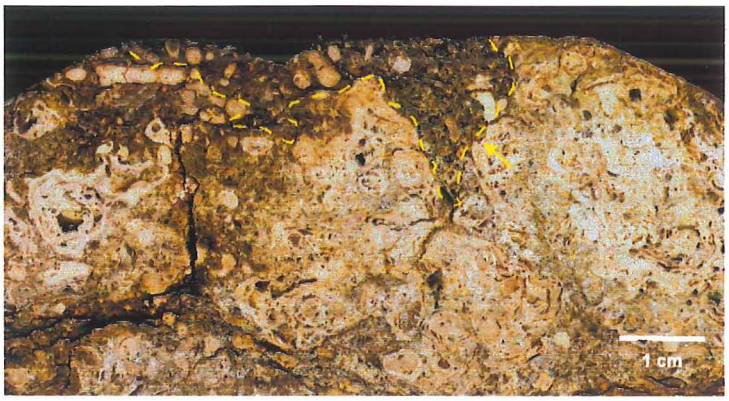

Figure 5.5: Differences in sediment within rhodoliths and in cavities.

The evidence for solution indicates a break in sedimentation, co-incidental with the change from dominantly sandy to dominantly calcareous sedimentation. On the north side of Kaipakati point, there is no cementation of the rhodolith band, and no evidence for long breaks in sedimentation. The lack of evidence of erosion is inferred to result from re-sedimentation of rhodoliths and glauconitic sandy sediment around the flanks of the rhodolith bar. A layer of poorly cemented orange sand, and a condensed section containing 25% bryozoa fragments represent a considerable break between the Island Sandstone and Tiropahi Limestone, and erosion of Island Sandstone has also occurred at Bullock Creek (Laird 1988). However, the outcrop at Seal Island is inaccessible due to the vertical nature of the cliff so information on the morphology of the upper surface of the rhodolith band is obtained primarily from examination of fallen blocks, and from photographs. Where the top can be observed, it is found to be very uneven and to contain solution cavities filled with the overlying limestone. The cavities and the solution of rhodoliths indicates an episode of sub-aerial exposure, resulting from a further drop in relative sea-level.

The presence of a large volume of calcareous material at Seal Island and the inferred presence of calcareous material (micrite and shells) in the matrix has meant that the rhodolith band itself and the sediment below are considerably more cemented than the corresponding sections at Pahautane and elsewhere. The rhodolith band has pervasive sparry calcite cement, which infills pore spaces and areas between successive algal layers, and has infilled, altered and enlarged conceptacles within the algal skeleton (fig. 5.6). The compression during diagenesis has also led to the formation of stylolites which cut across rhodoliths and concentrate fine quartz grains and iron oxides. Subsequently, probably during uplift, calcite veins developed cutting across rhodoliths and sediment equally. These diagenetic changes mean the sediment that infilled the cavities is just as cemented as the rest of the rhodolith

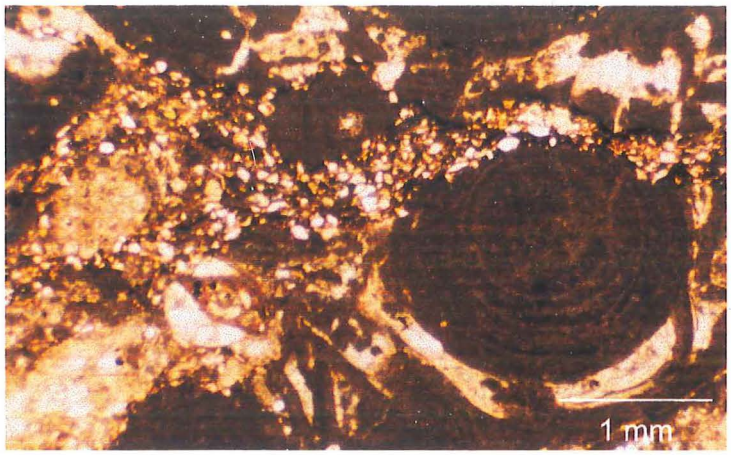

a: HLS 81a. Stylolites cutting a rhodolith and concentrating detrital sand. ppl.

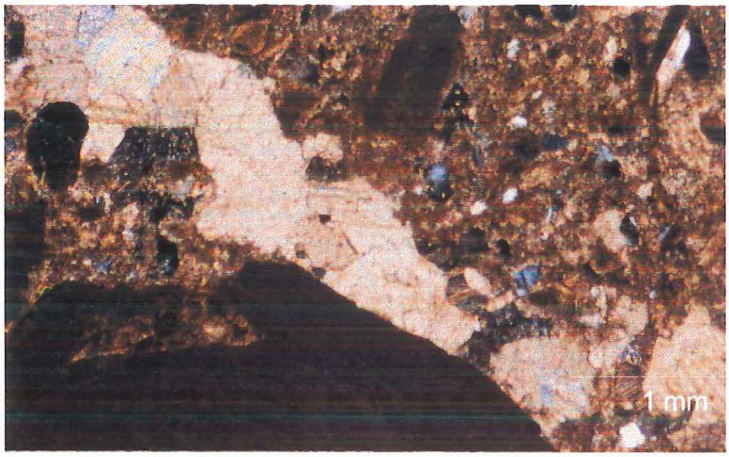

b: HLS 81b. Calcite vein along the edge of a rhodolith, with an open sediment infilled conceptacle (arrow). cpl.

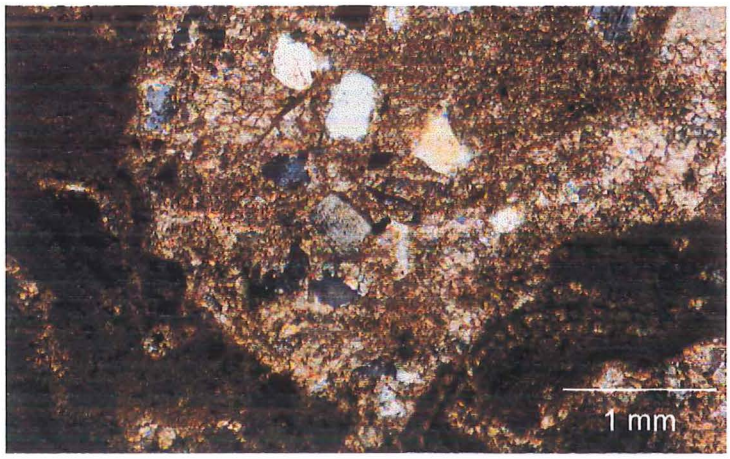

c: HLS 18. Calcite cementation of matrix. cpl.

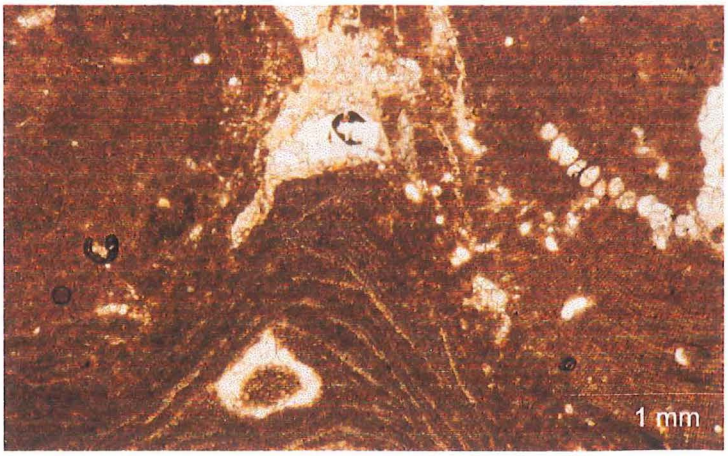

d: HLS 89. Sporolithon, showing infilling of conceptacles with spar and alteration of algal layers. ppl.

Figure 5.6: Alteration, cements, stylolites and veins.

band, and does not stand out at all during weathering, although the different colour of the sediment and the smooth edges of the cavities means they show up in the surfaces of cut blocks.

Interpretation

The occurrence of rhodoliths is limited to the boundary between the Rapahoe Group and the overlying Oligocene limestones of the Tiropahi Formation. The Waitakere Limestone is very similar in composition to the rhodolith bands, varying only in containing more branched forms of algal growth, presumably a consequence of lower energy conditions. The relatively large size of concentric laminated rhodoliths occurring at Woodpecker Bay argues for substantial currents turning the rhodoliths, and frequently algal balls may well have been swept off the bar where they formed and its immediate surroundings and distributed through the surrounding lower energy environments.

Other Similar Rhodolith Occurences:

MacGregor (1983) interprets the Waitakere limestone as having formed at a depth of 0-12 meters near shore in waters of about 15-20°C, and that the location was swept by tidal currents. Some foraminifera found in the Waitakere Limestone imply local sea-grass settings. The depth of growth of rhodoliths at Woodpecker Bay was probably similar to that proposed by MacGregor (1983) for the Waitakere Limestone. Storm events appear to have carried rhodoliths up to a kilometre from the inferred bar at Seal Island. The main concentration of rhodoliths at Seal Island was a build up of algal pebbles and cobbles surrounded by lower, muddy debris fields. The sediment deposited on the surrounding seafloor was a very calcareous, glauconitic muddy sand, bioturbated, with abundant shells and microfossils.

Several of the algal species found are more common in warm waters, however the limited number of studies on calcareous algae forming in temperate waters means that the inference of temperature ranges of these genera may be incomplete. Warm temperatures, similar to those proposed by MacGregor (1983) are supported by the occurrence of the warm water foraminifera *Asterigerina*. The algal band and the Waitakere Limestone appear to be of similar ages, although the age of the rhodolith band is poorly constrained.

Another occurrence of rhodoliths of a similar age occurs around Oamaru, where rhodoliths formed on the flanks of growing volcanic mounds of Runangan age (Lee *et al.* 1997), although Whaingaroan rhodoliths do occur in the area (D. Lee, pers. comm. 1998). These rhodoliths have far smoother surfaces than the rhodoliths at Woodpecker bay, and a far greater concentration and variety of other encrusting fauna, including corals, bryozoa, brachiopods, foraminifera and serpulid worms. The smoothness of the layers implies that the rhodoliths were turned more frequently than the Woodpecker bay rhodoliths. There are gaps in the rhodoliths apparently caused by boring fauna. Lee *et al.* (1997) infer a turning frequency of once to twice a year (based on size of encrusting fauna), paleobathymetry below wave base at around 25m and sea surface temperatures marginally subtropical. The rhodoliths lack many definite reproductive structures (conceptacles) making a positive identification of the algal genera present impossible.

Environment of deposition at Woodpecker Bay:

While encrusting organisms do occur on the rhodoliths at Woodpecker Bay, they are neither as frequent nor as diverse as the fauna from Oamaru. This may be caused by more frequent turning of the rhodoliths at Woodpecker Bay, Bryozoa do occur within the Rhodoliths (fig 5.3) but they do not attain a very large size before being broken and overgrown. Many fragments of branches occur both within rhodoliths and in the matrix between them. The

occurrence of upright branched forms implies that the rhodolith band was for the majority of the time below the level of significant wave action, although probably not below wave base, to cause the volume of small branch fragments. The depth probably did not exceed 20 m. Anderson (1984) presents evidence for the shallow depth of deposition of rhodoliths at Cape Foulwind, by showing the wave period and height necessary for moving rhodoliths at various depths. He concludes that the absolute maximum depth where the largest (150 mm) would be turned by storm events is 50 m. However, Harris *et al.* (1996) show that rhodoliths can be turned by shelf currents at moderate depths (40-140 m).

The transition from algal sands to algal gravels in the rhodolith layer implies shallowing conditions. While the sands may have been deposited after storms as deep as 20 meters, the rhodoliths in the upper parts of the layer were probably formed on the bar and turned by waves. Storms cut channels through the bar and probably eroded parts of it completely. During the period of solution, the rhodolith layer at seal island would have been at or above sea-level.

It is inferred that once rhodoliths began to accumulate, their size would make erosion of the rhodoliths more difficult, thereby aiding the growth and spread of the bar, until either the sedimentation rate increased, or all the algae were killed by some kind of environmental change or burial. When the bar of rhodoliths reached several tens of centimetres in thickness, the circulation of water through the sediment may have carried enough calcite to begin cementation. Cementation of the rhodoliths and algal fragments is inferred to have contributed to the permanence of the bar. Cementation of Mg-calcite is observed to occur in tropical algal-foraminifera reefs in Brazil, as far as several meters above the inter-tidal zone (Jindrich 1983). Coralline algal-serpulid boundstones on the modern day Freemantle Shelf (temperate waters) also contain hgh-Mg calcite cements (James and Bone 1992). Strong storms may have

succeeded in carrying rhodoliths up to 3 cm in diameter 1 km from the bar, but not in eroding the bar itself.

Sedimentation above and below Rhodoliths:

The increasing glauconite content and percentage of matrix in the Island Sandstone up to the rhodolith bar may imply that the sedimentation rate and the average energy of the environment was decreasing, although the sediment grain size was increasing. It may however also imply increasing deposition by short term, high-energy flows, which caught up detrital material, shells and glauconite and then rapidly dumped the sediment during waning flow. Deposition in this way would also explain the very poor sorting of the sediment. The glauconite in these sediments is likely to be transported, supporting deposition by short-term high-energy flows. Sedimentation by short-term high energy flows is inferred to be the main mechanism for deposition of the Island Sandstone. The Kaiata Mudstone, in contrast, has a much higher proportion of sediment deposited from suspension. The sediment beneath the rhodolith layers also contains an increasing proportion of larger shells, especially molluscs, probably caused by shallowing conditions upwards toward the layers.

The erosion event represented by the detrital sandstone horizon at Pahautane was followed by deposition of a limestone layer that contains 25% bryozoa fragments, although none of the bryozoa are in growth position. These fragments may have been washed down from a nearby shallow or shoreline area, which is not preserved, where bryozoa were abundant. At Seal Island the overlying glauconitic sandy algal limestone fills the cavities in the thick, cemented rhodolith layer, and gets progressively less glauconitic upwards.

Summary:

A major hiatus in sedimentation is implied by the presence of the rhodolith layers. The lack of sediment in parts of the thick, cemented layer that is composed of small fragments of algae

implies that sediment supply was very low. Also the frequency of storms that could carry such sediment was low. Calcareous algae grow in clear and/or shallow waters with abundant sunlight. The sea was likely to be cloudy due to the large amounts of silt and mud deposited in the surrounding areas, limiting the depth of growth of the algae to about 15 m maximum. The presence of supposedly "sub-tropical" genera in the rhodoliths does not necessarily imply that the seas in the Eocene to Oligocene were very warm, as rhodoliths have not been well studied in the Eocene and the environmental interpretations are based on more modern samples. However, their tolerances have probably not changed greatly since the Eocene, and the sea temperature at the time of deposition is inferred to be warm temperate at least.

The change vertically from algal sands to rhodoliths implies shallowing conditions, and the solution cavities in the top of the rhodolith band imply sub-aerial exposure to fresh water. Lateral changes within the bar from sands to rhodoliths probably represent channels caused by storm currents, which eroded parts of the bar. The rhodolith layers therefore represent a major break in sedimentation, and can be correlated with erosion or non-deposition events. recognised between the Island Sandstone and Nile Limestones in other locations.

Chapter 6

Fossils

Introduction

The Rapahoe Group contains a very diverse range of fossils. Calcareous micro and macrofossils have been examined for environmental interpretations. The calcareous encrusting algae are dealt with in Chapters 4 and 5. Previous work on the fossils was mainly restricted to the description of species found during mapping work that were useful for determining age. However, data has been published on some species of spatangoid echinoids, largely collected by H.G. Wellman (Henderson 1975). In addition some decapods discovered in the Island Sandstone were described by Feldman and Maxwell (1990), and some detailed sampling of Kaiata Mudstone sections was carried out by Srinivasan and Vella (1974) to determine foraminifera zones.

The Little Totara Sand has so far contributed no calcareous fossil material at all, except where it is inter-bedded with the Waitakere Limestone.

Macrofossils

Macrofossils recovered include arthropods, echinoderms, molluscs, brachiopods, worms, bryozoa and algae. The best preserved groups are those that originally had shells of calcite; most aragonitic shells have been dissolved, although occasionally their presence can be inferred from moulds in the sandstone or mudstone. Some aragonitic shells are preserved where the sediment is well cemented, especially near the top of the group where it is in contact with overlying limestones, and also where sedimentation has been rapid.

Another taphonomic characteristic of the Island Sandstone, is the occurrence around Perpendicular Point and Punakaiki of oval-shaped, concave-based accumulations of shells, frequently of only one or two species, especially when spatangoids and brachiopods are involved. Bryozoan fragments are the most common materials to occur in these oval accumulations. The accumulations tend to be elongate all in one direction, where three dimensions can be seen. The base of the accumulations are concave downwards, often with flattened upper surfaces (fig. 6.1). They range in size from 15 cm to about 45 cm long. These shell accumulations tend to occur together. The boturbation of the sediment around them means that they have probably been rearranged by burrowers, and may represent accumulations by burrowing animals. However, the accumulations are not associated with burrow structures, and the sorting of shells by size implies current deposition, as does the flattened upper surface. The accumulations probably represent deposits from currents in depressions on the sea floor, caused by current or storm wave activity. The collection of these accumulations into layers suggests deposition by an event occurring on the sea-floor, or storm reworking to a base within the sediment rather than collection by burrowing activities after deposition. The collection of small burrowing spatangoids into one of these masses may suggest that erosion of the sediment took place before the deposition of the accumulations.

a: Accumulation of juvenile spatangoids weathering out of the island Sandstone, fallen block, Perpendicular Point. F14P3.

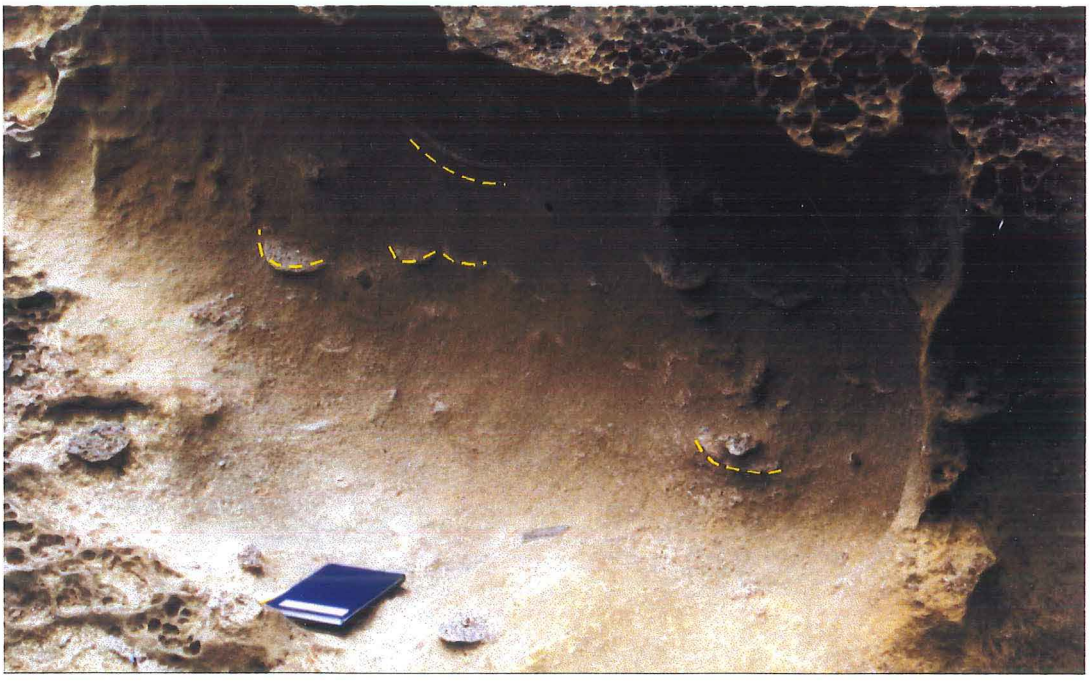

b: Layers of shell accumulations in bioturbated Island Sandstone, Perpendicular Point. Note the Concave bottom surfaces of the shell pockets. F14P4.

Figure 6.1: Shell accumulations in the Island Sandstone, Perpendicular Point.

Decapod Crustacea:

Decapod Crustacea are common in only one horizon within the Island Sandstone, and Feldmann and Maxwell (1990) described eight species of crab collected from a large sea cave at the end of the Truman Track, which leaves State Highway 6 about a kilometre north of Bullock Creek (fig 6.2). Crabs are also found in the same horizon to the north and south of this cave.

The fossil carapaces are found in the elliptical masses that occur frequently throughout the Island Sandstone in the Perpendicular Point to Punakaiki area. The shells occur in association with fecal pellets and spatangoids. *Duplipectin*, *Cirostrema,* two distinct brachiopod species, bryozoa fragments and other fragmentary fossil remains were also recorded by Feldmann and Maxwell (1990) from similar deposits as the crab fossils.

Feldmann and Maxwell (1990) identified *Laeviranina keyesi*, *L. pororariensis, Lyreidus bennetti*, *Rhachiosoma granuliferum*, *Pororaria eocenica*, *Carcinoplax temikoensis*, *Leptomithrax griffini* and *Notomithrax allani*. Eocene occurrences of *Lyreidus bennetti* are associated with sediments deposited in moderately high energy, inner-shelf environments, although extant species of *Lyreidus* occupy outer-shelf to bathyal habitats (Zinsmeister and Feldmann 1984, Feldmann and Maxwell 1990). *Rhachiosoma granuliferum* is a shelf form, endemic to New Zealand and found in both Westland and East Coast locations (Glaessner 1960, Glaessner 1980, Feldmann and Maxwell 1990). Modern *Carcinoplax* species are typically found in outer shelf and slope habitats (Feldmann and Maxwell 1990). Extant *Notomithrax* are associated with temperate habitats in Australia, the description of the Eocene species extends the time range of the genus and suggests a temperate southwestern Pacific origin (Feldmann and Maxwell 1990).

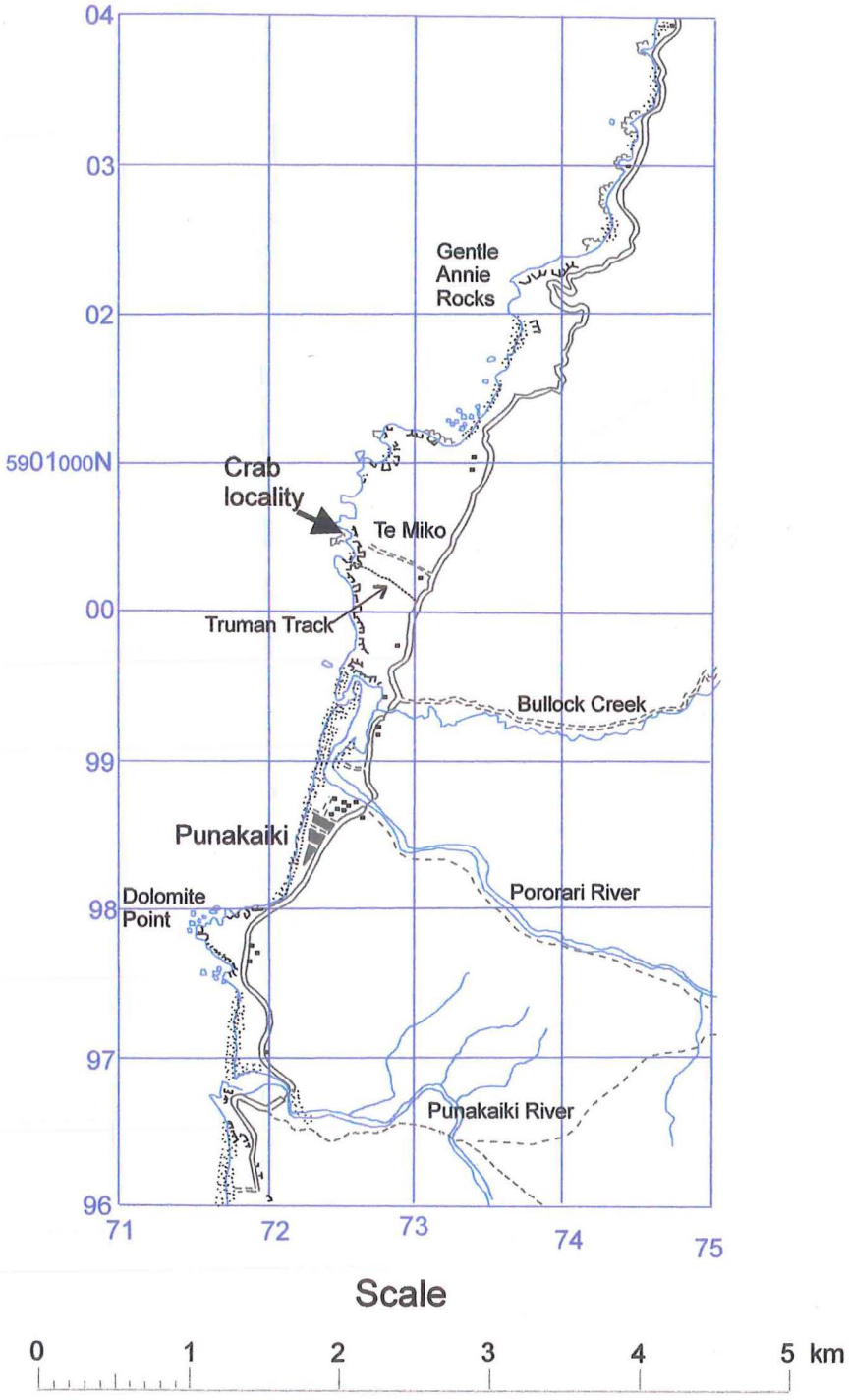

Figure 6.2: Location of sea cave containing many crustacean fossils

The only other Eocene crab fossil from the West Coast is *Tumidocarcinus tumidus* (Woodward) found at Woodpecker Bay (Feldmann and Maxwell 1990). This species lived over a wide bathymetric range but is not found in the crustacean assemblage at Truman Track, which Feldmann and Maxwell (1990) concluded may have been because the Island Sandstone here was deposited in shallower conditions than the species tolerates. The decapod Crustacea suggest a very shallow, moderate to high-energy conditions of deposition for the Island Sandstone around Punakaiki-Perpendicular Point.

Phyllum Echinodermata:

Crinoids tend to occur in deeper water, although some extant isocrinids live in shallower waters (Rasmussen in Moore and Teichert 1978). Crinoid stem plates are regularly encountered in thin sections, these have probably been redeposited from deeper environments by storm events. Crinoid stem ossicles are seen rarely that have glauconite precipitating within them, indicating a considerable time at or near the sediment-water interface. Other echinoderm plates may be from crinods or echinords.

Echinoids are the most common fossils over much of the Island Sandstone, with bivalves or bryozoa becoming more common in only a few places. Two major types of echinoid fossil are found: plates from echinoids, seen in thin section; and complete, broken or crushed specimens of spatangoids. The plates seen in thin section are generally rounded and most likely transported some distance before deposition. They may have come from regular echinoids rather than the spatangoids that burrowed into the sediment, although it is likely that some are from the irregular echinoids burrowing in the sediment as well as from crinoids.

It is rarely possible to be able to extract a spatangoid from the sediment, due to the calcite cementation of the Island Sandstone. Use of dilute (no greater than 10%) HCl acid, a scraping

instrument (knife), small wire pick and several brushes (wire and soft bristle) can effect separation of most of the fossil from the matrix.

The spatangoid fossils are commonly slightly crushed or deformed by burial pressures before cementation began. Fortunately, as spatangoids usually lie length parallel to bedding, and therefore perpendicular to burial pressure, the crushing compresses the test height. This crushing has the effect of obliterating any evidence for periproct shape and location, by causing the plates on the posterior margin to buckle and break.

Table 6.1: Fossil spatangoids collected from the Island Sandstone.

	Location	Name	Age
1	Smithy's Beach, Lower part	*Pericosmus annosus*	Kaiatan
2	Smithy's Beach	*Kina gracilus*	Kaiatan-Waitakian
3	Smithy's Beach	*Cardiaster*	
4	Smithy's Beach	*Schizaster (Paraster) exoletus*	Kaiatan-?Otaian
5	Smithy's Beach	*Cardiaster*	
6	Perpendicular Point	*Taimanawa prisca*	Kaiatan-Runangan

Table 6.1 shows only those fossils that could be collected in relatively good condition. Many fossils in the Island Sandstone cannot be removed, but show enough features to identify them (fig. 6.3).

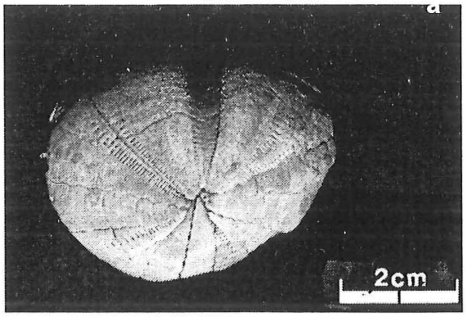

a and **b**: *Cardiaster* sp. from Smithy's Beach. The two specimens come from different parts of the section, **b** comes from near the top. No oral surfaces preserved. **a** is distorted and crushed.

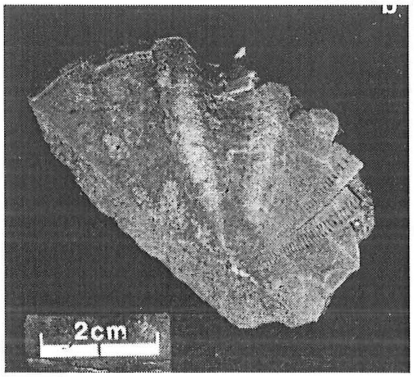

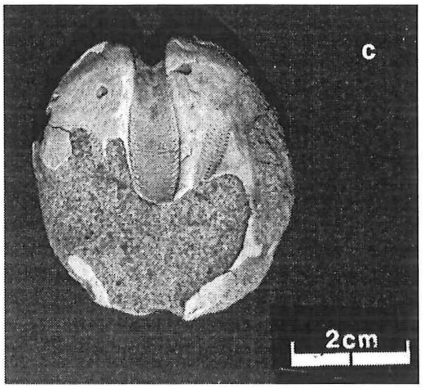

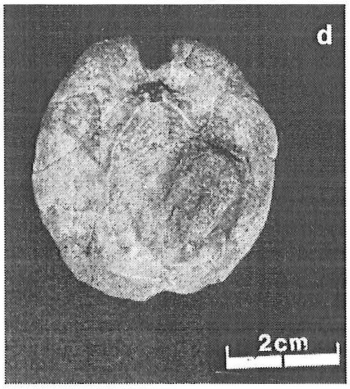

c and **d**: *Kina gracilus* from Smithy's Beach. **c** shows aboral surface with distinctive flaring ambulacra, **d** is the oral surface, showing deep frontal notch. Specimen crushed.

e and **f**: *Pericosmus annosus*, from Smithy's Beach. Specimen slightly crushed, **e** is aboral surface, **f** is oral surface.

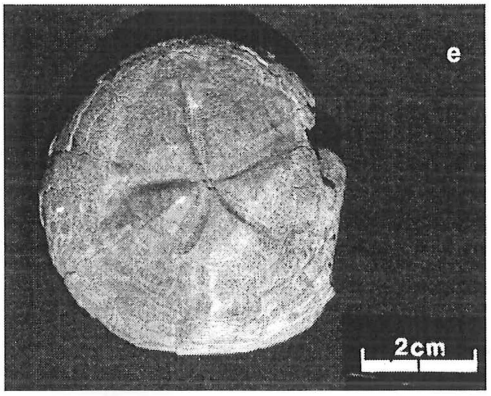

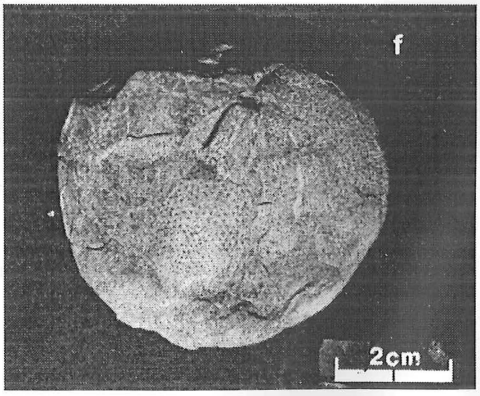

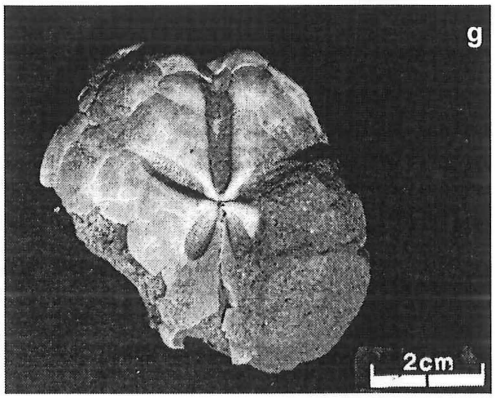

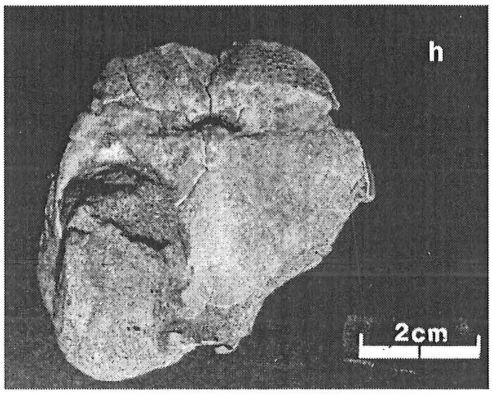

g and **h**: *Schizaster* sp., probably *Schizaster (Paraster) exoletus*. **g** is a view of the aboral surface, **h** shows the oral surface. Specimen is slightly crushed

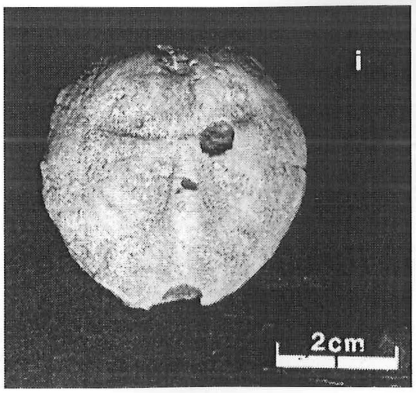

i: *Taimanawa prisca* from Perpendicular Point. Aboral surface only preserved.

Figure 6.3: Spatangoids from the Island Sandstone

The species of spatangoid found varies from place to place and within a section. At Smithy's Beach, the spatangoid commonly found near the bottom of the section is *Pericosmus annosus* (Henderson 1975), the holotype of which comes from the East Coast. The material used to define this species is poorly preserved (Henderson 1975), however direct comparisons of the type material held at Otago University with the fossils collected shows that they are the same species. *P. annosus* only occurs in the lower parts of the section at Smithy's beach. Further up the section, a *Schizaster* sp., probably *Schizaster (Paraster) exoletus* is common. A *Cardiaster* species and *Kina gracilus* (Henderson 1975) occur closer to the top of the Island Sandstone.

At Perpendicular Point, *Schizaster* sp. and *Taimanawa prisca* are the common spatangoids found. Spatangoids are only found in the parts of the succession that are bioturbated, hence at Perpendicular Point they are only found in the middle and upper part of the section, the rest shows primary stratification. Even in the largely bioturbated section there are erosion surfaces where spatangoid tests appear to have been concentrated in scours.

Echinoderms have broad environmental tolerances and there is little information on the environments favoured by the species identified. *Kina gracilus* and *Taimanawa prisca* are endemic to New Zealand, and restricted to the Eocene and Oligocene (Henderson 1975). The rest of the spatangoids are cosmopolitan in range, and the fauna has Tethyian influence (Henderson 1975). Henderson (1975) shows the present day distribution of many of the spatangoids is tropical to sub-tropical. Extant *Taimanawa* and *Pericosmus* species are tropical to sub-tropical. *Schizaster (Paraster)* ranges from tropical to temperate seas today. The low diversity of species in the sections (no more than 3 different species in any one part of the section) implies a lower temperature. The climatic conditions were most likely around the cooler limit of sub-tropical conditions. Feldmann and Maxwell (1990) suggest on the basis of previous studies of fossils and oxygen isotopes (e.g. Devereux 1967, Hornibrook *in* Suggate *et al.* 1978, Burns and Nelson

1981) and the ecological tolerances of extant spatangoid species that the New Zealand seas in the late Eocene were probably 5-10°C warmer than they are today.

Phylum Mollusca:

Bivalves are the most common mollusc found. They are usually a minor part of the assemblage or absent entirely, but become dominant in some horizons. Their abundance increases towards the top of the sections in the Kaipakati-Pahautane Point areas, and they are very common in and just below the overlying limestone. Here the most abundant shells are various species of *Duplipecten, Serripecten* or *Lentipecten,* but a giant oyster genus, probably *Crassostrea,* is more common than *Pectin* in the lower (Kaiatan) parts of the section. The oysters reach up to 25 cm long, and occur in large clusters that cannot have been transported far (see Chapter 4). Feldmann and Maxwell (1990 p. 783) tentatively identified a giant oyster they found in the Island Sandstone as a species of *Flemingostrea,* and used its presence and the presence of abundant Pectinidae as evidence for shallow water environments of deposition.

It is very rare to find molluscs in the Kaiata Mudstone: only one location, in the quarry at Cape Foulwind has yielded any fossils other than small, unidentifiable fragments. Here a fragment of *Pinna* was recovered, as was a single gastropod identified as a species of *Cirsotrema.* In other sections of the Kaiata Mudstone, casts of gastropods and bivalves are observed locally. *Pinna* is associated with mid to lower-shelf environments (Beu *et al.* 1990). *Cirsotrema* is unusual in that it has a calcitic shell.

Phyllum Brachiopoda

Brachiopods occur rarely in the Island Sandstone, and have not been found in the Kaiata Mudstone. Two types of brachiopod occur in the Island Sandstone: one is identified by Feldmann and Maxwell (1990) as a species of *Stethothyris*, which occurs singly and often crushed. The other, smaller brachiopod was tentatively assigned by Feldmann and Maxwell (1990) to *Terebratella*, but is closer to *Stethothyris tapirina* (Hutton 1873) from the Duntroonian of the East Coast (D.Lee pers.comm. 1998). These small (0.8 - 1.5 cm), smooth brachiopods are found in one locality, near where the crab fossils were found (Grid. Ref. 726003), and occur in the small oval collections mentioned previously. The brachiopods are frequently collected to the exclusion of all other fossil debris, which represents a degree of sorting in the currents that deposited them.

Microfossils

Microfossils recovered from the Rapahoe Group sediments are mainly foraminifera. Ostracods also occur, but very rarely. Only around Cape Foulwind, at Gibsons Beach and in the Cape Foulwind quarry are ostracods a dominant part of the microfossil assemblage.

Foraminifera

Foraminifera identified from each sample and age ranges are listed in Appendix III. The foraminiferal assemblage everywhere is dominated by benthic forms. Feldmann and Maxwell (1990) considered the foraminiferal assemblage found in the Island Sandstone near Punakaiki to be indicative of shallow water, containing mainly agglutinated species and some miliolids. In most sections, especially around the Punakaiki area, planktonic foraminifera are rare, and

frequently absent, especially in the coarser Island Sandstone. The diversity of the assemblages recovered from the sediments in the field area are also lower than those that occur in Island Sandstone and Kaiata Mudstone from the Greymouth region.

Srinivasan and Vella (1975) also noted the rarity of planktonic specimens at Cape Foulwind, and the dominance of porcelaneous foraminifera, from which they concluded that the water depths at Cape Foulwind were consistently less than 100 m. The low diversity indicates a more restricted circulation with the open sea. The maximum number of species that occur in a single sample is 14 identifiable specimens, from the Kaiata Mudstone at Gibsons Beach. Overall the Kaiata Mudstone has a higher diversity of both benthic and planktonic specimens than the Island Sandstone, which may reflect the higher energy, near shore conditions of Island Sandstone deposition. Most of the Kaiata Mudstone foraminifera assemblages suggest shelf to slope depths of deposition (Hornibrook *et al.* 1989), and genera such as *Stilostomella*, *Dentalia*, *Martinottiella*, *Cassidulina* and *Gyroidinoides* are suggestive of very quiet habitats with slow deposition (Hornibrook *et al.* 1989). The occurrence of some of the above genera in Island Sandstone samples is inferred to be due to the episodic nature of sedimentation for the Island Sandstone and Kaiata Mudstone. Strom events may have mixed assemblages from quieter, more offshore environments with assemblages from more active environments. Island Sandstone samples commonly contain *Arendosaria*, *Cibicides*, and *Melonis* genera, which are characteristic of shallow environments (Hornibrook *et al.* 1989).

Ostracods

Ostracods are only found commonly in Kaiata Mudstone samples from Gibsons Beach and the Cape Foulwind quarry, and also less commonly from Okari Lagoon locations. Most of the specimens are internal moulds, and almost 50% of the valves are conjoined, implying a high sedimentation rate which prevents bacterial action destroying the muscles holding the valves together, and means that the interstitial waters are undersaturated with respect to $CaCO_3$ (K.M. Swanson, pers. comm. 1998). However, the condensed section that occurs at Gibsons Beach yields ostracod specimens that are dominantly conjoined, so a high sedimentation rate is not needed to explain conjoined carapaces. Half of the specimens collected from the quarry are Platycopid ostracods of the genus *Cytherella*, including *C. splendida, C. micropustula*, and *C. hirsuta* (K.M. Swanson, pers. comm. 1998). The other Ostracods identified include *Bairdia* sp., *Philoneptunus* sp., *Bythocypis (Bythocypris)* sp., *Propontocypris* sp. and *Paracypris* sp., all of which have outer shelf affinities. The dominance by platycopid ostracods may be caused by an oxygen depleted environment (Whatley *et al.* 1994). The depth range indicated by the Ostracods is 500-1000 m (K.M. Swanson, pers. comm. 1998), but this is highly inconsistent with the location of the sample, within a few 10's of metres laterally of a shallow water algal limestone. The foraminifera samples from Gibsons Beach suggest water depths of less than 100 m (Srinivasan and Vella 1974), and that area is deeper than the area immediately around the quarry. The solution may be that the depth at which ostracods live may be controlled by the energy of the environment rather than the amount of water above them, and so the very quiet and sheltered environment in the basin probably meant that they lived at shallower depths. Another explanation is the probable deposition of deep water faunas close to shore during storm events.

Chapter 7:

Diagenesis

Cements

The majority of the Rapahoe group is cemented to varying degrees by calcite. The relatively low degree of compaction of matrix, fossils and trace fossils pre cement implies that the cementation happened relatively soon after deposition. The cement is frequently observed to overgrow echinoderm plates implying significant porosity during cementation, and to replace and alter bivalve and microfossil fragments. The cement is usually concentrated in layers of varying thickness and continuity (see Chapter 4). These layers can contain up to 64% $CaCO_3$. The rhythmic cementation that is observed in all outcrops of Island Sandstone and Kaiata Mudstone in the field area results from a variation in the amount of cement present, but as shown in Chapter 4, this variation in volume of cement is not related to textural differences (see fig. 4.6). In most samples, the cement appears to be replacing an original matrix, possibly of carbon rich clays.

The cause of the rhythmic cementation cannot be determined from the information available. Determining the chemical and physical conditions under which the calcite started to precipitate would help to work out the sequence of events, the timing and conditions of cementation. The composition, isotope chemistry and crystal structure of the calcite cement can be found by microprobe, bulk chemical analyses, XRD and SEM however, this problem is beyond the scope of this thesis. Some possibilities and evidence are presented here.

Literature on the subject of rhythmic cementation of sedimentary sequences ascribes

cementation as being related to textural differences in the sandstone and/or caused by diagenetic redistribution of biogenic calcite (fossils). In the case of textural differences often the better sorted or coarser sediments are preferentially cemented because their greater permeability allow for more calcite saturated pore waters to circulate (Hall *et al.* 1996). Other authors found that the cemented bands were created by the lateral joining of concretions. The rhythmic layering was caused by the distance between the concretion layers set by depletion of surrounding sediment of calcium carbonate (Bjørkum and Walderhaug 1990, 1993), or by separation of fossil rich beds that act as nuclei for the concretions (Fürsich 1982). Rhythmic cementation is ascribed to early calcite cementation on or just below the sea-floor (James and Bone 1992, Nelson 1988), often linked to organic matter degradation causing dissolution of $CaCO_2$ (Molenaar and Zijlstra 1997). In the case of the cementation related to the sea-floor (James and Bone 1992, Molenaar and Zijlstra 1997 especially) the surfaces of the cemented bands are frequently eroded and irregular, caused by syn- or post-cementation erosion. This irregularity is not observed in the Island Sandstone, and the association of cemented layers with layers of concretions tends to suggest that the layers are formed by merging concretions (fig. 7.1). The separation of these layers by irregular distances may be caused by the original cementation occurring at a specific horizon below the sea-floor. The complete bioturbation of the sediment, both in and out of cemented layers, means that cementation must have occured after bioturbation, and therefore below the sea-floor. The cemented layers may also be related to seasonal changes in pore-water temperature and composition, where the distance between cemented layers is controlled by the amount of deposition between seasons. Shells are not apparently concentrated in the cemented bands or depleted in surrounding less cemented horizons, although in general the sediments have few fossils preserved. Echinoderm fossils are found only in the less cemented layers, although thin sections of cemented layers show abundant fossil material, especially the more resistant calcite

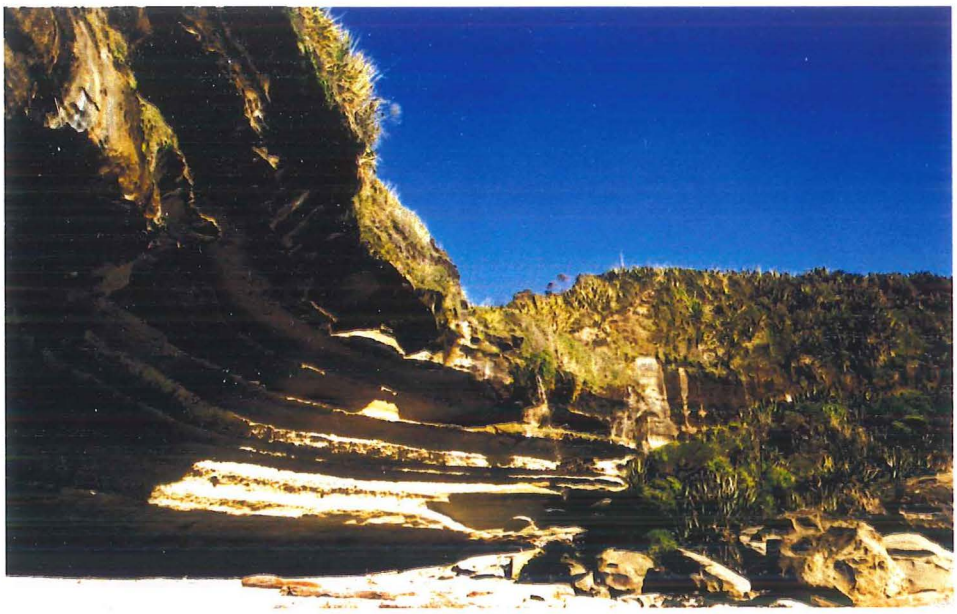

a: cemented layers weathering out with network trace fossils on the underside of the layers. Truman Track. F3P32.

b: cemented layers and strings of concretions, at Smithy's Beach. Pahautane Point (limestone) is in the distance. F1P17.

Figure 7.1: Rhythmic cementation in the Island Sandstone.

echinoderm fragments. The lower amount of small fossil fragments in the uncemented sandstones may reflect dissolution during the development of the cemented bands or an original heterogeneity that led to the nucleation of the calcite cementation in layers.

The thickness, continuity and frequency of the cemented layers decreases with decreasing grain size, that is, in the muddier parts of the Island Sandstone and Kaiata Mudstone the cemented bands are frequently bands of concretions and are separated by larger thicknesses of uncemented muddy sediment. The decreasing size and frequency of cemented bands may be caused by the presence of a higher quantities of clay in the sediments which inhibits cement formation, or because the process that causes the cementation does not reach into the deeper waters that these sediments were deposited in.

The occurrence of cement supported grains implies that the cement replaces a matrix (fig. 7.2a&b), so the inhibition of calcite cementation by clay presence is unlikely to be the dominant controlling factor. At the Gibsons Beach (Kaiata Mudstone) section especially, the number and frequency of cemented layers increases with increasing grain size (and trace fossil size), probably due to greater pore space. In the lower and middle parts of the section, the sediment is very muddy and there are no cemented bands, only three clay horizons. In the upper part, the sediment is distinctly siltier and the cemented bands increasingly common. Towards to top of the Kaiata Mudstone, the trace fossils begin to be filled with coarser sediments, sands and granules, indicating rapidly increasing energy (probably shallowing) conditions. It is at the top of the section that the cemented bands are at their greatest frequency and prominence. The shallowing may also be the reason that the cementation occurs: possibly because of increasing pore space due to increasing grain size; or by increasing the amount of biogenic calcium carbonate that is deposited in the sediments; or by changing the chemical conditions leading to solution and reprecipitation of calcium. Possibly land derived groundwaters mixing with saline porewaters,

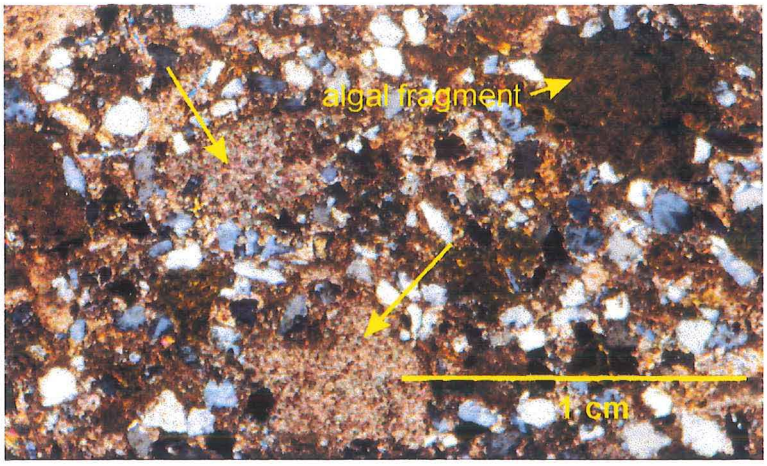

a: Calcite cement in Island Sandstone. Note the calcite overgrowths on echinoderm fragments (arrowed). HLS 2, cpl.

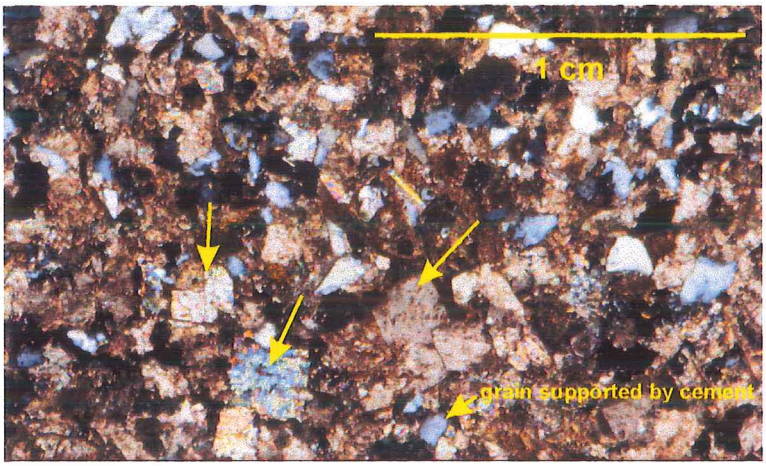

b: Euhedral calcite crystals (arrowed) in cemented Island Sandstone, Perpendicular Point. HLS 68, cpl.

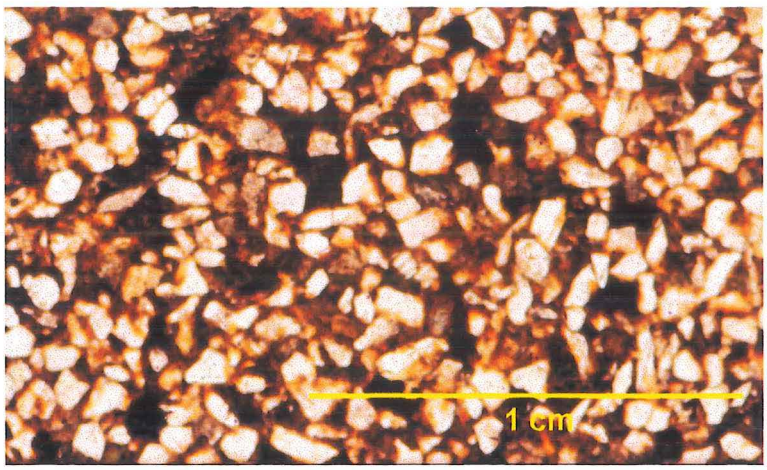

c: Iron oxide cement (probably hematite) in Island Sandstone from Punakaiki River Gorge. HLS 77, ppl.

Figure 7.2: Calcite and iron oxide cements from the Island Sandstone.

or seasonal changes in the supply of fresh water that changes the temperature and chemical conditions enough to begin cementation in the sediments.

The other major cement is an opaque cement, probably hematite. In most samples this occurs with a calcite cement, seeming to have developed simultaneously. The opaqueness of the cement makes determining the original texture of the sandstone and the textures of the cements difficult. The cement commonly appears red in thin section, the colour suggests that the mineral is hematite, and in the sample from the eastern side of the basin, beyond the Punakaiki River Gorge, a similar cement, here not mixed with calcite, displays uniaxial -ve interference figures (the hematite is not completely opaque in this case, but tanslucent and red, see fig 7.2c), supporting the identification of hematite as the cementing mineral. The source of the hematite in the Island Sandstone may be found in the common occurrence of euhedral to anhedral opaque black grains of detrital magnetite. Black opaque grains are often seen associated with the red coloured cement.

The third cement that occurs in the Island Sandstone is chalcedony cement. This cement occurs only at one horizon and the surrounding layers, in a small beach just south of Perpendicular Point (K30 728010). The cement occurs as infilling of porespaces, between grains and in fossils and veins, and also as replacement of detrital framework grains. It occurs after an early calcite cement, that can be seen fringing detrital grains and replacing aragonitic fossils (fig. 7.3). The chalcedony crystals are mainly length fast and microcrystalline chalcedony fabric is common (fig. 7.3). This cement has not as yet been found elsewhere in the Island Sandstone, and in restricted to a narrow (30 cm) zone in the outcrop, centred on the 5 cm layer containing pink coloured chalcedony concretions. The source of the silica is unknown, for while some quartz has been replaced with microcrystalline chalcedony, there is no evidence in the surrounding

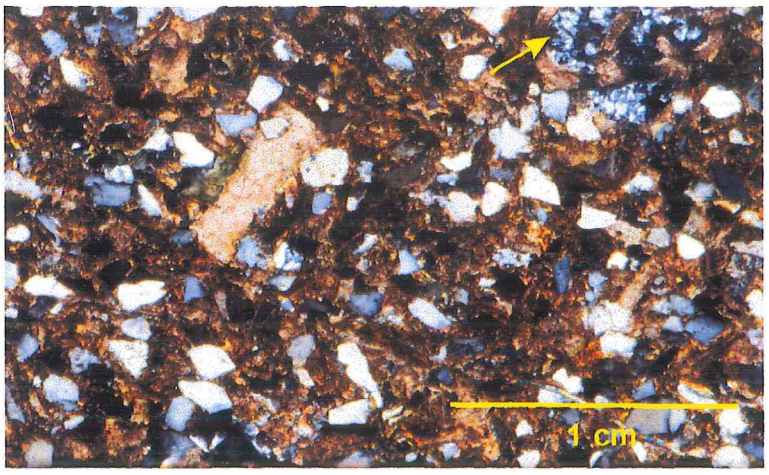

a: Chalcedony infilling a foraminifera test (arrowed). The rest of the view shows calcite cemented sands. HLS 67, cpl.

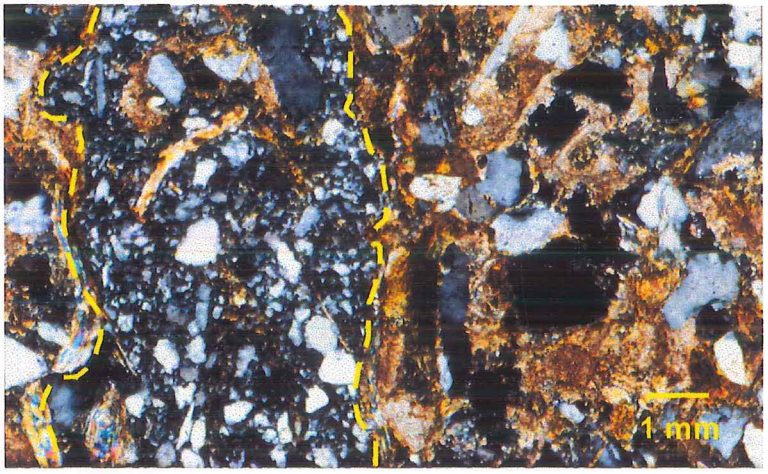

b: Chalcedony infilling a vein in Island Sandstone, to the left and right of the vein detrital sand, mica and fossils are cemented with calcite. HLS 85b, cpl.

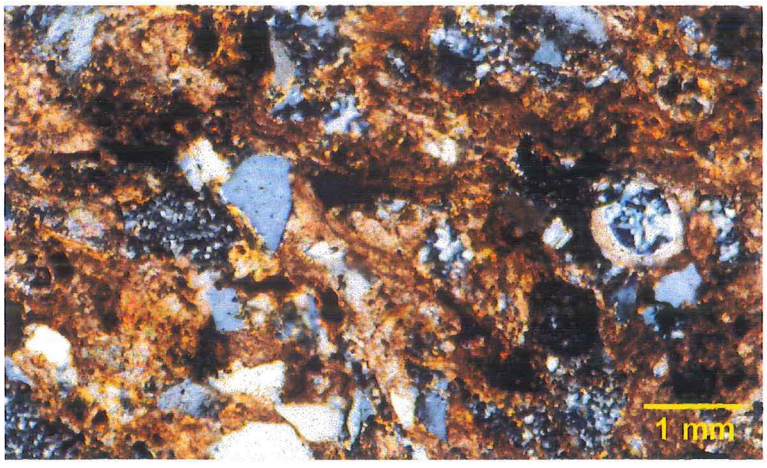

c: Chalcedony infilling dissolved pores and a foraminifera test. Microcrystaline fabric in most places, larger crystals extending from edge of microfossil. HLS 85b, cpl.

Figure 7.3: Chalcedony cement in the Island Sandstone, from south of Perpendicular Point.

sediments for dissolution of detrital quartz. Possible silica sources include dissolution of detrital quartz elsewhere, possibly by fluids given off during coalification of Brunner Coal Measures, siliceous microfossils such as diatoms and the smectite to illite transformation. The problem remains of why the cement is restricted to a very narrow horizon.

The layer containing chalcedony concretions occurs 50 cm above the beginning of bioturbation (see Chapter 4). The dissolution of the early calcite cement could have been related to chemical changes of the groundwaters, from marine to freshwater for example. However, unconformity-related silica precipitation would not have also deposited chalcedony cement in the sediment above the concretion layer (6% of the sample was chalcedony), and the layer itself should show uneven upper surfaces, which are not seen. The chalcedony cement must be diagenetic in origin. The dissolution of the early calcite cement and some fossils may in this case have been caused by solution by invading fluids, occurring in a relatively high calcite/original matrix layer. Hesse (1990) reviewed the literature on silicification of sediments and found that in carbonate sediments the silicification can occur before and with early carbonate cements and before, during and after both aragonite to calcite transformations and high-Mg Calcite stabilisation. Hesse (1987) found that silica could be sourced from pressure solution of quartz and feldspars in the host sediment and the smectite (montmorillonite) to illite transformation in associated shales. The Kaiata Mudstone contains no smectite clays and it is possible that the release of silica during the transformation of smectite to illite during diagenesis is the source of the silica cement. Alternatively, waters released during coalification could be responsible by dissolving quartz and feldspars in some other, unseen area then depositing it in this layer, although this seems unlikely.

Diagenetic changes also affected the clay mineral assemblage. Smectite and minor illite is the expected clay mineral expected to be deposited in marine pore-waters (Hesse 1987), but the Kaiata Mudstone contains Kaolinite, llite and Vermiculite, a diagenetic assemblage created

during burial not exceeding 4 km (Burley and MacQuaker 1992) by the alteration of biotite to vermiculite, smectite to illite and K-feldspars to kaolinite (Drits *et al.* 1997, Sakharov *et al.* 1999). Kaolinite could be sourced from erosion of Brunner Coal Measures, and can also be caused by weathering, as can vermiculite. The structural arrangement of the clays is unknown, the three clay minerals could occur individually or as a mixed-layer clay (Sakharov *et al.* 1999).

Burial History

Nathan *et al.* (1986: fig. 3.18) maps variation in vitrinite reflectance and Suggate Rank of the Brunner Coal Measures on the West Coast. The highest ranks and vitrinite reflectance values correspond to the higher maturation of the coal (Suggate 1959, 1974), which is caused by increasing depth *and/or* temperature. To interpret the maximum depth from vitrinite reflectance or rank data the geothermal gradient of the area at the time of burial must be known. However, an approximation of the maximum depth that the Eocene sediments reached can be estimated by examining the thickness of overlying sediments. On the western side of the Punakaiki-Charleston basin, where the Eocene units are thin, the Oligocene and Miocene deposits are also thin, and the maximum burial that the Eocene sediments could have been subjected to is about 1500 m. On the eastern side of the basin where the sediments are thicker, and in the axis of the 'Paparoa Trough', the Eocene to Pleistocene sediment thickness reaches up to 4000 m. These depth estimations are based on isopach maps in Nathan *et al.* (1986) and are in agreement with the rank and reflectance maps, which show the greatest values within the 'Paparoa Trough'. Eocene and Oligocene sedimentation was thickest in the trough, while Miocene sediments are more widespread, and thickest on the western side of the Paparoa Tectonic Zone and off-shore, reflecting the change in tectonic regime to compressional. The compressional regime resulted in the reactivation in the reverse sense of many of the basin margin faults, so that those areas where subsidence and therefore sediment thickness and burial depth were largest, the uplift was greatest. These areas are now exposed on plateaus and mountain ranges, and frequently as is the case east of the Paparoa Teconic Zone in the field area the Eocene sediments have been removed by erosion.

Chapter 8:

Basin Evolution

Introduction

From the physical properties, structure, sedimentology and paleontology, inferences about the environment of deposition of the sediments can be made. Much of the evidence comes from the sedimentology which was presented in detail in Chapter 4. The paleontological evidence can be found in Chapter 6. Mapping the changes in environment of deposition in the field area over time leads to a series of diagrams showing changing paleogeography. The changes in paleogeography over time reflect changes in relative sea level, tectonic subsidence and uplift in the basin and filling of accommodation space. From this information, the evolution of the basin through the Late Eocene and early Oligocene can be inferred.

Correlation of Stratigraphy

The first step in developing basin-wide paleogeographic maps is correlating the stratigraphy in various parts of the basin, to enable comparison of the sediments that were being deposited at a certain time. The lithological correlation presented in fig. 8.1 is partially based on measured sections (appendix I), some core logs from Nathan (1975b) and some estimations based on the mapped extent of the formations. The correlation is not based on the age of the sediments, but rather the overall lithology.

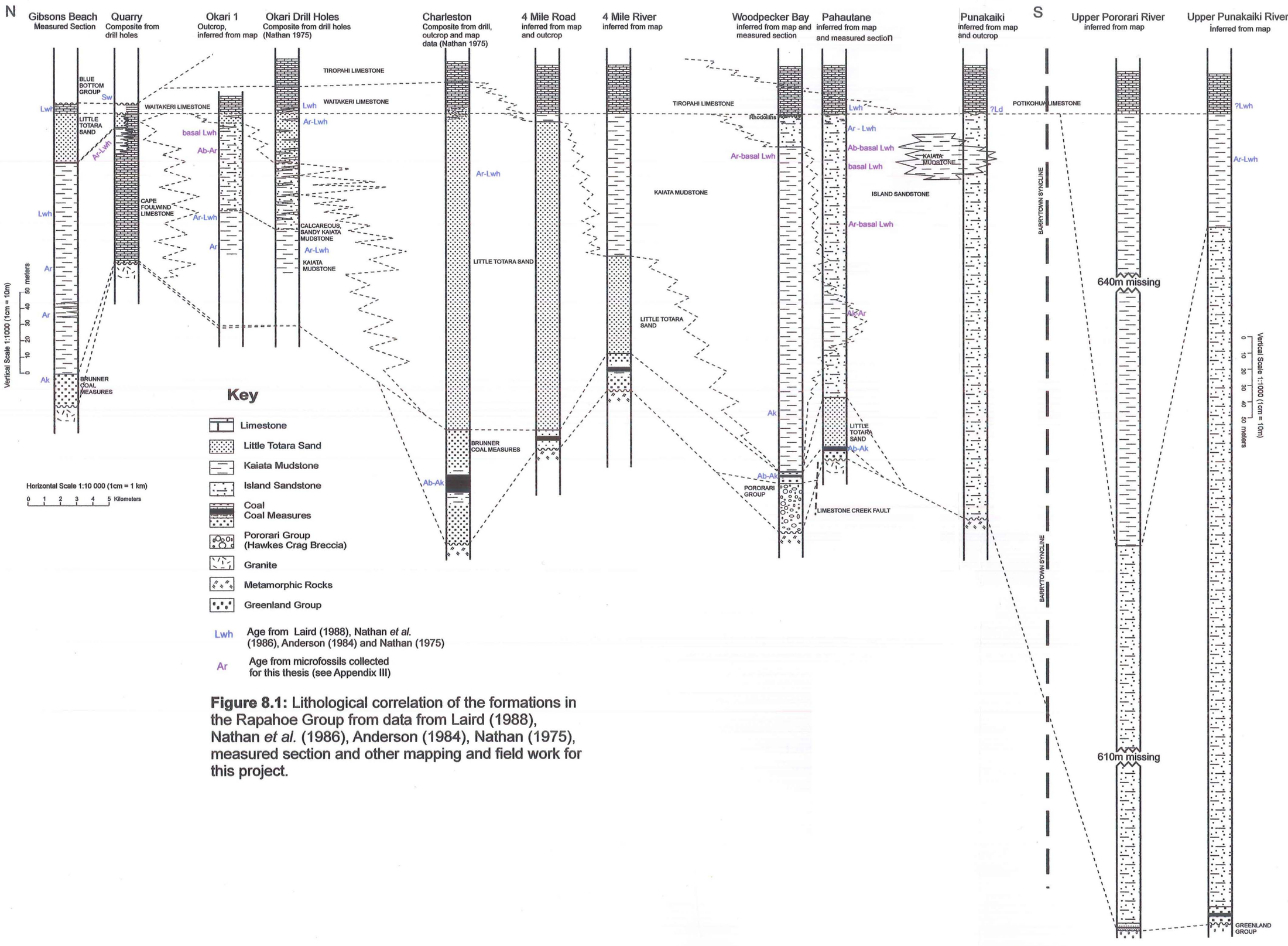

Figure 8.1: Lithological correlation of the formations in the Rapahoe Group from data from Laird (1988), Nathan *et al.* (1986), Anderson (1984), Nathan (1975), measured section and other mapping and field work for this project.

Dating the sediments is difficult, especially as the diversity of microfossils is relatively low and most of the planktonic zone fossils are missing (Chapter 6), and the macrofossils have broad age ranges or are unidentifiable. The sections based on outcrop patterns have little age control as the outcrop is very limited and very few samples could be collected. Approximate time horizons can be drawn across the correlation (fig. 8.2), which can be used to draw paleogeographic maps. The age of the overlying limestones is from Anderson (1984).

Environmental information

Little Totara Sand

The Little Totara Sand's many sections represent different environments, but all of these are part of a shoreline complex. The sand contains dune, beach and tidal channel and bar complexes (see Chapter 4). At Gibsons Beach the poor sorting, large scale cross bedding with well sorted laminations implies deposition in dune environments. In contrast, exposures around Charleston frequently show two directions of cross-bedding, sometimes with drapes of lighter mica. Herringbone cross bedding can be clearly seen in one road cutting, and reactivation surfaces have been identified in a cross-bedded unit. All these structures imply deposition in a tidal environment, probably a channel-bar complex. Other sections display no cross bedding, only indistinct bedding and lenses of coarse and fine material, disrupted by erosion and bioturbation. These sections are inferred to be beach deposits. The grain size analyses of Little Totara Sand samples shows a wide variability in distribution characteristics, largely because each analysed sample comes from a different section and usually a different environment of sedimentation.

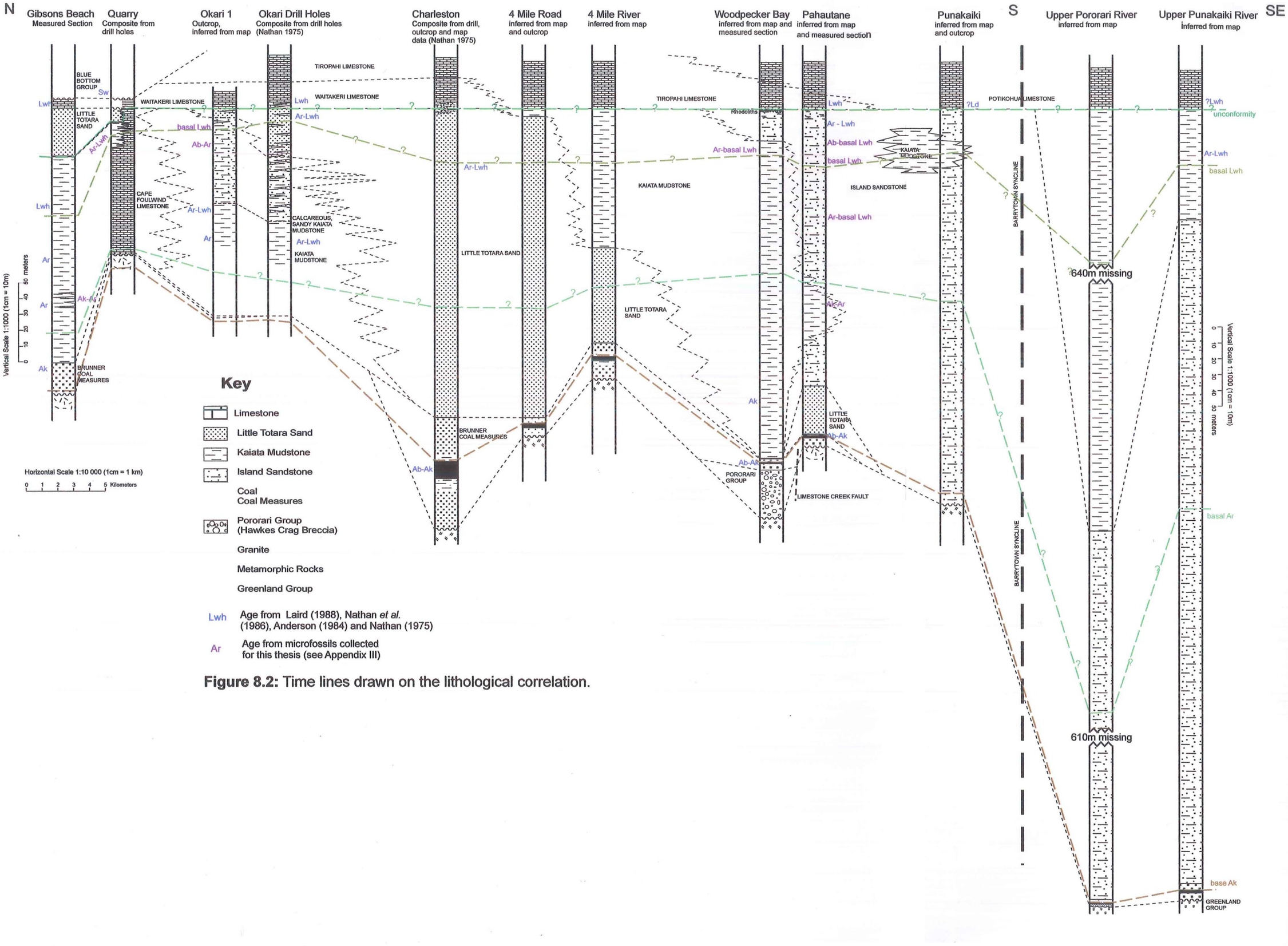

Figure 8.2: Time lines drawn on the lithological correlation.

The occurrence of Little Totara Sand is a convenient paleoshoreline indicator. Little Totara Sand occurs both under and over the limestone at the Cape Foulwind Quarry, proving that the unit is time transgressive. In the case of Gibsons Beach and the Cape Foulwind Quarry, the Little Totara Sand was deposited on and around the basement high, then retreated with the transgression, probably southwards and westwards, towards the inferred landmass to the west (see Introduction and later discussion), and the almost permanent beach/tidal bar accumulation around Charleston to the south. The later regression brought the Little Totara Sand back to the Gibsons/Quarry area.

The current directions obtained from cross-bedding in the Little Totara Sand (see fig. 4.20) show a wide variety of directions. The windblown sands at Gibsons Beach show a predominant wind direction towards the east and north, while tidal and current-deposited sands show overwhelming transport towards the southwest and southeast, largely parallel to the basin axis. This may represent long-shore currents running from one end of the basin to the other. In the vicinity of Charleston the Little Totara Sand is very thick and extensive, and is dominated by tidal bar, channel and beach deposits. This may represent a permanently shallow point in the basin close to emergent land (due to sedimentation keeping pace with subsidence and/or a paleogeographic high), or Charleston may represent the turning point of the transgression-regression cycle. The long period of time that the Little Totara Sand was deposited over (Kaiatan to Lower Whaingaroan) implies that the shoreline was relatively stable in this area, and therefore this area was a shallow point in the basin. The occurrence south of Charleston of Kaiata Mudstone, which overlies the Little Totara Sand and pinches out to the north, is inferred to have been deposited by the transgression gradually covering the Little Totara Sand deposits from the south to the north across the shallow area. The regression began before the shallowest region north of Charleston could have Kaiata Mudstone deposited on it. The transition from Little

Totara Sand to Kaiata Mudstone is unfortunately not exposed anywhere, the contacts mapped by Laird (1988) are inferred rather than seen, so it is unknown whether the contact is gradational or abrupt, or what the nature of the Little Totara Sand is directly below the contact. The occurrence of Kaiata Mudstone in this area rather than the Island Sandstone may be related to the apparent isolation of this section of the basin, between the high beach area to the north (Charleston) and the relatively shallow waters south of the Limestone Creek Fault (Pahautane). The sections from Woodpecker Bay to Charleston are dominated by muddy Kaiata Mudstone, that contains very few planktonic foraminifera, and was deposited in a very sheltered and quiet environment, probably not very deep. This may have meant that sands were only deposited close to shorelines and in very shallow waters. Around the Limestone Creek Fault, the thickness of Little Totara Sand (30 m to the south) drops abruptly to virtually nothing, and the Island Sandstone is not deposited north of the fault until the Lower Whaingaroan. This change in deposition across the fault implies that it was active for at least the Kaiatan and Runangan stages, and probably into Oligocene limestone deposition as well. The fault is inferred to be have had a down to the north sense of movement during deposition of the Rapahoe Group, the south side has thick shoreline and shallow marine deposits whereas the north side has Kaiata Mudstone, with basal lenses of Little Totara Sand, likely to be derived from the south side by storms or slumps. The fault was inferred to be present by Laird (1988) and can be clearly identified in parts of Limestone Creek, where the outcrops on either side of the creek do not match. The fault has been active after the Oligocene, with the same sense of motion as before, so that now limestone is in fault contact with Little Totara Sand in Limestone Creek.

Island Sandstone

The basal parts of the Island Sandstone around Punakaiki show clear evidence (hummocky cross-stratification, burrowed horizons, scours) of episodic deposition by storm events. The rhythmic cementation may also reflect episodic deposition (Chapter 7), and the shell accumulations that frequently occur throughout the Island Sandstone also imply episodic deposition by storm events (Chapter 6). The Island Sandstone is inferred to be deposited in shallow, shelf environments, above storm wave base and relatively close to shoreline. Laird (1988, p. 26) concluded that the environment of deposition was "shallow marine offshore, probably inner to middle shelf" and Feldmann and Maxwell (1990, pg. 783) found that "Paleontological evidence, such as it is, is in broad agreement with this assessment.". The macrofossils found in the Island Sandstone vary from very shallow crinoid and bryozoa fragments that are obviously transported (eroded edges), oysters that because of their large size cannot have been transported great distances, to spatangoids that lived more or less where found. The presence of shelly material from very shallow waters and giant oyster shells implies relatively shallow deposition. The spatangoids, unfortunately have large depth ranges, when such information is known.

Kaiata Mudstone

Laird (1998) place the deposition of the Kaiata Mudstone on the middle to outer shelf. The complete bioturbation of the Kaiata Mudstone indicates a low overall sedimentation rate. Like the Island Sandstone, the Kaiata Mudstone was probably deposited episodically, and the muddiest parts of the Kaiata Mudstone are therefore the furthest away from the sediment source and from disturbance by wave generated currents. However, the presence of *Pinna*, *Cirostrema*, large agglutinated foraminifera, giant *Crassostrea* and spatangoid fragments implies shallower

conditions. Srinivasan and Vella (1975) concluded from foraminiferal evidence that the depth of deposition of the Kaiata Mudstone at Gibsons Beach was less than 100 m. They also noted the rarity of planktonic specimens, which may indicate restricted circulation with the open ocean (Kear and Schofield 1959). Restricted circulation, such as occurs in an embayment or gulf, means less current and storm energy affecting sedimentation, and therefore quieter environments closer to shore than occurs in an open sea situation. Therefore the Kaiata Mudstone could have been deposited much closer to the shoreline and shallower than suggested by the clay and mud content.

The ostracods found in samples of Kaiata from the Cape Foulwind area are associated with low oxygen conditions or "kenoxic[1]" events (Chapter 6, Whatley *et al.* 1994). There are other indications that the Kaiata Mudstone was associated with low oxygen conditions, such as the growth of pyrite in the sediment, and the oxidised rims that occur on many burrows. Pyrite is formed by alteration of iron bearing minerals under reducing conditions. The process is aided by the presence of organic carbon compounds, which may be why the pyrite commonly occurs associated with burrows as well as disseminated through the sediment. The organic carbon provides electrons to convert the iron to the ferrous state and bond it to sulfur (Boggs 1987). Pale rims around burrows can form when the animal that created the burrow pumps oxygenated water from the surface through its burrow, which extends down into anoxic sediments (Bromley 1996). The presence of pyrite and haloed burrows indicate that the *sediment* was low in oxygen shortly after deposition, although the complete bioturbation implies enough oxygen at the sediment water interface to support abundant burrowers. The low oxygen may be associated with or caused by restricted circulation between the basin and the open sea. The presence of significant organic

[1] a kenoxic event is defined by Cepek and Kemper (1981 in Whatley *et al.* 1994) as an event where oxygen levels are depleted to result in dysaerobia, which some organisms were able to survive.

carbon in the Kaiata Mudstone (Nathan and Smale 1983) supports low oxygen in the sediment, which would inhibit bacterial breakdown of deposited organic carbon.

Srinivasan and Vella (1975) noted a change in the foraminiferal assemblage over the Runangan to Whaingaroan boundary. Porcelaneous (more delicate) faunas are more dominant in the Runangan and are partly displaced by Elphidiidae in the Whiangaroan, and a decrease in the total abundance of foraminifera also occurs in the Whaingaroan. Srinivasan and Vella attributed these observations to a difference in sedimentation rate, that is that the sedimentation was slow and the water quiet in the Runangan, and sedimentation was faster and conditions more turbulent in the Whaingaroan. The change in assemblage could also be caused by a change in the depth of deposition (Phleger 1960). The lower part of the section (Runangan) is muddier and contains at least one condensed section indicating quiet, slow deposition, while the upper (Whaingaroan) part of the section gets progressively siltier upwards and had more turbulence and a higher sedimentation rate, with increasing, coarser sediment supply indicating shallowing and deposition closer to the paleoshoreline.

Relative Sea Level Changes

All the beach sections that could be examined in detail showed changing lithology that can be related to changes in *relative* sea level. These three sections are at Gibsons Beach, Woodpecker Bay and Smithy's Beach. Also included is a composite section of several exposures including Perpendicular Point, road exposures, Bullock Creek and Punakaiki Township.

Gibsons Beach

At Gibsons Beach, the base of the Kaiata Mudstone is Runangan and represents relatively deep water deposition. The underlying ?Kaiatan sands are fluvial to marginal marine and are correlated

with Brunner Coal Measures, although no coal occurs at Gibsons Beach. The flow of debris from the nearby shallow water algal mound into the lower part of the Kaiata Mudstone indicates that the lower parts of this section were not far from a shoreline. The Kaiata Mudstone gets progressively muddier towards the middle of the section at Gibsons Beach, and in the muddiest part three clay layers occur that are interpreted as representing a fluctuating maximum of transgression (see Chapter 4). The foraminifera from either side of the clay layers give an age range of Ar-basal Lwh (HLS 88, Appendix III), and the location of the layers is around the boundary between the Runangan and Whaingaroan identified by Srinivasan and Vella (1975). Towards the top the sediment becomes siltier, then abruptly sandy, and considerable erosion has occurred before the deposition of shoreline lagoonal mud and beach and dune sands. The Gibsons beach section is inferred to show a gradual transgression (from fluvial-marginal marine "Brunner" sands to mudstone with no cemented bands), followed by a fluctuating maximum (several clay layers and condensed sections representing slow deposition, separated by sections of silty Kaiata), a gradual then abrupt regression (increasing silt content, followed by sand-granule deposition, followed by erosion of more than 4 m), then a slight transgression (lagoonal silt/muds and shoreline sands), followed eventually by a transgression leading to the deposition of the shallow water Waitakere Limestone.

Close by in the Cape Foulwind Quarry, the Little Totara Sand is found both under (Lewis pers. comm. 1999) and overlying the Cape Foulwind Limestone. As the Little Totara Sand is a shoreline deposit, this confirms the transgression-regression sequence from sub-aerial erosion - marginal marine - fully marine - marginal marine.

Woodpecker Bay

In the Woodpecker Bay section, the Kaiata Mudstone at the base of the sequence interfingers with shoreline Little Totara Sands (Laird 1988, pers. comm. 1999). The Kaiata Mudstone exposed at the base of the section is also sandier and contains more cemented layers, larger traces and *Ostrea* shells than the middle part. The Kaiata Mudstone exposed in the middle of the section at Woodpecker Bay is muddier, contains smaller traces fossils only and has fewer cemented bands. Towards the top of the section the cemented layers increase in frequency, and the Kaiata Mudstone grades up into silty Island Sandstone. The top of the Island Sandstone is marked by a layer of rhodoliths that increase of size from the bottom of the layer to top suggesting increasing energy suggesting shallowing, which is supported by the occurrence of dissolution due to sub-aerial exposure on the top surface of the rhodolith layer (see Chapter 5). The section at Woodpecker Bay therefore also shows a transgression-regression-transgression sequence, as occurs at Gibsons Beach.

Pahautane

The Smithy's Beach succession less than one kilometre to the south however, has a different appearance. The lowest parts of the section that can be seen are muddy, and about 6 m of Kaiata Mudstone can be seen at the bottom. Higher in the succession, the sediments become sandier, although more fluctuations from sandy to muddy sediments can be seen in this section than any other. Towards the top, however, the amount of mud decreases, and the amount of shelly material increases. The Glauconite content increases abruptly just before the top, as in the Woodpecker Bay section. The glauconite is transported into the sediment, rather than being formed where it was deposited, but implies that changing conditions favoured glauconite formation somewhere nearby. The top of the sandstone is marked by a less cemented layer of detrital sand that lies

between two well cemented, abundantly fossiliferous layers. The erosion between sandstone and limestone deposition is not as obvious here as it is a few kilometres south at Bullock Creek.

The exposed base of the Smithy's beach section is probably some stratigraphic height above the actual contact with Brunner Coal Measures. The Kaiata Mudstone occurrence at the base of exposure can probably be correlated with the muddiest part in Woodpecker Bay, and the sequence above to the gradual, fluctuating regression towards the top of the sequence. Unfortunately the age control on both of these sections is poor, so exact correlation is impossible.

Punakaiki

The Rapahoe Group at Punakaiki consists of Island Sandstone and some sandy Kaiata Mudstone in some sections. The base of the succession at Perpendicular Point rests on granite, and the Island Sandstone oversteps underlying Brunner Coal Measures and Little Totara Sand to onlap against what was a basement high. At the base the Island Sandstone is relatively well sorted and contains less mud than at the locations around Pahautane. Muddy sections still occur in the middle of the succession. Basal sandstone, with scours and hummocky cross-stratification passes up into muddier bioturbated rhythmically-cemented sandstone, a transition that probably represents a deepening in environment of deposition, to lessen the sediment supplied and the impact on the deposited sediment of major storm events (see Chapter 4). The rhythmically-bedded Island Sandstone is muddier, but passes up into well sorted sandstone towards the top of the section. The overlying contact with the ?Whaingaroan limestone is marked by an erosional surface and local discordance of up to 10° in Bullock Creek (Laird 1988): rare, isolated gneiss boulders occur along the contact around Punakaiki where it appears to be gradational (Laird 1970). The lowest part of the overlying limestones contains quartz pebbles and phosphatic nodules (Anderson 1984, Laird 1988).The erosion is inferred to be the result of the relative drop

in sea level indicated elsewhere in the basin.

Summary and Comparison to Global Eustacy

All the sections that are available for examination show a transgression-regression-transgression cycle. The first transgression is from estuarine/fluvial Brunner Coal Measures to a transgressive maximum marked by mud or clay deposition. The regression is marked by more silt then sand deposition, and ends in erosion and/or sub-aerial exposure wherever the contact can be examined in detail. After this erosion event, transgression begins again. The overall pattern is overprinted by minor fluctuations causing changes in lithology, condensed sections, clay layers, and firmgrounds throughout the sections (Lever 1998).

Correlating stratigraphy to global eustacy (e.g. Haq *et al.* 1987) has had limited success in New Zealand, largely due to the tectonic controls on New Zealand basins, rather than the accommodation space being controlled by sea-level and gradual subsidence alone. The global eustacy chart in fig. 8.3 (Abreu and Anderson 1998) is the latest chart published, and is based on a new oxygen isotope record. The isotope record is compared with a sequence stratigraphy-derived eustacy curve. The relative sea level curves produced for each section in the Punakiaki-Westport basin by examining the changes in lithology, fossils and trace fossils can then be drawn against the global sea level chart (fig. 8.3). The curves are approximate and the transgressions

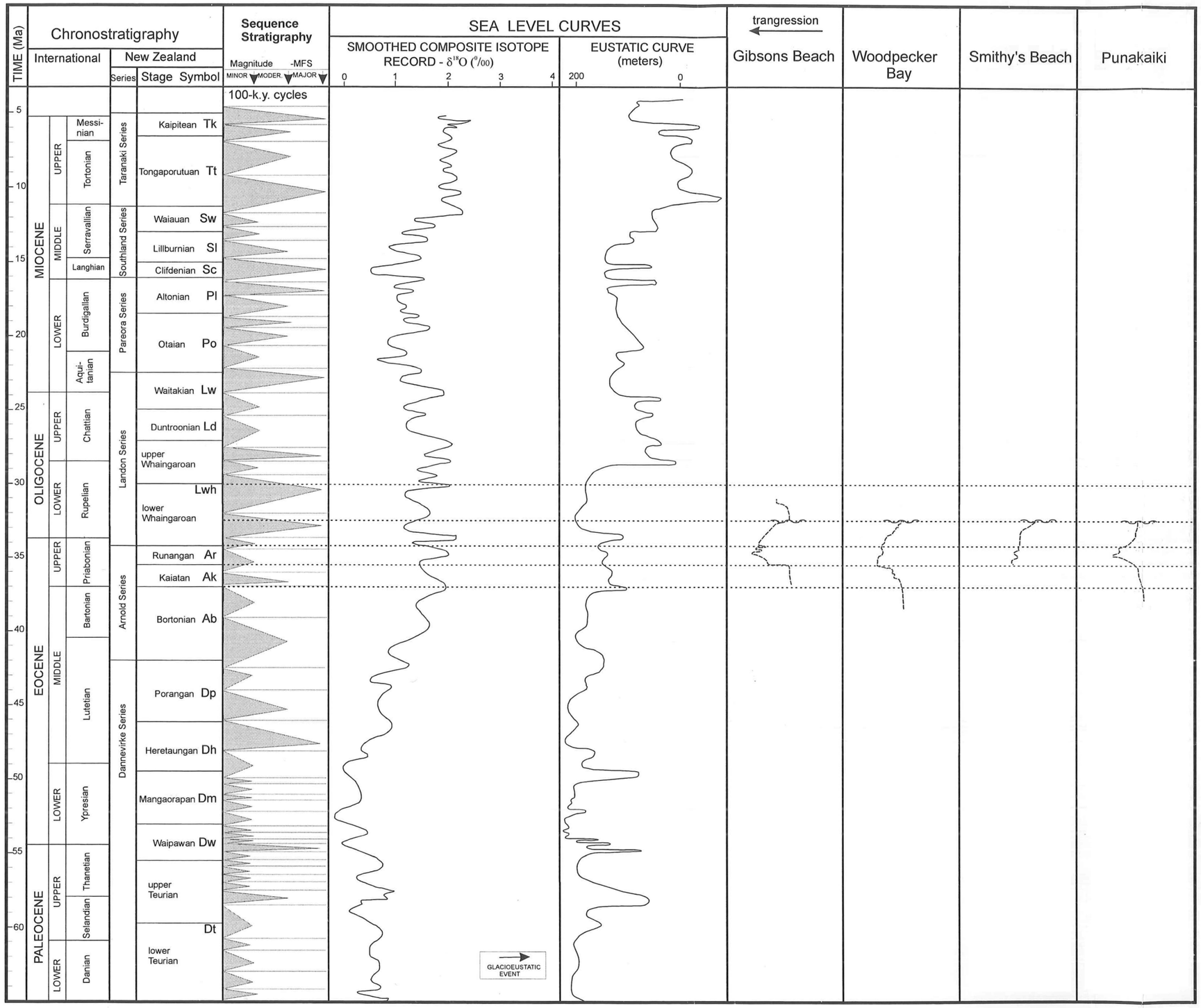

Figure 8.3: Global eustacy curves (from Abreu and Anderson 1998) compared to approximated relative sea-level at various exposures in the Punakaiki-Westport sub-basin.Even allowing for poor age control, the lithology derived curves do not compare well with the eustatic curves, indicating that global sea-level is not the dominant control on sedimentation in this basin.

and regressions are not shown to scale, so each curve shows only the shape of the transgressions and regressions that have occurred. The bottom part of each curve except the Smithy's Beach example is approximately sea-level, being the part of the sequence that is composed of fluvial/estuarine coal measures. The age control on the sections is not good and exact correlation with global eustacy is difficult. However, the basin curves do not have the same shape as any part of the eustatic curves, which is further evidence for a tectonic control on the relative sea-level in the Punakaiki-Westport basin.

Paleogeographic Interpretation

Basin Controls

The shape and subsidence of the Punakaiki to Westport basin is controlled by the Paparoa Tectonic Zone in the east (Laird 1968) and the Cape Foulwind Fault to the west (Nathan 1975b). Mapping of isopachs of the Rapahoe Sediments cannot unfortunately be used in reconstructing the basin shape and subsidence history, largely because outcrop is very poor, and no complete section of Rapahoe Group sediments is exposed anywhere. The thickness information that is used in the correlation diagram is largely gained by inference and calculation from well-separated outcrops and mapping of formations. Often the underlying units (Brunner Coal Measures) and the overlying units (limestones) are exposed, but the sediments inbetween are eroded or covered by Quaternary glacial and fluvial deposits. The reason for this lies in the softer nature of the Rapahoe Group sediments than the stratigraphically bounding units, and therefore they are preferentially eroded by rivers into broad forested valleys. The other problem with trying to map the thickness of the Cenozoic sediments on the West Coast in general is that the modern reverse

reactivation of faults that controlled Paleogene basins has removed many of the sediments that were deposited in the basin, so the complete story cannot be determined from mapping present thicknesses of the sediments. However, the observed dramatic thickening of the Rapahoe sediments towards the Paparoa Tectonic Zone implies that the basin was subsiding much more rapidly on the eastern side than on the west.

The Paparoa Tectonic zone was active from late Cretaceous times throughout the Cenozoic, although its sense of movement changed in the late Oligocene to Miocene. The tectonic zone has had a major effect on the location of sedimentary basins on the West Coast in the Cenozoic. Its activity during the deposition of the Rapahoe Group is shown by the large increase in thickness of Rapahoe sediments towards the Paparoa Tectonic Zone, and also the presence of conglomerate and breccia deposits of Eocene age (the Fossil Creek Formation, Laird 1988) along the eastern side of the basin. It is unfortunate that the Fossil Creek Formation has no sedimentary contacts with the other Rapahoe Group sediments, but they contain abundant pebbles of basement lithologies (gneiss, hornfels, quartz and undeformed granite), as well as mudstone and rare limestone clasts (one pebble bed only), possibly derived from sedimentation occurring close by (Laird pers. comm. 1999). The presence of rounded clasts is evidence for transport some distance before deposition, or for reworking of the clasts before deposition. However breccia occurrences implies some kind of land mass to the east for the clasts to be derived from.

Laird (1970) considered the breccia and conglomerates on the eastern side of the basin to be derived from the inferred land mass to the west, transported some distance in submarine canyons. Laird's main criterion for dismissing an eastern source is the current exposure of gneiss in this area, which could not have provided the source for the granite, vein quartz and hornfels which are dominant in the breccia and conglomerate deposits. However significant erosion of the area to the east of the basin has taken place, both in the Eocene-Oligocene and in more recent times

as the Paparoa Tectonic Zone uplifts the gniess. Undeformed granite, hornfels and quartz veins all occur with gneiss in the Charleston Metamorphic Complex, and Greenland Group rocks outcrop not far from the headwaters of Dilema and Fossil Creeks where the breccia and conglomerate deposits occur. It is more plausible that these slide deposits are derived from a local eastern source, than that they are transported across the width of the very shallow basin. The deposition of shallow lithofacies to the northwest and southwest indicates close land in these directions, however no disturbance of sedimentation great enough to accout for the thickness of Fossil Creek formation has been observed, although outcrop is poor. Directly west of the Fossil Creek formation, the sediments are quiet water muds, if the land mass was to the west the slide deposits would probably have ended up here. Similarly to the south of the Fossil Creek area a great thickness of Island Sandstone and Kaiata Mudstone accumulate without observed breccias and conglomerates, although the outcrop is very poor in this area. Therefore the land mass, and source of the rare limestone pebbles must lie to the east or northeast..

The rare limestone clasts may represent a nearer shore environment that the sediment passed through before being deposited here. Further upstream in Fossil Creek, limestones and conglomerates of the Welsh Creek Formation (Miocene) onlap onto Greenland Group basement (Laird pers. comm. 1999). The Miocene pebbly conglomerates contain granite, limestone and glauconitic sandstone and mudstone. The presence of granite pebbles in both the Fossil Creek Formation and the Miocene conglomerate is puzzling as no granites are found in the exposed basement rocks directly east of Fossil Creek. It is likely that the source of these granite pebbles is either presently covered by Neogene sediments, is buried in part of the Paparoa Tectonic Zone that is not seen, or that the basement has been eroded below the level of the possible original granite outcrop, due to the uplift east of the Paparoa Tectonic Zone since the Miocene. The onlap of Miocene limestone onto basement lithologies means that the area was either exposed during

the Miocene, although this could have been caused by the initiation of compressional tectonics along the Paparoa Tectonic Zone. An eastern or northeastern source of sediment for the Fossil Creek Formation is inferred, and it is likely that the land mass that was exposed in the Miocene was land or a high area during the Eocene and early Oligocene deposition.

Little is known about the Cape Foulwind Fault. It has been crossed by several seismic surveys, in which it appears as a ridge sub-parallel to the Paparoa Tectonic Zone, with a steep western face (probably fault bounded) and a shallower eastern side (Davey 1977). The ridge plunges to the north, where there is no discernable gap in sedimentation. However, around the Punakaiki region, sonobuoy and drillholes show a pre-Oligocene unconformity on the Western side of the fault (Davey 1977) that was used as evidence by Laird (1970) to support other evidence indicating a land mass offshore from Punakaiki during the Eocene to Oligocene (Anderson 1984). The Haku-1 well on the western side of the fault, SW of Punakaiki showed thin Kaiata Mudstone deposits and a thick Miocene succession, indicating that any exposed land on the western side of the fault was covered before the beginning of the Oligocene. Interestingly, no limestones occurred in the drillhole, although seismic data is interpreted to show limestone in nearby areas (Davey 1977). The land mass along the fault was gradually transgressed during the Eocene to Oligocene, and was probably completely covered by shallow waters by the Upper Whaingaroan. The Cape Foulwind fault runs very close to Cape Foulwind, and the basement high covered in algal limestones probably represents a hill extending basin-wards (to the east), that becomes an island as the transgression deepens.

Sedimentation in the Punakaiki section of the "Paparoa Trough" is not as simple as portrayed by Nathan *et al.* (1986). The great thickness of sediments in the headwaters of the Punakaiki and Pororari Rivers rests on thin Brunner Coal Measures and the basement (Laird 1988) yet the deposits in the Pike River Coalfield further east are resting on Paparoa Coal Measures, and

represent the continuation of subsidence in an older basin. The Eocene-Oligocene sediments in the headwaters of the Punakaiki and Pororari Rivers are thicker than those in the Pike area, and are inferred to be deposited in the most actively subsiding part of the basin. Any sediments deposited between these and the Pike River Rapahoe Group sediments have been eroded due to post-Oligocene uplift along the Paparoa Tectonic Zone. This area of the Paparoa Tectonic Zone is around the point at which the scissor movement pivots (Laird 1968). To the south the western side was down-faulted in the Eocene, to the north the eastern side was down-faulted. The faulting is complex around this area of the basin, with several faults acting at different times. During the deposition of the Paparoa Coal Measures at the Pike River Coal Field, several faults controlled the location and shape of the basin. Ferguson (1993) shows at least two normal faults on the eastern sides of two asymmetric rift basins (fig. 8.4a). These were active through the deposition of Cretaceous and Early Paleocene Paparoa Coal Measures. During the deposition of Brunner and Rapahoe sediments they were less active, but the thickness of sediments in the area indicates that the basin was deeper along these faults than elsewhere (fig. 8.4b). However, during the mid Eocene, another fault to the west (possibly the Canoe Fault) became the most active, and this is what controls the deposition in the headwaters of the Punakaiki and Pororari Rivers (fig. 8.4c). The Brunner Coal Measures here on-lap onto basement, indicating that this fault was not active during the Cretaceous and Paleocene. The shift of movement to this structure may have been caused by an unfavourable orientation of the faults controlling deposition in the Pike River Coalfield: Ferguson (1993) infers these to have a NNW-SSE orientation. Fault-bound blocks of Paparoa Coal Measures are found throughout the zone to the north. Significant erosion of uplifted areas within and to the east of the Paparoa Tectonic Zone has removed all evidence of sedimentation in this area, so the orientation, location, extent and duration of any deposition is unknown.

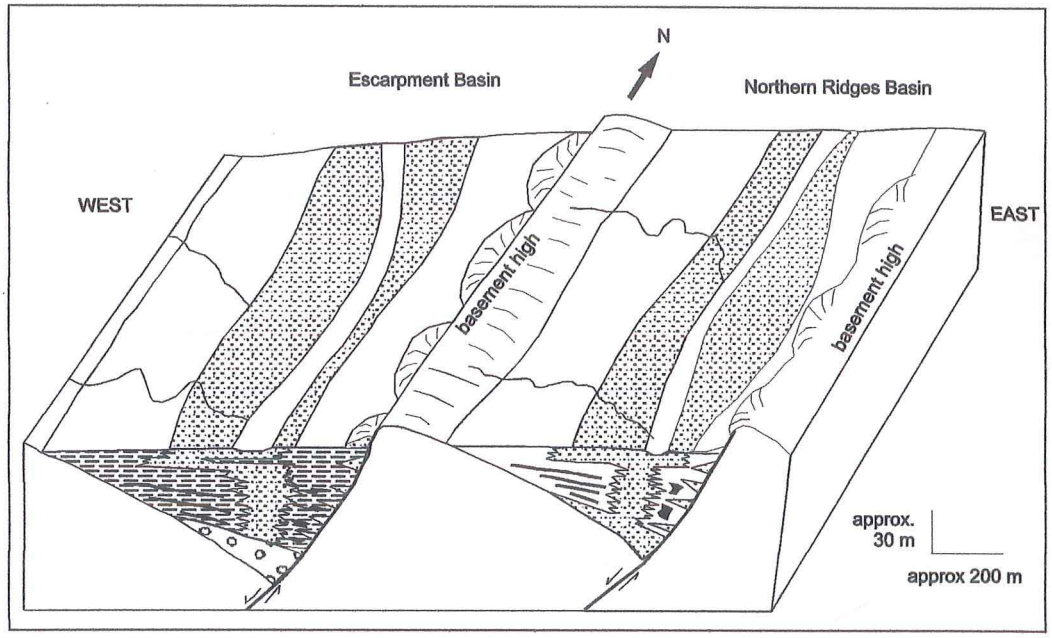

a: Model of deposition in the Pike River Coal Field in the Paleocene. Diagram from Ferguson (1993). Two asymmetric faults control deposition, these faults are inferred by Ferguson to be orientated NNW-SSE.

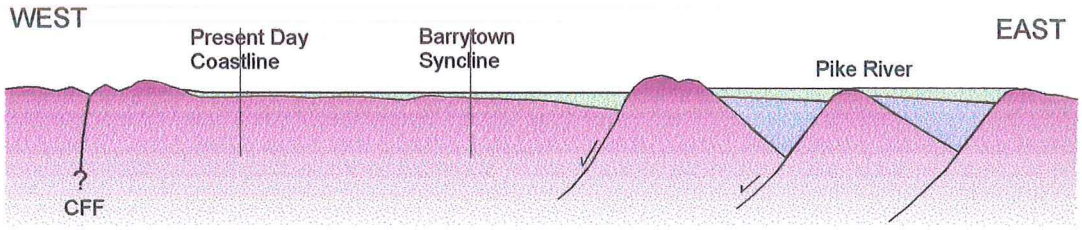

b: diagrammatic model of depositional controls on the Punakaiki area around the Bortonian-Kaiatan Boundary. The nature and location of the Cape Foulwind Fault (CFF) is unknown. The fault immediately east of the Barrytown syncline may be the Canoe Fault (Laird 1988). The eastern faults are after Ferguson (1993).

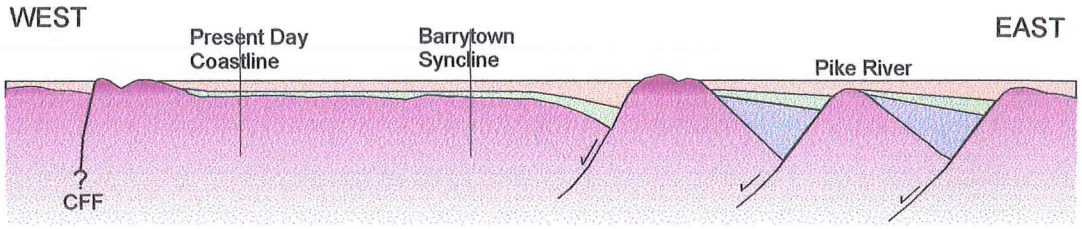

c: diagrammatic model of deposition during the Kaiatan-Runangan. High subsidence on the fault east of the Barrytown syncline is indicated by the thickness of sediment exposed there. The Pike River Faults are not very active in this time, but more sediment is deposited here than around the present day shoreline. Deposition west of the Cape Foulwind Fault (CFF) begins in the Runangan.

Basement Paparoa CM Brunner Rapahoe Group.

Figure 8.4: Model for the development of the Paparoa Trough around Punakaiki during the Eocene.

Laird (1968) and Nathan *et al.* (1986) based their reconstructions of the Paparoa Trough (see fig. 1.2) on assuming that coal isorank lines were continuous and parallel to the basin margins across this area where there is little information to confirm this assumption. The isorank lines then cross many structural elements in the Paparoa Tectonic Zone that may have been active throughout the Eocene and Oligocene. If active, they may have affected sediment thickness and burial depth, temperature and pressure. The various faults in the Paparoa Tectonic Zone around Punakaiki are so complex in their history and inter-relationship that such a generalisation cannot work completely. The assumption that sedimentation was relatively uniform over the inland Punakaiki to Fox River area may be incorrect. There may have been many islands and isolated basement highs caused by tectonic movements on a number of faults.

Lower Whaingaroan Unconformity

Laird (1970, 1988) noted several lines of evidence in the Punakaiki area to suggest that the contact between the Island Sandstone and the overlying Potikohua Limestone represented a considerable break in sedimentation and some erosion of the Island Sandstone. He noted a local discordance across the contact of up to 10° in Bullock Creek and the uneven nature of the contact there and the presence of phosphatic nodules and quartz pebbles in the basal few centimetres of the limestone (Laird 1988, page 29). Around Punakaiki Township itself, the Island apparently grades into the limestone, but Laird (1970) noted the presence of rare large boulders of gneiss within the transition and suggested "that a depositional break may be present." (Laird 1970, page 6).

Anderson (1984) dates the Potikohua Limestone at Punakaiki as Duntroonian to Waitakian but admits a possibility that it is Whaingaroan based on correlation with similar units. Nathan *et al.* (1986) notes the difficulty of identifying the Duntroonian stage on the West Coast region. The

underlying Island sandstone is basal Whaingaroan in age (Laird 1988). The age of the unconformity here is therefore unknown, but is probably Lower Whaingaroan.

The existence of an erosional event in the Lower Whaingaroan at Gibsons Beach and the Cape Foulwind Quarry has been pointed out to Stage 2 and 3 students from Canterbury University for years. The top of the Kaiata Mudstone in both locations is the flat upper surface of a cemented band, which contains abundant large burrows of *Thallasinoides*, which are filled with coarse sand and granules. The sand is not similar to the Little Totara Sand that occurs above the Kaiata in the sequence, and contains rounded fragments of algae, presumably derived from the local algal reef. The burrows could extend down from the surface up to 4 m (Bromley 1996), and the coarse sand was deposited above this level. However, since the sand was deposited and filled some of the burrows, at least 4 m of erosion has taken place. The sediment has been eroded down to the same level, that is the top of a cemented layer, consistently, producing what appears to be a sharp conformable contact between Kaiata Mudstone and Little Totara Sand (e.g. Nathan 1975b). This relationship suggests that the cemented layers were already partially cemented when the erosion occurred, this is supported by the lack of any cement in the overlying, highly porous Little Totara Sand.

Another deposit, not mentioned in previous publications, occurs between the Little Totara Sand and the Kaiata Mudstone. This is a dark, finely laminated mud and silt, with a very high carbon content, and lenses of coarser sand similar to the Little Totara Sand. The thickness of the silt varies from about 10 cm at Gibsons Beach to 50 cm at the quarry. The silts represent a lagoon that formed after the erosion, as part of a shoreline complex that included the Little Totara Sand. The break in sedimentation is well constrained here, as the underlying Kaiata Mudstone is dated as Lower Whaingaroan (Srinivasan and Vella 1975) and both the Little Totara Sand and overlying Waitakere Limestone are also Lower Whaingaroan in age.

At Pahautane Point, the contact of the Island Sandstone and the overlying Tiropahi Limestone is marked by a thin (about 10 cm) layer of orange coloured, less cemented detrital sand. This layer contains much less cement and fossil material than the underlying Island Sandstone. The contact appears conformable and planar in ooutcrop. The sand layer represents a break in normal sedimentation, although no other evidence of erosion is seen.

At Woodpecker Bay, the contact between Island Sandstone and Tiropahi Limestone is marked by a layer of rhodoliths (see Chapter 5). The layer at Seal Island shows clear evidence of shallowing conditions in the increase in size of rhodoliths and the decrease in smaller particles caused by the greater energy conditions. There are also channels cut through the layer, and the top surface has evidence for sub-aerial solution. Here there has been shallowing and erosion including sub-aerial exposure. At Woodpecker Bay and Pahautane the age of the unconformity is not precisely known; the top of the Island Sandstone is probably basal to Lower Whaingaroan, and the Limestone is Lower Whaingaroan (Anderson 1984).

Oligocene unconformities are mostly Upper Whaingaroan, Duntroonian and Waitakian in age on the East Coast of the South Island (Findlay 1980, Lewis and Belliss 1984, Kamp 1991, Lewis 1992, Lewis and Ekdale 1992, Brown 1995) and also in most of Westland (Nathan 1975b, Nathan 1978, Carter *et al.* 1982). These mid Oligocene unconformities are sometimes correlated with the separation of Australia and Antarctica and the initiation of the Circum Antarctic Currents (Carter and Landis 1972, Duff 1975, Carter *et al.* 1982, Fulthorpe *et al.* 1996). A paraconformity representing non-deposition for the entire Whaingaroan stage is identified by Leask (1993) between ?latest Runangan Brunner Coal Measures and Takaka Limestone in the Golden Bay area, but he concludes that this is caused by stability of the Golden Bay platform compared to rapidly subsiding basins on either side. Similar areas of non-deposition have been identified from cores in the Taranaki Basin. They can include all of the Arnold and much of the

Dannevirke series, and are of greater extent and duration in the south of the basin (Palmer 1985). Duff (1975) identified several unconformities in Oligocene sediments in DSDP legs 21 and 29, the unconformities in leg 21 (Lord Howe Rise) are Late Eocene (Kaiatan and Runangan) to Lower Whaingaroan. He also examined Lower Oligocene unconformities in onshore East Coast Basins, but suggested these were caused by epeirogenic movements, where he identified at least two episodes. Reay (1993) identified a Whaingaroan unconformity in the Middle Clarence Valley, but correlated it with the "Marshall Paraconformity". Field (1985) identified several unconformities in the Mount Somers area, the oldest indicating erosion in the mid Whaingaroan.

Carter *et al.* (1982) identified two major unconformities on the West Coast, an Early Oligocene unconformity, and later Duntroonian to Waitakian unconformity that they correlated to the "Marshall Paraconformity". In a section at Whitcliffs near Inangahua the older of the above is a low-angle unconformity between Maruia Group sediments (Eocene to Lower Whaingaroan) and overlying breccias and shallow marine beds (Lindqvist 1972, Carter *et al.* 1982). A similar unconformity has been noted in the Buller Gorge (Lindqvist pers. comm. 1999). This unconformity is not noted in sediments in the nearby Murchison Basin where the contact is apparently conformable (Suggate 1984). German (1976) noted the onset of breccia deposits in the Lower Whaingaroan at the Little Wanganui River mouth (the Kongahu Member). He interpreted these slide deposits as being derived from an emergent land-mass immediately west of the Cape Foulwind Fault. The slide deposits continued to be deposited until the Waitakian Stage (German 1976) although their inception could have been related to the unconformity in the Lower Whaingaroan. German noticed a decrease in angularity and in size of clast towards the top of the succession, where the beds also become thinner and further apart. This is related to the gradual transgression during the Whaingaroan and Duntroonian.

An angular unconformity occurs between Early Oligocene and older sediments at Avoca

(McLennan and Bradshaw 1984) but this is related by the authors to local uplift and normal faulting pre- or earliest Oligocene. Browne (1995) noted a Late Eocene-Oligocene episode of regional uplift and karstification in Marlborough.

In the southern part of the Punakaiki-Westport basin in the vicinity of Greymouth, Nathan (1978) noted two phosphatic, glauconitic and burrowed horizons in the Cobden Limestone, he places them at the Whaingaroan-Duntroonian and Duntroonian to Waitakian boundaries. The Kaiata Formation (Lwh at the top) grades into the Cobden Limestone over 3 m. However, Gage (1952) noted that the boundary between the Kaiata Mudstone and the Port Elizabeth beds was an obscure bored erosion surface (Gage 1952 in Srinivasan and Vella 1975). Srinivasan and Vella (1975) place the age of the contact as at the Runangan-Whaingaroan boundary, which is too early to be correlated to the Punakaiki to Westport successions. Unconformities from other basins that occur at approximately the same time as the unconformity in the Punakaiki to Westport Basin have been inferred by their discoverers to be caused by local tectonic movements. The unconformity in the Punakaiki-Westport Basin is local in extent, possibly having an effect in nearby Inangahua/Buller Gorge sedimentation and as far north as Little Wanganui River, but not affecting the Murchison Basin. Therefore it is inferred to have been caused by a local rather than regional or global event: probably a local tectonic movement.

Kaiatan

At the base of the Kaiatan Stage (fig. 8.5) fluvial/esturine coal measures were being deposited over much of the field area. The transgression from coal measures to marine sand and mud deposition occurred during the Kaiatan, from south to north. The coal measures in the south are older than those in the north, as is the base of the marine sequence. In the Pike river Coal Field the Brunner Coal measures are Bortonian (Ferguson 1993). The oldest marine sediments around Punakaiki are Kaiatan in age, whereas those around Cape Foulwind are Runangan, partly due to the topographic high that existed there. The Kaiata Mudstone on the Denniston Plateau is Kaiatan to Runangan, the coal measures underlying the Kaiata Mudstone are probably Kaiatan (Nathan *et al.* 1986), meaning that the transgression was not simply south to north, but also in this area east to west. The Denniston Plateau area was the down-faulted side of the Paparoa Tectonic Zone during Eocene-Oligocene times (Laird 1968). Some areas have local paleogeographic highs where the coal measures were not deposited. Cape Foulwind was such an area, although there are coal measures close by and the surface is deeply weathered and covered by sands of a similar age and appearance as the Brunner Coal Measures. At Meybille bay the coal measures pinch out against a granitic mound, and around K30 797136, the coal measures pinch out around a high in weathered Charleston Metamorphic Group. At the Brighton Coal Mine the Coal measures are slightly thicker, and become very thin north of the Limestone Creek Fault, suggesting this structure was active through the Kaiatan-Runangan. At Charleston the Brunner Coal Measures thicken dramatically, Nathan (1975b) suggested the abrupt thickening was due to infilling of a pre-Tertiary valley. No evidence was found to refute this. Other areas may have been basement highs, especially the footwall blocks of extensional asymmetric rifts, but these areas are usually eroded after post-Oligocene uplift.

Around the Punakaiki area, shallow marine sands were deposited shortly after if not at the base

of the Kaiatan stage. The Island Sandstone was deposited in the Punakaiki area from the Kaiatan to the Lower Whaingaroan.

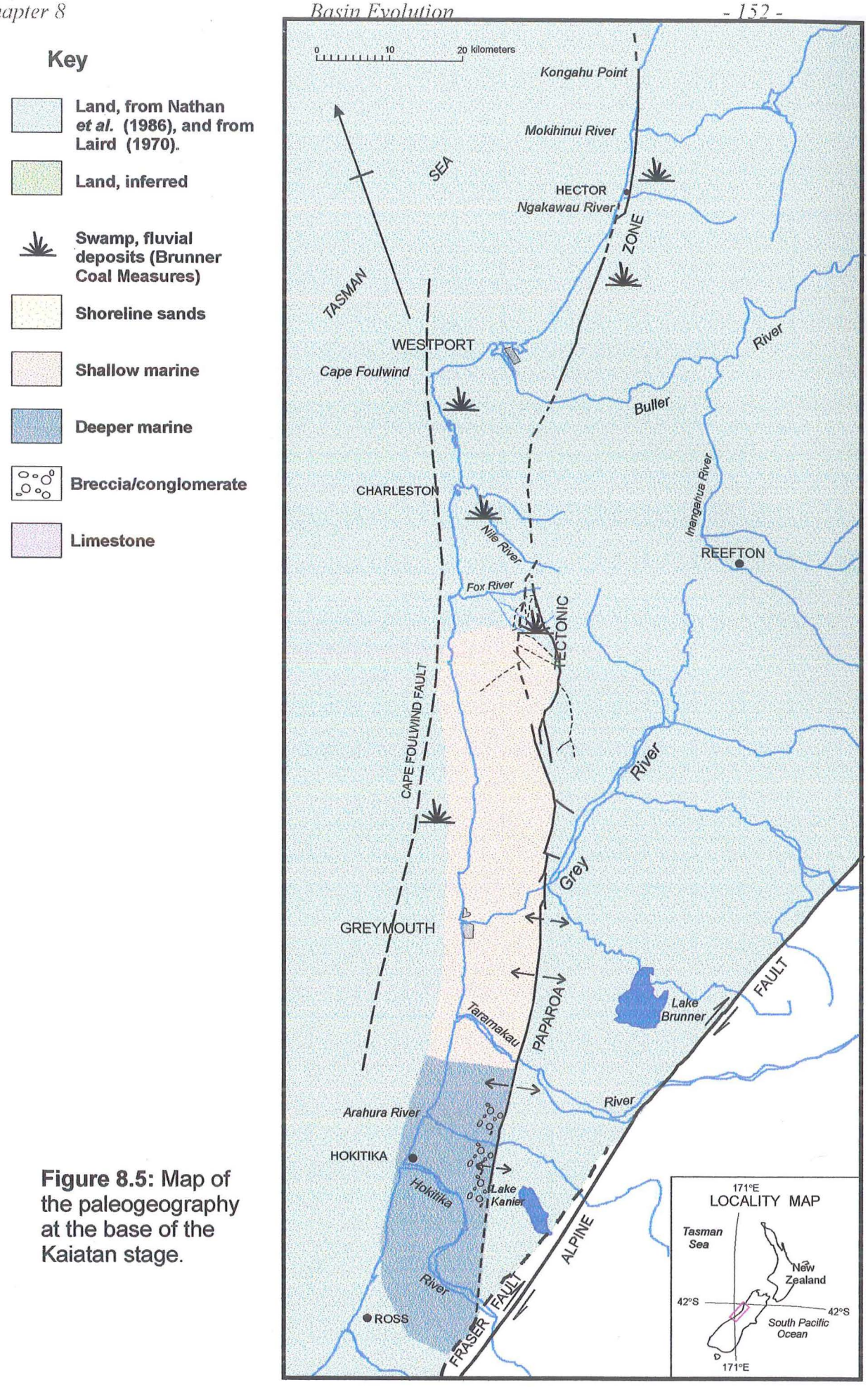

Figure 8.5: Map of the paleogeography at the base of the Kaiatan stage.

Runangan

By the base of the Runangan stage all low-lying areas were below sea-level (fig. 8.6). Laird (1970) inferred a land area to the west or southwest of Punakaiki because of the dominance of sandstones in this area, rather than the mudstones that occur to the north and south. In the Charleston region, only the shoreline Little Totara Sands were deposited from the Kaiatan to the Lower Whaingaroan. This is inferred to be due to a local paleogeographic high, that persisted due to high rates of deposition. Land is inferred to have existed on the eastern side of the basin, but probably only in small islands and blocks. To the far east, Nathan *et al.* (1986) inferred land to have existed at this time east of the headwaters of the Grey River. A channel to the open sea may have existed between Punakaiki and the location of the western landmass inferred by Nathan *et al.* (1986), and another connection probably existed to the north of Cape Foulwind. The shallowest area of the basin was around Charleston, but the basin probably deepened to the east. The shoreline sands were deposited in an increasingly narrow band as the transgression continued and reached the maximum late in the Runangan stage. The maximum transgression seems to have occurred just below the Runangan-Whaingaroan boundary, based on foraminiferal ages for sediments around the clay layers at Cape Foulwind in this thesis and Srinivasan and Vella (1975). The land mass to the southwest of Punakaiki must have been almost completely covered as Runangan aged Kaiata Mudstone is found in the Haku-1 drillhole, just west of the Cape Foulwind Fault. The area around Charleston continued to be a high area, depositing Little Totara Sand. Around Okari Lagoon, sandy Kaiata Mudstone was deposited , and Little Totara Sand occurs in the southern end. The land masses to the east continued to be uplifted and supplied sediment for breccias and conglomerates in the headwaters of the Fox River. The rapidly subsiding eastern basin margin (around the headwaters of the Punakaiki and Pororari Rivers)

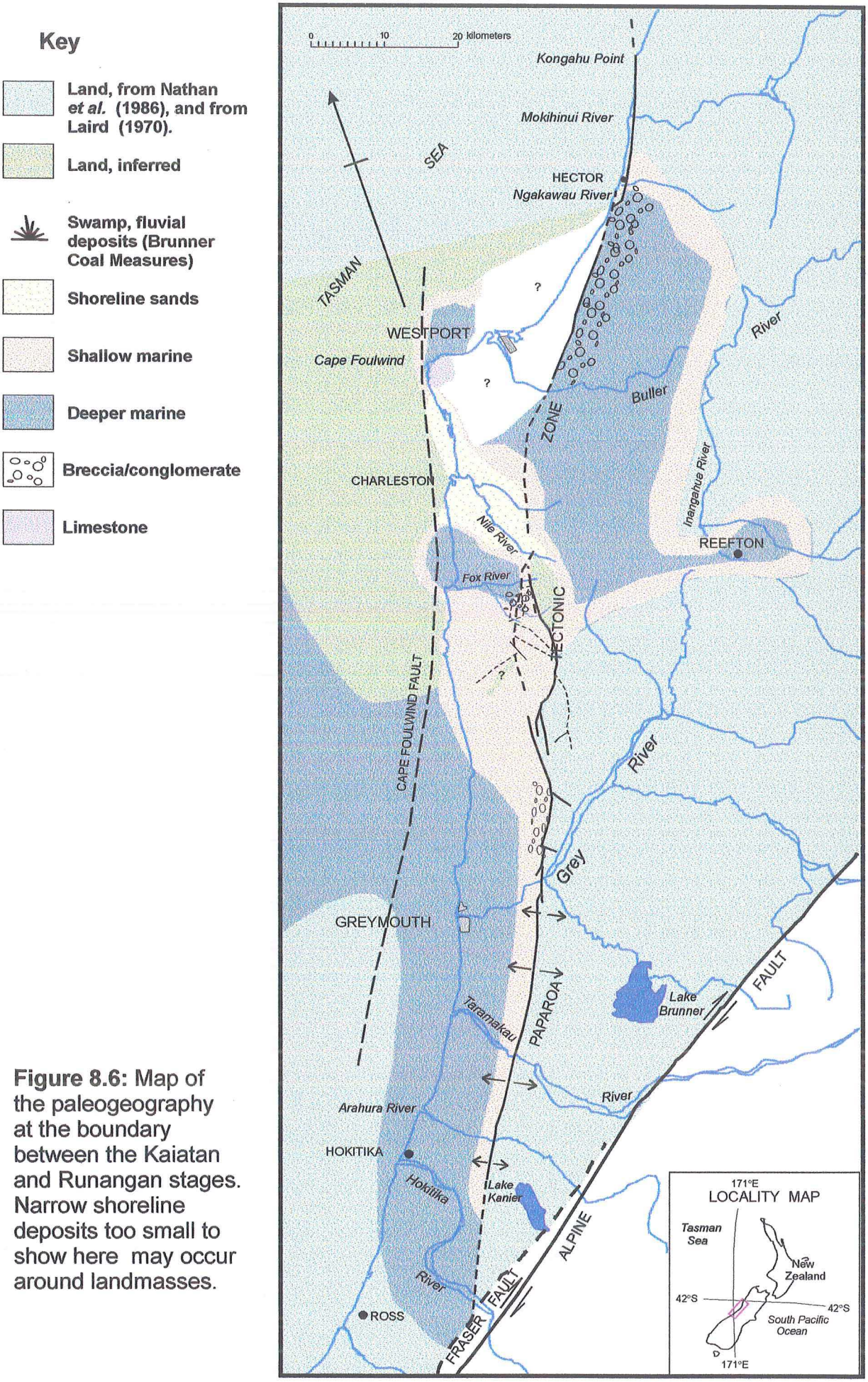

Figure 8.6: Map of the paleogeography at the boundary between the Kaiatan and Runangan stages. Narrow shoreline deposits too small to show here may occur around landmasses.

accumulated Island Sandstone, also implying a local source of sediment, and therefore an eastern to southeastern landmass.

Whaingaroan

In the Lower Whaingaroan, the regression was underway, and the sediments were rapidly becoming sandier. The base of the Whaingaroan stage, however, is the height of the transgression (fig. 8.7), and the muddiest sediments were deposited everywhere, except in the Charleston region, and around Punakaiki. In the Punakaiki area, the Island Sandstone is still being deposited in the Lower Whaingaroan, although it is muddier than the sediment above and below. Through the Whaingaroan the sediments become progressively sandier, until erosion, subaerial exposure and then transgression to limestone deposition occurs (fig. 8.8). Inland the eastern, rapidly subsiding part of the basin is accumulating Kaiata Mudstone in this time, possibly representing a shift of the shoreline away from the area as a result of the transgression or tectonic changes. In Dilemma and Fossil Creeks, slide deposits of breccia and conglomerates are still being deposited in the Lower Whaingaroan, indicating a possible emergent landmass to the east. To the north, the algal mound shrinks with the regression, and Kaiata Mudstone is deposited over much of the area formerly occupied by the algal reef. The sandy Kaiata continues to be deposited in the northern Okari area, and is followed by Little Totara Sand deposition. Not much is known about the top part of the sequence around Charleston, athought the top of the Little Totara Sand can be seen interfingering with overlying Lower Whaingaroan Waitakere Limestone, this is probably re-deposition of still exposed shoreline sands. The Lower Whaingaroan unconformity associated with the regression is not observed in the Charleston area, due mainly to the lack of outcrops in the area. The transgression culminates in limestone deposition over all of the basin by the

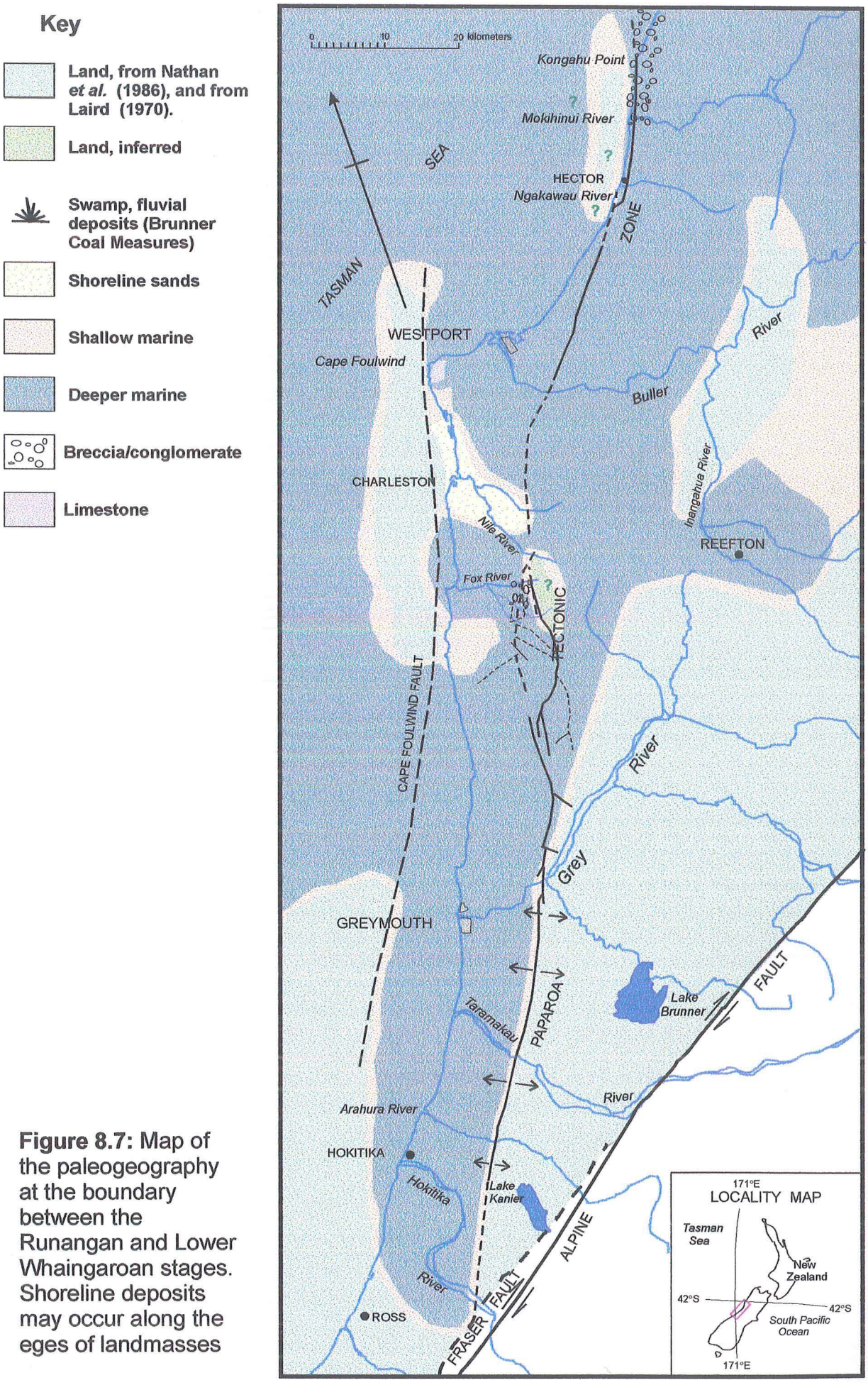

Figure 8.7: Map of the paleogeography at the boundary between the Runangan and Lower Whaingaroan stages. Shoreline deposits may occur along the eges of landmasses

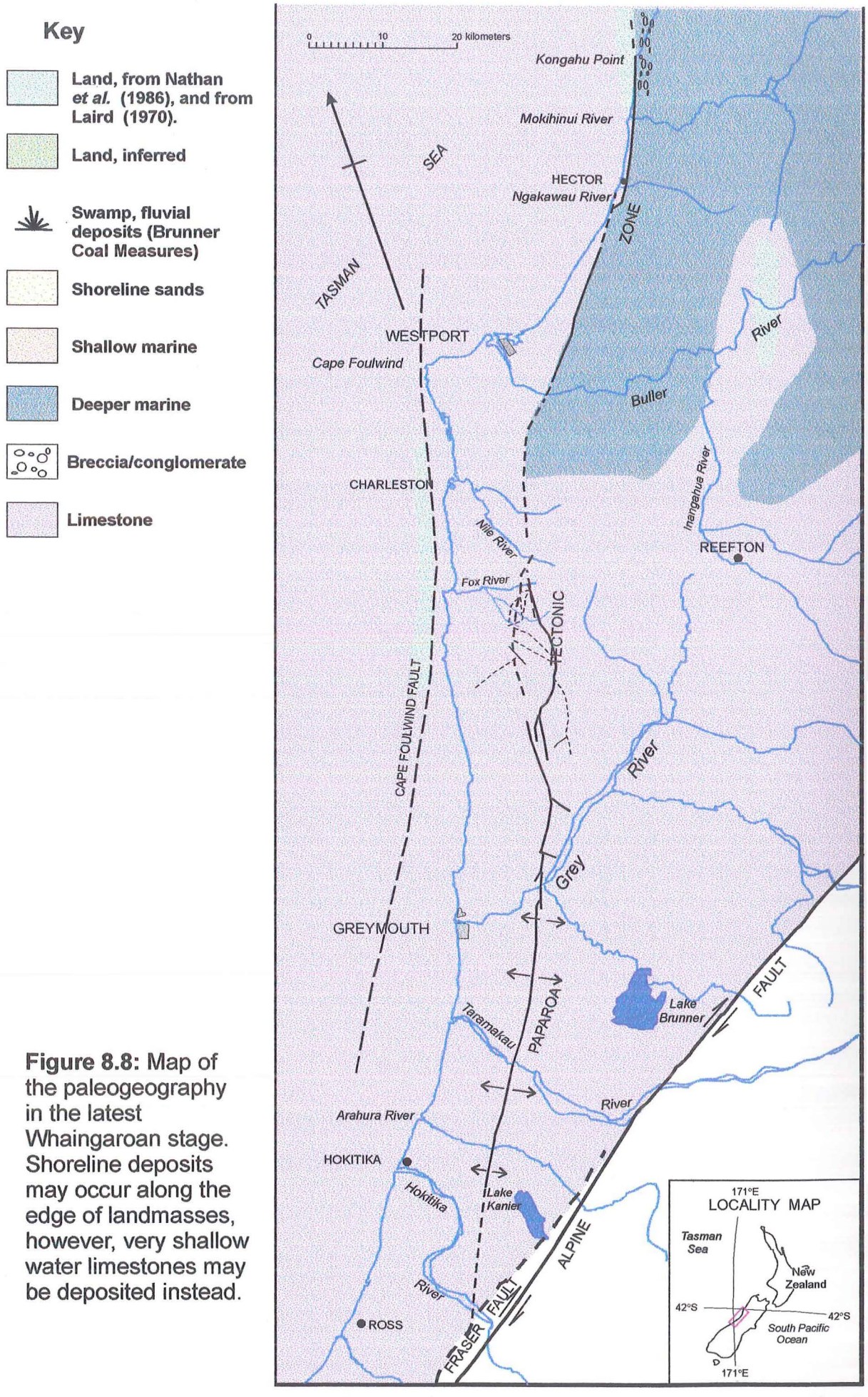

Figure 8.8: Map of the paleogeography in the latest Whaingaroan stage. Shoreline deposits may occur along the edge of landmasses, however, very shallow water limestones may be deposited instead.

Duntroonian stage, including those areas that were previously exposed in the east and west. The limestones are noted to be shallow water algal limestone facies in the north (Westport to Charleston) of the basin, deeper water glauconitic and sandy in the middle (Woodpecker and Pahautane) and more shallow water bryozoan packstones in the Punakaiki Area (Anderson 1984). Anderson (1984) suggests a land mass in the Lower Whaingaroan stretching south to Haku-1 based on the absence of Limestone in this area. However, Runangan mudstones occur in the drillhole, and the absence of limestone may be a local effect or subsequent erosion. German (1976) shows the conglomerate and breccia of the Kongahu Member around the mouth of the Little Wanganui River to the north of the field area as being deposited from the "Early Whaingaroan" into the Waitakian. The conglomerates are interpreted as slides off an emergent landmass on the western side of the Cape Foulwind Fault, about 5 km off the present day coastline. The conglomerate and breccia deposition may relate to the unconformity in the Lower Whaingaroan further south, but the age dating of the deposits is poor.

Chapter 9:

Conclusions

Basin History

1. The Rapahoe Group sediments between Punakaiki and Westport are confined to a relatively narrow and generally shallow basin bounded on both sides by faults. The eastern side of the basin subsided more rapidly throughout mid-upper Eocene and Early Oligocene times. Earlier fault bounded basins in the Pike River Coalfield continued to subside, but a new fault to the west of the Coalfield formed and was the most active probably due to a change in the extension direction between Paleocene and Eocene times.
2. The eastern side of the basin behaved like the Pike River basins: an asymmetric rift basin with a steep normal fault on the eastern margin (Ferguson 1993, fig. 8.4).
3. The western side of the basin was controlled in some way by the Cape Foulwind Fault. This structure remains enigmatic, but is inferred by Laird (1988) to be a normal fault with a currently downthrown western side, probably uplifted on the western side during much of the Eocene. The area around the fault and to the west remained above sea-level until the Runangan stage, when Kaiata Mudstone was deposited on the western side. Sediments are inferred to onlap either side of the structure until complete transgression in the early Miocene (Laird 1988).
4. Exposed basement is inferred to have existed to the east of the basin, in the Paparoa Tectonic Zone. The basement was probably exposed in several small blocks, the footwalls

of major basin boundary faults and probably also areas of uplift (or no subsidence) within the Paparoa Tectonic zone caused by the complex faulting in the area. The occurrences of breccias and conglomerates in the headwaters of the Fox River may imply exposed land mass(es) close by, although transport from the western landmass cannot be completely ruled out because of poor exposure of the sediments to the west.

5. All of the sequences that can be examined in detail show a transgression-regression-transgression sequence. The transgression occured from the Kaiatan to the latest Runangan: the regression occurs through to the Lower Whaingaroan where a lowstand unconformity can be recognised in all sections where this area of the sequence is seen, with erosion and sub-aerial exposure recognised from Punakaiki to Westport. The following transgression initiates widespread limestone deposition. The transgression can also be recognised by the overstepping of shallow and marginal marine deposits in the vicinity of Charleston by deeper marine Kaiata Mudstone sediments.

6. The Lower Whaingaroan unconformity cannot be correlated with the basal Lower Whaingaroan unconformities (Gage 1952) in Greymouth, but can possibly be correlated with similar erosional unconformities at Whitecliffs (Inangahua) and the Buller Gorge. Conglomerate and breccia deposits at the Little Wanganui River mouth are possibly initiated by the same event that causes the unconformity, they are dated as "early" Whaingaroan to Waitakian by German (1976). No similar unconformities occur in the Murchison Basin however. This implies a local tectonic cause for the regression and unconformity found in the Punakaiki to Westport Basin, that affected sediments as far north as Karamea, but not the Greymouth area. This may mean that only the northern part of the Paparoa Tectonic Zone was involved.

7. Microfossil information suggests that the Kaiata Mudstone is not an outer shelf deposit,

but rather was formed in quiet sedimentary environments closer to shore, but that it was protected from the open sea by land to the west and east. The lack of planktonic foraminifera and low oxygen association of the ostracods found support a sheltered, partially enclosed environment of deposition and shallow conditions.

8. The Little Totara Sand includes sections deposited in dune, beach, tidal channel and bar settings. The sand is time transgressive, and appears at both the top and the bottom of the sequence at Cape Foulwind (see Chapter 8).

9. The sediments were buried between 1.5 km (west side) and 4 km (east side) based on reconstructions of overburden thickness and coal rank (Nathan *et al.* 1986). This is consistent with the major subsidence in the basin being on the eastern side, so that in this area it appears that the Paparoa Tectonic Zone was acting as an eastern boundary fault (with complications) rather than a western boundary fault as occurs north of Westport. The area to the east of the zone has been uplifted and eroded since the Miocene, and any sediments deposited on the eastern side of the zone have been eroded.

10. Charleston appears to have been a paleogeographic high area, with only shoreline sands being deposited from Kaiatan to Lower Whaingaroan times, and the overlying limestone is a shallow water sandy algal limestone. The areas to the north and especially the south were deeper, but the basin shallowed again in the Punakaiki and Cape Foulwind areas. The basin became deeper east of Charleston, because of the more rapid subsidence along the eastern boundary. The shallowing to the south may have been controlled by the Limestone Creek Fault. On the south side of the fault, 30 m of Little Totara Sand was deposited, this is overlain by Island Sandstone, and Kaiata Mudstone does not occur extensively in this succession. To the north of the fault, Little Totara Sand exists as isolated lenses only in the base of the Kaiata Mudstone, these were probably deposited

in storm events from the beach near Pahautane. The nature of the Brunner-Rapahoe contact immediately north of the Limestone Creek Fault is unknown, as the fault has continued to be active with the norther side downthrown, and this has buried the contact far below ground surface. The basin between Pahautane and Charleston may have been isolated between two higher points to the south and north, a land mass to the west, and also possible land mass(es) to the east where the Fossil Creek Formation outcrops. It may also have been subsiding more rapidly along the Limestone Creek Fault.

11. In considering the definition of the Rapahoe Group, I have come to the conclusion that it would be better defined as all those marine and marginal marine sediments associated with the regional marine transgression in the Greymouth-Buller area, which includes the Brunner Coal Measures as they are marginal marine (estuarine) (Newman 1985) and represent the beginning of the regional transgression. Time and space constraints prevented the inclusion of any more than a cursory look at the Brunner Coal Measures in this thesis. The top of the Rapahoe Group in Greymouth-Buller area is the beginning of widespread limestone deposition: the Nile Group. This contact is an unconformity in the Punakaiki-Westport area, but appears to be gradational to the north and south. The limestone quarried at Cape Foulwind is not widespread, and is not, as previously classified, truly a part of the Waitakere Limestone. It is considerably older (Eocene), it inter-fingers with Kaiata Mudstone and it is separated from true, thin and widespread Waitakere Limestone by a possible unconformity (see Chapter 4). The limestone in the quarry should be considered as part of the transgressive sequence; therefore part of the Rapahoe Group, and I have provisionally named it the Cape Foulwind Limestone.

Future Work

During the progress of this thesis I have found many interesting problems that cannot be included here but which need further research. There are a great variety of different categories of project that could be done in this area, from structural, correlations, Palaeontology and Ichnology. Here is a list of the major problems that cannot be solved in this project:

1. The subaerial exposure of the rhodolith layer, which I have correlated with the erosion at Pahautane and Bullock Creek is probably contemporaneous with the disconformity below the Little Totara Sand around Westport. An erosional event to the top of a significant regression event in lower Whaingaroan times is therefore a basin-wide feature. Of interest is whether this regression and the associated unconformity are restricted to this basin or if it is of a more regional extent. The occurrences of breccia and conglomerate in mudstones to the north (German 1976) suggests that the cause of the unconformity may have been increased uplift of the western side of the Cape Foulwind Fault.
2. The trace fossils of the Rapahoe Group and the overlying sandy limestones are very diverse and interesting. There is a distinct facies control evident, in that the muddy sections of the Island Sandstone have a different assemblage to the sandier sections. There is also the occurrence of a highly unusual variety of *Teichichnus*, which is much larger than normal and appears like trough cross-bedding in outcrop. The sea-washed cliffs and bays in the vicinity of Woodpecker and Smithy's Bays provide excellent exposure of the traces.
3. The coralline algae of the Eocene and Oligocene need work done on them to determine the species present. From my observations, the genera present in the Eocene limestones are generally thought to be tropical, whereas the temperature in the Eocene in New Zealand did not become tropical. Little work has been done worldwide on Eocene and

Lower Oligocene tropical or temperate coralline algae, yet New Zealand has several extensive deposits of temperate coralline algae.

4. The Cape Foulwind Fault is an enigmatic feature of the Geology of the West Coast. It outcrops onshore to the south, but is thought to run just off the coast past Cape Foulwind and further north. It probably represents the western edge of the Eocene basin, but little is known about its geometry, exact location, the relative thickness and types/ages of sediments deposited on either side of it, and so a major part of the history of the area is guesswork only. It is unfortunately too close to shore and too shallow for ship based seismic lines, and one drill core only (Haku 1) has been sunk to see what lies on the other side of it. The fault needs further investigation and preferably some drill holes on either side in the vicinity of Westport, but this is likely to be a little too expensive for a university study!

5. The cementation or diagenetic history of the area, which can be looked at through the isotope chemistry, composition structure and distribution of Calcite cements, as well as the occurrence of chalcedony cements and also the rank of coal deposits in the underlying Brunner Coal Measures.

Acknowledgements

I would like to thank most sincerely my supervisor, Malcolm Laird, who has had his own ideas about this basin since he mapped it in the 1980's. His comments, discussion of various proofs, calmly reading all my draft chapters when he had better things to do, and providing me with information about the Rapahoe Group and surrounding sediments from his own experience is greatly appreciated. I also thank him for his enthusiasm for sediments and for leaping surging seas on slippery rocks! My associate supervisor, Doug Lewis, is responsible (whether he accepts it or not) for my own enthusiasm for sedimentary rocks, and I thank him for discussions on sedimentation, rhodoliths, solution, and especially for wandering up to one of my outcrops and saying "that's not cross-bedding, it's *Teichichnus*!" (or words to that effect). He is also thanked for the task of proof-reading my final draft, and providing always useful comments.

I would like to thank my flatmates for bearing with me and being supportive of a thesis in progress, my flatmate Rachelle for providing an example of how a thesis should be done (even if it's only arts), and my flatmate Zane for providing an example of how one shouldn't be done. Thanks guys!

John Southward has proven himself patient and sympathetic to cries of "help! the computer's eaten my thesis", and endless requests for more paper in the printers. We do appreciate you really John!!

Finally, I want to thank the people without whom this thesis wouldn't have happened, my family, especially my mother, who is a champion nagger, even if it is mostly by e-mail these days.

References

Abreu, V.S.; Anderson, J.B. 1998: Glacial eustacy during the Cenozoic: sequence stratigraphic implications. *AAPG Bulletin 82*: 1385-1400.

Adams, C.J.D.; Nathan, S. 1978: Cretaceous chronology of the Lower Buller Valley, South Island, New Zealand. *New Zealand Journal of Geology and Geophysics 21*: 455-462.

Adey, W.H.; MacIntyre, J.G. 1973: Crustose Coralline Algae: a re-evaluation in the geological sciences. *Geological Society of America Bulletin 84*: 883-904.

Andrews, P.B. and van der Lingen, G.J. 1969: Environmentally significant sedimentologic characteristics of beach sands. *New Zealand Journal of Geology and Geophysics 12*: 119-137.

Anderson, J.M. 1984: *The sedimentology and diagenesis of an Oligocene carbonate sequence (Nile Group), Westport to Punakaiki.* M.Sc Thesis, Victoria University, Wellington.

Baker, J.; Seward, D. 1996: Timing of Cretaceous and Miocene compression in northeast South Island, New Zealand: Constraints from Rb-Sr and fission-track dating of and igneous pluton. *Tectonics 15*: 976-983.

Banner, F.T., Simmons, M.D. 1994: Calcareous algae and foraminifera as water-depth indicators; and example from the Early Cretaceous carbonates of Northeast Arabia. in: Simmons, M.D. (ed): *Micropaleontology and hydrocarbon exploration in the Middle East.* Chapman and Hall, London: 243-252.

Beu, A.G.; Maxwell, P.A.; Brazier, R.C. 1990: Cenozoic Mollusca of New Zealand. *New Zealand Geological Survey Paleontological Bulletin 58*: 518 p.

Bishop, D.G. 1991: Cretaceous and Cenozoic tectonics of the West Coast region of the South Island. *Proceedings, 1991 N.Z. Oil Exploration Conference*: 122-133.

Bjørkum, P.A.; Walderhaug, O. 1993: Isotopic composition of a calcite-cemented layer in the Lower Jurassic Birdport Sands, southern England; implications for formation of laterally extensive calcite-cemented layers. *Journal of Sedimentary Petrology 63*: 678-682.

Bjørkum, P.A.; Walderhaug, O. 1990: Geometric arrangement of calcite cementation within shallow marine sandstones. *Earth-Science Reviews 29*: 145-161.

Bosence, D.W.J. 1976: Ecological studies on two unattached coralline algae from western Ireland. *Palaeontology 19*: 365-395.

Bosence, D.W.J. 1983a: Description and classification of rhodoliths (rhodoids, rhodolites). In: Peryt, T. (ed.): *Coated Grains.* Springer-Verlag, Berlin, p. 217-224.

Bosence, D.W.J. 1983b: The occurrence and ecology of recent rhodoliths – a review. In: Peryt, T. (ed.): *Coated Grains.* Springer-Verlag, Berlin, p. 225-242.

Bosellini, A.; Ginsburg, R.N. 1971: Form and internal structure of recent algal nodules (Rhodolites) from Bermuda. *Journal of Geology 79*: 669-682.

Bourrouilh, L.J.F.G. 1986: Tectonic drift versus climatic variations; rhodoliths as indicators of limits between tropical and nontropical sedimentary conditions; examples from Pacific Miocene. *AAPG Bulletin 10(5)*: 568.

Bradshaw, J.D. 1989: Cretaceous geotectonic patterns in the New Zealand region. *Tectonics 8*: 803-820.

Bradshaw, J.D. 1997: Notes for Canterbury University Geology course 324: History of New Zealand.

Bromley, R.G. 1996: *Trace Fossils. Biology, taphonomy and applications. 2nd edition.* Chapman and Hall, London.

Browne, G.H. 1995: Sedimentation patterns during the neogene in Marlborough, New Zealand. *Journal of the Royal Society of New Zealand 25*: 459-483.

Burgess, C.J.; Anderson, J.M. 1983: Rhodoids in temperate carbonates from the Cenozoic of New Zealand. In: Peryt, T. (ed.): *Coated Grains.* Springer-Verlag, Berlin, p. 243-258.

Burley, S.D.; MacQuaker, J.H.S. 1992: Authigenic clays, diagenetic sequences and conceptual models in contrasting basin-margin and basin-center North Sea Jurassic sandstones and mudstones. In: Houseknecht, D.W.; Pittman, E.D. (eds.): Origin, diagenesis, and petrophysics of clay minerals in sandstones. *Special Publication - SEPM 47*: 81-110.

Burns, D.A.; Nelson, C.S. 1981: Oxygen isotopic paleotemperatures across the Runangan-Whaingaroan (Eocene-Oligocene) boundary in a New Zealand shelf sequence. *New Zealand Journal of Geology and Geophysics 24*: 529-538.

Carter, R.M.; Landis, C.A. 1972: Correlative Oligocene unconformities in southern Australasia. *Nature 237(70)*: 12-13.

Carter, R.M.; Lindqvist, J.K.; Norris, R.J. 1982: Oligocene unconformities and nodular phosphate hargrounds in western Southland and northern West Coast. *Journal of the Royal Society of New Zealand 12*: 11-46.

Chamley, H. 1989: *Clay Sedimentology.* Springer-Verlag Berlin.

Davey, F.J. 1977: Marine Seismic Measurements in the New Zealand Region. *New Zealand Journal of Geology and Geophysics 20*: 719-777.

De Gilbert, J.M.; Martinell, J.; Domenech, R. 1995: The rosetted feeding trace fossils *Dactyloidites ottoi* (Geinitz) from the Miocene of Catalonia. *Geobios 28*: 796-776.

Devereux, I. 1967: Oxygen isotope paleotemperature measurements on New Zealand Tertiary fossils. *New Zealand Journal of Science 10*: 988-1011.

Drits, V.A.; Sakharov, B.A.; Lindgreen, H.; Salyn, A. 1997: Sequential structure transformationof illite-smectite-vermiculite during diagenesis of Upper Jurassic shales from the North Sea and Denmark. *Clay Minerals 32*: 351-371.

Duff, S.W. 1975: *Early Mid-Oligocene (Whaingaroan-Duntroonian) diastems marked by surfaces of biogenic excavation on the East Coast of the South Island, New Zealand.* M.Sc. Thesis, University of Canterbury.

Feldmann, R.M.; Maxwell, P.A. 1990: Late Eocene Decapod crustacea from north Westland, South Island, New Zealand. *Journal of Paleontology 64*: 779-797.

Ferguson, R.J. 1993: *Tectonic controls on basin development, fluvial architecture and coal occurrence in the Paparoa Coal Measures at the Pike River Coalfield, West Coast of the South Island.* M.Sc. Thesis, University of Canterbury, New Zealand.

Field, B.D. 1985: Mid Tertiary unconformities in the Mount Somers to Rangitata River area, Canterbury. *New Zealand Geological Survey Report SL* 1985, NZGS, Lower Hutt. 17 pp.

Findlay, R.H. 1980: The Marshall Paraconformity. Note. *New Zealand Journal of Geology and Geophysics 23*: 125-133.

Fulthorpe, C.S.; Carter, R.M.; Miller, K.G.; Wilson, J. 1996: Marshall Paraconformity; a mid-Oligocene record of inception of the Antarctic circumpolar current and coeval glacioi-eustatic lowstand?. *Marine and Petroleum Geology 13*: 61-77.

Fürsich, F.T. 1982: Rhythmic bedding and shell bed formation in the Upper Jurassic of East Greenland. In: Einsele, G.; Seilacher, A.: *Cyclic and Event Stratification*. Springer-Verlag, Berlin, p. 208-222.

Gage, M. 1945: The Tertiary and Quaternary Geology of Ross, Westland. *Transactions of the Royal Society of New Zealand 75*: 138-159.

Gage, M. 1952: The Greymouth Coalfield. *New Zealand Geological Survey Bulletin 45.*

Gage, M, 1975: Stratigraphic classification and nomenclature in Buller and North Westland, Comment. *N.Z. Journ. Geol. Geophys. 18*: 629-38.

Geinitz, H.B. 1849: Das Quadersandsteingebirge oder Kreidegebirge in Deutschland. 292 p. Craz und Gerlach, Freiberg.

German, R.C. 1976: Stratigraphy and sedimentology of the Nile Group (Oligocene) southwest Nelson. M.Sc. Thesis, held in the library, University of Canterbury.

Ghosh, A.K.; Maithy, P.K. 1996: On the present status of coralline red algaa *Archaeolithothamnium* Roth. from India. *Palaeobotanist 45*: 64-70.

Glaessner, M.F. 1960: The fossil decapod Crustacea of New Zealand and the evolution of the order Decapoda. *New Zealand Geological Survey Paleontological Bulletin 31*, 79 p.

Glaessner, M.F. 1980: New Cretaceous and Tertiary crabs (Crustacea: Brachyura) from Australia and New Zealand. *Trasactions of the Royal Society of South Australia 104*: 171-192.

Graham, I.J.; White P.J. 1990: Rb-Sr dating of Rahu Suite granitoids from the Paparoa Range, North Westland, New Zealand. *New Zealand Journal of Geology and Geophysics 33*: 11-22.

Hall, J.S.; Mozley, P.S.; Davis, J.M.; Delude, N.A. 1996: Evironments of formation and controls on the spatial distribution of calcite cements in the Sierra Ladrones Formation (Plio-Pliestocene), NM. *Abstracts with Programs - Geological Society of America 28*: 90.

Haq, B.U.; Hardenbol, J.; Vail, P.R. 1987: Chronology of fluctuating sea levels since the Triassic. *Science 235*: 1156-1167.

Harms, J.C.; Southard, J.B.; Spearing, D.R.; Walker, R.G. 1975: Depositional environments as interpreted from primary sedimentary structures and stratification sequences. *Soc. Econ. Paleontologists and Mineralogists Short Course no 2.*

Harris, P.T.; Tsuji, Y.; Marshall, J.F.; Davies, P.J.; Honda, N.; Matsuda, H. 1996: Sand and rhodolith-gravel entrainment on the mid- to outer-shelf under a western boundary current: Fraser Island continental shelf, eastern Australia. *Marine Geology 129*: 313-330.

Henderson, J. 1929: The Late Cretaceous and Tertiary Rocks of New Zealand. *Transactions of the Royal Society of New Zealand 294A*: 271-289.

Henderson, R.A. 1975: Cenozoic Spatangoid Echinoids from New Zealand. *N.Z. Geol. Surv. Paleont. Bull. 46*. 129p.

Hesse, R. 1987: Selective and reversible carbonate-silica replacements in Lower Cretaceous carbonate-bearing turbidites of the Eastern Alps. *Sedimentology 34*: 1055-1077.

Hesse, R. 1990: Silica Diagenesis: Origin of inorganic and replacement cherts. In: McIlreath, I.A.; Morrow, D.W.: *Diagenesis, Geoscience Canada reprint series 4,* p. 253-275.

Heward, A.P. 1981: A review of wave-dominated clastic shoreline deposits. *Earth-Science Reviews 17*: 223-276.

Hornibrook, N. de B.; Brazier, R.C.; Strong, C.P. 1989: Manual of New Zealand Permian to Pleistocene Foraminiferal Biostratigraphy. *New Zealand Geological Survey Paleontological Bulletin 56*, 175 p.

James, N.P.; Bone, Y. 1992: Synsedimentary cemented calcarenite layers in Oligo-Miocene cool-water shelf limestones, Eucla Platform, southern Australia. *Journal of Sedimentary Petrology 62*: 860-872.

Jindrich, V. 1983: Structure and diagenesis of recent algal-foraminifera reefs, Fernando de naronha, Brazil. *Journal of Sedimentary Petrology 53(2)*: 449-459.

Johnson, J.H. 1961: Limestone building algae and algal limestones. Johnson Publishing Company 297p.

Kamp, P.J.J. 1991: Late Oligocene Pacific-wide tectonic event. *Terra nova 3*: 65-69.

Kear, D.; Schofield, J.C. 1978: Geology of the Ngaruawahia subdivision. *New Zealand Geological Survey Bulletin 88*: 166p.

Kimbrough, D.L.; Tulloch, A.J. 1989: Early Cretaceous age of orthogneiss from the Charleston Metamorphic Group, New Zealand. *Earth and Planetary Science Letters 95*: 130-140.

Laird, M.G. 1968: The Paparoa Tectonic Zone. *New Zealand Journal of Geology and Geophysics 11*: 435-454.

Laird, M.G. 1970: *Notes on the paleogeography of the Haku 1 site and adjacent areas of West Coast.* Unpublished Petroleum Report Haku 1. PR 553. Held at the Geological Survey Library. Lower Hutt.

Laird, M.G. 1988: Sheet S37 Punakaiki (1st edition). Geological map of New Zealand 1:63 360. Map (1 sheet) and notes (48p.). New Zealand Department of Scientific and Industrial Research, Wellington.

Laird, M.G. 1994: Geological aspects of the opening of the Tasman Sea. In: Van der Lingen, G.J., Swanson, K.M., Muir, R.I. (eds.): *Evolution of the Tasman Sea Basin*, Rotterdam, Balkema, p. 1-18.

Laird, M.G.; Lewis, D.W. 1976: *Sedimentary Geology if Precambrian to Quaternary rocks, South Island (northern part), New Zealand.* Excursion guide 58C, 25th Geol. Congress Australia.

Lamarche, G.; Collot, J.-Y.; Wood, R.A.; Sosson, M.; Sutherland, R.; Delteil, J. 1997: The Oligocene-Miocene Pacific-Australia plate boundary, south of New Zealand: Evolution from oceanic spreading to strike-slip faulting. *Earth and Planetary Science Letters 148*: 129-139.

Leask, W.L. 1993: Brunner Coal Measures at Golden Bay, Nelson: an Eocene fluvial-esturine deposit. *New Zealand Journal of Geology and Geophysics 36*: 37-50.

Lee, D.E.; Scholz, J.; Gordon, D.P. 1997: Paleoecology of a late Eocene Mobile Rockground Biota from North Otago, New Zealand. *Palaios 12*: 568-581.

Lever, H. 1998: Paleogeography and basin development of the Eocene Rapahoe Group in the Punakaiki-Charleston area. *GSNZ/NZGS Joint Annual Conference 1998 Programme and Abstracts, Geol. Soc. New Zealand Misc. Publ. 101A*: 144.

Lewis, D.W. 1975: Stratigraphic classification and nomenclature in Buller and North Westland, Comment. *New Zealand Journal of Geology and Geophysics 18*: 638-42.

Lewis, D.W. 1992: Anatomy of an unconformity on Mid-Oligocene Amuri Limestone, Canterbury, New Zealand. *New Zealand Journal of Geology and Geophysics 35*: 463-475.

Lewis, D.W.; Belliss, S.E. 1984: Mid Tertiary unconformities in the Waitaki subdivision, North Otago. *Journal of the Royal Society of New Zealand 14*: 251-276.

Lewis, D.W.; Ekdale, A.A. 1992: Composite ichnofabric of a Mid-Tertary unconformity on pelagic Oligocene Amuri Limestone, Canterbury, New Zealand. *Palaios 7*: 222-235.

Lewis, D.W.; McConchie, D. 1994: *Analytical Sedimentology*. Chapman and Hall, London. 213p.

Lewthwaite, K.J. 1995: *The Charleston Metamorphic Group: Paleozoic and Cretaceous deformation and metamorphism, and development of the Paparoa Metamorphic Core Complex:* M.Sc. Thesis, University of Canterbury, New Zealand.

Lindqvist, J.K. 1972: Notocene stratigraphy of the Fletcher Creek and Inangahua areas, North Westland. Dip. Sci. Thesis, Otago University, Dunedin.

MacGregor, A.R. 1983: The Waitakere Limestone, a temperate algal carbonate in the lower Tertiary of New Zealand. *Journal of the Geological Society of London 140(3)*: 387-399.

Manker, J.P.; Carter, B.D. 1987: Paleoecology and Paleogeography of an Extensive Rhodolith Facies from the Lower Oligocene of South Georgia and North Florida. *Palaios 2*: 181-188.

Martin, J.M.; Braga, J.C.; Konishi, K.; Pigram, C.J. 1993: A model for the development of rhodoliths on platforms influenced by storms: Middle Miocene carbonates of the Marion Plateau (Northeastern Australia). *Proceedings of the Ocean Drilling Program, Scientific Results, 133*: 455-460.

McLennan, J.M.; Bradshaw, J.D. 1984: Angular unconformity between Oligocene and older Cenozoic rocks at Avoca, Canterbury, New Zealand. *New Zealand Journal of Geology and Geophysics 27*: 299-303.

Minnery, G.A. 1990: Crustose coralline algae form the Flower Garden Banks, northwestern Gulf of Mexico; controls on distribution and growth morphology. *Journal of Sedimentary Petrology 60*: 992-1007.

Molenar, N.; Zijlstra, J.J.P. 1997: Differential early diagenetic low-Mg calcite cementation and rhythmic harground development in Campaanian-Maastrichtian chalk. *Sedimentary Geology 109*: 261-281.

Moore, R.C.; Teichert, C. (eds.) 1978: *Treatise on Invertebrate Palaeontology, Part T, Echinodermata 2.* Geological Society of America and University of Kansas Press, Lawrence.

Morgan, P.G. 1911: The geology of the Greymouth subdivision, North Westland. *New Zealand Geological Survey Bulletin (n.s.) 13*: 159p.

Morgan, P.G.; Bartrum, J.A. 1915: The geology and mineral resources of the Buller-Mokihinui subdivision, Westport Division. *New Zealand Geological Survey Bulletin 17.*

Muir, R.J., Bradshaw, J.D., Weaver, S.D., Ireland, T.R. 1994: Crustal extension prior to the opening of the Tasman Sea Basin, Evidence from New Zealand granites. In: Van der Lingen, G.J., Swanson, K.M., Muir, R.I. (eds.): *Evolution of the Tasman Sea Basin*, Rotterdam Balkema, p. 55-72.

Nathan, S. 1974: Stratigraphic nomenclature for the Cretaceous-Lower Quaternary rocks of Buller and North Westland, West Coast, South Island, New Zealand. *New Zealand Journal of Geology and Geophysics 17*: 423-445.

Nathan, S. 1975a: Stratigraphic classification and nomenclature in Buller and North Westland, Reply. *New Zealand Journal of Geology and Geophysics 18*: 642-651.

Nathan, S. 1975b: Sheets S23 & S30 Foulwind and Charleston (1st edition). Geological map of New Zealand 1:63 360. Map (1 sheet) and notes (20p.). New Zealand Department of Scientific and Industrial Research, Wellington.

Nathan, S. 1978: Sheet S44 Greymouth. Geological map of New Zealand 1:63 360. Map (1 sheet) and notes (35p.). New Zealand Department of Scientific and Industrial Research, Wellington.

Nathan, S; Smale, D. 1983: Petrological studies of Cretaceous and Tertiary sediments from the West Coast region. *New Zealand Geological Survey Report G71.*

Nathan, S; Anderson, H.J.; Cook, R.A.; Herzer, R.H.; Hoskins, R.H.; Raine, J.I.; Smale, D. 1986: Cretaceous and Cenozoic sedimentary basins of the West Coast Region, South Island, New Zealand. *N.Z. Geological Survey Basin Studies 1.*

Nelson, C.S. 1978: Temperate shelf carbonate sediments in the Cenozoic of New Zealand. *Sedimentology 25*: 737-771.

Newman, J. 1985: *Paleoenvironments, coal properties, and their interrelationship in Paparoa and selected Brunner Coal Measures on the West Coast of the South Island.* Ph.D. Thesis, Canterbury University, New Zealand.

Nunweek, C.N. (in prep.) 1999: Depositional controls on peat accumulation and coal characteistics, Dunollie Coal Measures, Southern Rapahoe Sector, Greymouth. M.Sc. Thesis, University of Canterbury.

Palmer, J. 1985: Pre-Miocene lithostratigrahy of Taranaki Basin, New Zealand. *New Zealand Journal of Geology and Geophysics 28*: 197-216.

Pantin, H.M. 1969: The appearance and origin of colours in muddy marine sediments around New Zealand. *New Zealand Journal of Geology and Geophysics 12*: 51-66.

Peryt, T. 1983: Classification of coated grains. In: Peryt, T. (ed.): *Coated Grains.* Springer-Verlag, Berlin.

Phleger, F.B. 1960: *Ecology and distribution of recent Foraminifera.* John Hopkins, Baltimore. 296p.

Reay, M.B. 1975: *The nature, genesis and paleoenvironment of the Little Totara Sand Formation, North Westland, New Zealand.* Project for course 306, Geology Department, University of Canterbury.

Reay, M.B. 1993: Geology of the Middle Clarence Valley. Institute of Geologic and Nuclear Sciences Gological Map 10. IGNS Wellington.

Roder, G.H.; Suggate, R.P. 1990: Geologic map of NZ 1:50000 Sheet L29 BD Upper Buller Gorge. New Zealand Geological Survey, Welington.

Ruffell, A.H.; Rawson, P.F. 1994: Palaeoclimate control on sequence stratigraphic patterns in the Late Jurassic to Mid-Cretaceous, with a case study from eastern England. *Palaeogeography, Palaeoclimatology, Palaeoecology 110*: 43-54.

Sakharov, B.A.; Lindgreen, H.; Salyn, A.L.; Drits, V.A. 1999: Mixed-layer kaolinite-illite-vermiculite in North Sea shales. *Clay Minerals 34*

Smale, D. 1990: Distribution and Provenance of heavy minerals in the South Island; a review. *New Zealand Journal of Geology and Geophysics 33*: 557-571.

Soong, R.; Blattner, P. 1986: Biterminal authigenic super 18uO-enriched quartz in a subbituminous coal seam, Charleston, New Zealand. *New Zealand Journal of Geology and Geophysics 29*: 141-145.

Srinivasan, M.S.; Vella, P. 1974: Upper Eocene – Lower Oligocene benthonic foraminifera, Port Elizabeth and Cape Foulwind, New Zealand. *New Zealand Journal of Geology and Geophysics 18*: 21-37.

Suggate, R.P. 1959: New Zealand Coals. *New Zealand D.S.I.R. bulletin 134.* 113 p.

Suggate, R.P. 1974: Coal ranks in relation to depth and temperature in Australian and New Zealand oil and gas wells. *New Zealand Journal of Geology and Geophysics 17*: 149-167.

Suggate, R.P. 1984: Geologic map of NZ 1:50000 Sheet M29 AC Mangles Valley and notes (39 pp.). New Zealand Geologic Survey, Wellington.

Suggate, R.P.; Stevens, G.R.; Te Punga, M.T. (eds.) 1978: *The Geology of New Zealand.* Government Printer, Wellington, 820 p.

Sykes, R.; Lindqvist, J.K. 1993: Diagenetic quartz and amorphous silica in New Zealand coals. In: Stout, S.A.; Hower, J.C. (eds.): Collected papers from the ninth annual meeting of the Society for Organic Petrology. *Organic Geochemistry 20*: 855-866.

Tsuji, Y. 1993: Tide influenced high energy environments and rhodolith-associated carbonate deposition on the outer shelf and slope off the Miyako Islands, southern Ryukyu Island Arc, Japan. *Marine Geology 113*: 255-271.

Van der Lingen, G.J.; Andrews, P.B. 1968: Grain size parameters and sedimentary structures of a last intergalcial marine sand body, near Westport, New Zealand. *New Zealand Journal of Marine and Freshwater Research 2*: 447-471.

Visher, G.S. 1969: Grain size distributions and depositional processes. *Journal of Sedimentary Petrology 39*: 1074-1106.

Ward, S.D. 1997: *Lithostratigraphy, palynostratigraphy and basin analysis of the Lower Cretaceous to early Tertiary Paparoa Group, Greymouth Coalfield, New Zealand.* Ph.D. Thesis, Canterbury University.

Whatley, R.C.; Arias, C.F.; Comas-Rengifo M.J. 1994: The use of Ostracoda to detect kenoxic events: a case history from the Spanish Toarcian. *Geobios, M.S. 17*: 733-741.

White, P.J. 1994: Thermobarometry of the Charleston metamorphic group and implications for the evolution of the Paparoa metamorphic core complex, New Zealand. *New Zealand Journal of Geology and Geophysics 37*: 201-209.

Wood, R.; Lamarche, G.; Herzer, R.; Beltail, J.; Davy, B. 1996: Paleogene seafloor spreading in the southeast Tasman Sea. *Tectonics 15*: 966-975.

Wray, J.L. 1977: Calcereous Algae. *Developments in Paleontology and Stratigraphy 4.* Elsevier, Amsterdam.

Yetton, M. 1975: *The Texture and composition of the heavy minerals suites in Tertiary quartz sands near Westport.* Project for course 306, Geology Department, University of Canterbury.

Yoshihiro, T. 1993: Tide influences high-energy environments and rhodolith-associated carbonate deposition on the outer shelf and slope off the Miyako Islands, southern Ryukyu island arc, Japan. *Marine Geology 113*: 255-271.

Young, D.J. 1964: Ganister and silica sand deposits of the West Coast, South Island. *New Zealand Journal of Geology and Geophysics 7*: 508-524.

Zinsmeister, W.J.; Feldmann, R.M. 1984: Cenozoic high latitude heterochroneity of Southern Hemisphere marine faunas. *Science 224*: 281-283.

Zuffa, G.G. (ed.) 1985: *Provenance of Arenites.* D Reidel Publishing Co. Holland, 408p.

Appendix I

Measured Sections

This appendix gives the summary stratigraphic logs for the major sections that can be measured. Nowhere in the field area is a complete section exposed, the closest to a complete section is the Gibsons Beach section, where approximately 25 m of inferred Kaiata mudstone occurs below the last exposure to the approximate location of the contact with the underlying "Brunner" sands. In most river sections and inland sections the exposure is so limited that measured sections were not attempted. Kaiata Mudstone especially does not form good sections. The only sections suitable for logging occurred in the coastal cliffs, where they are continually eroded by the action of the sea. Measured sections were taken along Gibsons Beach, from Woodpecker Bay to Kaipakati Point and from Kaipakati Point to Pahautane. These sections show the locations of samples (HLS numbers), fossils (F numbers) and include brief discriptions of the textures, structures and trace fossils found.

Woodpecker Bay to Kaipakati Point: K30 749067-747068

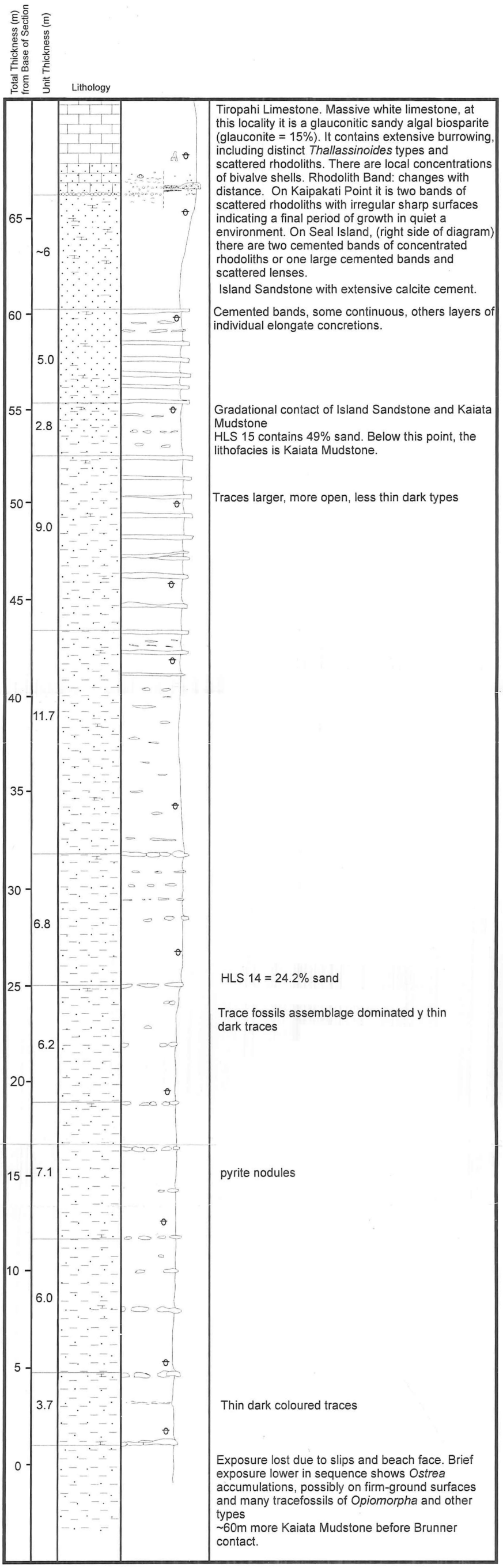

Gibsons Beach (Cape Foulwind) K29 834387-829387

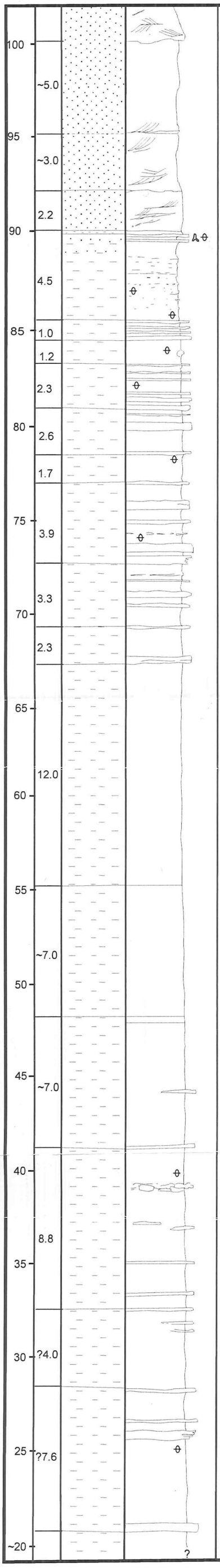

Nine Mile Formation (Quaternary Marine Sands).
Note: Rapahoe group is overlain conformably by Blue Bottom mudstones, close by this section, the quaternary marine sands top all the coastal cliffs in this area, an angular erosional unconformity.

Little Totara Sand. Overall poorly sorted, micaceous quartz sand, containing abundant cross-bedding structures, which separate grain sizes into well sorted laminae. Muscovite is the dominant mica.

?minor erosive surface.

Little Totara sand is white in colour with orange highlighting of cross-bedding, probably caused by iron mobalisation during quaternary marine weathering.

Surface of substantial erosion.
biotite present in sand
Mixture of very low angle single cross-beding and steeper varieties, mainly granule layers.
Black and brown laminated mud and silts.

Outstanding ~10cm thick laterally continuous cemented layers.

Scattered concretions, elongate and occuring in layers
Kaiata mudstone, micaceous, quartz rich very fine sand, silt and clay, normally grey in outcrop. Cemented bands range in thickness and lateral continuity, and frequently contain trace fossils, preserved uncompacted by the cementation, which probably was initiated shortly after deposition.
Burrows near the contact with the Little Totara Sand show increasing content of coarse sediment, shells, quartz sand, and algal grains, indicating that the conditions were shallowing, although the sediments deposited during this time have been eroded. The distinctive mud/silt layer between the Kaiata and LTS does not appear in any burrow fill, so it can be concluded that this was deposited after erosion of the coarser sediments, and in conditions unsuited to larger burrowers, probably in a lagoon or estuary. The presence of algal grains in the burrow fill shows the proximity of a bioherm, implying a nearby coastline. This bioherm may be the same as supplied algal detritus to the lower part of the Kaiata mudstone in this section.

A thin layer of clay, with no obvious change in grain size.

Two thin (2mm) layers of almost pure clay, marked by a change in the weathering pattern of the clif-face. The changein weathering pattern is related to an abrupt change across the upper layer from very muddy silts to less muddy silts.

Exposure limited due to cover by slips and beach sand.
All thickness approximate.

Pahautane to Kaipakati Point: K30 746053-746061

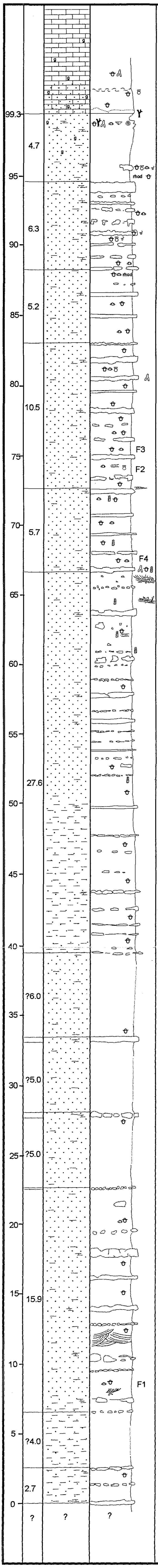

Tiropahi Limestone. Here the limestone is massive cream-brown glauconitic biosparite, with several layers of concentrated bivalves, and large amounts of bryozoa in the bottom-most part.

Shell band (bivalves). Lots of glauconite

Patches of ?bryozoa cementation
Eroded Soft sand
10-15% glauconite
Island sandstone, cream-brown to grey muddy sandstone, calcereous cemented bands common. Scattered echinoderm fossils, with worm tubes, bivalves, rhodoliths and brachiopods occurring in the upper part, close to the limestone contact.
HLS 5: 57% sand, angular quartz, mainly plagioclase feldspar, black/brown lithics and opaques, glauconite ~10-15%.

~5% glauconite

~5% glauconite, isolated rhodoliths, bioturbated

Rhodolith and cementation

~5% or less glauconite

Very little glauconite <<5%

Poorly sorted, muddy, no glauconite, trace fossils frequently have muddy rims. Iron concretions occur.

Some sedimentary structures preserved above concretion layer

Partly bioturbated sedimentary structures passing up into completely bioturbated sediments.

Lots of unjoined concretions.
Bioturbation not complete, broken shell accumulations and a little glauconite occur.
Obvious Ophiomorpha traces.
Narrow (5mm) dark rimmed traces, vertical, inclined and horizontal. Below this level these traces increase in frequency while ophiomorpha and other larger traces slowly decrease in frequency. Less Echinoderm fossils and traces.

HLS 7: 44% sand.

Iron concretions, heavily bioturbated

Last occurrence of narrow, dark edged trace fossils.
Iron concretions occur, even within calcitic concretions.

"Serpent holes", preferred erosion of trace fossils in concretions.
Many sedimentary structures, possible hummocky cross stratification, many scour surfaces.

Some sedimentary structures, intensity 4 bioturbation change in trace fossils
Highly bioturbated, grey, no sedimentary structures

HLS 12: 48% snad

Exposure ends due to change in orientation of coastal cliffs and dip of beds.

Appendix II

Sample Lists

The samples collected during field work are listed with brief descriptions of the formation collected from, the location, a grid reference and a note of whether grain size analysis (gs, see Appendix V), microfossil identification (m, see Appendix III) or thin sections (ts, see Appendix IV) were taken from the sample. Grid references are for the NZMS 260 series 1:50000 topographic maps, or alternatively, the geological map produced for this thesis in the back pocket. HLS numbers are used throughout the thesis, the UCL numbers are provided for future correlation with the University of Canterbury rock collection.

UCL	HLS	Description/Stratigraphic Location	Grid Reference	
17027	1	?hardgroud near lime/Island contact	K30 746053	ts
17028	2	sand/glauconite near lime/Island contact	K30 746053	ts
17029	3	bryozoan cementation above contact	K30 746053	ts
17030	4	Glauconitic Limestone	K30 746053	
17031	5	Island sandstone, glauconitic	K30 746053	gs, m
17032	6	Cemented Island sandstone	K30 746053	ts
17033	7	Island Sandstone	K30 746054	gs, m
17034	8	Island Sandstone	K30 746055	m
17035	9	Island Sandstone	K30 746056	m
17036	10	Island Stanstone and Fossils	K30 746055	m
17037	11	Cemented Island Sandstone, next to 10	K30 746055	ts
17038	12	Island/Kaiata	K30 746057	gs, m
17039	14	Kaiata Mudstone (Woodpeckers Bay)	K30 749067	gs, m
17040	15	Kaiata Mudstone (Woodpeckers Bay)	K30 748066	gs, m
17041	16	Kaiata-Island-Limestone 3.5m below rhodoliths	K30 747068	ts
17042	17	Kaiata-Island-Limestone 1.0m below rhodoliths	K30 747068	ts
17043	18	Rhodolith Band	K30 747068	ts
17044	20	Little Totara Sand, Pahautane	K30 751046	
17045	21	Little Totara Sand, Pahautane	K30 751046	

17046	22	Little Totara Sand	K30 753046	
17047	23	Quartz lag above Brunner	K30 753046	
17048	24	Qtz Sand interbedded with Limestone (HLS 27)	K29 834238	
17049	25	LT Sand near Charleston, Quarry wall	K29 830239	
17050	26	LT Sand near Charleston, Quarry wall	K29 830239	
17051	27	Limestone from interbedding with HLS 24	K29 834238	
17052	28	Transition Brunner --> LTSand	K30 804182	
17053	29	Transition Brunner --> LTSand	K30 804182	
17054	30	Transition Brunner --> LTSand	K30 804182	
17055	31	Transition Brunner --> LTSand	K30 804182	
17056	32	Transition Brunner --> LTSand Close	K30 804181	
17057	33	Transition Brunner --> LTSand Loose	K30 804181	
17058	34	Kaiata Mudstone from 4mile River	K30 808142	gs
17059	35	Kaiata Mudstone (Cape Foulwind)	K29 834387	
17060	36	Transition Layer (Mud-LTS)	K29 834387	
17061	37	LT Sand	K29 834387	gs
17062	38	LT Sand	K29 834387	gs
17063	39	Kaiata Mudstone	K29 830387	gs, m
17064	40	Cemented reef rubble in Kaiata	K29 830387	ts
17065	41	Kaiata Mudstone cemented band	K29 834387	ts
17066	42	Pleist., marine sand no fossils, above LT sand	K29 834387	
17067	43	Sandstone from Truman Track, fossils	K30 726003	m
17068	44	Sandstone from Truman Track, 2.3m above 43	K30 726003	m
17069	45	?Island Sandstone, road cutting	K30 73520128	m
17070	46	?Island Sandstone, road cutting	K30 73520128	gs, m
17071	47	?Island Sandstone, road cutting	K30 73450097	
17072	48	Road Cutting 25km bend, Brunner	K30 803144-142	
17073	49	Road Cutting 25km bend, Brunner	K30 803144-142	
17074	50	Road Cutting 25km bend, LT Sand	K30 803144-142	
17075	51	Road Cutting 25km bend, LT Sand	K30 803144-142	gs
17076	52	Road Cutting 25km bend, Brunner?	K30 803144-142	
17077	53	Road Cutting 25km bend, Brunner?	K30 803144-142	
17078	54	Road Cutting 25km bend, LT Sand	K30 803144-142	gs
17079	55	Road Cutting 25km bend, LT Sand	K30 803144-142	gs
17080	56	Road Cutting 25km bend, LT Sand	K30 803144-142	
17081	57	Road Cutting 25km bend, LT Sand, clay layer	K30 803144-142	
17082	58	??Little Totara Sand Okari Estuary	K29 828306	ts
17083	59	Island ss 2.3m below contact, Bullock Creek	K30 757000	gs, m

17084	60	Limestone close to contact, Bullock Creek	K30 757000	ts
17085	61	Coarse Burrow fill, below LT sand contact	K29 834387	ts
17086	62	Clayey material - discontinuity surface	K29 834387	
17087	63	Overlying 62 - coarse LTSand	K29 834387	gs
17088	64	Cemented and non cemented ?Kaiata, Okari	K29 824310	ts, m
17089	65	4.5m above 64, Okari Lagoon	K29 824312	m
17090	66	Kaiata mudstone, Okari Lagoon	K29 824315	gs, m
17091	67	Pink Cobbles in discontinuity layer, Island ss	K30 728010	ts
17092	68	Sed below surface HLS 67	K30 728010	ts
17093	69	Surface of thalassinoides rich band	K30 728011	ts
17094	70	Shell rich deposits	K30 728011	
17095	71	Wood?	K30 728011	
17096	72	Sediment and shells	K30 728011	
17097	73	Bryozoa layer and sediment. Island ss	K30 727993	ts
17098	74	Island/limestone, glauconitic, Limestone Ck	K30 751047	ts, m
17099	75	Muddy sediment beneath HLS 74	K30 751047	m
17100	76	Island sandstone upstream HLS 74&75	K30 751047	gs
17101	77	Island above Punakaiki River Gorge	K30 757927	ts
17102	78	Kaiata mudsone and layer of limestone blocks	K30 756928	gs, ts, m
17103	79	More rhodoliths from band	K30 747068	ts
17104	80	Sed (limestone) 1m above rhodolith band	K30 747068	ts
17105	81	Fallen blocks from rhodolith band	K30 748068	ts
17106	82	Sed below cemented band=unconformity	K30 746061	m
17107	83	Sed above cemented band=unconformity	K30 746061	m
17108	84	Shell fragments and brachs from HLS 44 loc.	K30 726003	
17109	85	Convoluted/laminated bedding + pink conc.	K30 728010	ts(2)
17110	86	Sediment immediately above pink conc. Layer	K30 728010	ts
17111	86'	Kaiata Mudstone from Quarry	K29 826363	m
17112	87	Mud/silt layers between Kaiata and LTS, Quarry	K29 826363	gs
17113	88	Clay layer and surrounding sed, Gibsons Beach.	K29 832387	gs(2), m(2)
17114	89	More rhodolith Blocks from Seal Island	K30 748068	ts
17115	90	Rotten and normal Limestone, Quarry	K29 827364	
17116	91	Limestone, Cape Foulwind Quarry	K29 826364	ts
17117	92	Limestone, Cape Foulwind Quarry	K29 827370	ts
17118	93	Brunner equivalent sandstone, Gibsons Beach.	K29 827388	

Appendix III

Microfossil List

The list presented in the following pages details specimens identified by Ms Alexa A. Cameron of the Geology Department at Canterbury University. The specimen lists do not include all microfossil material found in the sediments, but only those foraminifera specimens that could be identified, and especially concentrates on those that have useful age ranges for correlation purposes. The ostracods found in several samples are discussed in Chapter 6. The age range of identified species and the interpreted sample age is presented in the following table, this information is used in Chapter 8 for correlating sections within the basin. The data is such that frequently only an age range can be determined for a sample. This is largely because the foraminiferal zones that are best for dating samples rely on the appearance and disappearance of key species, that are not common in the samples extracted. This is especially the case in the planktonic zones which could not be used due to the rarity of planktonic specimens.

The microfossils were extracted by heating the sediment with a dispersant (detergent or Calgon) until completely disaggregated, then sieving and collecting the sand fraction. Microfossils were picked out with a brush under a binocular microscope, and collected in slides. Disaggregating more well cemented samples using hydrogen peroxide was attempted, but this was found to destroy most porcelaneous foraminifer and other microfossils, and even damage agglutinated foraminifera, so that few or no microfossils were recovered.

Sample	Species Present	Time Range	Sample Age
HLS 5	*Anomalinoides fasciatus* *Arendosaria antipoda* *Cibicides parki* *Lenticulina laculosa* *Melonis dorreeni* *Melonis maorica* *Vaginulina*	Ab-Po Ab-Tt Dp-base Lwh Ak-Wp Ab-Tt Ab-Tk	Ak-base Lwh
HLS 7	*Anomalinoides fasciatus* *Cassidulina subglobosa* *Cibicides parki* *Cibicides sp.* *Gyroidinoides allani* *Lenticulina sp.* *Sphaeroidina bulloides*	Ab-Po ? Dp-base Lwh Landon Ar-Rec.	basal Lwh
HLS 8	*Arendosaria antipoda* *Cibicides parki* *Cibicides sp.* *Cyclammina incisa* *Lenticulina sp.* *Gyroidina sp.* *Melonis maorica*	Ab-Tt Dp-base Lwh Arnold-Sthland Ab-Tk	Ab-basal Lwh
HLS 9	*Anomalinoides fasciatus* *Arendosaria antipoda* *Cibicides parki* *Gyroidinoides scrobiculata* *Lenticulina sp.* *Sphaeroidina bulloides*	Ab-Po Ab-Tt Dp-base Lwh Ab-? Ar-Rec.	Ar-basal Lwh
HLS 10	*Arendosaria antipoda* *Cibicides parki* *Cibicides cf. vortex* *Dorothia bulleta* *Gyroidina cf. scrobiculata* *Melonis maorica*	Ab-Tt Dp-base Lwh Ab-?Sw Cret-? Ab-? Ab-Tk	Ab-basal Lwh
HLS 12	*Cribrorotalia cf. tainuia* *Gyroidinoides* *Cassidulina* *Vaginulinopsis interrupta*	Ak-? Ak?Ar-Ld	Ak?

HLS 14	*Anomalinoides fasciatus*	Ab-Po	Ar-basal Lwh
	Arendosaria antipoda	Ab-Tt	
	Cassidulina subglobosa	?-Rec.	
	Cibicides parki	Dp-base Lwh	
	Hanzawaia (Discopulvinulina)	?Lwh-S	
	Dentalina		
	Gyroidinoides		
	Lenticulina sp.		
	Melonis maorica	Ab-Tk	
	Sphaeroidina bulloides	Ar-Rec.	
	Stilostomella pomuligera	Ab-T	
	Vaginulinopsis spinulosa	Ab-Ld	
HLS 15	*Anomalinoides sp.*		Ab-?Olig.
	Arendosaria antipoda	Ab-Tt	
	Dorothia bulleta	Cret-Olig?	
	Gyroidinoides sp.		
HLS 39	*Anomalinoides semiteres*	Ab-Ar	basal Ar (?Ab)
	Arendosaria antipoda	Ab-Tt	
	Bulimina bortonica	?Dp-Ab	
	Cassidulina sp.		
	Cibicides molestus	Ab-Wp	
	Cibicides parki	Dp-base Lwh	
	Gyroidinoides scrobiculata	Ab-?	
	Hoeglundina elegans	Ab-Rec.	
	Lenticulina		
	Melonis maorica	Ab-Tk	
	Nuttalidis truempyi	Dp-Ab	
	Rectuvigerina prisca	Ab-Ak	
	Sphaerodina bulloides	Ar-Rec	
	Uvigerina bortotara	Ab-Lwh	
HLS 43	*Anomalinoides fasciatus*	Ab-Po	Ar-Po
	Arendosaria antipoda	Ab-Tt	
	Gaudryina reussi	Ab-Po	
	Martinottiella communis	?-Rec.	
	Sphaerodina bulloides	Ar-Rec.	
HLS 44	*Anomalinoides fasciatus*	Ab-Po	Ar-Po
	Arendosaria antipoda	Ab-Tt	
	Cornuspira aerdinede	Cret.-Rec.	
	Cyclammine incisca	Arnold-Sthlnd	
	Pullenia quinqueloba		
	Sphaerodina bulloides	Ar-Rec	
HLS 45	*Cassidulina subglobosa*	?-Rec.	Ab-Tt
	Cibicides parki	Ab-Tt	
	Gyroidinoides sp.		
	Melonis doreeni	Ab-Tt	

HLS 46	*Cassidulina subglobosa* *Cibicides vortex* *Melonis doreeni* *Sphaerodina bulloides*	?-Rec. Ab-S Ab-Tt Ar-Rec.	Ar-S
HLS 59	*Arendosaria antipoda*	Ab-Tt	Ab-Tt
HLS 64	*Cibicides vortex* *Dentalia sp.* *Gyroidinoides allani* *Hoeglundina elegans* *Melonis doreeni* *Melonis maorica* *Rectuvigerina postprandia*	Ab-S Landon Ab-Rec. Ab-Tt Ab-Tk Ar-base Lwh	basal Lwh
HLS 65	*Anomalinoides fasciatus* *Cibicides parki* *Cibicides sp.* *Lenticulina sp.* *Melonis doreeni* *Polymorphina* *Uvigerina bortotara*	Ab-Po Ab-Tt Ab-Tt Ar?Lwh-P Ab-Lwh	Ar?-Lwh
HLS 66	*Bolivina sp.* *Cibicides molestus* *Cibicides parki* *Cyclammine incisca* *Gyroidinoides sp.* *Lenticulina sp.* *Loxostomoides bortonica* *Martinottiella communis* *Melonis doreeni* *Melonis maorica* *Vaginulina sp.*	 Ab-Wp Dp-base Lwh Arnold-Sthlnd Dw-Ar ?-Rec. Ab-Tt Ab-Tk	Ab-Ar
HLS 74	*Arendosaria antipoda* *Cibicides sp.* *Gyroidinoides sp.*	Ab-Tt	
HLS 75	*Anomalinoides fasciatus* *Arendosaria antipoda* *Cibicides sp.* *Melonis doreeni* *Melonis maorica* *Sphaerodina bulloides* *Tritaxia*	Ab-Po Ab-Tt Ab-Tt Ab-Tk Ar-Rec. D-S	Ar-Po

HLS 78	*Anomalinoides fasciatus* *Cibicides molestus* *Cibicides perforatus* *Cribrorotalia tainuia* *Guttulina problema* *Hoeglundina elegans* *Lenticulina sp.*	Ab-Po Ab-Wp Ak-Sc Ak-Lwh Ar-Lwh Ab-Rec.	Ar-Lwh
HLS 82	*Anomalinoides fasciatus* *Arendosaria antipoda* *Cibicides sp.* *Hoeglundina elegans* *Martinottiella communis* *Melonis doreeni*	Ab-Po Ab-Tt Ab-Rec. ?-Rec. Ab-Tt	Ab-Po
HLS 83	*Anomalinoides fasciatus* *Arendosaria antipoda* *Cibicides parki* *Gyroidinoides sp.* *Martinottiella communis* *Melonis doreeni*	Ab-Po Ab-Tt Ab-Tt ?-Rec. Ab-Tt	Ab-Po
HLS 86'	*Bulimina pupula* *Cibicides parki* *Glandulina symmetrica* *Guttulina problema* *Gyroidinoides sp.* *Lenticulina callifera* *Lenticulina loculosa* *Melonis doreeni* *Saracenaria*	A-P Ab-Tt Ar-Lwh Ar-Po Ak-Wp Ab-Tt Ab-W	Ar-Lwh
HLS 88u	*Arendosaria antipoda* *Cibicides molestus* *Cornuspira archivedus* *Dentalina sp* *Gullulina problema* *Gyroidinoides sp.* *Hoeglundina elegans* *Melonis doreeni* *Melonis maorica* *Rectuvigerina postprandia* *Stilostomella sp.*	Ab-Tt Ab-Wp Cret.-Rec. Ar-Lwh Ab-Rec. Ab-Tt Ab-Tk Ar-base Lwh	Ar-base Lwh

HLS 88o	*Arendosaria antipoda*	Ab-Tt	Ar-base Lwh
	Cibicides parki	Ab-Tt	
	Dentalina sp.		
	Gyroidinoides scrobiculatus	Ab-?	
	Hoeglundia elegans	Ab-Rec.	
	Lenticulina sp.		
	Rectuvigerina postprandia	Ar-base Lwh	

Appendix IV

Point Counting of Thin Sections.

This appendix lists all the samples that were thin sectioned, arranged by formation. The forms include information on the location and sample numbers, and also comments and rock names based on the examination of the thin sections. One thin section was made for each sample. Where possible these are cut across bedding to display the maximum variation in composition and structures. The percentage figures in each form are based on a count of at least 400 points, up to 600 points where variation within the thin section was large.

Sample Numbe	HLS 60	Formation	Potikohua Limestone
Location Detail	Bullock Creek, K30 757000		
Rock Name	sandy, glauconitic biosparite		
Comment	Stylolites common, glauconite and sand in layers = bedding. Microcline.		

Quartz	22.75%	Calcite Cemen	32.50%	Hornblende	
Plagioclase	2.00%	Quartz Cemen		Pyroxene	
K-Feldspar	5.50%	Authigenic Opaqu		Green grains	
Mica	1.25%	Calcareous Algae		Altered Grain	
Rock Fragments	1.75%	Bryozoa	4.75%		
Opaques		Foraminifer	7.00%	Glauconite	9.00%
Matri		Echinoderm	9.75%		
Clays		Other Shell	4.00%		

Sample Numbe	HLS 27	Formation	Waitakere Limestone
Location Detail	K29 834238, Charleston		
Rock Name	very coarse grainstone, hematitic algal biosparite		
Comment	Stylolites, white-pale pink coloured. Coarse sand common = LTS interbedded with this limestone.		

Quartz	0.40%	Calcite Cemen	13.00%	Hornblende	
Plagioclase	0.00%	Quartz Cemen		Pyroxene	
K-Feldspar	0.00%	Authigenic Opaqu		Green grains	
Mica	0.20%	Calcareous Algae	62.20%	Altered Grain	
Rock Fragments		Bryozoa	6.40%		
Opaques	3.00%	Foraminifer	3.20%	Glauconite	
Matri		Echinoderm			
Clays		Other Shell	3.20%		

Sample Numbe	HLS 78	Formation	Potikohua Limestone
Location Detail	Runakaiki River, K30 756928		
Rock Name	sandy bryozoan biosparite		
Comment	Sand in layers, high cementation, bluish in colour. Highly cemented, no stylolites.		

Quartz	11.25%	Calcite Cemen	37.00%	Hornblende	
Plagioclase	0.75%	Quartz Cemen		Pyroxene	
K-Feldspar	1.50%	Authigenic Opaqu		Green grains	
Mica	0.50%	Calcareous Algae		Altered Grain	
Rock Fragments		Bryozoa	24.25%		
Opaques	0.25%	Foraminifer	5.75%	Glauconite	0.50%
Matri		Echinoderm	11.75%		
Clays		Other Shell	6.50%		

Sample Numbe	HLS 80	Formation	Tiropahi Limestone
Location Detail	Kaipakati Point, K30 747068		
Rock Name	grainstone, galuconitic sandy algal biosparite		
Comment	Cream-green, rhodolith, glauconite fine sand.		

Quartz	8.50%	Calcite Cemen	34.00%	Hornblende	
Plagioclase	3.00%	Quartz Cemen		Pyroxene	
K-Feldspar	0.25%	Authigenic Opaqu		Green grains	
Mica	1.00%	Calcareous Algae	19.00%	Altered Grain	
Rock Fragments		Bryozoa	0.50%		
Opaques	2.50%	Foraminifer	5.50%	Glauconite	15.00%
Matri		Echinoderm	2.50%		
Clays		Other Shell	4.75%		

Sample Numbe	HLS 3	Formation	Tiropahi Limestone
Location Detail	Pahautane Point, K30 746053		
Rock Name	wackestone, glauconitic sandy bryozoan biosparite		
Comment	matrix supported(=calcite cement), detrital mode fine sand, largest bryozoa fragment ~5mm, bluecream		

Quartz	10.75%	Calcite Cemen	25.75%	Hornblende	
Plagioclase	1.25%	Quartz Cemen		Pyroxene	
K-Feldspar	1.75%	Authigenic Opaqu	5.50%	Green grains	
Mica	0.50%	Calcareous Algae		Altered Grain	
Rock Fragments	0.50%	Bryozoa	24.50%		
Opaques	3.50%	Foraminifer		Glauconite	8.25%
Matri	6.00%	Echinoderm			
Clays		Other Shell	11.75%		

Sample Numbe	HLS 58	Formation	Cape Foulwind Limestone
Location Detail	Okari Lagoon		
Rock Name	sandy algal biosparite		
Comment	Sporolithon, Lithophyllum. Large detritals, v. coarse sand, to fine sand size. Grain supported.		

Quartz	16.25%	Calcite Cemen	26.25%	Hornblende	
Plagioclase	1.25%	Quartz Cemen		Pyroxene	
K-Feldspar	2.00%	Authigenic Opaqu	0.50%	Green grains	
Mica	0.75%	Calcareous Algae	37.50%	Altered Grain	
Rock Fragments	9.00%	Bryozoa			
Opaques		Foraminifer	0.75%	Glauconite	
Matri		Echinoderm			
Clays		Other Shell	5.75%		

Sample Numbe	HLS 91	Formation	Cape Foulwind Limestone
Location Detail	Quarry		
Rock Name	algal biosparite		
Comment	Pink-cream rudstone, 96.5% CaCO3.		

Quartz		Calcite Cemen	17.75%	Hornblende	
Plagioclase		Quartz Cemen		Pyroxene	
K-Feldspar		Authigenic Opaqu	3.50%	Green grains	
Mica		Calcareous Algae	61.25%	Altered Grain	
Rock Fragments		Bryozoa	5.00%		
Opaques		Foraminifer	3.25%	Glauconite	
Matri	5.25%	Echinoderm	1.25%		
Clays		Other Shell	2.75%		

Sample Numbe	HLS 92	Formation	Cape Foulwind Limestone
Location Detail	Quarry		
Rock Name	sandy algal biosparite		
Comment	Blue-cream floatstone,		

Quartz	1.75%	Calcite Cemen	23.50%	Hornblende	
Plagioclase	0.75%	Quartz Cemen		Pyroxene	
K-Feldspar	0.50%	Authigenic Opaqu		Green grains	
Mica	0.50%	Calcareous Algae	56.25%	Altered Grain	
Rock Fragments	2.50%	Bryozoa	3.75%		
Opaques	2.00%	Foraminifer		Glauconite	0.25%
Matri	2.00%	Echinoderm			
Clays		Other Shell	6.25%		

Sample Numbe	HLS 1
Formation	Island Sandstone
Location Detail	Pahautane Point, K30 746053
Rock Name	
Comment	?firmground, bryozoa fragments, mud matrix now calcite cement.

Quartz	18.25%	Calcite Cemen	25.50%	Hornblende	
Plagioclase	2.75%	Quartz Cemen		Pyroxene	
K-Feldspar	0.75%	Authigenic Opaqu	20.75%	Green grains	
Mica	2.50%	Calcareous Algae		Altered Grain	
Rock Fragments	1.75%	Bryozoa	3.50%		
Opaques	2.00%	Foraminifer		Glauconite	8.75%
Matri		Echinoderm	3.50%		
Clays		Other Shell	9.00%		

Sample Numbe	HLS 2
Formation	Island Sandstone
Location Detail	Pahautane Point, K30 746053
Rock Name	calcite cemented, shelly, lith-feldsarenite
Comment	very coarse sand, mode is fine sand, grain supported.

Quartz	22.75%	Calcite Cemen	32.75%	Hornblende	
Plagioclase	1.75%	Quartz Cemen		Pyroxene	
K-Feldspar	2.75%	Authigenic Opaqu		Green grains	
Mica	1.50%	Calcareous Algae	5.50%	Altered Grain	
Rock Fragments	1.25%	Bryozoa	3.00%		
Opaques	3.50%	Foraminifer		Glauconite	13.00%
Matri		Echinoderm	2.25%		
Clays		Other Shell	10.50%		

Sample Numbe	HLS 6
Formation	Island Sandstone
Location Detail	Smithy's Beach, K30 746053
Rock Name	clacite cemented lithic feldsarenite.
Comment	Iron staining. Max = med sandm mode = fine sand, glauconite is transported.

Quartz	24.25%	Calcite Cemen	42.00%	Hornblende	
Plagioclase	2.25%	Quartz Cemen		Pyroxene	
K-Feldspar	2.50%	Authigenic Opaqu	3.50%	Green grains	5.00%
Mica	8.00%	Calcareous Algae		Altered Grain	
Rock Fragments	3.25%	Bryozoa			
Opaques	2.25%	Foraminifer		Glauconite	0.75%
Matri		Echinoderm			
Clays	5.25%	Other Shell	1.00%		

Sample Numbe	HLS 11
Formation	Island Sandstone
Location Detail	Smithy's Beach, K30 746053
Rock Name	calcite cemented lith-feldsarenite
Comment	Matrix = burrows/pellets Grain supported, max = med sand, mode = fine sand minor zircons

Quartz	33.75%	Calcite Cemen	37.75%	Hornblende	
Plagioclase	1.75%	Quartz Cemen		Pyroxene	
K-Feldspar	4.25%	Authigenic Opaqu	2.00%	Green grains	4.00%
Mica	4.50%	Calcareous Algae		Altered Grain	
Rock Fragments	4.00%	Bryozoa			
Opaques	1.75%	Foraminifer		Glauconite	0.50%
Matri		Echinoderm			
Clays	2.50%	Other Shell	3.25%		

Sample Numbe	HLS 16
Formation	Island Sandstone
Location Detail	Kaipakati Point, K30 747068
Rock Name	calcite cemented shelly feldsarenite
Comment	Grain supported, max = med sand, mode = fine sand, poorly sorted.

Quartz	29.50%	Calcite Cemen	39.75%	Hornblende	
Plagioclase	4.00%	Quartz Cemen		Pyroxene	
K-Feldspar	2.50%	Authigenic Opaqu		Green grains	1.00%
Mica	3.00%	Calcareous Algae		Altered Grain	
Rock Fragments	1.75%	Bryozoa			
Opaques	3.25%	Foraminifer	2.75%	Glauconite	7.25%
Matri		Echinoderm	0.75%		
Clays		Other Shell	4.50%		

Sample Numbe	HLS 17
Formation	Island Sandstone
Location Detail	Kaipakati Point, K30 747068
Rock Name	glauconitic sandy biosparite
Comment	Mostly grain supported, mode = fine-veryfine sand

Quartz	25.50%	Calcite Cemen	41.00%	Hornblende	
Plagioclase	4.00%	Quartz Cemen		Pyroxene	
K-Feldspar	1.25%	Authigenic Opaqu		Green grains	
Mica	2.25%	Calcareous Algae		Altered Grain	
Rock Fragments	1.00%	Bryozoa			
Opaques	3.50%	Foraminifer	4.25%	Glauconite	7.25%
Matri		Echinoderm	2.25%		
Clays		Other Shell	7.75%		

Sample Numbe	HLS 67	Formation	Island Sandstone
Location Detail	Perpendicular Point,		
Rock Name	chalcedony and calcite cemented feldsarenite		
Comment	Irregular masses, almost indistinguishable from matrix except by pink colour/higher chalcedony conc.		

Quartz	20.75%	Calcite Cemen	33.00%	Hornblende	
Plagioclase	2.75%	Quartz Cemen	19.25%	Pyroxene	
K-Feldspar	1.00%	Authigenic Opaqu	2.00%	Green grains	
Mica	3.25%	Calcareous Algae		Altered Grain	
Rock Fragments		Bryozoa			
Opaques	2.00%	Foraminifer	2.75%	Glauconite	
Matri		Echinoderm			
Clays		Other Shell	10.50%		

Sample Numbe	HLS 68	Formation	Island Sandstone
Location Detail	Perpendicular Point		
Rock Name	chalcedony and calcite cemented feldsarenite		
Comment	just below HLS 67		

Quartz	20.50%	Calcite Cemen	45.00%	Hornblende	
Plagioclase	4.75%	Quartz Cemen	2.00%	Pyroxene	
K-Feldspar	1.00%	Authigenic Opaqu	0.00%	Green grains	
Mica	2.75%	Calcareous Algae		Altered Grain	
Rock Fragments		Bryozoa			
Opaques	2.25%	Foraminifer	5.75%	Glauconite	
Matri		Echinoderm			
Clays		Other Shell	12.50%		

Sample Numbe HLS 69 Formation Island Sandstone

Location Detail Perpendicular Point K30 728011

Rock Name calcite cemented feldsarenite

Comment thalassinoides rich band. Max = 0.25mm, well sorted.

Quartz	11.00%	Calcite Cemen	53.25%	Hornblende	
Plagioclase	1.75%	Quartz Cemen		Pyroxene	
K-Feldspar	2.25%	Authigenic Opaqu	6.00%	Green grains	0.50%
Mica	2.75%	Calcareous Algae		Altered Grain	
Rock Fragments	0.50%	Bryozoa	4.75%		
Opaques	2.00%	Foraminifer	6.50%	Glauconite	0.75%
Matri		Echinoderm			
Clays		Other Shell	9.25%		

Sample Numbe HLS 73 Formation Island Sandstone

Location Detail Mouth of Pororari River

Rock Name calcite cemented feldspathic litharenite

Comment Grain supported, altered hornblende, max = med sand, mode = fine sand

Quartz	31.75%	Calcite Cemen	30.50%	Hornblende	1.50%
Plagioclase	2.50%	Quartz Cemen		Pyroxene	
K-Feldspar	2.75%	Authigenic Opaqu	2.75%	Green grains	
Mica	3.75%	Calcareous Algae		Altered Grain	
Rock Fragments	6.75%	Bryozoa			
Opaques	8.75%	Foraminifer	0.50%	Glauconite	
Matri	1.00%	Echinoderm			
Clays		Other Shell	7.50%		

Sample Numbe	HLS 74	Formation	Island Sandstone
Location Detail	Limestone Creek, K30 751047		
Rock Name	calcite cemented shelly lithfeldsarenite		
Comment	Unusual high glauconite content, lots shell material. Max = med sand, mode = fine sand, grain supported		

Quartz	16.25%	Calcite Cemen	23.50%	Hornblende	
Plagioclase	1.50%	Quartz Cemen		Pyroxene	
K-Feldspar	3.00%	Authigenic Opaqu	12.00%	Green grains	
Mica	2.25%	Calcareous Algae		Altered Grain	
Rock Fragments	2.00%	Bryozoa	1.75%		
Opaques	2.50%	Foraminifer	3.25%	Glauconite	10.25%
Matri		Echinoderm			
Clays		Other Shell	21.75%		

Sample Numbe	HLS 77	Formation	Island Sandstone
Location Detail	Punakaiki River Gorge		
Rock Name	siderite cemented feldspathic litharenite		
Comment	Iron rich cement (= matrix), possibly siderite. Grain supported, max = med sandm mode = fine sand		

Quartz	35.75%	Calcite Cemen		Hornblende	
Plagioclase	2.50%	Quartz Cemen		Pyroxene	2.75%
K-Feldspar	5.75%	Authigenic Opaqu		Green grains	
Mica	2.50%	Calcareous Algae		Altered Grain	4.50%
Rock Fragments	9.50%	Bryozoa			
Opaques	3.75%	Foraminifer		Glauconite	
Matri	33.00%	Echinoderm			
Clays		Other Shell			

Sample Numbe	HLS 85a	Formation	Island Sandstone
Location Detail	South Perpendicular Point, K30 728010		
Rock Name	calcite cemented shelly litharenite		
Comment	Laminations (different matrix(calcite) concentrations) are convoluted in outcrop. Detrital ?limonite		

Quartz	15.25%	Calcite Cemen	41.00%	Hornblende	
Plagioclase	1.25%	Quartz Cemen		Pyroxene	0.50%
K-Feldspar	1.25%	Authigenic Opaqu		Green grains	0.25%
Mica	2.50%	Calcareous Algae	6.25%	Altered Grain	1.50%
Rock Fragments	8.00%	Bryozoa			
Opaques	1.25%	Foraminifer	9.50%	Glauconite	
Matri		Echinoderm			
Clays		Other Shell	11.50%		

Sample Numbe	HLS 85b	Formation	Island Sandstone
Location Detail	South Perpendicular Point, K30 728010		
Rock Name	calcite and quartz cemented shelly sublitharenite		
Comment	Pink concretions: Quartz cement, mostly mosaic(length slow), some fibrous in voids (length fast).		

Quartz	17.50%	Calcite Cemen	26.00%	Hornblende	
Plagioclase	0.25%	Quartz Cemen	22.25%	Pyroxene	
K-Feldspar	0.50%	Authigenic Opaqu	5.50%	Green grains	1.00%
Mica	3.25%	Calcareous Algae		Altered Grain	
Rock Fragments	3.75%	Bryozoa			
Opaques	3.00%	Foraminifer	4.00%	Glauconite	1.25%
Matri		Echinoderm			
Clays		Other Shell	11.75%		

Sample Numbe	HLS 86	Formation	Island Sandstone
Location Detail	South Perpendicular Point, K30 728010		
Rock Name	quartz and calcite cemented shelly litharenite		
Comment	Immediately above HLS 85b. Detrital limonite and ?magnetite, dolomite rhombs, burrows (more matrix).		

Quartz	19.25%	Calcite Cemen	28.50%	Hornblende	
Plagioclase	0.50%	Quartz Cemen	6.00%	Pyroxene	
K-Feldspar	1.25%	Authigenic Opaqu		Green grains	0.50%
Mica	2.25%	Calcareous Algae		Altered Grain	
Rock Fragments	13.00%	Bryozoa			
Opaques	4.75%	Foraminifer	5.00%	Glauconite	4.50%
Matri		Echinoderm			
Clays		Other Shell	14.50%		

Sample Numbe	HLS 64	Formation	Kaiata/Island
Location Detail	Okari Lagoon		
Rock Name	calcite cemented shelly feldspathic litharenite		
Comment	max = coarse sand, mode = fine sand, very fine sand, muscovite common in mud layers, aligned.		

Quartz	18.25%	Calcite Cemen	37.00%	Hornblende	
Plagioclase	0.75%	Quartz Cemen		Pyroxene	
K-Feldspar	2.50%	Authigenic Opaqu	2.50%	Green grains	2.50%
Mica	3.75%	Calcareous Algae	6.50%	Altered Grain	
Rock Fragments	3.50%	Bryozoa			
Opaques	1.00%	Foraminifer	8.75%	Glauconite	
Matri	7.50%	Echinoderm			
Clays		Other Shell	7.75%		

Sample Numbe HLS 40 Formation Kaiata Mudstone

Location Detail Gibsons Beach

Rock Name pyritic algal biosparite

Comment Cemented reef rubble in Kaiata, large concentration of pyrite in one part of the slide.

Quartz	3.50%	Calcite Cemen	19.50%	Hornblende	
Plagioclase		Quartz Cemen		Pyroxene	
K-Feldspar	0.50%	Authigenic Opaqu	23.17%	Green grains	0.30%
Mica	0.50%	Calcareous Algae	34.00%	Altered Grain	
Rock Fragments		Bryozoa			
Opaques		Foraminifer	2.67%	Glauconite	0.50%
Matri	9.67%	Echinoderm			
Clays		Other Shell	4.50%		

Sample Numbe HLS 41 Formation Kaiata Mudstone

Location Detail Gibsons Beach

Rock Name pyritic calcite cemented siltstone.

Comment Clacite cement + matrix = original matrix. Bioturbation causes varying concentration of matrix, sand len

Quartz	14.50%	Calcite Cemen	24.75%	Hornblende	
Plagioclase	0.50%	Quartz Cemen		Pyroxene	
K-Feldspar	1.25%	Authigenic Opaqu	9.75%	Green grains	0.75%
Mica	3.25%	Calcareous Algae		Altered Grain	
Rock Fragments		Bryozoa			
Opaques		Foraminifer	1.25%	Glauconite	
Matri	40.00%	Echinoderm			
Clays		Other Shell	4.00%		

Sample Numbe	HLS 61	Formation	Kaiata Mudstone-burrow
Location Detail	Gibsons Beach		
Rock Name	calcite cemented algal feldspathic litharenite		
Comment	Coarse burrow fill imediately below contact with Little Totara Sand.		

Quartz	32.25%	Calcite Cemen	37.50%	Hornblende	
Plagioclase	1.50%	Quartz Cemen		Pyroxene	
K-Feldspar	2.25%	Authigenic Opaqu		Green grains	
Mica	1.75%	Calcareous Algae	5.50%	Altered Grain	
Rock Fragments	10.50%	Bryozoa	0.50%		
Opaques	1.25%	Foraminifer		Glauconite	
Matri		Echinoderm			
Clays	2.25%	Other Shell	4.75%		

Sample Numbe	HLS 18	Formation	Rhodolith Layers
Location Detail	Seal Island		
Rock Name	sandy algal biosparite		
Comment	?Lithophyllum, Sporolithon, Lithothamnion, ?mesophyllum.		

Quartz	5.50%	Calcite Cemen	39.50%	Hornblende	
Plagioclase	1.75%	Quartz Cemen		Pyroxene	
K-Feldspar	1.50%	Authigenic Opaqu	7.25%	Green grains	
Mica	0.75%	Calcareous Algae	36.75%	Altered Grain	
Rock Fragments		Bryozoa	2.25%		
Opaques	0.75%	Foraminifer	0.50%	Glauconite	1.50%
Matri		Echinoderm			
Clays		Other Shell	2.00%		

Sample Numbe	HLS 81b	Formation	Rhodolith Layers
Location Detail	Seal Island		
Rock Name	sandy slagl biosparite		
Comment	Lithothamnion, Lithophyllum. This count for algal part		

Quartz	2.50%	Calcite Cemen	22.50%	Hornblende	
Plagioclase	0.25%	Quartz Cemen		Pyroxene	
K-Feldspar		Authigenic Opaqu	2.50%	Green grains	
Mica	0.25%	Calcareous Algae	63.50%	Altered Grain	
Rock Fragments	0.25%	Bryozoa	6.25%		
Opaques		Foraminifer	0.75%	Glauconite	0.25%
Matri		Echinoderm			
Clays		Other Shell	1.00%		

Sample Numbe	HLS 81b	Formation	Rhodolith Layer
Location Detail	Seal Island		
Rock Name	sandy algal biosparite		
Comment	Lithothamnion, Lithophyllum. This count for sandy part		

Quartz	7.50%	Calcite Cemen	43.75%	Hornblende	
Plagioclase	0.25%	Quartz Cemen		Pyroxene	
K-Feldspar	1.25%	Authigenic Opaqu	4.75%	Green grains	
Mica	0.50%	Calcareous Algae	16.75%	Altered Grain	
Rock Fragments	0.75%	Bryozoa			
Opaques		Foraminifer	3.25%	Glauconite	9.75%
Matri	2.25%	Echinoderm			
Clays		Other Shell	9.25%		

Sample Numbe	HLS 89	Formation	Rhodolith Layer
Location Detail	Seal Island		
Rock Name	sandy algal biosparite		
Comment	Sporolithon, ?Lithophyllum. This count for algal part		

Quartz	6.00%	Calcite Cemen	29.75%	Hornblende	
Plagioclase	0.50%	Quartz Cemen		Pyroxene	
K-Feldspar	0.50%	Authigenic Opaqu	3.00%	Green grains	
Mica	0.25%	Calcareous Algae	49.00%	Altered Grain	
Rock Fragments	0.75%	Bryozoa	5.00%		
Opaques		Foraminifer	1.25%	Glauconite	0.25%
Matri		Echinoderm			
Clays		Other Shell	3.75%		

Sample Numbe	HLS 89	Formation	Rhodolith Layer
Location Detail	Seal Island		
Rock Name	glauconitic sandy algal biosparite.		
Comment	Sporolithon, Lithophyllum?. This count for sandy part.		

Quartz	12.75%	Calcite Cemen	39.50%	Hornblende	
Plagioclase	1.25%	Quartz Cemen		Pyroxene	
K-Feldspar	0.50%	Authigenic Opaqu	1.75%	Green grains	
Mica	1.50%	Calcareous Algae	20.50%	Altered Grain	
Rock Fragments	0.50%	Bryozoa	1.50%		
Opaques		Foraminifer	2.75%	Glauconite	15.00%
Matri		Echinoderm			
Clays		Other Shell	2.50%		

Appendix V

Textural Analyses

This appendix details the results of sieving analysis carried out on representative subsamples of the selected samples listed in Appendix II. Summary sheets for each formation list the statistical parameters calculated for each sample. The graphical representations of the data presented here are included in Chapter 4. Visual estimations of grain size and composition and grain counting of the Little Totara Sand are not included here as they are not used in this thesis. The Kaiata Mudstone and Island Sandstone tables are amalgamations of two different methods of grain size analysis, sieving and pipette analysis. The two analyses are included on the same table, the 4 phi size is repeated, the first is the last sieve and the second is part of the calculations for the pipette analysis.

Little Totara Sand

HLS 51 graphic mean $M_z = +1.38\phi$
standard deviation $\sigma_1 = 0.99\phi$ moderately sorted
graphic skewness $Sk_1 = +0.19$ fine skewed
graphic kurtosis $K_G = 0.77$ platykurtic
bimodal: coarse mode 0.0ϕ, fine mode +2.62ϕ
bimodal roundness; coarse quartz is mainly rounded, finer populations are angular

HLS 54 graphic mean $M_z = +0.80\phi$
standard deviation $\sigma_1 = 1.34\phi$ poorly sorted
graphic skewness $Sk_1 = +0.47$ very fine skewed
graphic kurtosis $K_G = 0.82$ platykurtic
bimodal: coarse mode -0.6ϕ, fine mode +2.62ϕ
bimodal roundness; coarse quartz is mainly rounded, finer populations are angular

HLS 55 graphic mean $M_z = +2.21\phi$
standard deviation $\sigma_1 = 1.92\phi$ poorly sorted
graphic skewness $Sk_1 = -0.095$ near symmetrical
graphic kurtosis $K_G = 1.64$ very leptokurtic
unimodal: fine mode +2.62ϕ
unimodal roundness; very few grains are rounded, main population is angular

HLS 37 graphic mean $M_z = +1.08\phi$
standard deviation $\sigma_1 = 1.16\phi$ poorly sorted
graphic skewness $Sk_1 = -0.23$ coarse skewed
graphic kurtosis $K_G = 0.80$ platykurtic
bimodal: coarse mode -1.37ϕ, fine mode +2.65ϕ
bimodal roundness, large pebbles/granules all rounded, some rounded grains also occur in smaller size fractions.

HLS 38 graphic mean $M_z = +0.90\phi$
standard deviation $\sigma_1 = 0.94\phi$ moderately sorted
graphic skewness $Sk_1 = -0.12$ coarse skewed
graphic kurtosis $K_G = 0.90$ mesokurtic
bimodal: coarse mode -0.6ϕ, fine mode +2.60ϕ
bimodal roundness, as above.

HLS 63 graphic mean $M_z = +0.90\phi$
standard deviation $\sigma_1 = 1.61\phi$ poorly sorted
graphic skewness $Sk_1 = +0.08$ near symmetrical
graphic kurtosis $K_G = 0.97$ mesokurtic
unimodal: +3.4ϕ
bimodal roundness, as above.

Sample Number: 54
Treatment: Drying, mechanical disaggregation, sieving for 10 minutes
Weight (g): Dry Sample: 51.58 Sand: 49.85 Mud: 0.2 Sand and Mud: 50.05

sieve diam. (ϕ)	exact diam. (ϕ)	weight beaker (g)	beaker & sample (g)	weight sample (g)	% aggs	corrected weight	cumulative weight	cumulative %	% shell	notes
-5.00				0		0.00	0.00	0.00		
-4.00				0		0.00	0.00	0.00		
-3.00				0		0.00	0.00	0.00		
-2.50				0		0.00	0.00	0.00		
-2.25				0		0.00	0.00	0.00		
-2.00				0		0.00	0.00	0.00		
-1.75	-1.72			0		0.00	0.00	0.00		
-1.50				0		0.00	0.00	0.00		
-1.25	-1.20	31.97	32.29	0.32	0	0.32	0.32	0.63		
-1.00		27.27	27.74	0.47	0	0.47	0.79	1.56		
-0.75	-0.74	27.53	29.07	1.54	1	1.52	2.31	4.57		
-0.50	-0.48	31.89	35.9	4.01	1	3.97	6.28	12.40		
-0.25	-0.20	29.19	33.66	4.47	1	4.43	10.71	21.13		
0.00		27.26	32.55	5.29	2	5.18	15.89	31.37		
0.25	0.28	28.51	35.42	6.91	1	6.84	22.73	44.87		
0.50	0.54	32.97	39.93	6.96	1	6.89	29.63	58.46		
0.75	0.78	31.97	34.93	2.96	2	2.90	32.53	64.19		
1.00	1.04	27.27	29.24	1.97	2	1.93	34.46	68.00		
1.25		27.53	28.49	0.96	2	0.94	35.40	69.85		
1.50	1.54	31.89	33.63	1.74	1	1.72	37.12	73.25		
1.75	1.72	29.19	30.45	1.26	1	1.25	38.37	75.72		
2.00		27.26	29.23	1.97	1	1.95	40.32	79.56		
2.25		28.51	30.88	2.37	1	2.35	42.66	84.19		
2.50	2.52	32.97	34.95	1.98	0	1.98	44.64	88.10		
2.75	2.72	31.97	34.14	2.17	0	2.17	46.81	92.38		
3.00	3.04	27.27	28.03	0.76	1	0.75	47.57	93.87		
3.25	3.28	27.53	27.96	0.43	1	0.43	47.99	94.71		
3.50	3.52	31.89	32.45	0.56	2	0.55	48.54	95.79		
3.75	3.70	29.19	29.49	0.3	1	0.30	48.84	96.38		
4.00	4.16	27.26	27.71	0.45	1	0.45	49.28	97.26		
4.25	4.34	28.51	28.71	0.2	0	0.20	49.48	97.65		
4.50										
4.75										
pan		32.97	34.16	1.19	0	1.19	50.67	100.00		~70/30 silt/clay
Total				51.24		50.67	50.67			

Sample Number: 55
Treatment: Drying, mechanical disaggregation, sieving for 10 minutes
Weight (g): Dry Sample: 53.38 Sand: 51.79 Mud: 1.66 Sand and Mud: 53.5

sieve diam. (ϕ)	exact diam. (ϕ)	weight beaker (g)	beaker & sample (g)	weight sample (g)	% aggs.	corrected weight	cumulative weight	cumulative %	% shell	notes
-5.00				0.00		0.00	0.00	0.00%		
-4.00				0.00		0.00	0.00	0.00%		
-3.00				0.00		0.00	0.00	0.00%		
-2.50				0.00		0.00	0.00	0.00%		
-2.25				0.00		0.00	0.00	0.00%		
-2.00				0.00		0.00	0.00	0.00%		
-1.75	-1.72			0.00		0.00	0.00	0.00%		
-1.50				0.00		0.00	0.00	0.00%		
-1.25	-1.20			0.00		0.00	0.00	0.00%		
-1.00		31.97	31.97	0.00	0	0.00	0.00	0.00%		
-0.75	-0.74	27.27	27.29	0.02	20	0.02	0.02	0.03%		
-0.50	-0.48	27.53	27.55	0.02	99	0.00	0.02	0.03%		
-0.25	-0.20	31.89	31.90	0.01	50	0.00	0.02	0.04%		
0.00		29.19	29.23	0.04	20	0.03	0.05	0.10%		
0.25	0.28	27.26	27.31	0.05	10	0.04	0.10	0.18%		
0.50	0.54	28.51	28.61	0.10	10	0.09	0.19	0.35%		
0.75	0.78	32.97	33.17	0.20	10	0.18	0.37	0.69%		
1.00	1.04	31.97	32.43	0.46	1	0.46	0.82	1.55%		
1.25		27.27	27.89	0.62	2	0.61	1.43	2.69%		
1.50	1.54	27.53	29.65	2.12	2	2.08	3.51	6.59%		
1.75	1.72	31.89	34.33	2.44	1	2.42	5.92	11.13%		
2.00		29.19	34.60	5.41	1	5.36	11.28	21.19%		
2.25		27.26	35.84	8.58	0	8.58	19.86	37.30%		
2.50	2.52	28.51	40.61	12.10	0	12.10	31.96	60.03%		
2.75	2.72	31.97	44.94	12.97	0	12.97	44.93	84.39%		
3.00	3.04	27.27	31.02	3.75	0	3.75	48.68	91.44%		
3.25	3.28	27.53	28.44	0.91	0	0.91	49.59	93.14%		
3.50	3.52	31.89	32.87	0.98	0	0.98	50.57	94.98%		
3.75	3.70	29.19	29.61	0.42	0	0.42	50.99	95.77%		
4.00	4.16	27.26	27.85	0.59	0	0.59	51.58	96.88%		
4.25	4.34	28.51	28.79	0.28	0	0.28	51.86	97.41%		
4.50										
4.75										
pan		32.97	34.35	1.38	0	1.38	53.24	100.00 %		mainly silt
Total				53.45		53.24	53.24			

Sample Number: 38
Treatment: Drying, mechanical disaggregation, sieving for 10 minutes
Weight (g): Dry Sample: 61.46 Sand: 59.83 Mud: 0.45 Sand and Mud: 60.26

sieve diam. (ϕ)	exact diam. (ϕ)	weight beaker (g)	beaker & sample (g)	weight sample (g)	% aggs	corrected weight	cumulative weight	cumulative %	% shell	notes
-5.00				0.00		0.00	0.00	0.00%		
-4.00				0.00		0.00	0.00	0.00%		
-3.00				0.00		0.00	0.00	0.00%		
-2.50				0.00		0.00	0.00	0.00%		
-2.25				0.00		0.00	0.00	0.00%		
-2.00				0.00		0.00	0.00	0.00%		
-1.75	-1.72			0.00		0.00	0.00	0.00%		
-1.50		31.97	32.04	0.07	0	0.07	0.07	0.12%		
-1.25	-1.20	27.27	27.64	0.37	0	0.37	0.44	0.73%		
-1.00		27.53	27.99	0.46	0	0.46	0.90	1.49%		
-0.75	-0.74	31.89	32.89	1.00	5	0.95	1.85	3.07%		
-0.50	-0.48	29.19	31.25	2.06	5	1.96	3.81	6.32%		
-0.25	-0.20	27.26	28.91	1.65	5	1.57	5.37	8.92%		
0.00		31.97	34.40	2.43	0	2.43	7.80	12.95%		
0.25	0.28	27.27	30.25	2.98	1	2.95	10.75	17.84%		
0.50	0.54	27.53	32.15	4.62	2	4.53	15.28	25.35%		
0.75	0.78	31.89	36.22	4.33	1	4.29	19.57	32.46%		
1.00	1.04	29.19	35.30	6.11	1	6.05	25.62	42.50%		
1.25		27.26	31.48	4.22	1	4.18	29.80	49.43%		
1.50	1.54	28.51	38.01	9.50	1	9.41	39.20	65.03%		
1.75	1.72	32.97	38.75	5.78	0	5.78	44.98	74.62%		
2.00		27.50	33.04	5.54	0	5.54	50.52	83.81%		
2.25		31.97	35.08	3.11	0	3.11	53.63	88.97%		
2.50	2.52	27.27	29.18	1.91	0	1.91	55.54	92.14%		
2.75	2.72	27.53	29.56	2.03	1	2.01	57.55	95.47%		
3.00	3.04	31.89	33.00	1.11	0	1.11	58.66	97.31%		
3.25	3.28	29.19	29.68	0.49	0	0.49	59.15	98.13%		
3.50	3.52	27.26	27.62	0.36	0	0.36	59.51	98.72%		
3.75	3.70	28.51	28.65	0.14	1	0.14	59.65	98.95%		
4.00	4.16	32.97	33.15	0.18	0	0.18	59.83	99.25%		
4.25	4.34	27.50	27.57	0.07	0	0.07	59.90	99.37%		
4.50										
4.75										
pan		27.63	28.01	0.38	0	0.38	60.28	100.00 %		~60/40 silt/clay
Total				60.90		60.28	60.28			

Sample Number: 37
Treatment: Drying, mechanical disaggregation, sieving for 10 minutes
Weight (g): Dry Sample: 55.80 Sand: 54.5 Mud: 0.41 Sand and Mud: 54.91

sieve diam. (ϕ)	exact diam. (ϕ)	weight beaker (g)	beaker & sample (g)	weight sample (g)	% aggs	corrected weight	cumulative weight	cumulative %	% shell	notes
-5.00				0.00		0.00	0.00	0.00%		
-4.00				0.00		0.00	0.00	0.00%		
-3.00				0.00		0.00	0.00	0.00%		
-2.50				0.00		0.00	0.00	0.00%		
-2.25				0.00		0.00	0.00	0.00%		
-2.00		31.97	32.14	0.17	0	0.17	0.17	0.31%		
-1.75	-1.72	27.27	27.57	0.30	0	0.30	0.47	0.86%		
-1.50		27.53	27.87	0.34	0	0.34	0.81	1.48%		
-1.25	-1.20	31.89	33.09	1.20	1	1.19	2.00	3.64%		
-1.00		29.19	30.20	1.01	2	0.99	2.99	5.44%		
-0.75	-0.74	27.26	28.79	1.53	1	1.51	4.50	8.20%		
-0.50	-0.48	28.51	30.80	2.29	5	2.18	6.68	12.16%		
-0.25	-0.20	32.97	35.18	2.21	2	2.17	8.84	16.11%		
0.00		31.97	34.38	2.41	1	2.39	11.23	20.45%		
0.25	0.28	27.27	29.68	2.41	1	2.39	13.62	24.79%		
0.50	0.54	27.53	30.47	2.94	1	2.91	16.53	30.10%		
0.75	0.78	31.89	34.56	2.67	1	2.64	19.17	34.91%		
1.00	1.04	29.19	32.92	3.73	1	3.69	22.86	41.63%		
1.25		27.26	29.89	2.63	0	2.63	25.49	46.42%		
1.50	1.54	28.51	35.65	7.14	0	7.14	32.63	59.43%		
1.75	1.72	32.97	37.42	4.45	0	4.45	37.08	67.53%		
2.00		27.50	33.54	6.04	0	6.04	43.12	78.53%		
2.25		31.97	36.44	4.47	1	4.43	47.55	86.59%		
2.50	2.52	27.27	29.64	2.37	0	2.37	49.92	90.90%		
2.75	2.72	27.53	29.65	2.12	0	2.12	52.04	94.76%		
3.00	3.04	31.89	32.87	0.98	0	0.98	53.02	96.55%		
3.25	3.28	29.19	29.74	0.55	0	0.55	53.57	97.55%		
3.50	3.52	27.26	27.76	0.50	0	0.50	54.07	98.46%		
3.75	3.70	28.51	28.71	0.20	1	0.20	54.27	98.82%		
4.00	4.16	32.97	33.21	0.24	1	0.24	54.50	99.25%		
4.25	4.34	27.50	27.58	0.08	0	0.08	54.58	99.40%		
4.50										
4.75										
pan		27.63	27.96	0.33	0	0.33	54.91	100%		~10% or less clay
Total				55.31		54.91	54.91			

Sample Number: 63
Treatment: Drying, mechanical disaggregation, sieving for 10 minutes
Weight (g): Dry Sample: 57.90 Sand: 55.18 Mud: 1.69 Sand and Mud: 56.87

sieve diam. (ϕ)	exact diam. (ϕ)	weight beaker (g)	beaker & sample (g)	weight sample (g)	% aggs	corrected weight	cumulative weight	cumulative %	% shell	notes
-5.00				0.00		0.00	0.00	0.00%		
-4.00				0.00		0.00	0.00	0.00%		
-3.00				0.00		0.00	0.00	0.00%		
-2.50		27.63	28.70	1.07	0	1.07	1.07	1.88%		
-2.25				0.00		0.00	1.07	1.88%		
-2.00		32.45	32.96	0.51	0	0.51	1.58	2.78%		
-1.75	-1.72	33.18	34.05	0.87	0	0.87	2.45	4.31%		
-1.50		32.12	33.05	0.93	0	0.93	3.38	5.94%		
-1.25	-1.20	31.97	33.68	1.71	0	1.71	5.09	8.95%		
-1.00		27.27	28.86	1.59	1	1.57	6.66	11.72%		
-0.75	-0.74	27.53	29.61	2.08	2	2.04	8.70	15.30%		
-0.50	-0.48	31.89	35.45	3.56	1	3.52	12.23	21.50%		
-0.25	-0.20	29.19	32.27	3.08	1	3.05	15.28	26.86%		
0.00		27.26	30.59	3.33	2	3.26	18.54	32.60%		
0.25	0.28	28.51	31.90	3.39	1	3.36	21.90	38.50%		
0.50	0.54	32.97	36.66	3.69	1	3.65	25.55	44.92%		
0.75	0.78	31.97	34.77	2.80	2	2.74	28.29	49.75%		
1.00	1.04	27.27	30.76	3.49	1	3.46	31.75	55.82%		
1.25		27.53	29.87	2.34	1	2.32	34.06	59.90%		
1.50	1.54	31.89	36.21	4.32	2	4.23	38.30	67.34%		
1.75	1.72	29.19	31.50	2.31	1	2.29	40.58	71.36%		
2.00		27.26	29.81	2.55	1	2.52	43.11	75.80%		
2.25		28.51	30.82	2.31	2	2.26	45.37	79.78%		
2.50	2.52	32.97	34.57	1.60	2	1.57	46.94	82.54%		
2.75	2.72	31.97	34.01	2.04	2	2.00	48.94	86.05%		
3.00	3.04	27.27	28.98	1.71	1	1.69	50.63	89.03%		
3.25	3.28	27.53	28.99	1.46	1	1.45	52.08	91.57%		
3.50	3.52	31.89	33.51	1.62	1	1.60	53.68	94.39%		
3.75	3.70	29.19	29.91	0.72	1	0.71	54.40	95.65%		
4.00	4.16	27.26	28.05	0.79	1	0.78	55.18	97.02%		
4.25	4.34	28.51	28.79	0.28	2	0.27	55.45	97.50%		
4.50										
4.75										
pan		32.97	34.39	1.42	0	1.42	56.87	100.00 %		~20% clay
Total				57.57		56.87	56.87			

Sample Number: 51
Treatment: Drying, mechanical disaggregation, sieving for 10 minutes
Weight (g): Dry Sample: 50.04 Sand: 48.11 Mud: 0.76 Sand and Mud: 48.87

sieve diam. (ϕ)	exact diam. (ϕ)	weight beaker (g)	beaker & sample (g)	weight sample (g)	% aggs	corrected weight	cumulative weight	cumulative %	% shell	notes
-5.00				0.00		0.00	0.00	0.00%		
-4.00				0.00		0.00	0.00	0.00%		
-3.00				0.00		0.00	0.00	0.00%		
-2.50				0.00		0.00	0.00	0.00%		
-2.25				0.00		0.00	0.00	0.00%		
-2.00				0.00		0.00	0.00	0.00%		
-1.75	-1.72			0.00		0.00	0.00	0.00%		
-1.50				0.00		0.00	0.00	0.00%		
-1.25	-1.20	31.97	32.06	0.09	75	0.02	0.02	0.05%		
-1.00		27.27	27.33	0.06	75	0.01	0.04	0.08%		
-0.75	-0.74	27.53	27.65	0.12	75	0.03	0.07	0.14%		
-0.50	-0.48	31.89	32.06	0.17	60	0.07	0.14	0.28%		
-0.25	-0.20	29.19	29.61	0.42	30	0.29	0.43	0.88%		
0.00		27.26	28.53	1.27	10	1.14	1.57	3.22%		
0.25	0.28	28.51	31.90	3.39	1	3.36	4.93	10.08%		
0.50	0.54	32.97	39.47	6.50	1	6.44	11.36	23.25%		
0.75	0.78	31.97	37.65	5.68	1	5.62	16.99	34.76%		
1.00	1.04	27.27	31.41	4.14	1	4.10	21.09	43.15%		
1.25		27.53	29.67	2.14	1	2.12	23.20	47.48%		
1.50	1.54	31.89	36.41	4.52	2	4.43	27.63	56.54%		
1.75	1.72	29.19	32.68	3.49	1	3.46	31.09	63.61%		
2.00		27.26	32.05	4.79	0	4.79	35.88	73.42%		
2.25		28.51	32.90	4.39	1	4.35	40.22	82.31%		
2.50	2.52	32.97	35.48	2.51	2	2.46	42.68	87.34%		
2.75	2.72	31.97	34.50	2.53	2	2.48	45.16	92.42%		
3.00	3.04	27.27	28.61	1.34	2	1.31	46.48	95.10%		
3.25	3.28	27.53	28.10	0.57	1	0.56	47.04	96.26%		
3.50	3.52	31.89	32.45	0.56	1	0.55	47.60	97.39%		
3.75	3.70	29.19	29.42	0.23	1	0.23	47.82	97.86%		
4.00	4.16	27.26	27.55	0.29	1	0.29	48.11	98.44%		
4.25	4.34	28.51	28.64	0.13	0	0.13	48.24	98.71%		
4.50										
4.75										
pan		32.97	33.60	0.63	0	0.63	48.87	100.00 %		mostly silt
Total				49.96		48.87	48.87			

Island Sandstone

HLS 5 graphic mean $M_z = +4.25\phi$
standard deviation $\sigma_1 = 1.61\phi$ poorly sorted
graphic skewness $Sk_1 = +0.54$ very fine skewed
graphic kurtosis $K_G = +1.64$ very leptokurtic
modes: $+0.43\phi$ and $+3.42\phi$

HLS 7 graphic mean $M_z = +4.39\phi$
standard deviation $\sigma_1 = 1.55\phi$ poorly sorted
graphic skewness $Sk_1 = +0.47$ very fine skewed
graphic kurtosis $K_G = +1.62$ very leptokurtic
modes: $+0.7\phi$, $+3.40\phi$ and $+4.35\phi$

HLS 12 graphic mean $M_z = +4.47\phi$
standard deviation $\sigma_1 = 1.57\phi$ poorly sorted
graphic skewness $Sk_1 = +0.46$ very fine skewed
graphic kurtosis $K_G = +1.52$ very leptokurtic
modes: $+0.9\phi$, $+3.40\phi$ and $+4.35\phi$

HLS 46 graphic mean $M_z = +4.30\phi$
standard deviation $\sigma_1 = 1.19\phi$ poorly sorted
graphic skewness $Sk_1 = +0.37$ very fine skewed
graphic kurtosis $K_G = +1.10$ mesokurtic
modes: $+3.18\phi$ and $+4.38\phi$

HLS 59 graphic mean $M_z = +3.74\phi$
standard deviation $\sigma_1 = 0.85\phi$ moderately
graphic skewness $Sk_1 = +0.50$ very fine skewed
graphic kurtosis $K_G = +1.43$ very leptokurtic
modes: $+3.41\phi$ and $+4.31\phi$

HLS 76 graphic mean $M_z = +4.25\phi$
standard deviation $\sigma_1 = 1.08\phi$ poorly sorted
graphic skewness $Sk_1 = +0.31$ very fine skewed
graphic kurtosis $K_G = +1.41$ leptokurtic
modes: $+3.43\phi$ and $+4.38\phi$

Sample Number: 5

Treatment: Heating with 5g/l Calgon, some mechanical disaggregation, wet sieving, sand fraction dry sieved. Mud fraction: pipette analysis.

Weight (g): Dry Sample: 38.77 Sand: 17.7 Mud: 13.57 Sand and Mud: 31.27

sieve diam. (ϕ)	exact diam. (ϕ)	weight beaker (g)	beaker & sample (g)	weight sample (g)	% aggs	corrected weight	cumulative weight	cumulative %	% shell	notes
-5.00				0.00		0.00	0.00	0.00%		
-4.00				0.00		0.00	0.00	0.00%		
-3.00				0.00		0.00	0.00	0.00%		
-2.50				0.00		0.00	0.00	0.00%		
-2.25				0.00		0.00	0.00	0.00%		
-2.00				0.00		0.00	0.00	0.00%		
-1.75	-1.72			0.00		0.00	0.00	0.00%		
-1.50				0.00		0.00	0.00	0.00%		
-1.25	-1.20			0.00		0.00	0.00	0.00%		
-1.00				0.00		0.00	0.00	0.00%		
-0.75	-0.74			0.00		0.00	0.00	0.00%		Aggregates= crust (rare).
-0.50	-0.48			0.00		0.00	0.00	0.00%		pellets, broken pellets and
-0.25	-0.20	26.53	26.93	0.40	99	0.00	0.00	0.00%	2	misccellaneous,
0.00		29.23	29.56	0.33	98	0.01	0.01	0.02%		unidentifiable aggs.
0.25	0.28	29.58	30.05	0.47	98	0.01	0.02	0.05%	5	2% glauconite
0.50	0.54	29.27	29.95	0.68	93	0.05	0.06	0.20%	6	4% g.
0.75	0.78	28.53	29.22	0.69	88	0.08	0.15	0.47%	5	5% g.
1.00	1.04	25.22	26.28	1.06	88	0.13	0.27	0.87%	3	6% g.
1.25		29.86	30.73	0.87	89	0.10	0.37	1.18%	3	8% g.
1.50	1.54	25.42	27.23	1.81	86	0.25	0.62	1.99%	2	6% g.
1.75	1.72	29.29	30.53	1.24	88	0.15	0.77	2.47%	2	8% g.
2.00		26.53	28.26	1.73	85	0.26	1.03	3.30%	2	4% g.
2.25		29.23	30.87	1.64	85	0.25	1.28	4.08%	2	3% g.
2.50	2.62	29.58	31.07	1.49	80	0.30	1.58	5.04%		
2.75	2.72	29.27	31.47	2.20	60	0.88	2.46	7.85%		
3.00	3.04	28.53	30.79	2.26	40	1.36	3.81	12.19%		
3.25	3.28	25.22	27.93	2.71	20	2.17	5.98	19.12%		
3.50	3.52	29.86	36.83	6.97	10	6.27	12.25	39.18%		
3.75	3.70	25.42	28.03	2.61	5	2.48	14.73	47.11%		
4.00	4.16	29.29	32.36	3.07	1	3.04	17.77	56.83%		
4.00		7.04	7.32	0.28		4.00	21.77	56.83%		
4.50		7.47	7.67	0.20		2.00	23.77	69.62%		
5.00		5.33	5.49	0.16		3.50	27.27	76.02%		
6.00		7.08	7.17	0.09		1.00	28.27	87.21%		
7.00		7.47	7.54	0.07		1.00	29.27	90.41%		
8.00		7.08	7.13	0.05		0.50	29.77	93.60%		
9.00		6.87	6.91	0.04		0.50	30.27	95.20%		
10.0		7.47	7.50	0.03		1	31.27	96.80%		
Total				33.15		31.27	31.27			

Sample Number: 7

Treatment: Heating with 5g/l Calgon, some mechanical disaggregation, wet sieving, sand fraction dry sieved. Mud fraction: pipette analysis.

Weight (g): Dry Sample: 37.18 Sand: 16.6 Mud: 21.5 Sand and Mud: 38.1

sieve diam. (ϕ)	exact diam. (ϕ)	weight beaker (g)	beaker & sample (g)	weight sample (g)	% aggs	corrected weight	cumulative weight	cumulative %	% shell	notes
-5.00				0.00		0.00	0.00	0.00%		
-4.00				0.00		0.00	0.00	0.00%		
-3.00				0.00		0.00	0.00	0.00%		
-2.50				0.00		0.00	0.00	0.00%		
-2.25				0.00		0.00	0.00	0.00%		
-2.00				0.00		0.00	0.00	0.00%		
-1.75	-1.72			0.00		0.00	0.00	0.00%		
-1.50				0.00		0.00	0.00	0.00%		
-1.25	-1.20			0.00		0.00	0.00	0.00%		
-1.00				0.00		0.00	0.00	0.00%		
-0.75	-0.74			0.00		0.00	0.00	0.00%		
-0.50	-0.48			0.00		0.00	0.00	0.00%		
-0.25	-0.20	26.53	26.63	0.10	99	0.00	0.00	0.00%		Aggregates = pellets, crust,
0.00		29.23	29.31	0.08	99	0.00	0.00	0.00%		and other unidentidied
0.25	0.28	29.58	29.68	0.10	99	0.00	0.00	0.00%		aggregates.
0.50	0.54	29.27	29.45	0.18	92	0.01	0.01	0.04%	2	
0.75	0.78	28.53	28.75	0.22	90	0.02	0.04	0.10%	4	
1.00	1.04	25.22	25.60	0.38	92	0.03	0.07	0.18%	3	
1.25		29.86	30.17	0.31	89	0.03	0.10	0.26%	2	1% glauconite
1.50	1.54	25.42	26.24	0.82	93	0.06	0.16	0.42%	1	
1.75	1.72	29.29	29.86	0.57	88	0.07	0.23	0.60%	2	
2.00		26.53	27.41	0.88	88	0.11	0.33	0.87%		
2.25		29.23	30.16	0.93	80	0.19	0.52	1.36%		
2.50	2.52	29.58	30.52	0.94	70	0.28	0.80	2.10%		
2.75	2.72	29.27	31.15	1.88	60	0.75	1.55	4.07%		
3.00	3.04	28.53	30.87	2.34	40	1.40	2.96	7.76%		
3.25	3.28	25.22	28.54	3.32	20	2.66	5.61	14.73%		
3.50	3.52	29.86	36.68	6.82	5	6.48	12.09	31.74%		
3.75	3.70	25.42	27.66	2.24	1	2.22	14.31	37.56%		
4.00	4.16	29.29	31.58	2.29	0	2.29	16.60	43.57%		
4.00		6.85	7.29	0.44		9.50	26.10	43.57%		
4.50		7.08	7.33	0.25		2.50	28.60	68.50%		
5.00		7.08	7.28	0.20		2.50	31.10	75.07%		
5.50		6.89	7.04	0.15		3.00	34.10	81.63%		
6.50		7.71	7.80	0.09		0.50	34.60	89.50%		
7.00		7.46	7.54	0.08		1.00	35.60	90.81%		
8.00		6.89	6.95	0.06		0.50	36.10	93.44%		
9.00		7.06	7.11	0.05		1.50	37.60	94.75%		
10		7.08	7.10	0.02		0.50	38.10	98.69%		
Total				25.74		38.10	38.10			

Sample Number: 12

Treatment: Heating with 5g/l Calgon, some mechanical disaggregation, wet sieving, sand fraction dry sieved. Mud fraction: pipette analysis.

Weight (g): Dry Sample: 32.23 Sand: 12.91 Mud: 14.5 Sand and Mud: 27.41

sieve diam. (ϕ)	exact diam. (ϕ)	weight beaker (g)	beaker & sample (g)	weight sample (g)	% aggs	corrected weight	cumulative weight	cumulative %	% shell	notes
-5.00				0.00		0.00	0.00	0.00%		
-4.00				0.00		0.00	0.00	0.00%		
-3.00				0.00		0.00	0.00	0.00%		
-2.50				0.00		0.00	0.00	0.00%		
-2.25				0.00		0.00	0.00	0.00%		
-2.00				0.00		0.00	0.00	0.00%		
-1.75	-1.72			0.00		0.00	0.00	0.00%		
-1.50				0.00		0.00	0.00	0.00%		
-1.25	-1.20			0.00		0.00	0.00	0.00%		
-1.00				0.00		0.00	0.00	0.00%		
-0.75	-0.74			0.00		0.00	0.00	0.00%		
-0.50	-0.48			0.00		0.00	0.00	0.00%		Aggregates = pellets (most
-0.25	-0.20	26.53	26.53	0.00		0.00	0.00	0.00%		common), crust, glauc.
0.00		29.23	29.24	0.01	99	0.00	0.00	0.00%		pellets, and unidentifiable
0.25	0.28	29.58	29.60	0.02	90	0.00	0.00	0.01%		aggregates.
0.50	0.54	29.27	29.29	0.02	60	0.01	0.01	0.03%		Lots of rounded Quartz
0.75	0.78	28.53	28.56	0.03	60	0.01	0.02	0.07%		grains in this sample
1.00	1.04	25.22	25.36	0.14	60	0.06	0.08	0.25%		
1.25		29.86	30.04	0.18	60	0.07	0.15	0.48%	1	
1.50	1.54	25.42	25.97	0.55	70	0.16	0.31	1.01%	2	
1.75	1.72	29.29	29.74	0.45	60	0.18	0.49	1.58%	2	10% glauconite
2.00		26.53	27.23	0.70	40	0.42	0.91	2.93%	2	7% glauconite
2.25		29.23	29.93	0.70	50	0.35	1.27	4.05%	1	
2.50	2.52	29.58	30.30	0.72	50	0.36	1.63	5.20%	1	
2.75	2.72	29.27	30.36	1.09	40	0.65	2.28	7.29%	2	
3.00	3.04	28.53	29.77	1.24	30	0.87	3.15	10.06%	1	
3.25	3.28	25.22	26.90	1.68	10	1.51	4.66	14.90%		
3.50	3.52	29.86	34.92	5.06	2	4.96	9.62	30.76%		
3.75	3.70	25.42	27.11	1.69	2	1.66	11.27	36.05%		
4.00	4.16	29.29	30.94	1.65	1	1.63	12.91	47.09%		
4.00		6.94	7.24	0.30		6.00	18.91	47.10%		
4.50		7.40	7.58	0.18		1.50	20.41	68.99%		
5.00		7.33	7.48	0.15		2.50	22.91	74.46%		
6.00		6.86	6.96	0.10		2.00	24.91	83.58%		
7.00		7.07	7.13	0.06		1.00	25.91	90.88%		
8.00		7.36	7.40	0.04		0.50	26.41	94.53%		
9.00		7.50	7.53	0.03		0.50	26.91	96.35%		
10.0		7.08	7.10	0.02		0.5	27.41	98.18%		
Total				16.81		27.41	27.41			

Sample Number: 46

Treatment: Heating with 5g/l Calgon, some mechanical disaggregation, wet sieving, sand fraction dry sieved. Mud fraction: pipette analysis.

Weight (g): Dry Sample: 35.73 Sand: 17.19 Mud: 24 Sand and Mud: 41.19

sieve diam. (ϕ)	exact diam. (ϕ)	weight beaker (g)	beaker & sample (g)	weight sample (g)	% aggs	corrected weight	cumulative weight	cumulative %	% shell	notes
-5.00				0.00		0.00	0.00	0.00%		
-4.00				0.00		0.00	0.00	0.00%		
-3.00				0.00		0.00	0.00	0.00%		
-2.50				0.00		0.00	0.00	0.00%		
-2.25				0.00		0.00	0.00	0.00%		
-2.00				0.00		0.00	0.00	0.00%		
-1.75	-1.72			0.00		0.00	0.00	0.00%		
-1.50				0.00		0.00	0.00	0.00%		
-1.25	-1.20			0.00		0.00	0.00	0.00%		
-1.00				0.00		0.00	0.00	0.00%		
-0.75	-0.74			0.00		0.00	0.00	0.00%		
-0.50	-0.48			0.00		0.00	0.00	0.00%		
-0.25	-0.20	26.53	26.69	0.16	100	0.00	0.00	0.00%		
0.00		29.23	29.30	0.07	100	0.00	0.00	0.00%		
0.25	0.28	29.58	29.71	0.13	100	0.00	0.00	0.00%		
0.50	0.54	29.27	29.39	0.12	97	0.00	0.00	0.01%	3	
0.75	0.78	28.53	28.65	0.12	97	0.00	0.01	0.02%	1	
1.00	1.04	25.22	25.37	0.15	90	0.02	0.02	0.05%	5	
1.25		29.86	29.97	0.11	95	0.01	0.03	0.07%	3	
1.50	1.54	25.42	25.62	0.20	90	0.02	0.05	0.12%	3	1% glauconite
1.75	1.72	29.29	29.43	0.14	85	0.02	0.07	0.17%	2	
2.00		26.53	26.72	0.19	65	0.07	0.14	0.33%	4	
2.25		29.23	29.43	0.20	60	0.08	0.22	0.52%	4	
2.50	2.52	29.58	29.80	0.22	50	0.11	0.33	0.79%	1	
2.75	2.72	29.27	29.81	0.54	40	0.32	0.65	1.58%		
3.00	3.04	28.53	30.06	1.53	30	1.07	1.72	4.18%		
3.25	3.28	25.22	29.40	4.18	15	3.55	5.27	12.80%		
3.50	3.52	29.86	37.70	7.84	5	7.45	12.72	30.88%		
3.75	3.70	25.42	27.89	2.47	1	2.45	15.17	36.82%		
4.00	4.16	29.29	31.31	2.02	0	2.02	17.19	41.72%		
4.00		6.87	7.36	0.49		10.50	27.69	41.73%		
4.50		7.06	7.34	0.28		3.50	31.19	67.23%		
5.00		7.03	7.24	0.21		3.50	34.69	75.72%		
5.50		7.07	7.21	0.14		1.00	35.69	84.22%		
6.00		6.76	6.88	0.12		3.00	38.69	86.65%		
7.00		7.08	7.14	0.06		1.50	40.19	93.93%		
8.00		7.35	7.38	0.03		0.50	40.69	97.57%		
9.00		7.46	7.48	0.02		0.50	41.19	98.79%		
10.00		7.46	7.47	0.01		0	41.19	100.00%		
Total				21.75		41.19	41.19			

Sample Number: 59

Treatment: Heating with 5g/l Calgon, some mechanical disaggregation, wet sieving, sand fraction dry sieved. Mud fraction: pipette analysis.

Weight (g): Dry Sample: 50.83 Sand: 29.78 Mud: 14.5 Sand and Mud: 44.28

sieve diam. (ϕ)	exact diam. (ϕ)	weight beaker (g)	beaker & sample (g)	weight sample (g)	% aggs	corrected weight	cumulative weight	cumulative %	% shell	notes
-5.00				0.00		0.00	0.00	0.00%		
-4.00				0.00		0.00	0.00	0.00%		
-3.00				0.00		0.00	0.00	0.00%		
-2.50				0.00		0.00	0.00	0.00%		
-2.25				0.00		0.00	0.00	0.00%		
-2.00				0.00		0.00	0.00	0.00%		
-1.75	-1.72			0.00		0.00	0.00	0.00%		
-1.50				0.00		0.00	0.00	0.00%		
-1.25	-1.20			0.00		0.00	0.00	0.00%		
-1.00				0.00		0.00	0.00	0.00%		
-0.75	-0.74			0.00		0.00	0.00	0.00%		
-0.50	-0.48			0.00		0.00	0.00	0.00%		
-0.25	-0.20	26.53	26.57	0.04	99	0.00	0.00	0.00%		
0.00		29.23	29.34	0.11	90	0.01	0.01	0.02%		
0.25	0.28	29.58	29.79	0.21	90	0.02	0.03	0.07%		
0.50	0.54	29.27	29.62	0.35	95	0.02	0.05	0.11%	2	
0.75	0.78	28.53	28.91	0.38	90	0.04	0.09	0.20%	2	
1.00	1.04	25.22	25.76	0.54	90	0.05	0.14	0.32%	2	lots bryozoa fragments
1.25		29.86	30.26	0.40	90	0.04	0.18	0.41%	2	
1.50	1.54	25.42	26.32	0.90	85	0.14	0.32	0.71%	2	
1.75	1.72	29.29	29.92	0.63	90	0.06	0.38	0.86%	0	
2.00		26.53	27.40	0.87	88	0.10	0.48	1.09%	2	
2.25		29.23	30.18	0.95	85	0.14	0.63	1.41%		
2.50	2.52	29.58	30.61	1.03	75	0.26	0.88	2.00%		
2.75	2.72	29.27	31.21	1.94	30	1.36	2.24	5.06%		
3.00	3.04	28.53	31.70	3.17	6	2.98	5.22	11.79%		
3.25	3.28	25.22	31.87	6.65	2	6.52	11.74	26.51%		
3.50	3.52	29.86	42.21	12.35	1	12.23	23.97	54.12%		
3.75	3.70	25.42	28.23	2.81	0	2.81	26.78	60.47%		
4.00	4.16	29.29	32.29	3.00	0	3.00	29.78	67.24%		
4.00		7.11	7.41	0.30		7.00	36.78	67.25%		
4.50		6.86	7.02	0.16		3.00	39.78	83.06%		
5.00		7.07	7.17	0.10		1.50	41.28	89.84%		
5.50		7.02	7.09	0.07		1.00	42.28	93.22%		
6.00		7.47	7.52	0.05		1.00	43.28	95.48%		
7.00		7.46	7.49	0.03		1.00	44.28	97.74%		
8.00		7.46	7.47	0.01		0.00	44.28	100.00 %		
9.00		7.48	7.49	0.01		0.00	44.28	100.00 %		
10.0		6.93	6.94	0.01		0.00	44.28	100.00 %		
Total				37.07		44.28	44.28			

Sample Number: 76

Treatment: Heating with 5g/l Calgon, some mechanical disaggregation, wet sieving, sand fraction dry sieved. Mud fraction: pipette analysis.

Weight (g): Dry Sample: 45.73 Sand: 16.95 Mud: 24.5 Sand and Mud: 41.45

sieve diam. (ϕ)	exact diam. (ϕ)	weight beaker (g)	beaker & sample (g)	weight sample (g)	% aggs	corrected weight	cumulative weight	cumulative %	% shell	notes
-5.00				0.00		0.00	0.00	0.00%		
-4.00				0.00		0.00	0.00	0.00%		
-3.00				0.00		0.00	0.00	0.00%		
-2.50				0.00		0.00	0.00	0.00%		
-2.25				0.00		0.00	0.00	0.00%		
-2.00				0.00		0.00	0.00	0.00%		
-1.75	-1.72			0.00		0.00	0.00	0.00%		
-1.50				0.00		0.00	0.00	0.00%		
-1.25	-1.20			0.00		0.00	0.00	0.00%		
-1.00		.		0.00		0.00	0.00	0.00%		
-0.75	-0.74			0.00		0.00	0.00	0.00%		
-0.50	-0.48			0.00		0.00	0.00	0.00%		
-0.25	-0.20	26.53	27.33	0.80	98	0.02	0.02	0.04%	2	Aggregates mainly pellets
0.00		29.23	29.40	0.17	99	0.00	0.02	0.04%	1	and broken pellets
0.25	0.28	29.58	29.83	0.25	96	0.01	0.03	0.07%	2	
0.50	0.54	29.27	29.72	0.45	97	0.01	0.04	0.10%	2	
0.75	0.78	28.53	29.00	0.47	95	0.02	0.06	0.16%	1	
1.00	1.04	25.22	25.92	0.70	93	0.05	0.11	0.27%	2	1% glauconite
1.25		29.86	30.37	0.51	92	0.04	0.15	0.37%	1	1% glauconite
1.50	1.54	25.42	26.38	0.96	92	0.08	0.23	0.56%	2	1% glauconite
1.75	1.72	29.29	29.93	0.64	91	0.06	0.29	0.70%	1	1% glauconite
2.00		26.53	27.53	1.00	88	0.12	0.41	0.99%	1	1% glauconite
2.25		29.23	30.22	0.99	80	0.20	0.61	1.46%	1	1% glauconite
2.50	2.52	29.58	30.55	0.97	65	0.34	0.95	2.28%	0	1% glauconite
2.75	2.72	29.27	30.83	1.56	60	0.62	1.57	3.79%	1	1% glauconite
3.00	3.04	28.53	30.17	1.64	35	1.07	2.64	6.36%		1% glauconite
3.25	3.28	25.22	27.29	2.07	10	1.86	4.50	10.86%		1% glauconite
3.50	3.52	29.86	37.47	7.61	2	7.46	11.96	28.85%		
3.75	3.70	25.42	28.39	2.97	1	2.94	14.90	35.94%		
4.00	4.16	29.29	31.34	2.05	0	2.05	16.95	40.89%		
4.00		7.06	7.56	0.50		13.00	29.95	40.89%		
4.50		6.93	7.17	0.24		3.50	33.45	72.26%		
5.00		6.92	7.09	0.17		3.00	36.45	80.70%		
5.50		6.90	7.01	0.11		1.00	37.45	87.94%		
6.00		7.46	7.55	0.09		2.00	39.45	90.35%		
7.00		7.06	7.11	0.05		1.50	40.95	95.17%		
8.00		7.07	7.09	0.02		0.50	41.45	98.79%		
9.00		7.47	7.48	0.01		0.00	41.45	100.00 %		
10.00		6.90	6.91	0.01		0.00	41.45	100.00 %		
Total				27.01		41.45	41.45			

Kaiata Mudstone

HLS 14	graphic mean	$M_z = +4.87\phi$	
	standard deviation	$\sigma_1 = 1.91\phi$	poorly sorted
	graphic skewness	$Sk_1 = +0.45$	very fine skewed
	graphic kurtosis	$K_G = +2.00$	very leptokurtic
	modes: +3.41ϕ and +4.37ϕ		
HLS 15	graphic mean	$M_z = +4.11\phi$	
	standard deviation	$\sigma_1 = 1.11\phi$	poorly sorted
	graphic skewness	$Sk_1 = +0.12$	fine skewed
	graphic kurtosis	$K_G = +1.65$	very leptokurtic
	modes: +3.39ϕ and +4.39ϕ		
HLS 66	graphic mean	$M_z = +4.30\phi$	
	standard deviation	$\sigma_1 = 2.54\phi$	very poorly sorted
	graphic skewness	$Sk_1 = +0.67$	very fine skewed
	graphic kurtosis	$K_G = +1.20$	leptokurtic
	modes: +2.62ϕ and +4.34ϕ		
HLS 34	graphic mean	$M_z = +3.74\phi$	
	standard deviation	$\sigma_1 = 1.38\phi$	poorly sorted
	graphic sewness	$Sk_1 = +0.61$	very fine skewed
	graphic kurtosis	$K_G = +1.09$	mesokurtic
	modes: +2.62ϕ and +4.37ϕ		
HLS 39	graphic mean	$M_z = +5.64\phi$	
	standard deviation	$\sigma_1 = 1.90\phi$	poorly sorted
	graphic skewness	$Sk_1 = +0.51$	very fine skewed
	graphic kurtosis	$K_G = +1.23$	leptokurtic
	modes: (+0.72), +3.39ϕ and +4.38ϕ		
HLS 78	graphic mean	$M_z = +5.64\phi$	
	standard deviation	$\sigma_1 = 1.70\phi$	poorly sorted
	graphic skewness	$Sk_1 = +0.44$	very fine skewed
	graphic kurtosis	$K_G = +1.10$	mesokurtic
	modes: +0.50, (+3.23ϕ) and +4.38ϕ		

Sample Number: 14

Treatment: Heating with 5g/l Calgon, some mechanical disaggregation, wet sieving, sand fraction dry sieved. Mud fraction: pipette analysis.

Weight (g): Dry Sample: 35.89 Sand: 7.82 Mud: 24.5 Sand and Mud: 32.32

sieve diam. (ϕ)	exact diam. (ϕ)	weight beaker (g)	beaker & sample (g)	weight sample (g)	% aggs	corrected weight	cumulative weight	cumulative %	% shell	notes
-5.00				0.00		0.00	0.00	0.00%		
-4.00				0.00		0.00	0.00	0.00%		
-3.00				0.00		0.00	0.00	0.00%		
-2.50				0.00		0.00	0.00	0.00%		
-2.25				0.00		0.00	0.00	0.00%		
-2.00				0.00		0.00	0.00	0.00%		
-1.75	-1.72			0.00		0.00	0.00	0.00%		
-1.50				0.00		0.00	0.00	0.00%		
-1.25	-1.20			0.00		0.00	0.00	0.00%		
-1.00				0.00		0.00	0.00	0.00%		
-0.75	-0.74			0.00		0.00	0.00	0.00%		
-0.50	-0.48			0.00		0.00	0.00	0.00%		
-0.25	-0.20	26.53	26.56	0.03		0.00	0.00	0.00%		
0.00		29.23	29.56	0.33	99	0.00	0.00	0.00%		
0.25	0.28	29.58	30.21	0.63	99	0.01	0.01	0.02%		
0.50	0.54	29.27	30.10	0.83	97	0.02	0.03	0.10%	2	
0.75	0.78	28.53	29.26	0.73	98	0.01	0.05	0.14%	1	
1.00	1.04	25.22	26.28	1.06	97	0.03	0.08	0.24%	2	
1.25		29.86	30.63	0.77	98	0.02	0.09	0.29%	1	
1.50	1.54	25.42	27.01	1.59	97	0.05	0.14	0.44%	2	
1.75	1.72	29.29	30.31	1.02	95	0.05	0.19	0.59%	2	
2.00		26.53	28.06	1.53	92	0.12	0.31	0.97%	1	
2.25		29.23	30.68	1.45	92	0.12	0.43	1.33%	1	
2.50	2.52	29.58	30.87	1.29	90	0.13	0.56	1.73%		
2.75	2.72	29.27	31.35	2.08	70	0.62	1.18	3.66%		
3.00	3.04	28.53	30.34	1.81	40	1.09	2.27	7.02%		
3.25	3.28	25.22	26.93	1.71	20	1.37	3.64	11.25%		
3.50	3.52	29.86	32.73	2.87	10	2.58	6.22	19.25%		
3.75	3.70	25.42	26.38	0.96	5	0.91	7.13	22.07%		
4.00	4.16	29.29	29.99	0.70	2	0.69	7.82	24.19%		
4.00		25.80	26.30	0.50		9.50	17.32	24.20%		
4.50		31.84	32.15	0.31		4.50	21.82	53.59%		
5.00		32.44	32.66	0.22		2.00	23.82	67.51%		
5.50		32.11	32.29	0.18		1.50	25.32	73.70%		
6.00		35.61	35.76	0.15		2.50	27.82	78.34%		
7.00		26.40	26.50	0.10		1.50	29.32	86.08%		
8.00		31.88	31.95	0.07		1.00	30.32	90.72%		
9.00		30.24	30.29	0.05		0.50	30.82	93.81%		
10.00		33.60	33.64	0.04		1.50	32.32	95.36%		
Total				21.39		32.32	32.32			

Sample Number: 39

Treatment: Heating with 5g/l Calgon, some mechanical disaggregation, wet sieving, sand fraction dry sieved. Mud fraction: pipette analysis.

Weight (g): Dry Sample: 36.99 Sand: 3.71 Mud: 25.25 Sand and Mud: 28.96

sieve diam. (ϕ)	exact diam. (ϕ)	weight beaker (g)	beaker & sample (g)	weight sample (g)	% aggs	corrected weight	cumulative weight	cumulative %	% shell	notes
-5.00				0.00		0.00	0.00	0.00%		
-4.00				0.00		0.00	0.00	0.00%		
-3.00				0.00		0.00	0.00	0.00%		
-2.50				0.00		0.00	0.00	0.00%		
-2.25				0.00		0.00	0.00	0.00%		
-2.00				0.00		0.00	0.00	0.00%		
-1.75	-1.72			0.00		0.00	0.00	0.00%		
-1.50				0.00		0.00	0.00	0.00%		
-1.25	-1.20			0.00		0.00	0.00	0.00%		
-1.00				0.00		0.00	0.00	0.00%		
-0.75	-0.74			0.00		0.00	0.00	0.00%		Aggregates are crust,
-0.50	-0.48			0.00		0.00	0.00	0.00%		pellets and broken pellets.
-0.25	-0.20	26.53	27.14	0.61	99	0.01	0.01	0.02%	1	
0.00		29.23	29.58	0.35	98	0.01	0.01	0.05%	2	microfossils
0.25	0.28	29.58	30.03	0.45	98	0.01	0.02	0.08%	2	
0.50	0.54	29.27	29.99	0.72	97	0.02	0.04	0.15%	2	1 round qtz grain
0.75	0.78	28.53	29.27	0.74	96	0.03	0.07	0.25%	3	1 angular qtz grain
1.00	1.04	25.22	26.28	1.06	94	0.06	0.14	0.47%	4	ang. qtz, 1% glauconite
1.25		29.86	30.68	0.82	92	0.07	0.20	0.70%	5	1% glauc
1.50	1.54	25.42	27.11	1.69	92	0.14	0.34	1.17%	5	1% glauc
1.75	1.72	29.29	30.46	1.17	92	0.09	0.43	1.49%	6	1% glauc
2.00		26.53	28.13	1.60	92	0.13	0.56	1.93%	6	1% glauc
2.25		29.23	30.91	1.68	93	0.12	0.68	2.34%	5	1% glauc
2.50	2.52	29.58	31.04	1.46	93	0.10	0.78	2.69%	4	1% glauc
2.75	2.72	29.27	31.54	2.27	94	0.14	0.92	3.16%	2	1% glauc, shell=fragments.
3.00	3.04	28.53	30.42	1.89	92	0.15	1.07	3.68%	2	1% glauc
3.25	3.28	25.22	26.78	1.56	67	0.51	1.58	5.46%	2	1% glauc
3.50	3.52	29.86	31.96	2.10	50	1.05	2.63	9.09%	1	1% glauc
3.75	3.70	25.42	26.31	0.89	40	0.53	3.17	10.93%	1	
4.00	4.16	29.29	29.97	0.68	20	0.54	3.71	12.81%	1	
4.00		32.43	32.94	0.51		7.00	10.71	13.67%		
4.50		27.63	28.00	0.37		3.50	14.21	37.85%		
5.00		27.17	27.47	0.30		2.50	16.71	49.93%		
5.50		34.15	34.40	0.25		2.00	18.71	58.56%		
6.00		29.80	30.01	0.21		3.50	22.21	65.47%		
7.00		38.97	39.11	0.14		2.50	24.71	77.56%		
8.00		27.71	27.80	0.09		1.50	26.21	86.19%		
9.00		32.45	32.51	0.06		1.00	27.21	91.37%		
10.0		26.15	26.19	0.04		1.75	28.96	94.82%		
Total				21.74		28.96	28.96			

Sample Number: 66

Treatment: Heating with 5g/l Calgon, some mechanical disaggregation, wet sieving, sand fraction dry sieved. Mud fraction: pipette analysis.

Weight (g): Dry Sample: 58.41 Sand: 31.09 Mud: 23.5 Sand and Mud: 54.59

sieve diam. (ϕ)	exact diam. (ϕ)	weight beaker (g)	beaker & sample (g)	weight sample (g)	% aggs	corrected weight	cumulative weight	cumulative %	% shell	notes
-5.00				0.00		0.00	0.00	0.00%		
-4.00				0.00		0.00	0.00	0.00%		
-3.00				0.00		0.00	0.00	0.00%		
-2.50				0.00		0.00	0.00	0.00%		
-2.25				0.00		0.00	0.00	0.00%		
-2.00				0.00		0.00	0.00	0.00%		
-1.75	-1.72			0.00		0.00	0.00	0.00%		
-1.50				0.00		0.00	0.00	0.00%		
-1.25	-1.20			0.00		0.00	0.00	0.00%		
-1.00				0.00		0.00	0.00	0.00%		
-0.75	-0.74			0.00		0.00	0.00	0.00%		
-0.50	-0.48			0.00		0.00	0.00	0.00%		
-0.25	-0.20	26.53	26.59	0.06	99	0.00	0.00	0.00%		large musc. flakes are the
0.00		29.23	29.31	0.08	70	0.02	0.02	0.05%		only grains
0.25	0.28	29.58	29.72	0.14	68	0.04	0.07	0.13%	2	
0.50	0.54	29.27	29.55	0.28	50	0.14	0.21	0.38%	1	
0.75	0.78	28.53	28.80	0.27	50	0.14	0.34	0.63%	5	qtz and muscovite
1.00	1.04	25.22	25.71	0.49	45	0.27	0.61	1.12%	5	
1.25		29.86	30.29	0.43	30	0.30	0.91	1.68%	5	
1.50	1.54	25.42	26.52	1.10	25	0.82	1.74	3.19%	4	
1.75	1.72	29.29	30.22	0.93	25	0.70	2.44	4.46%	4	
2.00		26.53	28.24	1.71	25	1.28	3.72	6.81%	3	
2.25		29.23	31.80	2.57	22	2.00	5.72	10.49%	2	
2.50	2.52	29.58	33.96	4.38	12	3.85	9.58	17.55%	1	
2.75	2.72	29.27	41.01	11.74	5	11.15	20.73	37.98%		
3.00	3.04	28.53	33.66	5.13	5	4.87	25.61	46.90%		
3.25	3.28	25.22	27.26	2.04	2	2.00	27.60	50.57%		
3.50	3.52	29.86	32.02	2.16	3	2.10	29.70	54.41%		
3.75	3.70	25.42	26.17	0.75	1	0.74	30.44	55.77%		
4.00	4.16	29.29	29.94	0.65	1	0.64	31.09	56.94%		
4.00		26.53	27.01	0.48		5.00	207.39	56.95%		
4.50		29.23	29.61	0.38		3.00	210.39	66.11%		
5.00		29.58	29.90	0.32		1.50	211.89	71.61%		
5.50		29.27	29.56	0.29		2.00	213.89	74.35%		
6.00		28.53	28.78	0.25		3.00	216.89	78.02%		
7.00		25.22	25.41	0.19		2.00	218.89	83.51%		
8.00		29.86	30.01	0.15		2.00	220.89	87.18%		
9.00		25.42	25.53	0.11		1.50	222.39	90.84%		
10.0		29.29	29.37	0.08		3.50	225.89	93.59%		
Total				34.91		54.59	54.59			

Sample Number: 15

Treatment: Heating with 5g/l Calgon, some mechanical disaggregation, wet sieving, sand fraction dry sieved. Mud fraction: pipette analysis.

Weight (g): Dry Sample: 41.48 Sand: 17.82 Mud: 18.5 Sand and Mud: 36.32

sieve diam. (ϕ)	exact diam. (ϕ)	weight beaker (g)	beaker & sample (g)	weight sample (g)	% aggs	corrected weight	cumulative weight	cumulative %	% shell	notes
-5.00				0.00		0.00	0.00	0.00%		
-4.00				0.00		0.00	0.00	0.00%		
-3.00				0.00		0.00	0.00	0.00%		
-2.50				0.00		0.00	0.00	0.00%		
-2.25				0.00		0.00	0.00	0.00%		
-2.00				0.00		0.00	0.00	0.00%		
-1.75	-1.72			0.00		0.00	0.00	0.00%		
-1.50				0.00		0.00	0.00	0.00%		
-1.25	-1.20			0.00		0.00	0.00	0.00%		
-1.00				0.00		0.00	0.00	0.00%		
-0.75	-0.74			0.00		0.00	0.00	0.00%		
-0.50	-0.48			0.00		0.00	0.00	0.00%		
-0.25	-0.20	26.53	26.53	0.00		0.00	0.00	0.00%		
0.00		29.23	29.23	0.00		0.00	0.00	0.00%		
0.25	0.28	29.58	29.60	0.02	99	0.00	0.00	0.00%	1	
0.50	0.54	29.27	29.32	0.05	96	0.00	0.00	0.01%	2	angular qtz, broken shells
0.75	0.78	28.53	28.78	0.25	94	0.02	0.02	0.05%	5	broken shells +
1.00	1.04	25.22	25.65	0.43	94	0.03	0.04	0.12%	3	microfossils
1.25		29.86	30.19	0.33	95	0.02	0.06	0.16%	3	1% glauconite
1.50	1.54	25.42	26.14	0.72	93	0.05	0.11	0.30%	2	1% glauconite
1.75	1.72	29.29	29.49	0.20	91	0.02	0.13	0.35%	2	1% glauconite
2.00		26.53	27.32	0.79	87	0.10	0.23	0.63%	1	2% glauconite
2.25		29.23	30.01	0.78	56	0.34	0.57	1.58%	1	3% glauconite
2.50	2.52	29.58	30.37	0.79	50	0.40	0.97	2.67%	1	5% glauconite
2.75	2.72	29.27	30.68	1.41	45	0.78	1.74	4.80%	1	4% glauconite
3.00	3.04	28.53	30.25	1.72	30	1.20	2.95	8.12%		
3.25	3.28	25.22	29.49	4.27	10	3.84	6.79	18.70%		
3.50	3.52	29.86	38.20	8.34	2	8.17	14.96	41.20%		
3.75	3.70	25.42	26.94	1.52	1	1.50	16.47	45.34%		
4.00	4.16	29.29	30.65	1.36	1	1.35	17.82	49.05%		
4.00		30.62	31.00	0.38		10.50	28.32	49.06%		
4.50		31.95	32.12	0.17		2.50	30.82	77.97%		
5.00		32.10	32.22	0.12		1.00	31.82	84.86%		
5.50		33.17	33.27	0.10		1.00	32.82	87.61%		
6.00		32.47	32.55	0.08		1.50	34.32	90.36%		
7.00		31.23	31.28	0.05		1.00	35.32	94.49%		
8.00		29.86	29.89	0.03		1.00	36.32	97.25%		
9.00		29.10	29.11	0.01		0.00	36.32	100.00 %		
10.0		30.90	30.91	0.01		0.00	36.32	100.00 %		
Total				22.98		36.32	36.32			

Sample Number: 78

Treatment: Heating with 5g/l Calgon, some mechanical disaggregation, wet sieving, sand fraction dry sieved. Mud fraction: pipette analysis.

Weight (g): Dry Sample: 44.2 Sand: 2.78 Mud: 31.25 Sand and Mud: 33.03

sieve diam. (ϕ)	exact diam. (ϕ)	weight beaker (g)	beaker & sample (g)	weight sample (g)	% aggs	corrected weight	cumulative weight	cumulative %	% shell	notes
-5.00				0.00		0.00	0.00	0.00%		
-4.00				0.00		0.00	0.00	0.00%		
-3.00				0.00		0.00	0.00	0.00%		
-2.50				0.00		0.00	0.00	0.00%		
-2.25				0.00		0.00	0.00	0.00%		
-2.00				0.00		0.00	0.00	0.00%		
-1.75	-1.72			0.00		0.00	0.00	0.00%		
-1.50				0.00		0.00	0.00	0.00%		
-1.25	-1.20			0.00		0.00	0.00	0.00%		
-1.00				0.00		0.00	0.00	0.00%		
-0.75	-0.74			0.00		0.00	0.00	0.00%		
-0.50	-0.48			0.00		0.00	0.00	0.00%		
-0.25	-0.20	26.53	28.14	1.61	99	0.02	0.02	0.05%	1	Limestone fragments and
0.00		29.23	29.91	0.68	99	0.01	0.02	0.07%	1	pellets = aggregates
0.25	0.28	29.58	30.37	0.79	99	0.01	0.03	0.09%		
0.50	0.54	29.27	30.37	1.10	98	0.02	0.04	0.14%	1	rounded qtz grain
0.75	0.78	28.53	29.51	0.98	96	0.04	0.08	0.25%	1	rounded and ang qtz
1.00	1.04	25.22	26.51	1.29	96	0.05	0.14	0.41%	1	rounded and ang qtz
1.25		29.86	30.85	0.99	95	0.05	0.19	0.56%	2	rounded and ang qtz
1.50	1.54	25.42	27.55	2.13	94	0.13	0.31	0.95%	1	musc. and biotite and qtz
1.75	1.72	29.29	30.64	1.35	94	0.08	0.39	1.19%	1	
2.00		26.53	28.12	1.59	93	0.11	0.51	1.53%	1	
2.25		29.23	31.07	1.84	93	0.13	0.63	1.92%		
2.50	2.52	29.58	31.27	1.69	92	0.14	0.77	2.33%		
2.75	2.72	29.27	31.43	2.16	90	0.22	0.99	2.98%		
3.00	3.04	28.53	30.35	1.82	80	0.36	1.35	4.09%		
3.25	3.28	25.22	26.66	1.44	70	0.43	1.78	5.39%		
3.50	3.52	29.86	31.61	1.75	65	0.61	2.39	7.25%		
3.75	3.70	25.42	25.90	0.48	50	0.24	2.63	7.97%		
4.00	4.16	29.29	29.55	0.26	45	0.14	2.78	8.41%		
4.00		28.03	28.64	0.61		8.00	10.78	9.17%		
4.50		31.68	32.13	0.45		5.00	15.78	33.39%		
5.00		31.54	31.89	0.35		3.00	18.78	48.53%		
5.50		29.82	30.11	0.29		2.50	21.28	57.61%		
6.00		32.63	32.87	0.24		4.50	25.78	65.18%		
7.00		36.26	36.41	0.15		3.00	28.78	78.81%		
8.00		32.33	32.42	0.09		2.00	30.78	87.89%		
9.00		31.55	31.60	0.05		1.50	32.28	93.94%		
10.0		33.75	33.77	0.02		0.75	33.03	98.49%		
Total				23.95		33.03	33.03			

Sample Number: 34

Treatment: Heating with 5g/l Calgon, some mechanical disaggregation, wet sieving, sand fraction dry sieved. Mud fraction: pipette analysis.

Weight (g): Dry Sample: 41.56 Sand: 23.67 Mud: 17.0 Sand and Mud: 40.67

sieve diam. (ϕ)	exact diam. (ϕ)	weight beaker (g)	beaker & sample (g)	weight sample (g)	% aggs	corrected weight	cumulative weight	cumulative %	% shell	notes
-5.00				0.00		0.00	0.00	0.00%		
-4.00				0.00		0.00	0.00	0.00%		
-3.00				0.00		0.00	0.00	0.00%		
-2.50				0.00		0.00	0.00	0.00%		
-2.25				0.00		0.00	0.00	0.00%		
-2.00				0.00		0.00	0.00	0.00%		
-1.75	-1.72			0.00		0.00	0.00	0.00%		
-1.50				0.00		0.00	0.00	0.00%		
-1.25	-1.20			0.00		0.00	0.00	0.00%		
-1.00				0.00		0.00	0.00	0.00%		
-0.75	-0.74			0.00		0.00	0.00	0.00%		
-0.50	-0.48			0.00		0.00	0.00	0.00%		
-0.25	-0.20	26.53	26.53	0.00		0.00	0.00	0.00%		
0.00		29.23	29.24	0.01	99	0.00	0.00	0.00%		muscovite flakes
0.25	0.28	29.58	29.59	0.01	98	0.00	0.00	0.00%		
0.50	0.54	29.27	29.29	0.02	90	0.00	0.00	0.01%		biotite and muscovite
0.75	0.78	28.53	28.56	0.03	50	0.01	0.02	0.04%		
1.00	1.04	25.22	25.29	0.07	60	0.03	0.05	0.11%	5	microfossils and pellets
1.25		29.86	29.92	0.06	30	0.04	0.09	0.21%	9	
1.50	1.54	25.42	25.61	0.19	40	0.11	0.20	0.49%	5	
1.75	1.72	29.29	29.49	0.20	30	0.14	0.34	0.84%	4	
2.00		26.53	26.93	0.40	15	0.34	0.68	1.68%	2	
2.25		29.23	29.91	0.68	15	0.58	1.26	3.10%	3	
2.50	2.52	29.58	30.86	1.28	7	1.19	2.45	6.02%	2	
2.75	2.72	29.27	36.00	6.73	3	6.53	8.98	22.07%	1	
3.00	3.04	28.53	36.30	7.77	1	7.69	16.67	40.99%		
3.25	3.28	25.22	29.25	4.03	1	3.99	20.66	50.80%		
3.50	3.52	29.86	32.52	2.66	2	2.61	23.27	57.21%		
3.75	3.70	25.42	25.70	0.28	4	0.27	23.54	57.87%		
4.00	4.16	29.29	29.43	0.14	5	0.13	23.67	58.20%		
4.00		25.27	25.62	0.35		6.00	29.67	58.20%		
4.50		32.31	32.54	0.23		3.00	32.67	72.95%		
5.00		32.19	32.36	0.17		2.50	35.17	80.33%		
5.50		32.49	32.61	0.12		1.00	36.17	86.48%		
6.00		27.40	27.50	0.10		2.00	38.17	88.94%		
7.00		31.59	31.65	0.06		1.50	39.67	93.85%		
8.00		27.45	27.48	0.03		0.00	39.67	97.54%		
9.00		31.53	31.56	0.03		0.50	40.17	97.54%		
10.0		34.75	34.77	0.02		0.50	40.67	98.77%		
Total				24.56		40.67	40.67			

HLS 87	Peptizer = Calgon, 1gm			Total Sand:		12.0%
	Lagoon deposit from C. Foulwind Quarry			Total Mud:	Measured:	25.05g
					Calculated:	23.5g
Size (phi)	W(sample+ beaker)	W(beaker)	W(sample)	W(finer)	W(fraction)	
4	7.83	7.34	0.49	23.5		
4.5	7.36	7.06	0.3	14	9.5	9.5
5	7.94	7.69	0.25	11.5	2.5	12
5.5	7.28	7.07	0.21	9.5	2	14
6	7.26	7.07	0.19	8.5	1	15
7	7.62	7.46	0.16	7	1.5	16.5
8	6.9	6.76	0.14	6	1	17.5
9	7.04	6.91	0.13	5.5	0.5	18

HLS 88o	Peptizer = Calgon, 1gm			Total Sand:		4.2%
	over clay layer, Gibsons Beach			Total Mud:	Measured:	22.41g
					Calculated:	22g
Size (phi)	W(sam+b)	W(b)	W(sample)	W(finer)		
4	5.79	5.33	0.46	22		
4.5	7.5	7.1	0.4	19	3	3
5	7.36	7.01	0.35	16.5	2.5	5.5
5.5	7.34	7.03	0.31	14.5	2	7.5
6	7.72	7.46	0.26	12	2.5	10
7	7.63	7.46	0.17	7.5	4.5	14.5
8	6.98	6.86	0.12	5	2.5	17
9	7.54	7.46	0.08	3	2	19

HLS 88u	Peptizer = Calgon, 1gm			Total Sand:		1.33%
	under clay layer, Gibsons Beach			Total Mud:	Measured:	25.14g
					Calculated:	24.5g
Size (phi)	W(sam+b)	W(b)	W(sample)	W(finer)		
4	7.39	6.88	0.51	24.5		
4.5	7.95	7.47	.0.48	23	1.5	1.5
5	7.33	6.9	0.43	20.5	2.5	4
5.5	7.27	6.88	0.39	18.5	2	6
6	7.79	7.45	0.34	16	2.5	8.5
7	7.13	6.86	0.27	12.5	3.5	12
8	7.11	6.92	0.19	8.5	4	16
9	7.6	7.47	0.13	5.5	3	19

Appendix VI

Photograph List

This list is of every photograph that was taken while doing field work. Figures containing photographs list the reference number of the photograph, and this list provides the details of the location of the photograph.

Film	Photo	Description and Location
1	1	Kaiata Mudstone-Limestone with rhodolith layer, increasing sand content
1	2	towards rhodolith band = contact. More loose rhodoliths and shells
1	3	"
1	4	Location: Woodpeckers Bay, NZMS 260 K30 747068
1	5	"
1	6	"
1	7	"
1	8	"
1	9	"
1	10	Sedimentary structures in Island Sandstone (road exposure); 10 and 11 are
1	11	small scale scour structures
1	12	12,13,14 & 15 are hummocky cross stratification in close up and
1	13	general views.
1	14	Location: Irimahwharo Point (above Gentle Annie Rocks)
1	15	"
1	16	Wave eroded cave, joint plane, Nt1P2, K30 746057
1	17	cemented layers, dip measured, Nt1p3, K30 746057
1	18	Ophiomorpha, near Pahautane Point, Nt1P3, K30 746054
1	19	Worm Shells preserved in concretion, Nt1P3, K30 746054
1	20	Trace fossils in concretion, Nt1P3, K30 746054
1	21	Part of sand-limestone contact zone, Nt1P3&3.5, K30 746053
1	22	Part of sand-limestone contact zone, Nt1P3&3.5, K30 746053
1	23	Part of sand-limestone contact zone, Nt1P3&3.5, K30 746053
1	24	Echinoid in Island Sandstone Nt1P3, K30 746058, HLF1, MS105
1	25	Scour surface and channels in concretions K30 746057

2	1	Brunner overlain by LT Sand
2	2	LT Sand interbedded with Waitakeri Limestone K29 833238
2	3	Lense (hammer end)of Waitakeri Limestone in LT Sand K29 833238
2	4	Similar cyclic/rhythmic patterns in seds of same age far north of south Island
2	5	Section near limestone contact, Pahautane Point, MS101, K30 746053
2	6	Section near limestone contact, Pahautane Point, MS101, K30 746053
2	7	Section over previous photos
2	8	Surface showing shell band and isolated rhodolith, end scallop 2cm, MS101
2	9	Surface showing shell band and isolated rhodolith, blue shell 4.2cm across
2	10	Brachiopod MS101 K30 746053
2	11	Rhodolith and echinoid spine MS101, K30 746053
2	12	Scallop shells MS101, K30 746053
2	13	Worm tubes and echinoid traces MS101, K30 746053
2	14	Worm tubes and echinoid traces in concretions MS101, K30 746053
2	15	Ichnofabric MS102, K30 746053
2	16	Thalassinoides in Island, MS102 K30 746054
2	17	Ophiomorpha andother traces, MS103 K30 746054
2	18	Cemented Band, cross bedding, bioturbated Island, MS103, K30 746056
2	19	Change in ichnofabric, long purple thin traces occur MS105, K30 746058
2	20	many sedimentary structures MS105, K30 746058
2	21	many sedimentary structures MS105, K30 746058
2	22	change from no sed structures (grey) to some sed structures (cream) MS105
2	23	change from no sed structures (grey) to some sed structures (cream) MS105
2	24	change from no sed structures (grey) to some sed structures (cream) MS105
2	25	angular unconformity MS105, K30 746061
2	26	angular unconformity MS105, K30 746061
3	1	angular unconformity MS105, K30 746061
3	2	angular unconformity MS105, K30 746061
3	3	angular unconformity; ?sole marks (118) MS105, K30 746061
3	4	angular unconformity, ophiomorpha in cemeted band MS105, K30 746061
3	5	Ichnofabric MS105, K30 746059, Nt1P5
3	6	Ichnofabric MS105, K30 746059, Nt1P6
3	7	Ichnofabric MS105, K30 746059, Nt1P6
3	8	Ichnofabric MS105, K30 746059, Nt1P6
3	9	Ichnofabric MS105, K30 746059, Nt1P7
3	10	Change in bioturbation, larger burrows MS104, K30 746057, Nt1P7
3	11	Ophiomorpha MS104, K30 746057, Nt1P7
3	12	Lateral variation in concretion style, MS105, K30 746061, Nt1P7

3	13	Views across inlet in Kaipakati point of rhodolith band and Island-Limestone
3	14	transition. K30 746059, Nt1P7
3	15	Views across inlet in Kaipakati point of rhodolith band and Island-Limestone
3	16	transition. K30 746059, Nt1P7
3	17	oysters encrusted K30 755069, Nt1P8
3	18	Several layers in Kaiata, K30 755069, Nt1P8
3	19	oysters encrusted K30 755069, Nt1P8
3	20	oysters encrusted K30 755069, Nt1P8
3	21	Traces in Kaiata K30 755069, Nt1P8
3	22	Ichnofabric K30 755069, Nt1P9
3	23	Ichnofabric, change to narrow burrows K30 749067, Nt1P9
3	24	Agglomerate of small rhodoliths K30 747068, Nt1p10
3	25	Vertical section over rhodolith band occurrence K30 747068, Nt1p10
3	26	Vertical section over rhodolith band occurrence K30 747068, Nt1p10
3	27	Vertical section over rhodolith band occurrence K30 747068, Nt1p10
3	28	Rhodolith band some 15m from 25-26, out on point. K30 747068, Nt1p10
3	29	Rhodolith band some 15m from 25-26, out on point. K30 747068, Nt1p10
3	30	Oblique burrow sections, Truman Track, K30 725004, Nt1P10
3	31	Pretty Picture of Overhanging shelves, Truman Track.
3	32	Thalassinoides? Truman Track, in overhanging ledges K30 725004, Nt1P10
3	33	Thalassinoides? Truman Track, in overhanging ledges K30 725004, Nt1P10
3	34	Shell concentration in sandstone, Truman track K30 725004, Nt1P10
3	35	Iron staining in Little Totara Sand, Brighton Mine, K30 751046
3	36	Iron staining in Little Totara Sand, Brighton Mine, K30 751046
3	37	Iron staining in Little Totara Sand, Brighton Mine, K30 751046
3	38	Outcrop from opposite side of valley
4	1	Outcrop from opposite side of valley
4	2	Outcrop from opposite side of valley
4	3	Pretty Picture of Rata forest, Brighton Mine
4	4	Granule layers in LTSand, Brighton Mine, K30 753046
4	5	Structures in LT Sand, Brighton Mine, K30 753046
4	6	Structures in LT Sand, Brighton Mine, K30 753046
4	7	Structures in LT Sand, Brighton Mine, K30 753046
4	8	Structures in LT Sand, Brighton Mine, K30 753046
4	9	Pretty Picture out of Brighton Mine from K30 753046
4	10	Inaccessible part of outcrop, Brighton Mine, K30 753046
4	11	Brunner Coal, Lag, LT Sand, Brighton Mine, K30 753046
4	12	Brunner Coal, Lag, LT Sand, Brighton Mine, K30 753046

4	13	
4	14	View from end of Brighton Mine, K30 753046, gently East dipping Island
4	15	McLaughlins Pit, K29 830239, LT Sand
4	16	McLaughlins Pit, K29 830239, LT Sand
4	17	McLaughlins Pit, K29 830239, LT Sand
4	18	
4	19	
4	20	Transition section Brunner-LT Sand, K30 804181-804182
4	21	Transition from packed to loose LT Sand
4	22	Quaternary marine terrace overlying 20-21
4	23	Four Mile Road Brunner-LTS contact
4	24	Fallen limestoneBlock in 4mile river K30 808142
4	25	Fallen limestoneBlock in 4mile river K30 808142
4	26	Kaiata Mudstone cemented outcrop K30 808142
4	27	Pretty picture of forest
4	28	Open cast mine Brunner-LTS
4	29	Island Sandstone in Mine exposures, Redjacket Mine
4	30	Bullock Creek Road Island-Limestone contact
4	31	Bullock Creek Road Island-Limestone contact
4	32	Bullock Creek Road Island-Limestone contact
4	33	View North from lookout
4	34	View South from Lookout, Perpendicular Point
4	35	Thalassinoides in Kaiata K29 834387
4	36	Thalassinoides in Kaiata K29 834387
4	37	Kaiata to LT Sand Transition K29 834387
5	1	Sed structures in LT Sand, Nt1P20, K29 834387
5	2	LT Sand 10m above kaiata contact K29 834387, Nt1P21, MS110
5	3	Trace fossils in Kaiata Mudstone K29 834387, Nt1P21, MS111
5	4	Layer in Kaiata, MS111, Nt1P21, difference in weathering structures
5	5	Kaiata-LT Sand from West side
5	6	Kaiata-LT Sand from West side
5	7	Kaiata-LT Sand from West side
5	8	Contact from east side with half-moon in sky.....
5	9	Trace fossils in Kaiata 250cm below contact, on east side, echinoid spine
5	10	in burrow and narrow dark traces which are not present in F5P3.
5	11	
5	30	Kaiate/Island Sandstone K30 735012, Nt1P23
5	31	Kaiata/Island Sandstone exposed on two different levels, K30 734009, Nt1P24

5	32	Pretty Pictures, Inland Packtrack Pororari River crossing
5	33	Pretty Pictures, Inland Packtrack Pororari River crossing
5	34	Contact with Brunner Seds, 25km bend, K30 803144-142, Nt1P26
5	35	Contact with Brunner Seds, 25km bend, K30 803144-142, Nt1P26
5	36	Contact round cornor, 25km bend, K30 803144-142, Nt1P26
5	37	Contact round cornor, 25km bend, K30 803144-142, Nt1P26
5	38	Photo of Sample Location, K30 803144-142, Nt1P27
5	39	Photo of Sample Location, K30 803144-142, Nt1P27
6	1	Exposures above 38&39, K30 803144-142, Nt1P27
6	2	Exposures above 38&39, K30 803144-142, Nt1P27
6	3	Exposures above 38&39, K30 803144-142, Nt1P27
6	4	After sampling, K30 803144-142, Nt1P28
6	5	Photo of exposure with carbonaceous siltstone at base, K30 803143, Nt1P29
6	6	LT sand, with change in structure, appearance, K30 803143, Nt1P29
6	7	Cross bedding in LT sand, K30 803142, Nt1P29
6	8	
6	9	
6	10	
6	11	View of 7-10 and 12,13.....
6	12	Clay layer in LT sand marks change from cross-bedded to massive and
6	13	finer to coarse sand. K30 803142, Nt1P30
6	14	Okari Lagoon, ?little totara sand. K29 828306, Nt1P31
6	15	Contact Island sandstone-limestone Bullock Creek, K30 757000, Nt1P31
6	16	Contact Island sandstone-limestone Bullock Creek, K30 757000, Nt1P31
6	17	Coarse burrow fills, K29 834387, Nt1P32
6	18	Coarse burrow fills, K29 834387, Nt1P32
6	19	walled and unwalled coarse filled burrows, K29 834387, Nt1P33
6	20	walled and unwalled coarse filled burrows, K29 834387, Nt1P33
6	21	pyrite surrounded burrows, K29 834387, Nt1P33
6	22	shell and sand filled burrows, K29 834387, Nt1P33
6	23	Contact LT sand and BB grp, overlain by pliocene marine sands, K29 834387
6	24	Clayey surface within LT sand, right of 23, K29 834387, Nt1P34
6	25	?Kaiata Mudstone, Okari Lagoon K29 824310, Nt1P35
6	26	Interference ripples (current lft-rgt, wind see water) Okari Lagoon
6	27	Trace fossils in top layer of F6P25, K29 824310, Nt1P35
6	28	Trace fossils and cemented layer, K29 824310, Nt1P35
6	29	Hilside with exposure of Kaiata mudstone, K29 824312, Nt1P35
6	30	Modern river gravels overly Kaiata mudstone K29824315, Nt1P35

6	31	New slump exposes sedimentary structures in sand K29 804181, Nt1P36&16
6	32	"
6	33	"
6	34	loose packed overlying sand.....
6	35	View in rain from roadside.....
6	36	Woodpecker Bay, Paparoa Coal Measures, Seal Island, Rain and mist (scenic)
6	37	"
6	38	"
7	1	Cliffs above Perpendicular Point, Map2pnt5, Nt1P37
7	2	Cliffs above Perpendicular Point, Map2pnt4, Nt1P37
7	3	Island ss cliffs north Perpendicular Point, Nt1P37
7	4	Island ss, discontinuity, laminations, convoluted bedding, fossils K30 728010
7	5	Oysters, Island ss K30 728010 Nt1P32
7	6	convoluted bedding, as above
7	7	laminations-bioturbation transition, as above
7	8	Pink cobble layer, as above
7	9	trace fossils on underside of layer above F7P8, loc as above
7	10	trace fossils on underside of layer above F7P8, loc as above
7	11	convoluted bedding, as above
7	12	convoluted bedding, as above
7	13	Oysters occurring above thal. Horizon, K30 728011, Nt1P38
7	14	Oysters occurring above thal. Horizon, K30 728011, Nt1P38
7	15	Oyster encrustation above thal. layer, location as above
7	16	Base of thalassinoides horizon, rubbish chambers, largest ~70cm long
7	17	Thalassinoides traces brought out by weathering
7	18	Thalassinoides traces brought out by weathering
7	19	layers in Island ss, location as above
7	20	shell rich horizon, location as above
7	21	wood? In Island horizon, location as above
7	22	boundary between thal horizons, location as above
7	23	algal layers, scattered layer beneath thick cemented bands, K30 748068, Nt1P39
7	24	algal layers, scattered layer beneath thick cemented bands, K30 748068, Nt1P39
7	26	algal layers, scattered layer beneath thick cemented bands, K30 748068, Nt1P39
7	27	algal layers, scattered layer beneath thick cemented bands, K30 748068, Nt1P39
7	29	LT sand overlying Brunner sands and Charl. Met. complex, K30 798137, Nt1P37
7	30	LT sand, Brunner, Charl. Met. Com. and fault (SW side down ~1.8m), Nt1P37,
7	31	K30 797136.
7	32	tracefossils in Island ss K30 727993

7	33	Bryozoa layer in Island ss K30 727993
7	34	Bryozoa layer in Island ss K30 727993
7	35	location of 33 and 34
7	36	Echinoid, K30 727993
7	37	Bryozoa fragments above thallassinoides horizon.
8	1	Island ss?/limestone with lots of glauconite, smeared by scraping K30 751047
8	2	Same as 8/1
8	3	Location of 8/1
8	4	Island ss ~10m upstream 8/1&2
8	5	Kaiata mudstone outcrop = mudslide, very dangerous, Punakaiki river gorge
8	6	Bedding in outcrop of Island, above Punakaiki gorge, K30 757927
8	7	Details of bedding in 8/6
8	8	Details of bedding in 8/6, E is 1 cm long
8	9	More bedding, and steeper joints
8	10	Concretions and tracefossils in Island ss, 15m downstream last locality
8	11	as above
8	12	as above
8	13	Bedding dipping opposite way, fallen block
8	14	Kaiata mudstone on track in gorge, not contains blocks of ?limestone.
8	15	Kaiata mudstone on track in gorge, not contains blocks of ?limestone.
8	16	Kaiata mudstone on track in gorge, not contains blocks of ?limestone.
8	17	Worm encrusted echinoderm, and free rhodoliths, fallen block K30 747068
8	18	Bryozoa, rhodoliths, fallen block, K30 747068
8	19	Surface of rhodolith band and encrusting oysters, fallen block K30 747068
8	20	Details of rhodolith band on point K30 747068
8	21	Details of rhodolith band on Seal island K30 748068
8	22	Details of rhodolith band on Seal island K30 748068
8	23	Bird
8	24	Fallen blocks showing internal structure of rhodolith band, K30 748068
8	25	Fallen blocks showing internal structure of rhodolith band, K30 748068
8	26	Details of rhodolith band on Seal island K30 748068
8	27	Fallen blocks showing internal structure of rhodolith band, K30 748068
8	28	Details of rhodolith band on Seal island K30 748068
8	29	Birds
8	30	Rhodolith Band Nth side Smithy's beach, K30 746059
8	31	Rhodolith Band Nth side Smithy's beach, K30 746059
8	32	Trace fossils on underside of cemented layer = base of unconformity 746061
8	33	Trace fossils on underside of cemented layer = base of unconformity 746061

9	1	Rhodolith Samples, polished sides. Samples from HLS 18 and 81.
9	2	Rhodolith Samples, polished sides. Samples from HLS 18 and 81.
9	3	Rhodolith Samples, polished sides. Samples from HLS 18 and 81.
9	4	Rhodolith Samples, polished sides. Samples from HLS 18 and 81.
9	5	Rhodolith Samples, polished sides. Samples from HLS 18 and 81.
9	6	Rhodolith Samples, polished sides. Samples from HLS 18 and 81.
9	7	Rhodolith Samples, polished sides. Samples from HLS 18 and 81.
9	8	Rhodolith Samples, polished sides. Samples from HLS 18 and 81.
9	9	Rhodolith Samples, polished sides. Samples from HLS 18 and 81.
9	10	Rhodolith Samples, polished sides. Samples from HLS 18 and 81.
9	11	Rhodolith Samples, polished sides. Samples from HLS 18 and 81.
9	12	Rhodolith Samples, polished sides. Samples from HLS 18 and 81.
10	1	Brachiopod, HLS 44 loc. Truman Track K30 726004, looking down on bedding
10	2	Fossil accumulation, as above
10	3	Trace fossils as above
10	4	Bryozoa in shell accumulation, as above
10	5	Shell accumulation close to HLS 43 Loc. Looking up at underside of bed
10	6	as above, brachiopod showing ?interior.
10	7	Hummocky x-stratification and escape structures, Smithy's beach K30 746058
10	8	Hummocky x-stratification and escape structures, Smithy's beach K30 746058
10	9	Hummocky x-stratification and escape structures, Smithy's beach K30 746058
10	10	Echinoderm locations
10	11	Echinoderm locations
10	12	Bryozoa/corralline algae on ?hardground, below limestone contact K30 746053
10	13	Bryozoa/corralline algae on ?hardground, below limestone contact K30 746053
10	14	Bryozoa and ostrea in shell accumulation, above limestone contact, K30 746053
10	15	Bryozoa and ostrea in shell accumulation, above limestone contact, K30 746053
10	16	Glauconite infilled burrows in limestone above P15
10	17	Outcrop showing progressive changes in limestone, K30 746053
10	18	Outcrop showing progressive changes in limestone, K30 746053
10	19	Echinoderm locations
10	20	Cemented band at non-conformity, K30 746061
10	21	Cemented band at non-conformity, K30 746061
10	22	join of cemented bands below and above non-conformity K30 746061
10	23	Convoluted Bedding K30 728010
10	24	Convoluted Bedding K30 728010
10	25	Pink Concretion Band and surrounding layers K30 728010
10	26	Pink Concretion band and surrounding layers K30 728010

10	27	Diruption in Pink concretion layer, K30 728010
10	28	Panorama of Bay, laminated sands above bioturbated
10	29	Panorama of Bay, laminated sands above bioturbated
10	30	Panorama of Bay, laminated sands above bioturbated
10	31	Panorama of Bay, laminated sands above bioturbated
10	32	Panorama of Bay, laminated sands above bioturbated
10	33	Panorama of Bay, laminated sands above bioturbated
10	34	Panorama of Bay, laminated sands above bioturbated
10	35	Second year field trip, Kaiata Outcrop, Dave Shelley speaketh. K29 826388
10	36	Railway cutting, Malcolm + Brunner equivalents, (prob. marine sands) K29 826388
10	37	Second year field trip, Brunner equivalents.
10	38	Second year field trip, Brunner equivalents.
10	39	Students from second year field trip. Railway cutting, k30 826388
11	1	View of Quarry
11	2	Limestone from Quarry
11	3	View of Quarry, eastern side, Kaiata overlies and grades laterally into Limestone.
11	4	Silty layers 'tween kaiata and LTS, eastern side of Quarry
11	5	Silty layers 'tween kaiata and LTS, eastern side of Quarry
11	6	LTS structure
11	7	LTS(covered by mud slick)-congl.-BB group-Quaternary marine sands (Noel Win)
11	8	LTS-congl.-BB group-Quaternary marine sands (Noel Win is Scale)
11	9	Overview of Eastern face of Quarry
11	10	Surface in Kaiata, muddy beneath, silty above, rubbery black clay between.
11	11	Surface in Kaiata as above, Gibsons Beach, K29 830387
11	12	Surface in Kaiata, is two surfaces close together, location of 10+11 K29 830387
11	13	Surface in Kaiata, is two surfaces close together, location of 10+11 K29 830387
11	14	Algal debris in Kaiata K29 828387
11	15	Two surfaces in Kaiata. K29 830387
11	16	Another surface in Kaiata, above previous two.
11	17	Fallen block showing rhodoliths, Seal island K30 748068
11	18	Fallen block showing rhodoliths, Seal island K30 748068
11	19	Fallen block showing rhodoliths, Seal island K30 748068
11	20	More rhodolith bands further north on Seal Island, appear to dip other way
11	21	Sed infilled hollows, fallen block Seal Island, K30 748068
11	22	Band with Zoom, Seal Island
11	23	More ?karst features on blocks, Seal Island K30 748068

11	24	Block from band, no sed K30 748068
11	25	Well bored block K30 748068
11	26	Block with patches of sed, K30 748068
11	27	Block with progression from no sed, to lots sed K30 748068
12	1	Cross bedding in McLaughlins Pit. Nt2P2
12	2	Cross bedding in McLaughlins Pit. Nt2P2
12	3	Cross bedding in McLaughlins Pit. Nt2P2
12	4	Face of LTS and McLaughlins Pit. Nt2P2
12	5	Exposure of Upper Part of LTS in Road Cutting K29 829238, Nt2P2
12	6	Exposure of Upper Part of LTS in Road Cutting K29 829238, Nt2P2
12	7	Small Scale steep x-beds, Upper LTS road Exp as above, Nt2P3
12	8	Small Scale steep x-beds, Upper LTS road Exp as above, Nt2P3
12	9	X-beds in LTS, Pit on 4 Mile Road.
12	10	Onlap of Brunner and LTS onto weathered met basement, K30 798137, F7P29
12	11	As above, Nt2P4
12	12	Gauge from fault zone, K30 798137, see F7P30
12	13	Sunshine Coal Mine k30 792133
12	14	Sunshine Coal Mine k30 792133
12	15	Pretty Picture of Gibsons Beach after a Nor'west storm
12	16	Shells on Waitakere limestone surface, fallen Block, K29 836388
12	17	karst features on top of Waitakere limestone, K29 836388
12	18	karst features on top of Waitakere limestone, K29 836388
12	19	LTS to congl. To Bluebottom Cape Foulwind Quarry, Nt2P6, K29 830366
12	20	Very Coarse LTS, Quarry, K29 8303666
12	21	Quarry Overview, see sketch Nt2P7
12	22	Lmst to Rotten Limestone to kaiata, Nt2P8, K29 826264
12	23	View across small pit in Quarry, location 6, Nt2P8
12	24	Thin bedded Limestone/kaiata K29 825364, location 2 Nt2P8
12	25	Thin bedded Limestone/kaiata K29 825364, location 2 Nt2P8
12	26	limestone passing laterally into Kaiata Mudstone, Quarry.
13	1	Quarry Wall, locations 3-4, Nt2P9
13	2	Location 7 thicker limestone and mudstone bands, Quarry
13	3	Location 1 Waitakeri Limestone at top of cliff
13	4	Location 1 Waitakeri Limestone at top of cliff
13	5	Solid vertically jointed limestone opposite road from locations 3-4
13	6	karst formation in Waitakeri and underlying limestone (Quat??)
13	7	Muddy Layers at Location 8
13	8	Muddy Layers at Location 8

13	9	Coarse sand = HLS 93 equiv. Brunner, note opposite Railway Cutting see F11
13	10	Location of P9, Nt2P11
13	11	LTS at Gibsons Beach, Nt2P12
13	12	LTS at Gibsons Beach, Nt2P12
13	13	Carbonaceous layers in LTS, to of bottom part of LTS Gibsons Beach
13	14	Cross Bedding, Bottom part of LTS, Gibsons Beach
13	15	Pericosmos barraeus? F1
13	16	Kina gracilus? F2
14	1	shell accumulation, worm tubes+broken shellls. Beach below Perpendicular Point
14	2	shell accumulation, worm tubes+broken shellls. Beach below Perpendicular Point
14	3	accumulation of small spatangoids, ?channel. Beach below Perpendicular Point
14	4	pockets of worm tubes in ~round hollows. Beach below Perpendicular Point
14	5	A swale-->hummock, laminated Island ss, Beach below Perpendicular Point
14	6	convoluted bedding in Island sandstone, Beach below Perpendicular Point
14	7	Two episodes of bioerosion-->channeling..... Beach below Perpendicular Point
14	8	Coarse filled burrows below erosion surface, upper surface in F14P7
14	9	Swale cut off by erosion surface. Beach below Perpendicular Point
14	10	Hummocky cross stratification. Beach below Perpendicular Point
14	11	Hummock cut off by large channel. Beach below Perpendicular Point
14	12	Zoom of transition laminated sands-->muddy rhythmic cementation. P. Point.
14	13	Perpendicular Point cliff face.
14	14	Perpendicular Point cliff face.
14	15	Slip exposing Kaiata Mudstone above track to Gibsons Beach.
15	1	Teichichnus sp. In Island Sandstone, Smithy's Beach K30 746057
15	2	Teichichnus sp. In Island Sandstone, Smithy's Beach K30 746057
15	3	Teichichnus sp. In Island Sandstone, Smithy's Beach K30 746057
15	4	Teichichnus sp. In Island Sandstone, Smithy's Beach K30 746057
15	5	Teichichnus sp. In Island Sandstone, Smithy's Beach K30 746057
15	6	Teichichnus sp. In Island Sandstone, Smithy's Beach K30 746057
15	7	Multiple Thallassinoides burrows in Limestone-Island Contact, K30 746053
15	8	Malcolm and Doug examine Limestone, Pahautane Point, K30 746053
15	9	Teichichnus sp. In Island Sandstone, Smithy's Beach K30 746057
15	10	Teichichnus sp. In Island Sandstone, Smithy's Beach K30 746057
15	11	Teichichnus sp. In Island Sandstone, Smithy's Beach K30 746057
15	12	Herringbone Cross Bedding in Little Totara Sand road cutting, K30 798137
15	13	Herringbone Cross Bedding in Little Totara Sand road cutting, K30 798137
15	14	Herringbone Cross Bedding in Little Totara Sand road cutting, K30 798137